Inventory and Probabilistic Function of Natural Hazards in the United States

July 19, 2018 – September 18, 2018

Alan W. Black[1,2,3] and Vincent M. Brown[1,2]

1 Southern Climate Impacts Planning Program
2 Louisiana State University
3 Southern Illinois University Edwardsville

NREL Technical Monitors: Kate Anderson, Scott Belding, and Lissa Myers

NREL is a national laboratory of the U.S. Department of Energy
Office of Energy Efficiency & Renewable Energy
Operated by the Alliance for Sustainable Energy, LLC

This report is available at no cost from the National Renewable Energy Laboratory (NREL) at www.nrel.gov/publications.

Contract No. DE-AC36-08GO28308

Subcontract Report
NREL/SR-7A40-75493
January 2020

Inventory and Probabilistic Function of Natural Hazards in the United States

July 19, 2018 – September 18, 2018

Alan W. Black[1,2,3] and Vincent M. Brown[1,2]

1 Southern Climate Impacts Planning Program
2 Louisiana State University
3 Southern Illinois University Edwardsville

NREL Technical Monitors: Kate Anderson, Scott Belding, and Lissa Myers

Suggested Citation
Black, Alan W. and Vincent M. Brown. 2020. *Inventory and Probabilistic Function of Natural Hazards in the United States: July 19, 2018 – September 18, 2018*. Golden, CO: National Renewable Energy Laboratory. NREL/SR-7A40-75493. https://www.nrel.gov/docs/fy20osti/75493.pdf.

NREL is a national laboratory of the U.S. Department of Energy
Office of Energy Efficiency & Renewable Energy
Operated by the Alliance for Sustainable Energy, LLC

This report is available at no cost from the National Renewable Energy Laboratory (NREL) at www.nrel.gov/publications.

Contract No. DE-AC36-08GO28308

Subcontract Report
NREL/SR-7A40-75493
January 2020

National Renewable Energy Laboratory
15013 Denver West Parkway
Golden, CO 80401
303-275-3000 • www.nrel.gov

This publication received minimal editorial review at NREL.

NOTICE

This work was authored in part by the National Renewable Energy Laboratory, operated by Alliance for Sustainable Energy, LLC, for the U.S. Department of Energy (DOE) under Contract No. DE-AC36-08GO28308. Funding provided by the U.S. Air Force Civil Engineering Center. The views expressed herein do not necessarily represent the views of the DOE or the U.S. Government.

Cover Photos by Dennis Schroeder: (clockwise, left to right) NREL 51934, NREL 45897, NREL 42160, NREL 45891, NREL 48097, NREL 46526.

Acknowledgments

This work was initially funded by the U.S. Air Force Civil Engineering Center.

NREL thanks the researchers from the Southern Climate Impacts Planning Program and Louisiana State University who authored the regional reports, including Nicholas Grondin, Barry Keim, Stephen Kreller, Derek Thompson, and all others.

Executive Summary

The U.S. Department of Energy's National Renewable Energy Laboratory (NREL) developed a standardized risk assessment process that considers the location-specific vulnerabilities and threats (climate-related as well as human-caused) at a site to generate a ranked list of organizational risks and associated mitigation options for reducing those risks.

To support this effort, the Southern Climate Impacts Planning Program (SCIPP), a National Oceanic and Atmospheric (NOAA) Regional Integrated Sciences and Assessments (RISA) team, was selected to provide climate science expertise to develop a comprehensive inventory and probabilistic function of natural hazards (e.g., hurricanes, tornados, flooding, and sea level rise) for the entire United States by region. The inventory of climate-related hazards and the associated likelihood scores are incorporated into a companion risk assessment tool enabling standardized comparisons of risk at sites across the country.

The analysis included the division of the United States into nine regions that correspond to the regions examined in the Fourth National Climate Assessment (NCA), released in 2018 (see Figure ES-1). For each region, several climate-related stressors were evaluated in broad categories, such as temperature, precipitation, and other weather conditions and hazards. Stressors were evaluated for their changes in the near- (2021-2050), mid- (2041-2070), and late-century (2071-2099), relative to their occurrence in the period from the early 1900s to early 2000s, based on several different scenarios. These scenarios represent possible future climates based on global action (or inaction) to reduce greenhouse gas emissions.

Data were gathered from the Climate Science Special Report (CSSR) for the Fourth NCA, the Third NCA, and peer-reviewed scientific articles addressing various stressors in a changing climate. This analysis included data from two major scientific efforts to understand and model future climate: Phases 3 and 5 of the Coupled Model Intercomparison Project (CMIP). Regional model data from North America (NARCCAP) were also utilized. These climate model sources are detailed in Table ES-1.

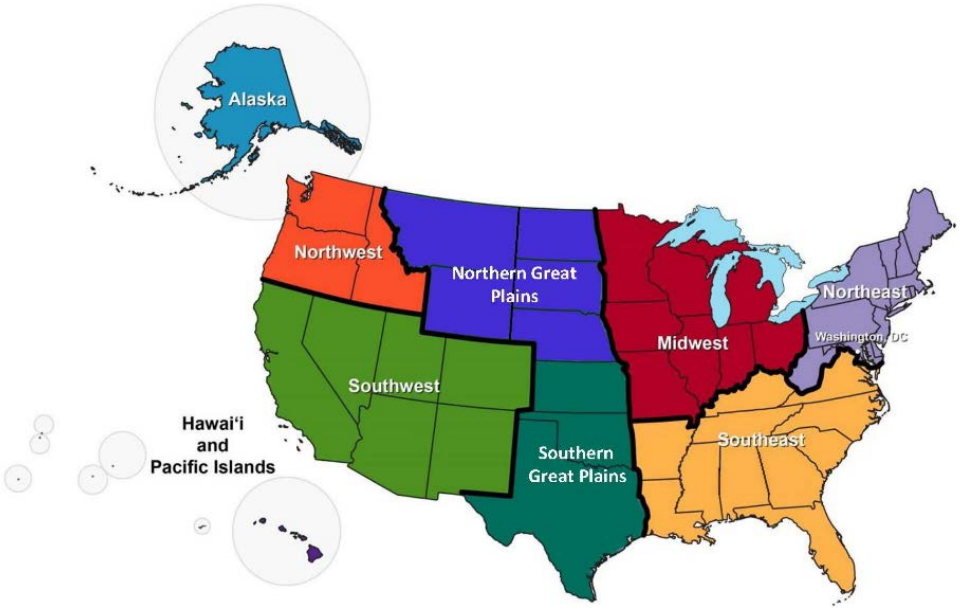

Figure ES-1. Regional division of the United States (Figure source: Melillo et al. 2014).

The results of this analysis are summarized in 11 reports. Nine of the reports are organized by region and cover the stressors with the greatest amount of data available that enabled detailed regional analysis. Because coastal communities have very specific climate-related issues to consider even within a region, a separate Coastal Communities report was also created. Lastly, a summary report on Other Stressors was created for those stressors, such as wind, that generally have insufficient data available to provide more regionally differentiated assessments. In assigning specific likelihood scores between 1 (low) and 10 (high) for each regional stressor (Table ES-2), professional judgment was exercised to evaluate the agreement among climate models, and between those models and peer-reviewed literature data. The most significant projected changes from each report are summarized below.

Table ES-1. Climate Model Sources Used in Analysis

Abbrev.	Year	Title	Models Included	Basis for Scenarios	Scenario(s)	Est. Avg. Temp. Increase by 2100 (IPCC 2007; Hayhoe 2017)	Est. GHG Conc. (CO_2e) in 2100 (ARC)
NARCCAP	2007 (upd. 2014)	North American Regional Climate Change Assessment Program (Mearns 2007)	10	GHG Emissions	High: A2	3.4 °C/6.1 °F	
CMIP3	2010	Coupled Model Intercomparison Project, Phase 3	24	GHG Emissions:	Low: B1 Balanced: A1B High: A2	1.8 °C/3.2 °F 2.8 °C/5.0 °F 3.4 °C/6.1 °F	
CMIP5	2014	Coupled Model Intercomparison Project, Phase 5 (Collins 2013)	61	Radiative Forcing (W/m^2):	RCP 2.6 RCP 4.5 RCP 6.0 RCP 8.5	1.0 °C/1.8 °F 1.8 °C/3.2 °F 2.2 °C/4.0 °F 3.7 °C/6.7 °F	475 ppm 630 ppm 800 ppm 1313 ppm

Table ES-2. Regional Likelihood Scores for Analyzed Stressors

Region	Northeast		Southeast		Midwest		N Great Plains		S Great Plains		Southwest		Northwest		Alaska		Hawai'i	
Stressor Change	Increase	Decrease	Increase	Decrease	Increase	Decrease	Increase	Decrease	Increase	Decrease	Increase	Decrease	Increase	Decrease	Increase	Decrease	Increase	Decrease
Temperature:																		
Annual average temperatures	8	2	8	2	9	1	9	1	6	4	8	2	8	2	8	2	6	3
Magnitude of hottest annual temperature	7	3	3	7	7	3	4	6	3	7	8	2	7	3	6	4	6	3
Magnitude of lowest annual temperature	9	1	5	5	9	1	8	1	8	1	7	3	8	2	6	4	6	3
Number of days with temperatures ≥ 95°F	6	3	9	1	7	3	8	2	9	1	8	2	6	4	6	4	5	4
Number of days with freezing temperatures	2	8	1	9	2	8	1	9	2	8	2	8	3	7	4	6	1	1
Minimum nighttime temperatures	7	2	6	4	8	2	8	2	7	3	8	2	8	2	8	2	7	3
Daily temperature range	4	5	3	7	4	5	2	7	2	8	3	7	3	7	3	7	4	5
Precipitation:																		
Annual precipitation	6	4	5	5	7	3	6	4	6	4	5	5	5	5	7	3	4	5
Rainfall amounts on days with rain (intensity)	8	2	8	2	8	2	8	2	8	2	5	5	6	4	8	2	4	5
Number of days with heavy rainfall	6	4	7	3	5	5	8	2	8	2	6	4	6	4	6	4	4	5
Increase in precipitation seasonality	6		6		7		7		6		5		5		5		6	
Other Stressors in Regional Reports:																		
Chance of flooding/high water levels	7	3	9	1	7	3	7	3	7	3	6	4	6	4	7	3	10	1
Chance of drought/low water levels	5	5	5	5	5	5	8	2	8	2	7	3	7	3	5	5	4	7
Wildfire occurrence	2	2	5	5	2	2	8	2	8	2	7	3	7	3	7	3	5	5
Length of fire season	2	1	6	4	2	1	5	5	7	3	6	4	6	4	6	4	5	5
Intensity of winter storms	5	5	5	5	5	5	6	4	6	4	5	5	5	5	5	5	1	1
Snowfall totals (by storm/annual)	4	5	4	6	5	4	6	4	4	6	5	5	4	6	4	6	1	1
Occurrence of ice storms/freezing rain	5	5	4	6	5	5	6	4	6	4	3	7	3	7	5	5	1	1
Other Stressors:																		
Average wind speed	3	7	3	7	3	7	3	7	5	5	3	7	3	7	3	7	3	7
Number of days with high winds	3	5	3	5	3	5	3	5	3	5	3	5	3	5	3	5	3	5
Number of days with thunderstorms/lightning	6	5	6	5	6	5	6	5	6	5	6	5	6	5	6	5	6	5
Occurrence of severe thunderstorms	5	5	5	5	5	5	5	5	5	5	5	5	5	5	5	5	5	5
Occurrence of tornadoes	5	5	5	5	5	5	5	5	5	5	5	5	5	5	5	5	5	5
Humidity (dewpoint)	7	3	7	3	7	3	7	3	7	3	7	3	7	3	7	3	7	3
Increase in vector-borne disease occurrence	6		6		6		6		6		6		6		6		6	
Decrease in water quality	6		6		6		6		6		6		6		6		6	
Coastal Issues:																		
Intensity of hurricanes	6	4	6	4	NA		NA		NA		6	4	6	4	6	4	6	4
Increased sea level	9		9		NA		NA		NA		8		8		9		8	
Increased coastal flooding	8		9		NA		NA		NA		8		8		9		8	
Increased storm surge due to hurricanes	7		8		NA		NA		NA		7		7		7		7	
Increased coastal erosion	7		8		NA		NA		NA		8		7		8		7	

Regional Report Summaries

Northeast Region

Temperature

The most significant projected temperature changes in the Northeast region include: an increase in annual average temperatures, an increase in the magnitude of hottest annual temperatures, a decrease in the number of days with freezing temperatures, and an increase in overnight minimum temperatures. These effects are likely to be modulated by coastal and mountainous areas within the region. Urban heat island effects are also prevalent in the Northeast.

Precipitation

The most significant projected precipitation changes in the Northeast region include: an increase in rainfall intensity. Local effects are prevalent (orographic, leeward versus windward, and so on) in the region.

Other Stressors

The most significant projected other stressor(s) in the Northeast region include: an increase in flood risk and an increase in drought risk.

Southeast Region

Temperature

The most significant projected temperature changes in the Southeast region include: an increase in annual average temperatures, a decrease in the magnitude of hottest annual temperatures, an increase in the number of days with temperatures $\geq 90°F$, a decrease in the number of days with freezing temperatures, an increase in overnight minimum temperature, and a decrease in the average daily temperature range.

Precipitation

The most significant projected precipitation changes in the Southeast region include: an increase in rainfall intensity, an increase in the number of days with heavy rainfall, a decrease in overall snowfall, and increased precipitation seasonality (variability).

Other Stressors

The most significant projected other stressors in the Southeast region include: an increase in sea level (sea-level rise), an increase in flood risk, and increased fire season length.

Midwest Region

Temperature

The most significant projected temperature changes in the Midwest region include: an increase in annual average temperatures, an increase in the magnitude of lowest annual temperatures, a decrease in the number of days with freezing temperatures, and an increase in minimum overnight temperatures. Some of these effects are likely to be more pronounced in the northern parts of the region and dampened along river valleys.

Precipitation
The most significant projected precipitation changes in the Midwest region include: an increase in annual precipitation (accumulation), an increase in the number of days with heavy rainfall, an increase in rainfall intensity, and increased precipitation seasonality (variability). Local factors may lead some areas of the region to experience muted effects.

Other Stressors
The most significant projected other stressors in the Midwest region include: an increase in flood risk.

Northern Great Plains Region

Temperature
The most significant projected temperature changes in the Northern Great Plains region include: an increase in annual average temperatures, an increase in magnitude of the lowest annual temperatures, an increase in the number of days with temperatures ≥ 90°F, a decrease in the number of days with freezing temperatures, an increase in overnight minimum temperatures, and a decrease in the daily average temperature range.

Precipitation
The most significant projected precipitation changes in the Northern Great Plains region include: an increase in rainfall intensity, an increase in number of days with heavy rainfall, an increase in snowfall, and increased precipitation seasonality (variability).

Other Stressors
The most significant projected other stressors in the Northern Great Plains region include: an increase in flood risk, an increase in drought risk, and increased frequency of wildfire.

Southern Great Plains Region

Temperature
The most significant projected temperature changes in the Southern Great Plains region include: an increase in the average annual temperatures, an increase in the number of days with temperatures ≥ 90°F, a decrease in the number of days with freezing temperatures, increased annual average minimum temperatures, and a decrease in the daily average temperature range.

Precipitation
The most significant projected precipitation changes in the Southern Great Plains region include: an increase in the number of days with heavy rainfall and increased rainfall intensity. These changes are less likely to be found in western Texas.

Other Stressors
The most significant projected other stressors in the Southern Great Plains region include: an increase in flooding risk, an increase in drought risk, an increase in the frequency of wildfire, and an increase in fire season length.

Southwest Region

Temperature

The most significant projected temperature changes in the Southwest region include: an increase in annual average temperatures, an increase in the magnitude of hottest annual temperatures, an increase in the magnitude of lowest annual temperatures, an increase in the number of days with temperatures ≥90°F, a decrease in the number of days with freezing temperatures, and a decrease in the daily average temperature range.

Precipitation

The most significant projected precipitation changes in the Southwest region include: an increase in the number of days with heavy rainfall. Mountainous terrain will experience the greatest variability in precipitation due to complex topography, orographic effects, and leeward versus windward airflow.

Other Stressors

The most significant projected other stressors in the Southwest region include: an increase in drought risk, an increase frequency of wildfire, an increase wildfire burned area, an increase in fire season length, a decrease in snowpack, and a decreased frequency of ice storms/freezing rain.

Northwest Region

Temperature

The most significant projected temperature changes in the Northwest region include: an increase in annual average temperatures, an increase in the magnitude of hottest annual temperatures, an increase in the magnitude of the lowest annual temperatures, an increase in the number of days with temperatures ≥ 90°F in areas that already experience these days, a decrease in the number of days with freezing temperatures, and a decrease in the daily average temperature range. Sub-regions along the Pacific coast will be moderated by the ocean, while the southeast portion of the region is projected to have the more significant changes.

Precipitation

The most significant projected precipitation changes in the Northwest region include: an increase in extreme precipitation events and a decrease in average snowpack. Coastal proximity and elevation are strong local determinants of precipitation effects.

Other Stressors

The most significant projected other stressors in the Northwest region include: an increase in sea level (sea-level rise), an increase in wildfire frequency, and an increase in length of the fire season.

Alaska

Temperature

Determining historical temperature trends in Alaska is complicated by the lack of sufficient long-term measurement stations. With that caveat, the most significant projected temperature changes in Alaska include: an increase in annual average temperatures, an increase in annual minimum temperatures, an increase in the number of days with temperatures > 90th percentile, an increase in overnight minimum temperatures, and a decrease in the daily average temperature range.

Changes will be unevenly distributed across the state because of the complex topography and localized (geographical) factors.

Precipitation
The most significant projected precipitation changes in Alaska include: an increase in annual precipitation and increased rainfall intensity.

Other Stressors
The most significant projected other stressors in Alaska include: an increase in sea level (with strong regional variability), an increase in flood risk, and increased wildfire frequency.

Hawai‘i

Temperature
Climate models are limited in their ability to resolve surface temperature on small Pacific islands. Hawai‘i’s temperature changes will be largely dictated by changes in ocean temperatures and ocean heat content. With those caveats, the most significant projected temperature changes in Hawai‘i include: an increase in annual average temperatures, an increase in the magnitude of the hottest annual temperatures, an increase in the magnitude of lowest annual temperatures, and an increase in overnight minimum temperatures.

Precipitation
Climate model resolution for precipitation on Hawai‘i is poor. With that caveat, the most significant predicted precipitation effects in Hawai‘i include: an increase in precipitation seasonality (variability).

Other Stressors
The most significant projected other stressors in Hawai‘i include: an increase in sea level (sea-level rise) and an increased flood risk.

Other Stressors

The most significant projected other stressors include: an increase in average wind speed across the Southern Great Plains region; a decrease in average wind speed across the Southwest, Northwest, and Northern Great Plains; an increase in humidity (dew point); an increase in conditions conducive to severe thunderstorms; an increase in geographic range for vector-borne diseases; and a decrease in overall average water quality.

Coastal Regions

The most significant projected coastal stressors include: an increase in tropical cyclone intensity, an increase in sea level (sea-level rise), an increase in storm surge frequency, an increase in storm surge intensity, an increase in flood frequency, an increase in flood intensity, and an increase in coastal erosion and land loss.

Table of Contents

1 Introduction

The U.S. Department of Energy's National Renewable Energy Laboratory (NREL) was tasked with developing a standardized risk assessment process that could be used at sites across the United States. The methodology will consider the vulnerabilities and threats (climate-related as well as human-caused) specific to each installation, resulting in a ranked list of organizational risks and associated mitigation options for reducing those risks.

To support this effort, the Southern Climate Impacts Planning Program (SCIPP), a National Oceanic and Atmospheric (NOAA) Regional Integrated Sciences and Assessments (RISA) team was selected to provide climate science expertise focused on developing a comprehensive inventory and probabilistic function of natural hazards (e.g., hurricanes, tornados, flooding, and sea level rise) for the entire United States by regions. The inventory of climate-related hazards and the associated likelihood scores were incorporated into a companion risk assessment tool enabling standardized comparisons of risk across all U.S. sites.

The analysis included the division of the United States into nine regions that correspond to the regions examined in the Fourth National Climate Assessment (NCA), released in late 2018. This was done to help users of this document locate additional information on climate and climate change contained within that report. For each region, several climate-related stressors were evaluated in broad categories, such as temperature, precipitation, other weather conditions and hazards, and coastal hazards. Data were gathered from the Climate Science Special Report (CSSR) for the Fourth NCA, the Third NCA (published in 2014), and peer-reviewed scientific articles addressing various stressors in a changing climate. This analysis included data from two major scientific efforts to understand and model future climate. The first is the Coupled Model Intercomparison Project Phase 3 (CMIP3), consisting of 24 separate models from 17 research groups in 12 countries. The second is the Coupled Model Intercomparison Project Phase 5 (CMIP5), consisting of 61 models from 28 research groups in 14 countries. Stressors were evaluated for their change in the years 2050, 2075, and 2100 relative to their occurrence in the period from the early 1900s to early 2000s based on several different future emissions scenarios. These scenarios represent possible future climates based on global action (or inaction) to reduce greenhouse gas emissions.

The results of this analysis are summarized in 11 reports. Nine of the reports are organized by region and cover the stressors with the greatest amount of data available that enabled detailed regional analysis. A summary report on other stressors was created for those stressors, such as wind, that have insufficient data available to provide more regionally differentiated assessments. Lastly, because coastal communities have very specific climate related issues to consider even within a region, a separate coastal regions report was also created.

2 Northeast Region

2.1 Summary of Climate Projections for the Northeast Region

2.1.1 Temperature

The Northeast region experienced slight increases in annual temperature (1.43°F), with more warming (>1.5°F) found in the New England and the mid-Atlantic metro areas (e.g. New York City, Washington, D.C, etc.) compared to Appalachia. This is found by comparing the present-day average temperature (averaged from 1986-2016) against the 1901-1960 averages. The difference in warming is largely due to the urban heat island effect—as the northeastern seaboard from Boston to Washington, D.C. is densely populated and heavily urbanized. In general, the warming has been more notable during winter (DJF) compared to summer (JJA), while parts of Appalachia have trended slightly cooler during the summer (USGCRP 2017, p. 188; Figure 2-1).

Warming is expected to continue by mid-century under both lower and higher emission scenarios; both of which show an increase of roughly 4-5°F from present-day by 2065. The models diverge by the late century (2070-2099) with the lower emissions scenario showing an average increase of 5.2°F from present-day, while the higher emissions scenario shows an average increase of over 9°F (USGCRP 2017, p.195-196). Warming is expected to be more significant further north in the region, especially across upstate New York and northern New England, while the coastal regions' increase will be moderated by the nearby ocean. While the models do not have the spatial resolution to resolve this, the proximity to the Great Lakes will also impact the magnitude of warming in northwestern Pennsylvania (Erie) and western New York (Buffalo).

Temperatures are unlikely to decrease in the region over the next century, as model output for the different emissions scenarios show warming across the entirety of the region. While the models diverge in the magnitude of warming in later periods, neither model realizes a cooling effect within the region (USGCRP 2017, p.195-196). The magnitude of increase could be dampened for coastal locations, such as eastern Massachusetts and coastal Maine due to proximity to water.

There has been a decrease in the hottest annual temperatures (roughly 1°F), comparing present-day to the 1901-1960 average, with the most significant decreases in rural areas and away from the coast. Nationally, this is result of peak warmth in the 1930s (Dust Bowl Era) – after a sharp drop throughout the 1940s and 1950s, there has been a steady increase since the mid-1960s (USGCRP 2017 p. 190). Contrary to present day observed trends, models expect a statistically significant increase in hottest annual temperatures by mid-century. For the Northeast region, an increase of 6.51°F is expected under the higher emission scenarios (USGCRP 2017, p.197-198). Under lower emission scenarios, warming is still expected but the magnitude is less, closer to 3-4°F (Melillo et al. 2014, p. 39).

Due to the proximity of the Atlantic Ocean, coastal regions in the northeast will experience less of an increase in magnitude of hottest annual temperatures. Although, this may be countered in urban locations on the coasts due to the urban heat island effect. Terrain effects in Appalachia may also temper the magnitude of increase. There does not seem to be any indication that the

magnitude of hottest annual temperature will decrease in the future (USGCRP 2017 p. 197-198, Melillo et al. 2014 p. 39); however, rural areas that do not have a significant urban heat island effect (such as central Pennsylvania, upstate New York, and northern New England), may see limited increases in the hottest annual temperatures as they do not have as much man-made material to absorb heat, such as roads and large buildings.

The largest projected increase in the lowest annual temperatures is found across the northern portion of the United States, including the Northeast region (USGCRP 2017, p.197-198). This continues the trend of warmer lowest annual temperatures that has been observed nationally and primarily across the Northeast region. The few exceptions are in portions of West Virginia and central New York (USGCRP 2017, p.190). On average, the change from near present (1976-2005) to the mid-century (2036-2065) is expected to be roughly 9.51°F under higher emission scenarios but could be over 10°F by the end of the century (USGCRP 2017 p.198 and Melillo et al. 2014 p. 39; Figure 2-2). Lower emission scenarios yield less warming and show an increase of 6-8°F across most of the region by the end of the century. Despite this divergence, even the coastal areas see an increase in the lowest annual temperatures, especially as the region's coast is largely urbanized. There is high confidence the lowest annual temperatures will rise, with little evidence to support a decrease or even unchanged values in the future.

Nationally, there has been an increase in the frequency of heat waves (consecutive days with 90°F or higher) and daily record highs set (not necessarily 90°F+ temps) since 1990 (USGCRP 2017, p.192). Average annual maximum temperatures have also increased nationally and in the Northeast region, comparing present day averages (1986-2016) to the first half of the century (1901-1960) (USGCRP 2017, p.187); however, even under the most extreme scenarios (high emissions), the Northeast region has large variability in the projected increase in number of days ≥ 90°F. Under lower emissions scenarios, some portions of the region show a negligible increase or no changes in the number of days, especially in northern New England, upstate New York, and down through the Appalachian Mountains into eastern West Virginia. However, since some of these areas experience few, if any, days above 90°F, even an increase of two or three days could double the current number days above 90°F (Melillo et al. 2014). While it seems more likely that the region as a whole will experience more 90°F+ days, the variation within the region itself and the differences between the high emissions and low emissions models lead to a higher uncertainty.

There is a wide range of variability in the region regarding the projected increase in extremely hot days. Model output for both low and high emissions scenarios show the effects of urban heat islands with more days over 90°F near Boston, New York City, Baltimore/Washington, the I-91 corridor in Connecticut and Massachusetts (New Haven, Hartford, and Springfield), and the I-90 corridor in upstate New York (Buffalo, Rochester, Syracuse, and Albany), especially in the higher emissions scenarios. Terrain is also a significant factor in the region, with higher elevations in West Virginia, Pennsylvania, New York, and northern New England expecting a smaller increase in days over 90°F in both outputs, with a near zero increase in some areas (Figure 2-3).

Average temperatures across the contiguous United States have increased and there has been a reduction in the number of days with freezing temperatures. Models continue to project increased temperatures, leading to fewer days with freezing temperatures (USGCRP 2017 p.188 and 197).

In the higher emissions scenarios, most of the Northeast region is expected to have fewer days with freezing temperatures by mid-century, compared to present day averages (1976-2005) (Figure 2-4). Lower emissions scenarios also show a decrease in days with freezing temperatures in the Northeast region. Terrain and proximity to water may play a role in the number of freezing days, but there is relatively high confidence the number of days with freezing temperatures will not increase.

The Connecticut River Valley and valleys within the Appalachian Mountains and Adirondack Mountains may not experience the same decrease in freezing temperature days as surrounding locations (possibly seeing no change at all). On the other hand, locations heavily modulated by the Atlantic Ocean, such as eastern Massachusetts, the Delmarva Peninsula, and coastal Maine may see a greater reduction of freezing temperature days due to moderating effect of the ocean.

Warmer nighttime temperatures have been observed in many locations over the past fifty years, especially in urban areas (Melillo et al. 2014, p. 9, 377). In recent years, many record-high low temperatures have been set across the country during the record-breaking summer of 2012 (Melillo et al. 2014 p. 38). Warmer overnight temperatures are expected in urbanized areas due to the urban heat island effect that is consequential in the highly developed and densely populated coastal Northeast. According to the Climate Science Special Report (USGCRP 2017 p. 277), the urban heat island effect can lead to nighttime temperatures 1.5°F to 4.5° warmer than adjacent rural areas.

With current observations and model projections, nighttime temperatures, on average, will likely be higher in the future. In lower emission scenarios, the Northeast region is projected to experience ~30-70 more days with "hot nights" during the late century period (2070-2099) compared to prior century (1971-2000). A "hot night" is defined as warmer than 98% of minimum nighttime temperatures from 1971-2000. Since the National Climate Assessment (Melillo et al. 2014) and the Climate Science Special Report (USGCRP 2017) do not directly assess the increase in nighttime temperatures, but instead focus on "hot nights", there is some uncertainty for this stressor. Beyond the general gradient of number of "hot nights" (Figure 2-5), local effects could also play a significant role. First, the urban heat island effect will be more pronounced in the Northeast region than some other regions of the country (e.g. the Northern Great Plains) due to the densely populated and urbanized "Bos-Wash" corridor through southern New England, southern New York, New Jersey, eastern Pennsylvania, Maryland, Delaware, and ending in the Washington, D.C. metropolitan area. These "hot nights" and thus, increased minimum nighttime temperatures are more likely in urban areas (Melillo et al. 2014, p.377).

None of the recent climate assessments (Karl et al. 2009, Melillo et al. 2014, and USGCRP 2017) have documented any changes to diurnal temperature range in the Northeast region. A search of literature on climate change and diurnal temperature range seems to focus on effects to agriculture and does not discuss exact magnitude of change for this region. However, if minimum temperatures continue to rise more than maximum temperatures, it is expected the daily temperature range will constrict.

2.1.2 Precipitation

According to the Climate Science Special Report (USGCRP 2017, p.208-209), average annual precipitation across the United States rose by approximately 4% from 1901 to 2015. This increase, however, was not evenly distributed across the country. Locations in the Northeast generally showed a slight increase in accumulation, but the region as a whole did not show a statistically significant trend. Within the region, increases were not as significant around New York City. Most of Pennsylvania (especially central) and West Virginia had more similarities in precipitation with the Southeast region, rather than the Northeast (USGCRP 2017, p. 209; Figure 2-6).

Future projections show an increase in annual precipitation (accumulation) for the Northeast United States. The magnitude varies by location, with northern locations in the region expecting higher precipitation throughout the year, with minimal increases expected for West Virginia and parts of Maryland by the late century (2071-2100) (USGCRP 2017 p.217 and Melillo et al. 2014 p. 35). Confidence is high that annual precipitation will increase—extending back to the 2nd National Climate Assessment (Karl et al. 2009); however, even by the late period there is some uncertainty on how much of an increase will occur in particular locations.

Local effects will be extremely important in this region and may not be adequately resolved in climate models. An example can be seen with tropical cyclones, which can cause large interannual variability in precipitation accumulation. The frequency of tropical cyclones (and if they make landfall) will likely be important for precipitation trends in the region. In addition, terrain can affect precipitation in the region. Effects of terrain will vary by location and will affect year-to-year variability, especially in the Appalachian Mountains.

With uncertainty in the frequency of tropical cyclone impacts on the region and the lack of the spatial ability to see the effects of the complex terrain in the Appalachian Mountains, there could be locations that experience no increase or a slight decrease in annual precipitation, especially in the short term following a lower emissions scenario, which is omitted from inclusion in the 2nd and 3rd National Climate Assessments (Karl et al. 2009 and Melillo et al. 2014) and the Climate Science Special Report (USGCRP 2017). The confidence in change is low, but scenarios and models both show that the region should experience slightly more accumulation through time.

In the Northeast region, there has been a 55% increase in the amount of rain falling during the top 1% of non-zero rainfall events from 1958-2016. There has also been a 27% increase in the five-year maximum precipitation from 1901-2016 (USGCRP 2017, p. 212). The increase in both parameters are the highest of all regions in the Climate Science Special Report for the Continental United States. Model projections are confident that the amount of rain falling during intense events will increase, regardless of scenarios. Both scenarios project an increase of 10% and 13% from present-day in the twenty-year return period amount by mid-century (the 20-yr return period is the precipitation amount that on average would occur once every 20 years). By the late century, the models diverge, with the higher emissions scenario showing a 22% increase and the lower emissions scenario a 14% increase from present-day. These projections indicate a "more extreme precipitation climate" (USGCRP 2017 p. 220). While localized factors may reduce or mitigate the projected increases in intensity, averaged as a whole, the region is very likely to experience an increase in precipitation intensity.

Models suggest the number of days with precipitation amounts greater than the 95th percentile of non-zero precipitation days will increase by ≥ 25%, while days in lower percentiles (10-80th) decrease across the country (USGCRP 2017 p. 220). For the Northeast, both high and low emission scenarios show slight increases in heavy precipitation days by 2050 and 2070, but diverge at end of the 21st century, with higher emissions scenarios showing more heavy rainfall days; however, there is large variability in the model.

The slight increases by mid-century are effectively no larger than the statistical variation in the data. This lack of confidence in change in the short term, coupled with the diverging outcomes in the late century runs, yields a lower overall likelihood/confidence. It is important to note that models tend to have difficulty with precipitation and projecting precipitation days, explaining the high deviation at longer durations. Terrain induced rainfall in Appalachia and coastal storms generated by sea breezes along the Atlantic could lead to locally higher numbers of days with heavy rainfall; however, climate model data do not have the appropriate resolution to show smaller scale interactions.

Precipitation changed in the Northeast seasonally, comparing the present-day average (1986-2015) to the historical average (1901-1960). During winter (DJF), central New England and eastern Massachusetts were wetter than other sectors of the region, which either had a very small increase in precipitation or a decrease in precipitation. In spring (MAM), western Pennsylvania got notably drier. During summer (JJA) precipitation showed an increasing trend in the northern part of the region, while precipitation decreased further south. The trend during fall (SON) showed increased precipitation for the whole region (USGCRP 2017 p.209).

According to the 3rd National Climate Assessment (Melillo et al. 2014) precipitation is expected to increase by mid-century (2041-2070) compared to the last three decades of the 20th century. The most pronounced increase is anticipated in winter and spring, particularly in the higher emission scenarios. By the late century (2070-2099), under higher emissions scenarios, winters and springs are expected to increase by ~20% or more compared to the 1976-2005 average. In general, summer and fall are expected to have a slightly higher amount of precipitation, but not nearly the magnitude as winter and spring (USGCRP 2017 p.217).

In the observational record, portions of West Virginia and Appalachia showed decreased precipitation in spring, summer, and winter and an increase in precipitation during fall (USGCRP 2017 p.209). Therefore, the models may not be resolving the complex terrain, despite the models projecting West Virginia and Appalachia to act similar to the rest of the region. Greater increases in precipitation are favored during winter further north in the region (USGCRP 2017 p.217 and Melillo et al. 2014). In addition, tropical cyclone activity may affect precipitation totals in summer and fall and may not be adequately initialized in the models. Additionally, lake effect precipitation in western Pennsylvania and New York, may also not be resolved by models due to localized effects of lake effect precipitation.

2.1.3 Other Stressors

The Northeast region has and still is at risk for flooding and high water levels. The region is vulnerable to tropical cyclones and storm surge, which will likely be exacerbated by rising seas (sea-level has risen in the region by roughly 1-2 ft. on average) (Melillo et al. 2014 p. 370-375). Inland regions are also prone to flooding, especially river valleys with complex terrain where

more intense precipitation events are likely to occur, thus leading to an increased flood risk for the region (Melillo et al. 2014 p. 370-375). Spatially, floods have generally increased in magnitude in the Hudson River valley and northern New Jersey, while regions of Pennsylvania have seen a decrease. Floods of varying magnitudes were observed across the rest of the region (Melillo et al. 2014 p.40). In the future, sea-level rise is expected to increase nationally, especially in the Northeast region (Melillo et al. 2014 p. 374). In addition, higher rainfall intensities are expected, leading to an increased potential for flooding. While local variability is large, generally, the entire region as a whole is expected to have more frequent flooding events.

The 3rd National Climate Assessment revealed that drought risk is expected to increase in the Northeast region, particularly in summer and fall, as a result of decreased snowmelt and higher temperatures causing increased plant transpiration (Melillo et al. 2014 p. 374). Model output described by Sun et al. (2015) showed that in high emissions scenarios by mid-century, the Northeast region's longest dry spells will increase by a few days compared to the 1981-2000 average. This implies that droughts may become more prevalent during these dry spells or more importantly, as population expands and the demand for water increases, there may not be enough water to meet demand. This projection makes sense in the context of the other rainfall stressors that imply extreme rainfall events will increase in frequency, but possibly not much of an increase in annual precipitation.

Humans are the main cause of wildfire events in the northeastern United States. In the decade from 1999 to 2009, wildfires were frequent during spring (April and May) and generally occurred in more rural areas, such as central and western Massachusetts and central and northeastern Pennsylvania. Although it should be noted that developed regions (suburban Boston and New York City) also had (minimal) wildfires during this decade (Pollina et al. 2013).

According to Pollina et al. (2013), wildfires are prevalent in the region during dry conditions and atmospheric subsidence (sinking air), the latter common during mild, dry spring days. The synoptic (large-scale) patterns that promote wildfires in the region involve the migration of high-pressure systems and mid-latitude cyclones – all projected to be modified in a changing climate. Wildfires were also found to occur when the relative humidity anomaly was 10-25% below normal. Due to relative infrequency and the lack of more recent research on the effects of climate change on wildfires, and the large human component to wildfire causation, there is low confidence in projecting the change in wildfire frequency in the next century. Wildfires are almost certain to occur but determining changes in frequency has proven to be difficult. There is also somewhat low confidence in changes to the fire season length. Results indicate no significant changes in the number of days with fire or the window of time in which wildfires occur in the region.

The Climate Science Special Report (USGCRP 2017 p.217) suggested an increase in precipitation during winter under the higher emission scenarios by the late century in the Northeast region. Along with the increasing frequency of extreme storms nationally in recent decades, it is probable that this trend will continue in the region. This could be countered by the suggestion (found in the Second National Climate Assessment) that more winter precipitation may fall as rain rather than snow by late century, especially in higher emissions scenarios (Karl et al. 2009). Some studies show that icing events may become more prevalent, as the temperatures warm and transition from snow to rain, but uncertainty is high.

This discussion does not apply to winter storms at higher elevations, such as Mount Washington. Winter storms may become less frequent in southern sections of the region, and thus their intensity may be limited. Locations adjacent to Lakes Erie and Ontario may be subjected to intense lake effect snow, which (due to inadequate spatial resolution) cannot be resolved by climate models. According to Kunkel et al. (2013), observations have not shown meaningful trends in high or low snowfall in the last century. Although Northeast region winter precipitation is expected to increase (USGCRP 2017 p.217) by the late century under some climate change scenarios, the second National Climate Assessment details that this precipitation is likely to be rain, rather than snow. This is especially true for southern sections of the region, where an increase in temperatures would eliminate many days where snow could occur (Karl et al. 2009 p.107, USGCRP 2017 p.196).

It is possible that increases in snowfall totals could be limited due to warming temperatures, despite increased winter precipitation. In the short-term or in lower emissions scenarios, which have less warming than higher emissions scenarios, winter precipitation could increase, but there is no continuity to the last century, making it difficult to determine. Therefore, as a result of possible differences in the near and short-term and its dependence on the exact magnitude of warming, there is very high uncertainty in this climate stressor.

2.2 Tables and Figures: Northeast Region

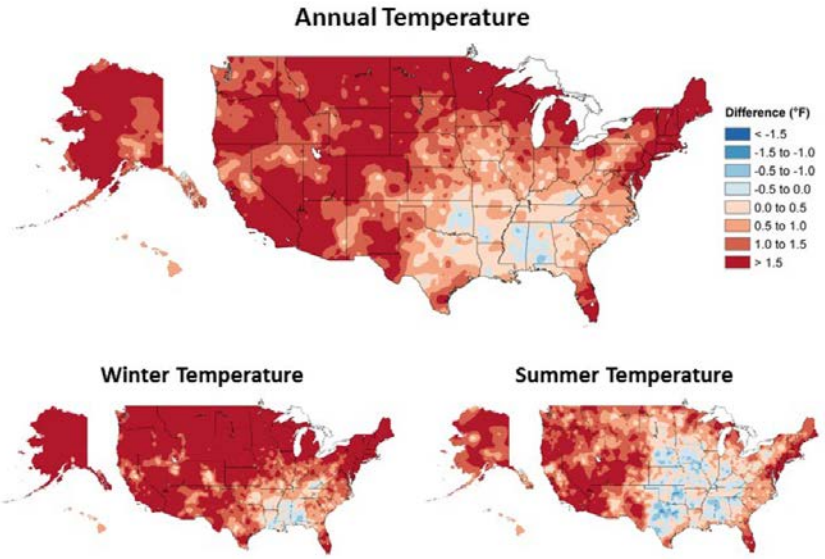

Figure 2-1. Observed changes in annual, winter, and summer temperature (°F) between present-day (1986–2016) averages and 1901–1960 (continental United States)/1925–1960 (Alaska & Hawai'i) averages. Estimates are derived from the nClimDiv dataset. Figure and caption adapted from USGCRP 2017 p. 188.

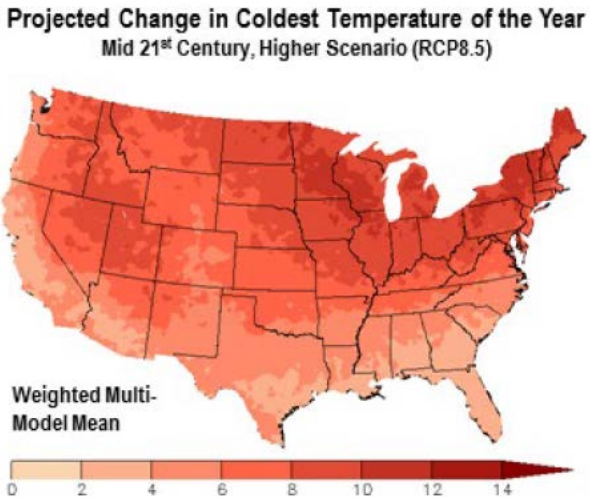

Figure 2-2. Projected changes in the higher emissions scenarios in the coldest daily temperatures (°F) of the year in the lower forty-eight between the mid-century (2036–2065) average and the average for near-present (1976–2005). Increases are statistically significant in all. Figure and caption adapted from USGCRP 2017 p. 198.

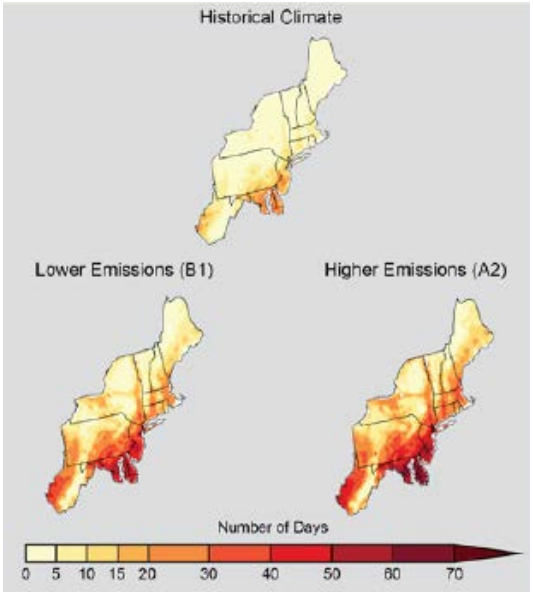

Figure 2-3. Map showing annual projected increases in the number of days over 90°F by mid-century (2041-2070) compared to 1971-2000 averages under both lower and higher emissions scenarios. (Figure source: Melillo et al. 2014 p. 374).

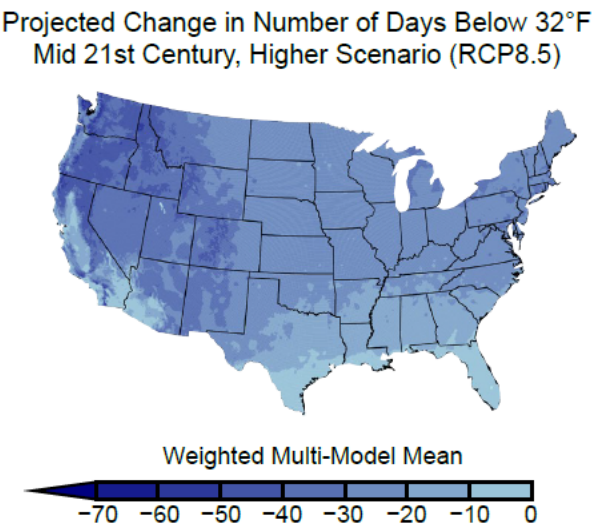

Figure 2-4. Projected changes under higher emissions scenarios in the number of days per year with a minimum temperature under 32°F in the lower forty-eight between the mid-century (2036–2065) average and the near-present (1976–2005) averages. Changes are statistically significant in all areas. Map and caption adapted from USGCRP 2017 p.199.

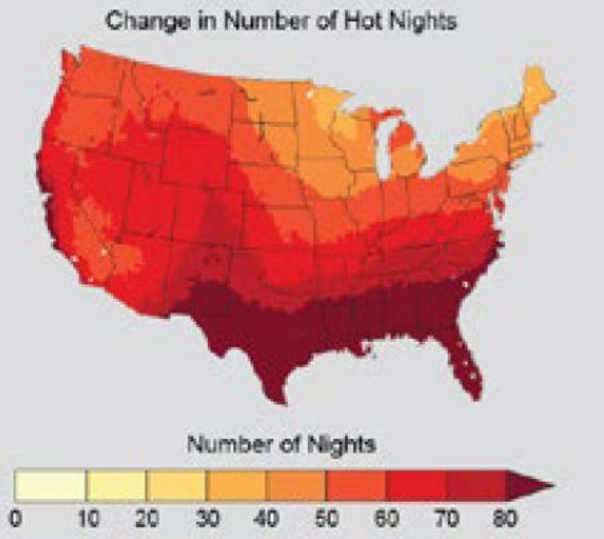

Figure 2-5. Map showing the change in number of hot nights by the end of the century (2070-2099) compared to 1971-2000 under high emissions scenarios. Map and caption adapted from Melillo et al. 2014 p.155.

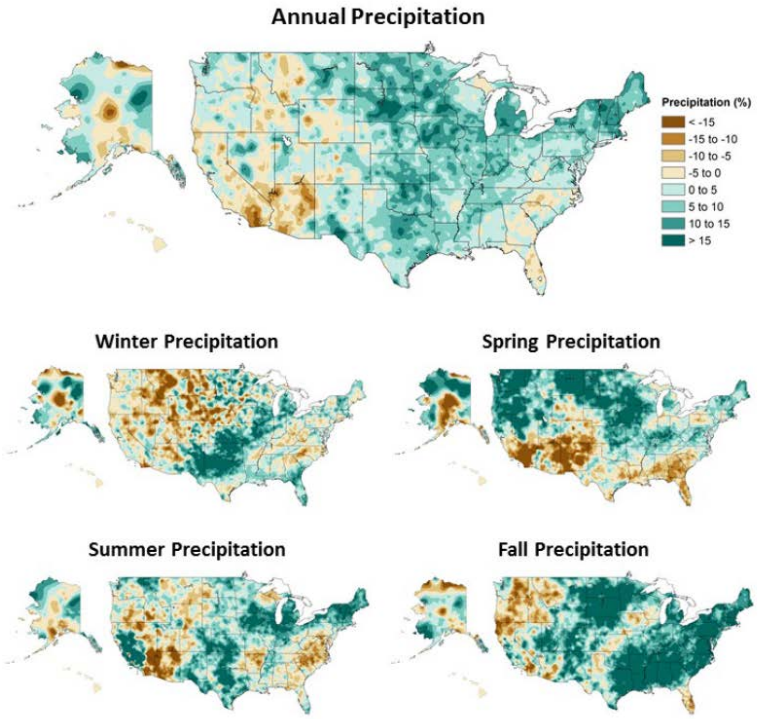

Figure 2-6. Annual and seasonal changes in precipitation over the United States. Changes are the average for present-day (1986–2015) minus the average for the first half of the last century (1901–1960 for the contiguous United States, 1925–1960 for Alaska and Hawai'i) divided by the average for the first half of the century. Maps and caption adapted from USGCRP 2017 p. 209.

3 Southeast Region

3.1 A Summary of Climate Projections for the Southeast Region

3.1.1 Temperature

While the Southeast experienced the lowest increase in average annual temperatures compared to other regions (Figure 3-1), projections indicate annual average temperatures will continue to increase in the coming decades under both emissions scenarios. There is a low probability annual average temperatures decrease across the region; however, sub-regional variability, especially at the local level, is evident. Mountainous areas, especially on the leeward side, may exhibit different changes in average annual temperatures.

The Southeast is not expected to have an increase in the magnitude of the hottest annual temperatures. Historically, the Southeast has had the 2nd largest decrease in the average hottest annual temperatures behind only the Midwest region (Figure 3-2). The decreasing trend in annual high temperatures is spatially consistent across the Southeastern region with only small increases near coastal Georgia. While the region is projected to warm, observational data leads most models to continue to forecast a decrease in the magnitude of the hottest annual temperatures. Basically, the hottest days of the year will not become hotter; however, the number of days with temperatures above 90°F is expected to rise (Figure 3-3), similar to what has been observed.

According to the Climate Science Special Report, the Southeast is projected to experience the greatest increase in frequency of days above 90°F in the contiguous United States. Under the higher emissions scenario (RCP8.5), roughly 70 more days annually are expected to reach temperatures over 90°F by the 2036-2065 period (Figure 3-3). As annual average temperatures rise, the number of days above 90°F will also rise, but this does not largely affect the "hottest annual temperatures." Florida is projected to see the largest increase in days above 90°F (>70 days) and the Appalachians are expected to see the lowest increase (10-20 days). However, despite variability, confidence is high that the number of days above 90°F will increase across the region.

As average annual temperatures increase across the region, the number of days with freezing temperatures is expected to broadly decrease. High elevation areas may not experience this decrease, but most of the region will. The Southeast will see a decrease in days below 32°F by 0-40 days depending on location (Figure 3-3).

Historically the number of nights with a low temperature of ≥ 75°F has increased across the Southeast, which has caused a decrease in the daily temperature range. The daily temperature range has already decreased broadly across the region and it is projected to decrease further, mainly due to rising minimum daily temperatures. Alabama and Mississippi have shown cooling trends over the last ~100 years so confidence in warming of overnight temperatures is less; however, models are in agreement that overnight temperatures will continue to increase across the region, continuing to constrict the daily temperature range.

3.1.2 Precipitation

Annual precipitation has slightly decreased in the Southeast over the past 100 years, driven by slightly drier springs and summers that are not balanced out by the substantially wetter fall season (Figure 3-4). Winter accumulations have remained stable over the past 100 years. Seasonal projections show high variability in accumulation. Differences in seasonal accumulation are expected in the region because of large observed variances. Fall precipitation has increased >15% over most of the region and spring precipitation amounts have decreased by about 10% (Figure 3-5). Winter is projected to become slightly wetter along with spring for a majority of the region excluding Louisiana. Summer is broadly projected to be drier and fall slightly wetter (Figure 3-5); however, annual accumulation is not expected to change significantly because of increases and decreases in seasonal precipitation.

Observations across the region have shown an increase in the 99th percentile of daily precipitation from 1958-2016, an increase in the frequency of 2-day events that have a precipitation total exceeding the largest 2-day amount that is expected to occur on average once every 5 years for both 1901-2016 and 1958-2016 (Figure 3-6). Fall has also observed a steady increase in daily 20-year return period precipitation (Figure 3-7). Models project heavy precipitation events will continue into the future. Under all scenarios, the frequency of extreme events that exceed a five-year return period are projected to increase (Figure 3-8).

Research has demonstrated that as temperatures rise, the amount of moisture the atmosphere can hold increases, resulting in more moisture available for storms (moisture convergence). The projected change in the 20-year return period amount for daily precipitation is expected to increase by roughly 10% by mid-century under both low and high emissions scenarios, while the late-century is projected to increase by between 13% (lower emissions scenario) and 21% (higher emissions scenario) (Figure 3-9). However, models that project precipitation changes, especially heavy and extreme precipitation changes, are limited, mainly due to difficulty quantifying how thunderstorms, tropical systems, and other types of events that cause heavy and extreme precipitation will change. Nonetheless, as temperatures rise, it is expected that more moisture will be available for storms, causing more frequent extreme events. High elevation areas near eastern Tennessee, southwestern North Carolina, and northern Georgia have different precipitation regimes (orthographic rainfall) that may not drastically change under future scenarios.

Much of the coastal region is susceptible to extreme precipitation from tropical cyclones. Average tropical rainfall rates within 300 miles of the tropical storm center are projected to increase by 8-17% due to the projected increase of water vapor in the atmosphere. Events like Hurricane Harvey give credit to these projections, and as such, heavy and extreme precipitation events induced by tropical cyclones are projected to become slightly heavier.

3.1.3 Other Stressors

As the average temperature around the globe increases, mean sea-level will rise (thermal expansion) placing coastal communities at risk to inundation and even more susceptible to storm surge. Tidal flooding (or nuisance flooding) across the region has broadly increased. An increase in intensity and frequency of heavy precipitation events will increase flash flooding and river flooding risks throughout the entire Southeast. The conversion of natural landscapes to impervious surfaces is increasing rainfall-induced flooding. Storm surge and sea-level rise is a

significant risk across the entire coastline. The Louisiana coast is particularly at risk due to the erosion of the coastal wetlands. As erosion progresses, the state will become more susceptible to storm surge events.

Drought is an issue in the Southeast, but there is a lack of evidence to indicate if drought frequency or intensity will change in the region. Previous droughts have occurred in Georgia but have caused agricultural issues in the Carolinas and Florida. Wildfires occur across the region and historical trends indicate increased frequency through time and models indicate the length of wildfire season will increase due to warmer temperatures. If spring and summer continue the drying trend as indicated in an earlier stressor, the wildfire season could potentially be longer.

The northern sector of the region is more susceptible to changes in snowfall totals, as states such as Virginia and Kentucky receive more snowfall annually. Southern states will likely experience less frequent snowfall events, decreasing overall snowfall totals. This change is mostly driven by projected changes in winter temperatures.

3.2 Tables and Figures: Southeast Region

Table 3-1. Observed changes in annual average temperature (°F) for each National Climate Assessment region. Changes are the difference between the average for present-day (1986–2016) and the average for the first half of the last century (1901–1960 for the contiguous United States, 1925–1960 for Alaska, Hawai'i, and the Caribbean). (Source: USGCRP 2017 p. 190).

NCA Region	Change in Coldest Day of the Year	Change in Warmest Day of the Year
Northeast	2.83°F	−0.92°F
Southeast	1.13°F	−1.49°F
Midwest	2.93°F	−2.22°F
Great Plains North	4.40°F	−1.08°F
Great Plains South	3.25°F	−1.07°F
Southwest	3.99°F	0.50°F
Northwest	4.78°F	−0.17°F

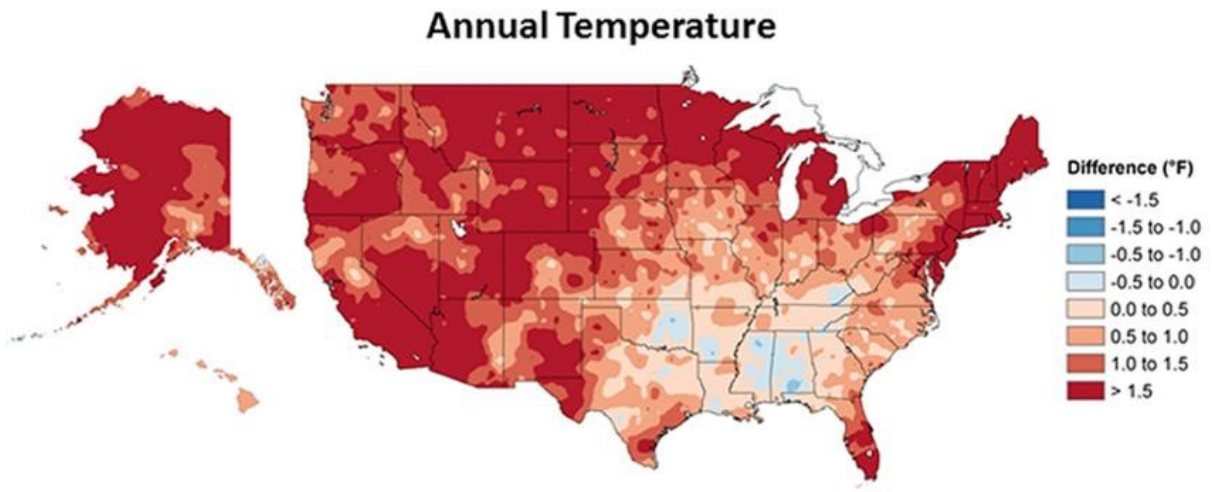

Figure 3-1. Observed changes in annual temperature (°F). Changes are the difference between the average for present-day (1986–2016) and the average for the first half of the last century (1901–1960 for the contiguous United States (Figure source: USGCRP 2017 p. 188).

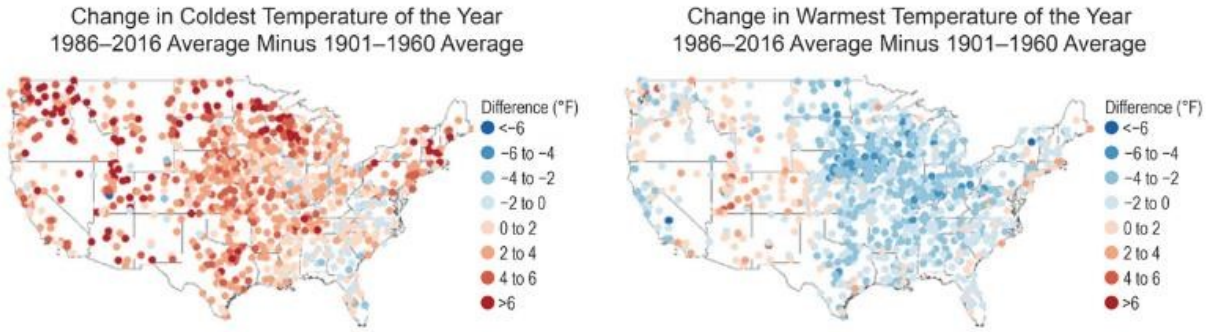

Figure 3-2. Observed changes in the coldest and warmest daily temperatures (°F) of the year in the contiguous United States. Maps depict changes at stations; changes are the difference between the average for present-day (1986–2016) and the average for the first half of the last century (1901–1960) (Figure source: USGCRP 2017 p. 190).

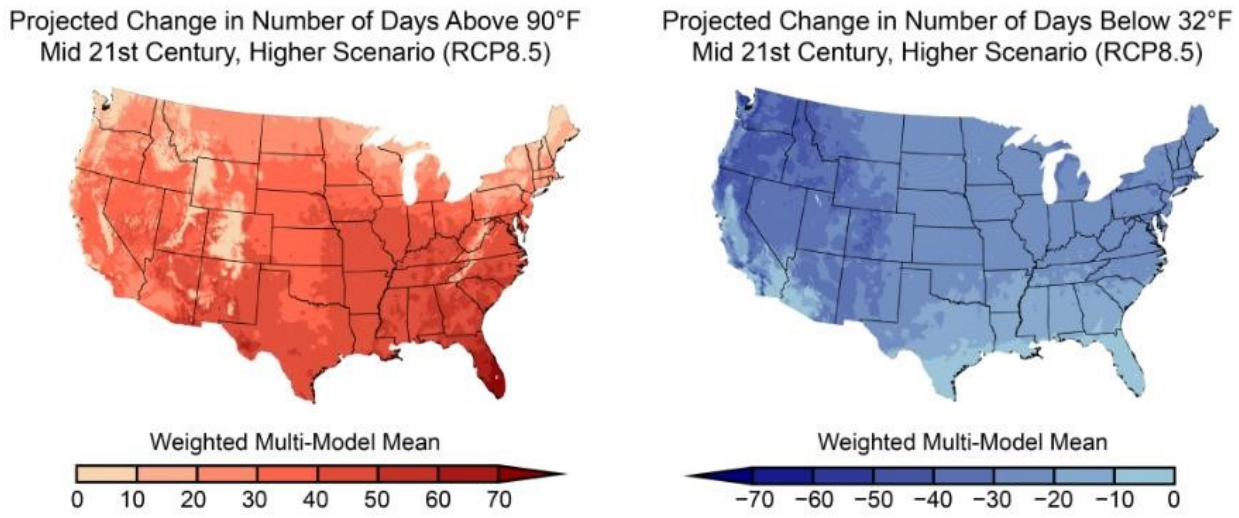

Figure 3-3. Projected changes in the number of days per year with a maximum temperature above 90°F and a minimum temperature below 32°F in the contiguous United States. Changes are the difference between the average for mid-century (2036–2065) and the average for near-present (1976–2005) under the higher scenario (RCP8.5) (Figure source: USGCRP 2017 p. 199).

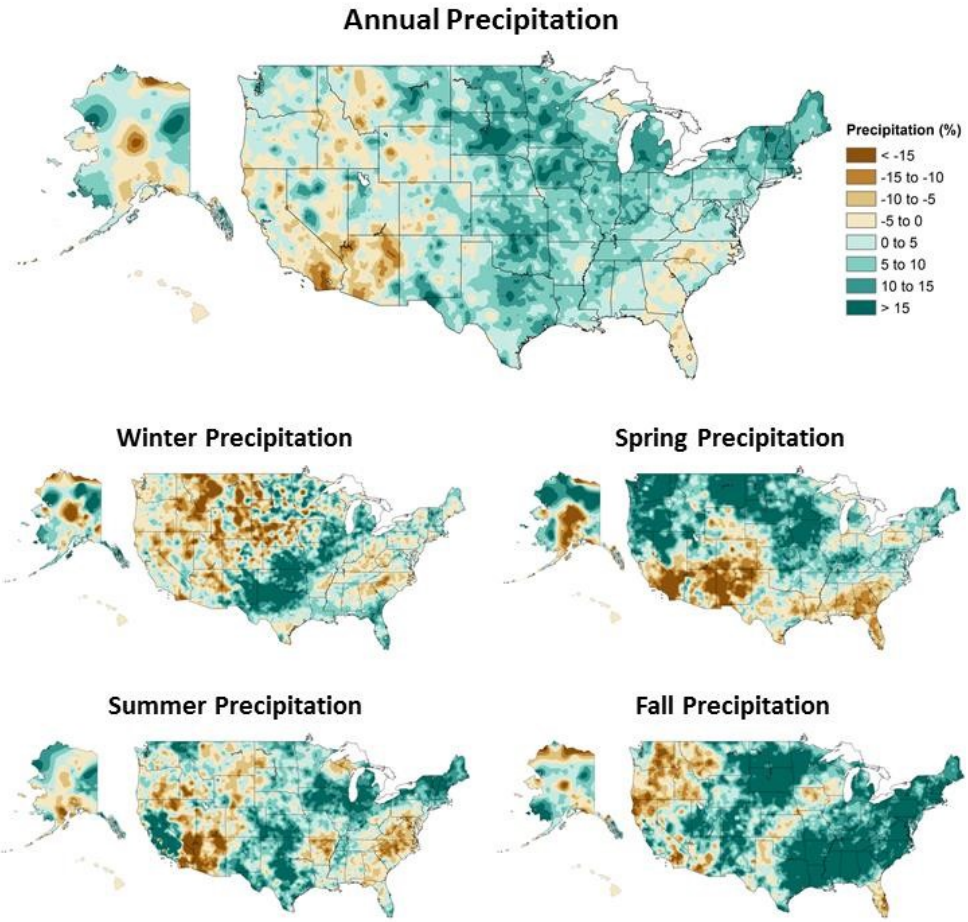

Figure 3-4. Annual and seasonal changes in precipitation over the United States. Changes are the average for present-day (1986–2015) minus the average for the first half of the last century (1901–1960 for the contiguous United States (Figure source: USGCRP 2017 p. 209).

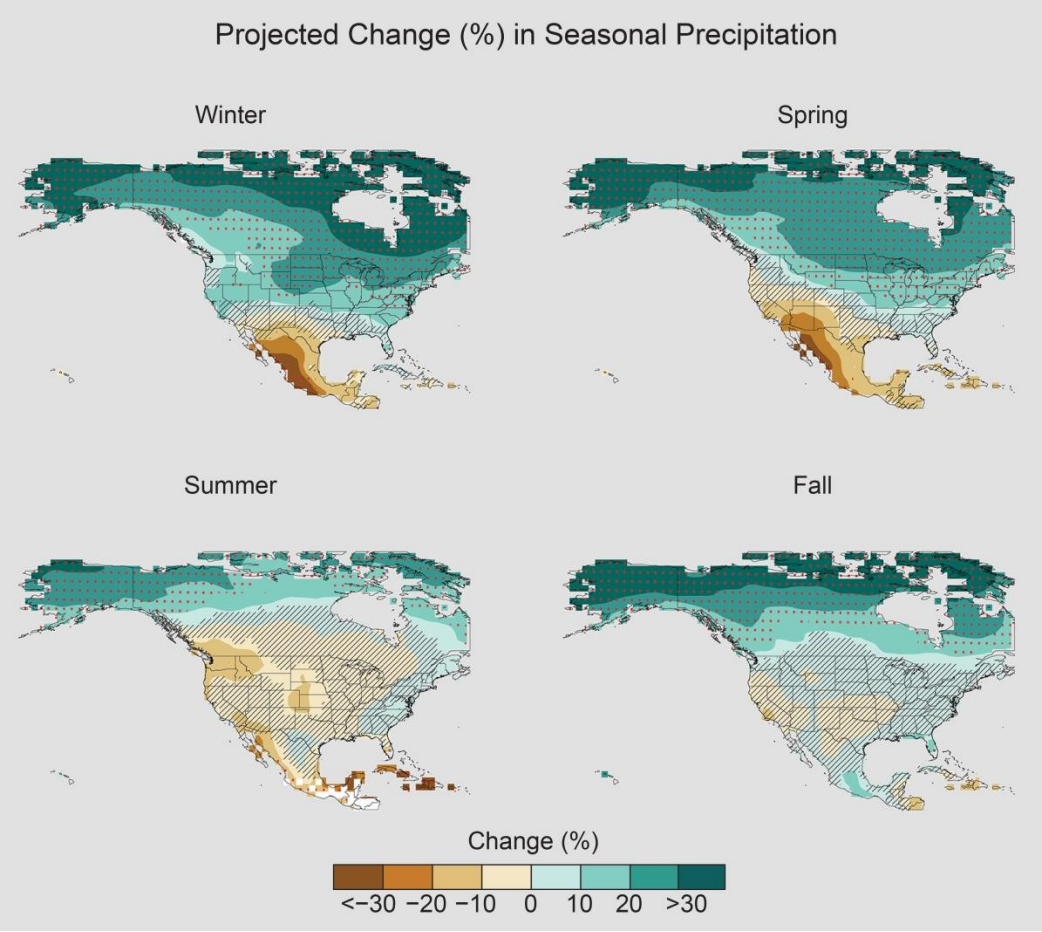

Figure 3-5. Projected change (%) in total seasonal precipitation from CMIP5 simulations for 2070–2099. The values are weighted multimodel means and expressed as the percent change relative to the 1976–2005 average. These are results for the higher scenario (RCP8.5). Stippling indicates that changes are assessed to be large compared to natural variations. Hatching indicates that changes are assessed to be small compared to natural variations. Blank regions (if any) are where projections are assessed to be inconclusive (Figure source: USGCRP 2017 p. 217).

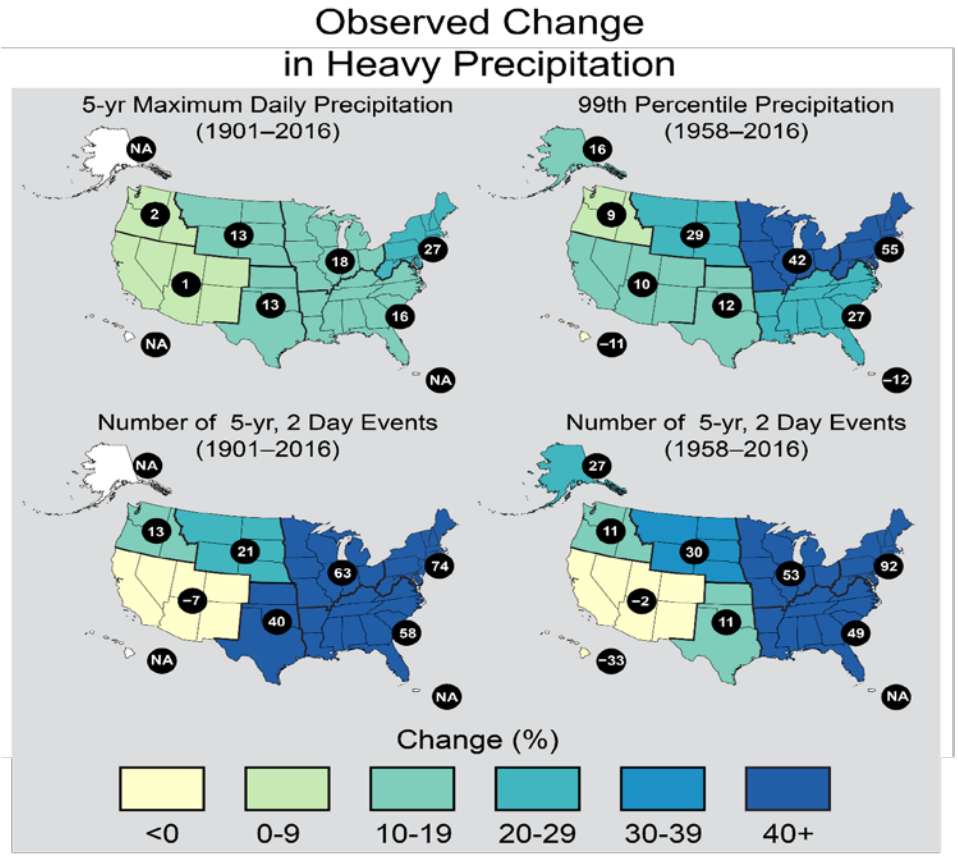

Figure 3-6. These maps show the change in several metrics of extreme precipitation by NCA4 region, including (upper left) the maximum daily precipitation in consecutive 5-year blocks, (upper right) the amount of precipitation falling in daily events that exceed the 99th percentile of all non-zero precipitation days, (lower left) the number of 2-day events with a precipitation total exceeding the largest 2-day amount that is expected to occur, on average, only once every 5 years, as calculated over 1901–2016, and (lower right) the number of 2-day events with a precipitation total exceeding the largest 2-day amount that is expected to occur, on average, only once every 5 years, as calculated over 1958–2016. The numerical value is the percent change over the entire period, either 1901–2016 or 1958–2016. The percentages are first calculated for individual stations, then averaged over 2° latitude by 2° longitude grid boxes, and finally averaged over each NCA4 region (Figure source: USGCRP 2017 p. 212).

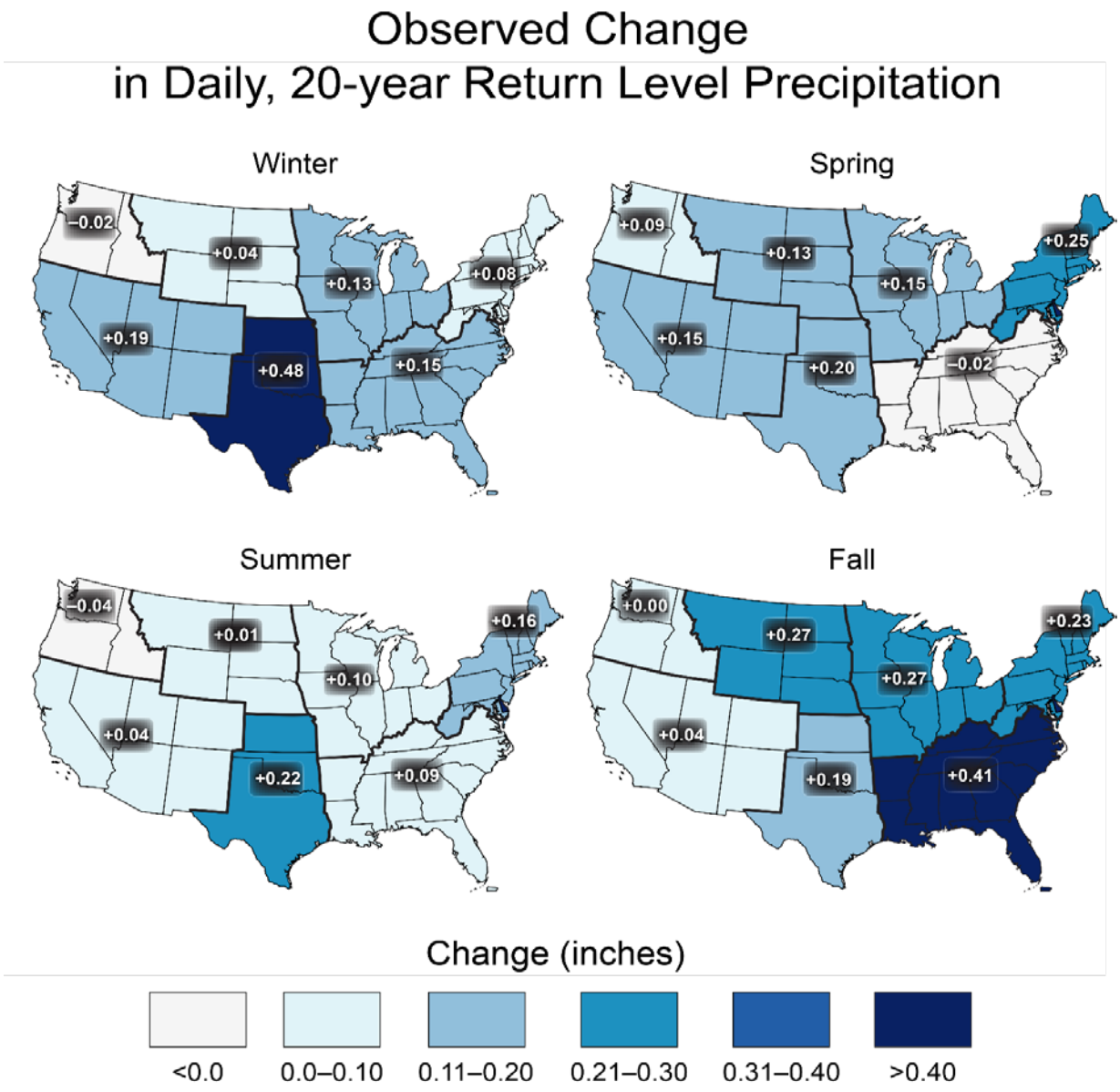

Figure 3-7. Observed changes in the 20-year return value of the seasonal daily precipitation totals for the contiguous United States over the period 1948 to 2015 using data from the Global Historical Climatology Network (GHCN) dataset (Figure source: USGCRP 2017 p. 211).

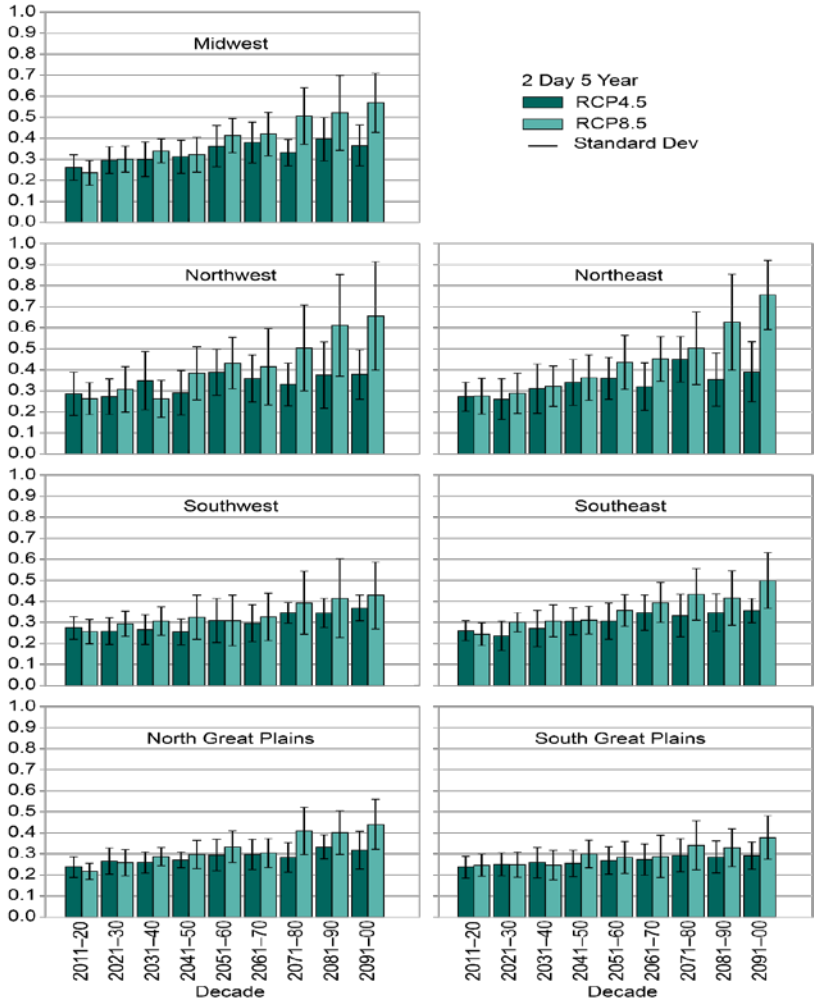

Figure 3-8. Regional extreme precipitation event frequency for a lower scenario (RCP4.5) (green; 16 CMIP5 models) and the higher scenario (RCP8.5) (blue; 14 CMIP5 models) for a 2-day duration and 5-year return. Calculated for 2006–2100 but decadal anomalies begin in 2011. Error bars are ±1 standard deviation; standard deviation is calculated from the 14 or 16 model values that represent the aggregated average over the regions, over the decades, and over the ensemble members of each model. The average frequency for the historical reference period is 0.2 by definition and the values in this graph should be interpreted with respect to a comparison with this historical average value (Figure source: USGCRP 2017 p. 219).

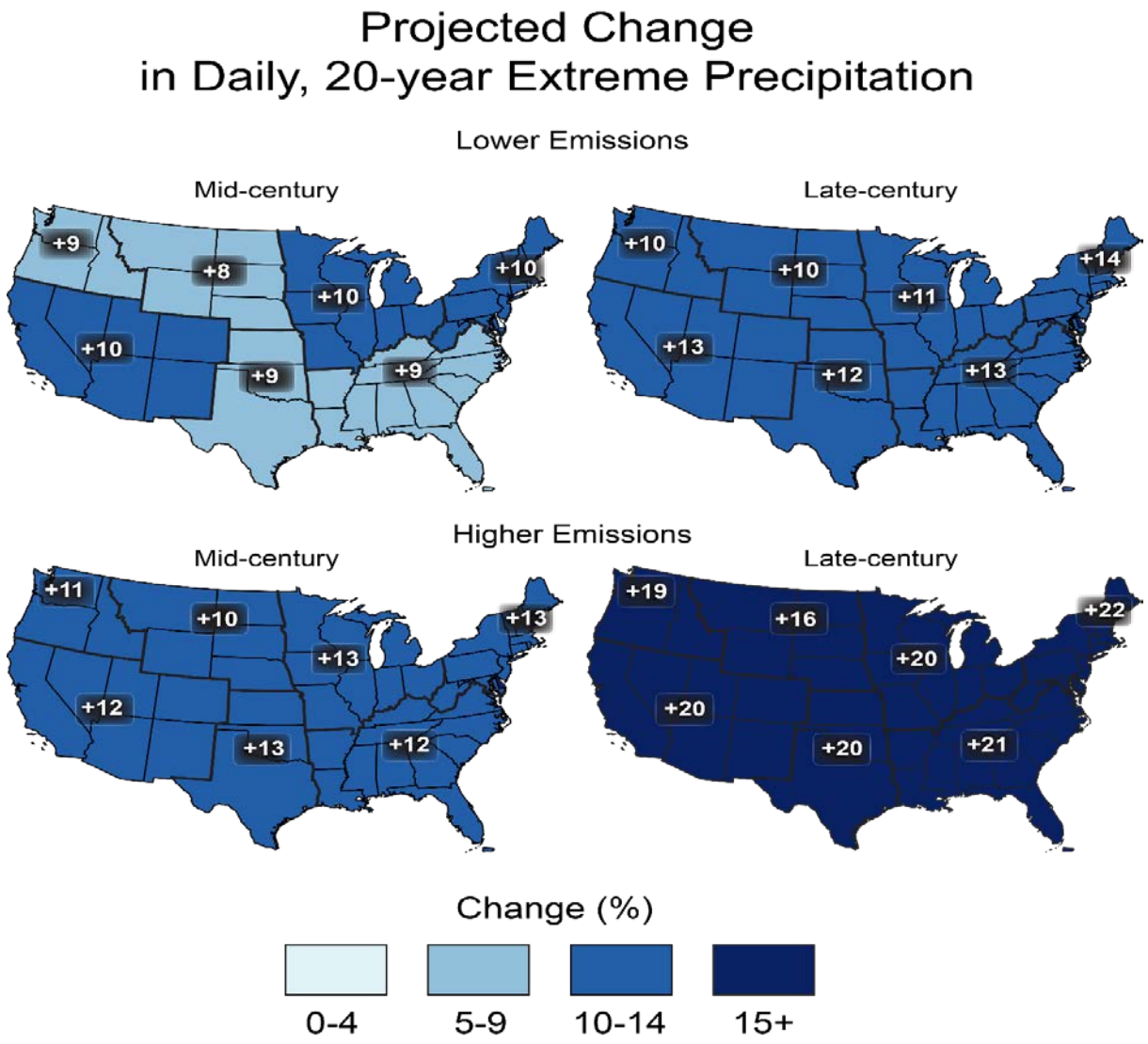

Figure 3-9. Projected change in the 20-year return period amount for daily precipitation for mid- (left maps) and late-21st century (right maps). Results are shown for a lower scenario (top maps; RCP4.5) and for a higher scenario (bottom maps, RCP8.5). These results are calculated from the LOCA downscaled data (Figure source: USGCRP 2017 p. 220).

4 Midwest Region

4.1 Summary of Climate Projections for the Midwest Region

4.1.1 Temperature

The Midwest region experienced slight increases in annual temperature (1.26°F), with more warming (>1.5°F) found in northern Minnesota, Wisconsin, and Michigan, and less warming across Iowa, Missouri, and the Ohio River valley. This is found by comparing present-day average temperature (1986-2016) against the 1901-1960 average. In general, the warming has been more notable during winter (DJF) compared to summer (JJA), with large sections of the region showing no change or slight cooling during summer (USGCRP 2017, p. 188, Figure 4-1).

Warming is expected by mid-century under both lower and higher emission scenarios; both show an increase of 4-8°F from present-day by 2065, with an average of 4.21°F over the region. The models diverge by the late century (2070-2099) with the lower emissions scenario only showing an overall increase of 5.57°F from present day, while the higher emissions scenario shows an increase of 9.49°F (USGCRP 2017, p.195-196). Warming is expected to be more significant further north in the region, particularly in northern Minnesota, Wisconsin, and the Upper Peninsula of Michigan. The effect is noticeable by mid-century under lower emissions scenarios. While the models do not have the spatial resolution to describe regional or localized factors, proximity to the Great Lakes will impact the magnitude of warming in regions adjacent to Lakes Michigan, Superior, Huron, and Erie.

Temperatures are unlikely to decrease in the region over the next century, as model output for different emissions scenarios shows warming across the entire region. The models diverge in the magnitude of the warming in later periods, but neither model shows a cooling effect in the region (USGCRP 2017, p.195-196). While cooling is not expected for the Midwest region, the magnitude of increase could be dampened for river valleys, such as the Ohio River valley. However, it is unlikely that the region will experience a decrease in annual temperatures.

Observed data show a decrease in the hottest annual temperatures for many locations across the Midwest. The most pronounced decreases are seen in rural areas away from the Great Lakes. Models expect a statistically significant increase in the hottest annual temperature by mid-century. Specifically, an increase of roughly 6.71°F is expected under high emissions scenarios (USGCRP 2017, p.197-198), while lower emissions scenarios have the hottest annual temperatures warming closer to 3-4°F (Melillo et al. 2014, p. 39). Since the observed data show that the hottest annual temperatures have decreased, confidence is lower that the hottest annual temperatures will increase by 2050 than by 2100; however, models seem to be congruent and tend to show broad increases.

In terms of the lowest annual temperatures, the largest increases are expected to be contained in the northern half of the United States, including the Midwest (USGCRP 2017, p.197-198; Figure 4-2). This continues the trend of warmer lowest annual temperatures that has been observed nationally and in most of the Midwest. The few exceptions are scattered throughout the region in both urban and rural areas (USGCRP 2019, p.190). On average, the change from the near-present (1976-2005) to the mid-century (2036-2065) is expected to be about 9.44 °F under

high emissions scenarios, and could be over 15°F by the end of the century (USGCRP 2017 p.198 and Melillo et al. 2014 p. 39, Figure 4-2). Lower emissions scenarios yield less warming, with an increase of only 6-10°F across most of the region by the end of the century. Despite this divergence, the region shows a uniform increase in the lowest annual temperatures. The lowest annual temperatures are not expected to decrease or even stay relatively similar. Due to terrain effects, the magnitude of warming in the lowest annual temperature in the Ohio and Mississippi River valleys might be lower. A similar phenomenon may be found adjacent to the Great Lakes. Urban locations, such as Cincinnati, St. Louis, and Minneapolis/St. Paul may also see a greater magnitude of warming than nearby rural areas due to the urban heat island effect.

Under the most extreme scenarios, the Midwest region has a wide variability in the increase in the frequency of days at or over 90°F by mid-century, when compared to 1976-2005 averages. The most pronounced increase in 90°F days are expected, in these higher emission scenarios, in Missouri, Illinois, and Indiana, with anywhere from 50-70 more days over 90°F. Conversely, the Upper Peninsula of Michigan, northern Minnesota, and northern Wisconsin are expected to add fewer days, ~10-30. The remainder of the region, in general, could see 30-50 more days over 90°F (USGCRP 2017 p. 199). The 3rd National Climate Assessment (Melillo et al. 2014) also provides information about days over 95°F for this region in lower emissions scenarios (Figure 4-3). Most of Missouri, as well as southern Illinois, and southwestern Indiana (Evansville) could see 20 more days over 95°F by mid-century compared to 1971-2000 averages. This increase decreases northward in the region, with an increase of ≤ 5 days for the Upper Peninsula of Michigan, northern Wisconsin, and northern Minnesota. It is possible, due to variability and uncertainty in models, parts of the Midwest could see no meaningful increase in the frequency of days over 90°F. While it is unlikely, model outputs, especially under reduced emissions scenarios (Figure 4-3), show a limited change in the frequency of days over 90°. The level of uncertainty described in the prior stressor is again shown here.

It is implied that as average temperatures increase, the number of days with freezing temperatures will decrease. In higher emissions scenarios, most of the Midwest is expected to have 30-50 fewer days with freezing temperatures by mid-century compared to present-day averages (1976-2005) (Figure 4-4). Therefore, while the higher emissions and related scenarios are the "worst-case", even lower emissions scenarios yield a decrease in days with freezing temperatures. It is unlikely days with freezing temperatures will increase.

Warmer overnight temperatures are expected in urbanized areas due to the urban heat island effect, which is very consequential in the highly developed and densely populated regions of the Midwest, such as Chicagoland and the Auto Belt (southern Michigan and northern Ohio). According to the Climate Science Special Report (USGCRP 2017 p. 277), the urban heat island effect can lead to overnight temperatures 1.5°F to 4.5° warmer than adjacent rural areas.

With current observations and model projections, temperatures on average will be higher in the coming years. In the low emissions scenario, the Midwest region will feature anywhere from ~30-70 more days with "hot nights" during the late century period (2070-2099) compared to one century earlier (1971-2000). A "hot night" is defined as warmer than 98% of minimum nighttime temperatures from 1971-2000. Beyond the general gradient in the frequency of "hot nights" (Figure 4-5), local effects could also play a significant role in this region. First, the urban heat island effect will be more pronounced in the Midwest region than some other regions of the

country (e.g. the Northern Great Plains) due to the densely populated metropolitan areas (such as Chicagoland, Minneapolis/St. Paul, St. Louis, and Indianapolis), yielding a sharp contrast to the rural adjacent area. These "hot nights" and increased minimum nighttime temperatures are likely in urban areas, especially compared to the adjacent rural areas (Melillo et al. 2014, p.377).

The decrease in the diurnal temperature range over the past 30 years (1986-2016), compared to 1901-1960 averages due to a differential rate of warming of average maximum temperatures compared to average minimum temperatures in this region (USGCRP 2017 p. 186-187), leads to the conclusion that this trend may continue into the future. None of the recent climate assessments (Karl et al. 2009, Melillo et al. 2014, and USGCRP 2017) have documented any possible change to the diurnal temperature range in the Midwest region. A search of literature on climate change and diurnal temperature range seems to revolve mainly around effects to agriculture and does not discuss the exact magnitude of change for this region. However, if maximum temperatures do not increase as much as minimum temperatures, then it is expected that the diurnal temperature range will shrink. This constriction of the daily temperature range is seen in various regions throughout the United States.

4.1.2 Precipitation

According to the Climate Science Special Report (USGCRP 2017, p.208-209), average annual precipitation across the United States rose by approximately 4% from 1901 to 2015. This increase was not evenly distributed across the country. The Midwest generally saw an increase, but the increase was less in Wisconsin and southern Ohio, while the eastern half of the Upper Peninsula of Michigan and some locations in Wisconsin showed a slight decrease. More significant increases were found in the states adjacent to the Great Plains (e.g. Iowa) (USGCRP 2017, p. 209; Figure 4-6).

Future projections show an increase in annual precipitation for the Midwest United States. The magnitude varies by location, with extreme northern locations in the region having higher precipitation throughout the year, with less of an increase projected for Missouri and the Ohio River valley by the late century (2071-2100) (USGCRP 2017 p.217 and Melillo et al. 2014 p. 35). Confidence is high that annual precipitation will increase; this confidence extends back to at least the 2nd National Climate Assessment (Karl et al. 2009). However, there is some uncertainty in the mid-century on how much of an increase in annual precipitation will occur in various locations.

Local effects will be extremely prevalent in this region and may not have been adequately shown in climate models. Most notable are tropical cyclones. While they obviously do not make landfall in the region, tropical cyclone-induced precipitation can lead to differences in annual year-to-year precipitation and spatially within this region. There is some uncertainty in the amount, frequency, and strength of tropical cyclone effects in climate models (USGCRP 2017 p. 22). Terrain can affect precipitation in the region as well. The effects of terrain will vary by location and will affect year to year variability, especially in the Ozark Mountains in southwestern Missouri.

With the lack of spatial resolution to see the effects of the complex terrain in the Ozark Mountains and lake effect precipitation, there could be locations that experience no increase or a slight decrease in annual precipitation, especially in the short term. However, models generally

project an increase in precipitation, leading to a low probability of a decrease in annual precipitation.

In the Midwest, there has been a 42% increase in the amount of rain falling during the top 1% of non-zero rainfall events from 1958-2016. Also, there has been an 18% increase in the five-year maximum precipitation from 1901-2016 (USGCRP 2017, p. 212). Model projections are confident that the amount of rain falling during intense rainfall events will increase, no matter the emissions scenario. Both the low and high emissions scenarios project an increase of 10-13%, respectively, from present-day in the twenty-year return period amount by mid-century. The twenty-year return period amount is the precipitation amount that on average would occur every twenty years.

By the late century, the models diverge, with the higher emissions scenario having a 20% increase, while the lower emissions scenario has an 11% increase from present-day. These projections, for this region and nationally, indicate a "more extreme precipitation climate" (USGCRP 2017 p. 220). While some regions of the United States have experienced decreases in rainfall intensity, as measured by a variety of parameters, the Midwest is not one of them (Figure 4-6). In fact, for all observed parameters discussed by the Climate Science Special Report (USGCRP 2017), the Midwest region had the second highest increase in rainfall intensity.

Across the U.S., there has been an increase in the amount of precipitation falling in two-day events since the 1970s (USGCRP 2017 p. 211). There does not seem to be any specific data to discuss this for the Midwest region in particular for annual counts, but the non-summer seasons, especially the fall, have been trending toward more heavy rainfall days. However, there are model data that suggest that the number of days with precipitation amounts greater than the 95th percentile of non-zero precipitation days will increase by over 25%, while days in lower percentiles (10-80th) decrease across the country (USGCRP 2017 p. 220). For the Midwest region, both high and low emissions scenarios limited increases in heavy precipitation days by around 2050 and 2070, but diverge by end of the 21st century, with higher emissions scenarios showing a slight increase in rainfall days, especially when considering the possible error.

Precipitation has changed in the Midwest seasonally when comparing the present-day average (1986-2015) to the historical average (1901-1960). In winter (DJF), southern areas in the region (Missouri, Illinois, Indiana, Ohio, and Michigan's lower peninsula) became wetter than other sections of the region, which either had a very small increase in precipitation or, especially in Ohio, a decrease in precipitation. In spring (MAM), large parts of the eastern Midwest region got notably drier while the Ohio River valley and the western Midwest region got significantly wetter. The trend during the summer months (JJA) was less precipitation in Wisconsin's Iron Range, the Ohio River valley, most Missouri, and Michigan's Upper Peninsula and greater precipitation in a strip across the Midwest from Cleveland toward western Iowa, while the trend during the fall has been increased precipitation for the whole region, except Iowa and adjacent regions of southern Minnesota and Wisconsin (USGCRP 2017 p.209).

According to the 3rd National Climate Assessment (Melillo et al. 2014), precipitation is expected to increase by mid-century (2041-2070) when compared to last three decades of the 20th century, most notably during winter and spring, especially in higher emissions scenarios in the upper

Midwest states (Minnesota, Wisconsin, and Michigan). Summers are expected to get increasingly drier. While late century (2070-2099), under higher emissions scenarios, winters and spring precipitation are expected to increase by 20-30% compared to the 1976-2005 average, summers are expected to dry by 10% or more across the region, although the increase will be small "compared to natural variations." (USGCRP 2017 p.217). However, it is important to note the difficulty climate models have with resolution precipitation.

4.1.3 Other Stressors

The Midwest region has been and is still at risk for flooding and high water levels. Floods have been increasing in magnitude throughout most of the region, especially in states adjacent to the Great Plains (Minnesota, Iowa, and Missouri) and south of Lake Michigan (Illinois and Indiana). Decreases in magnitude were minor and dispersed around the region, with the exception of Wisconsin, which has seen minor and some more pronounced decreases in flood magnitude (Melillo et al. 2014 p. 40). Unlike the coastal regions of the United States, the Midwest region is not directly affected by sea level rise. Higher rainfall intensity is expected in the region and flooding has increased over the last century and is expected to continue to increase (Melillo et al. p. 419). Uncertainty in these predictions is related to the sub-regional variability present.

The United States has experienced all types of drought (meteorological, agricultural, and hydrological) over the past decade, although, according to the Climate Science Special Report, they were at least partially as a result of natural variation in annual and seasonal rainfall amounts (USGCRP 2017 p.232). Notably, the Climate Assignment Special Report (USGCRP 2017 p.233) mentions that there is conflicting evidence regarding drought in the United States in terms of climate change. Model output described by Sun et al. (2015) and Melillo et al. (2014, p. 425) show that in high emissions scenarios by mid-century, most of the Midwest region's longest dry spells will increase by 0-4 days compared to the 1981-2000 and 1971-2000 averages, respectively. This implies that droughts may become more prevalent during these dry spells or more importantly, as population grows and the demand for water increases, there may simply not be enough water to go around. This projection makes sense in the context of the other rainfall stressors that imply extreme rainfall events will increase, but possibly not much of an increase in annual precipitation.

A search of literature found two papers that discuss Midwest region wildfires, one of which focused exclusively Minnesota, Michigan, and Wisconsin. Both of these papers are outlined in Plucinski (2012) and argue that 96-97% of wildfires were human caused, with some of the remainder being attributed to temperature and precipitation. The 2nd and 3rd National Climate Assessments, as well as the Climate Science Special Report (Karl et al. 2009, Melillo et al. 2014, and USGCRP 2017) do not describe any climatic effects on Midwestern wildfires. A literature search on future projections of Midwest wildfires was similarly unsuccessful. It is possible that wildfires could increase from the already relatively low number of incidences. There is also a chance of changes in the length of fire season in this region.

According to Kunkel et al. (2013) extreme winter storms occurred more frequently during wetter and colder than average seasons over the past century. Although, according to the authors, 30% of extreme winter storms occurred during drier seasons and 35% of extreme winter storms occurred during warmer seasons. In the future, the frequency of the heavy snow events may match that of the 2013-14 and 2014-15 seasons (USGCRP 2017 p. 264-265). Across the nation,

the number of severe regional snowstorms that occurred from 1960–2011 was more than double the number of storms than occurred during the preceding sixty years (Kunkel et al. 2013).

The Climate Science Special Report (USGCRP 2017 p.217) suggests an increase in precipitation during winter under the highest emissions scenarios by late century in the Midwest region. It is probable that this trend may continue in the region. This could be countered by the suggestion in the Second National Climate Assessment that winter precipitation may increasingly fall as rain rather than as snow by late century, especially in higher emissions scenarios (Karl et al. 2009). In the short term, trends suggest a temporary continued increase in the intensity of storms, but with warming winters, this may change at later time periods. Overall, there is considerable uncertainty in these projections. Winter storms may become less frequent in southern sections in the region, and thus their intensity may be limited. In addition, locations adjacent to the Great Lakes may be subjected to intense lake effect snow, which cannot be resolved by climate models and is not addressed in detail in recent climate assessments.

According to Kunkel et al. (2013), observations have not shown meaningful trends in high or low snowfall in the last century. Although Midwest region winter precipitation is expected to increase (USGCRP 2017 p.217) by late century under some climate change scenarios, the second National Climate Assessment details that this precipitation is more likely to be in the form of rain, rather than snow. This is especially true for southern sections of the Midwest region (e.g. Missouri and southern Illinois) whose increase in temperatures would eliminate many days where snow could fall (Karl et al. 2009 p.107, USGCRP 2017 p.196).

Considering the above, it is possible that any increases in snowfall totals could be limited due to warming annual temperatures, despite increased winter precipitation. In the short-term or in lower emissions scenarios, both of which have less warming than higher emissions scenarios, winter precipitation could increase and fall as snow, but it is difficult to determine this with much certainty. Terrain may affect snow accumulation, especially in Appalachian Ohio and the Ozark Mountains, where snow accumulation at higher elevations may not change in the same manner as adjacent lower elevations. In addition, further south in region, any decreases might be amplified due to general warmer temperatures when compared to northern sections of the region. Ultimately there is considerable uncertainty about changes in winter precipitation in the region.

In the Midwest region, there are no systematic trends in ice storms or freezing rain over the past century (Kunkel et al. 2013). However, precipitation during winter is expected to increase, as well as temperature, especially under higher emissions scenarios (USGCRP 2017 p. 196 and 217). These ingredients could be supportive of increase freezing rain occurrence and ice storm frequency in the Midwest region. However, “the frequency of ice storms has not been derived from climate models” (Melillo et al. 2014 p. 148) and much uncertainty exists in these predictions.

4.2 Tables and Figures: Midwest Region

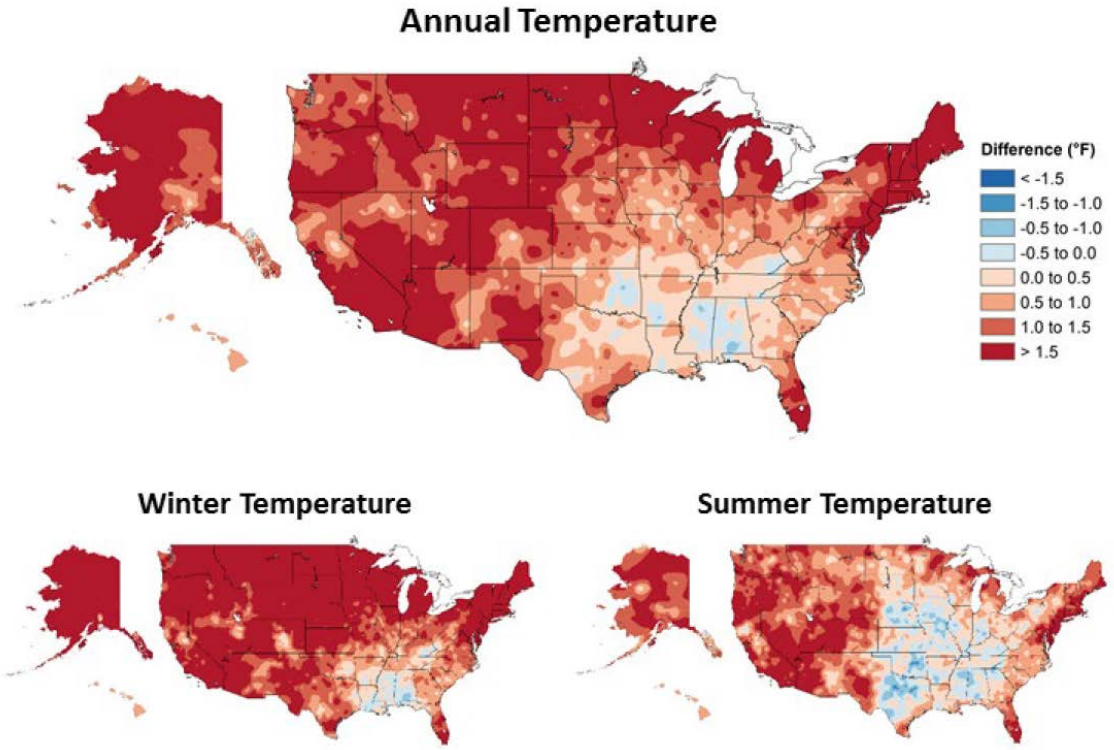

Figure 4-1. Observed changes in annual, winter, and summer temperature (°F) between present-day (1986–2016) averages and 1901–1960 (continental United States)/1925–1960 (Alaska & Hawai'i) averages. Estimates are derived from the nClimDiv dataset (Figure source: USGCRP 2017 p. 188).

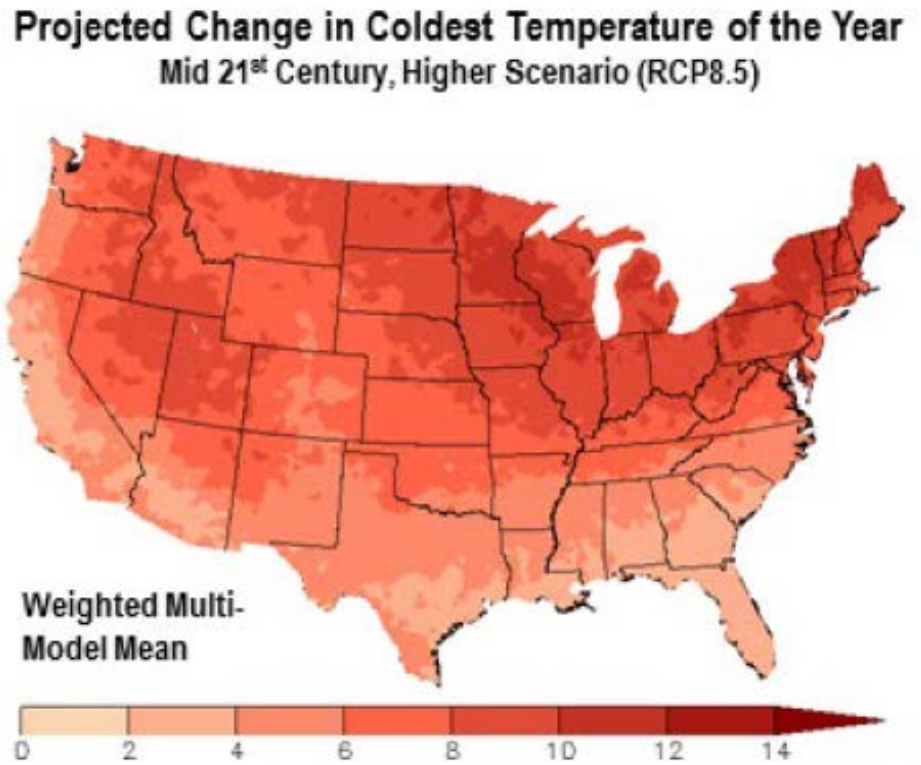

Figure 4-2. Projected changes in the higher emissions scenarios in the coldest daily temperatures (°F) of the year in the U.S. between the mid-century (2036–2065) average and the average for near-present (1976–2005). Increases are all statistically significant (Figure source: USGCRP 2017 p. 198).

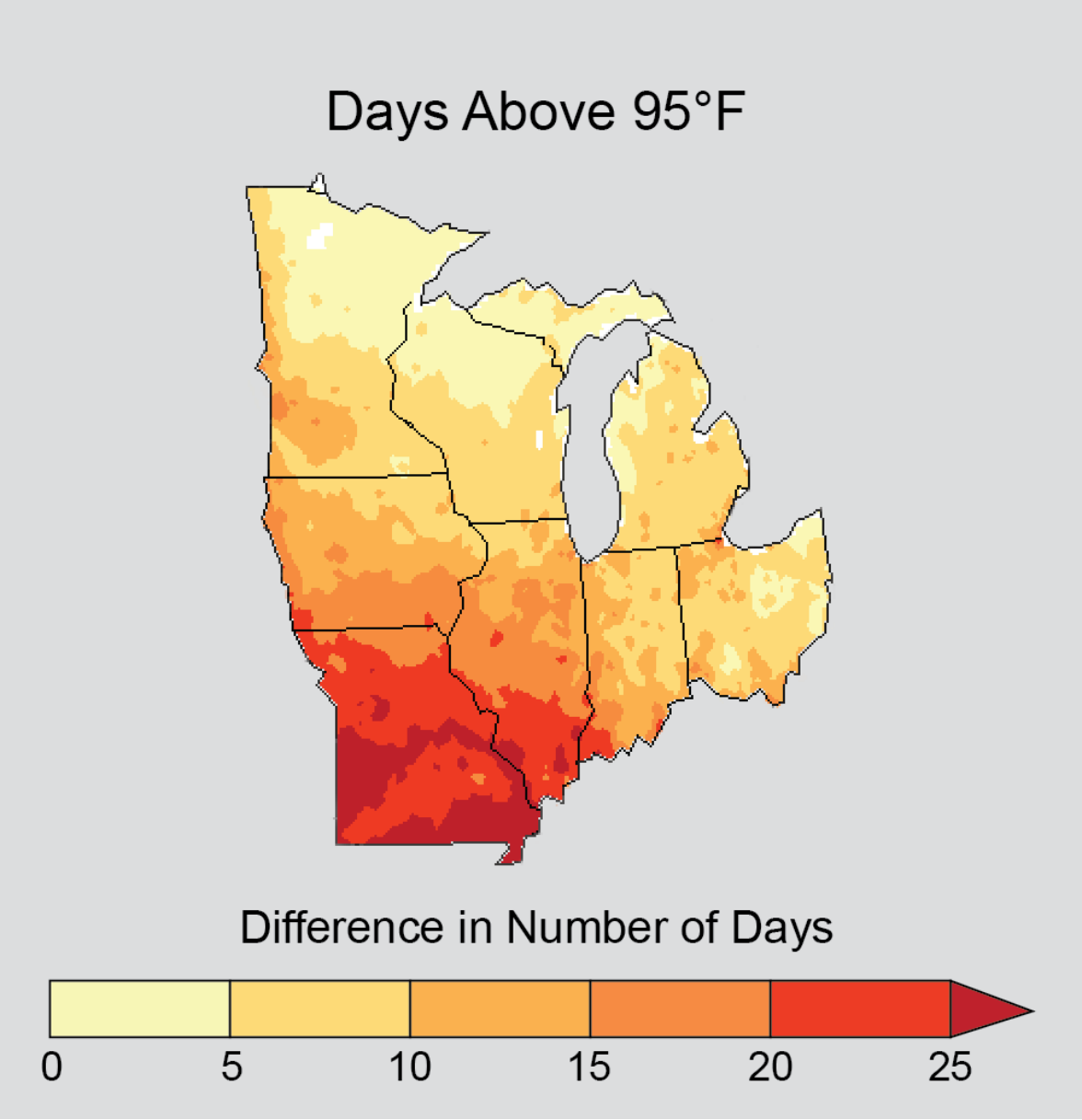

Figure 4-3. Map showing annual projected increases in the number of days over 95°F by mid-century (2041-2070) compared to 1971-2000 averages under higher emissions (Figure source: Melillo et al. 2014 p. 421).

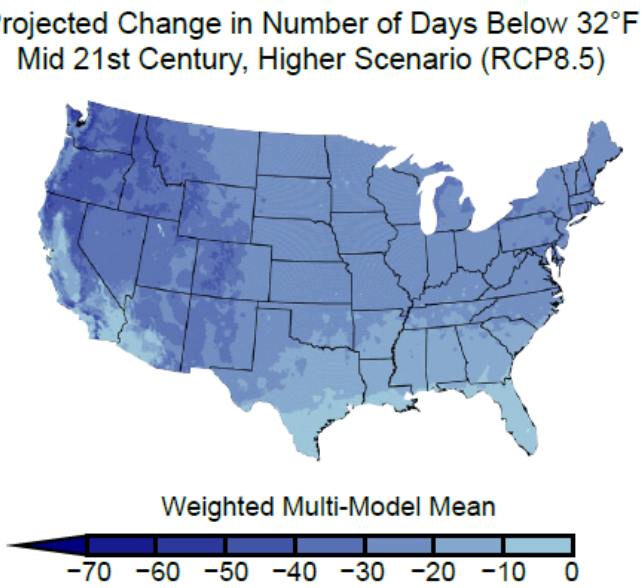

Figure 4-4. Projected changes under higher emissions scenarios in the number of days per year with a minimum temperature under 32°F in the lower forty-eight between the mid-century (2036–2065) average and the near-present (1976–2005) averages. Changes are statistically significant in all areas (Figure source: USGCRP 2017 p. 199).

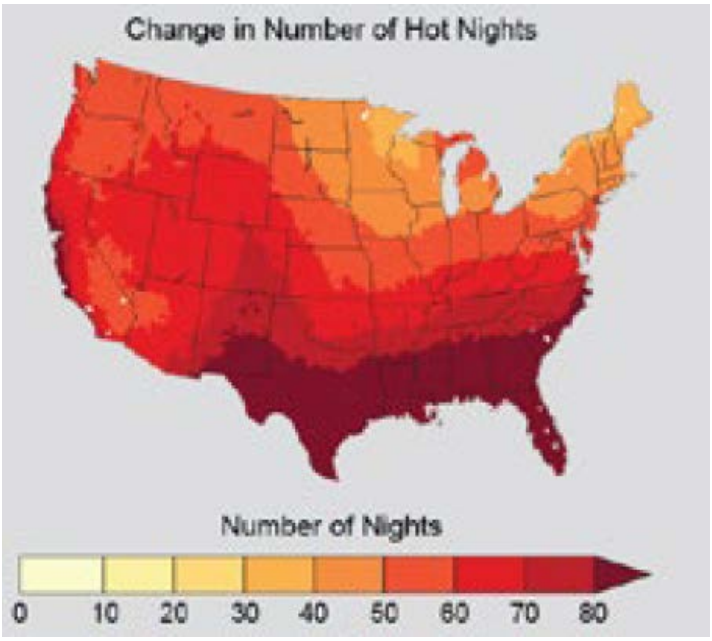

Figure 4-5. Map showing the change in number of hot nights by the end of the century (2070-2099) compared to 1971-2000 under high emissions scenarios (Figure source: Melillo et al. 2014 p.155).

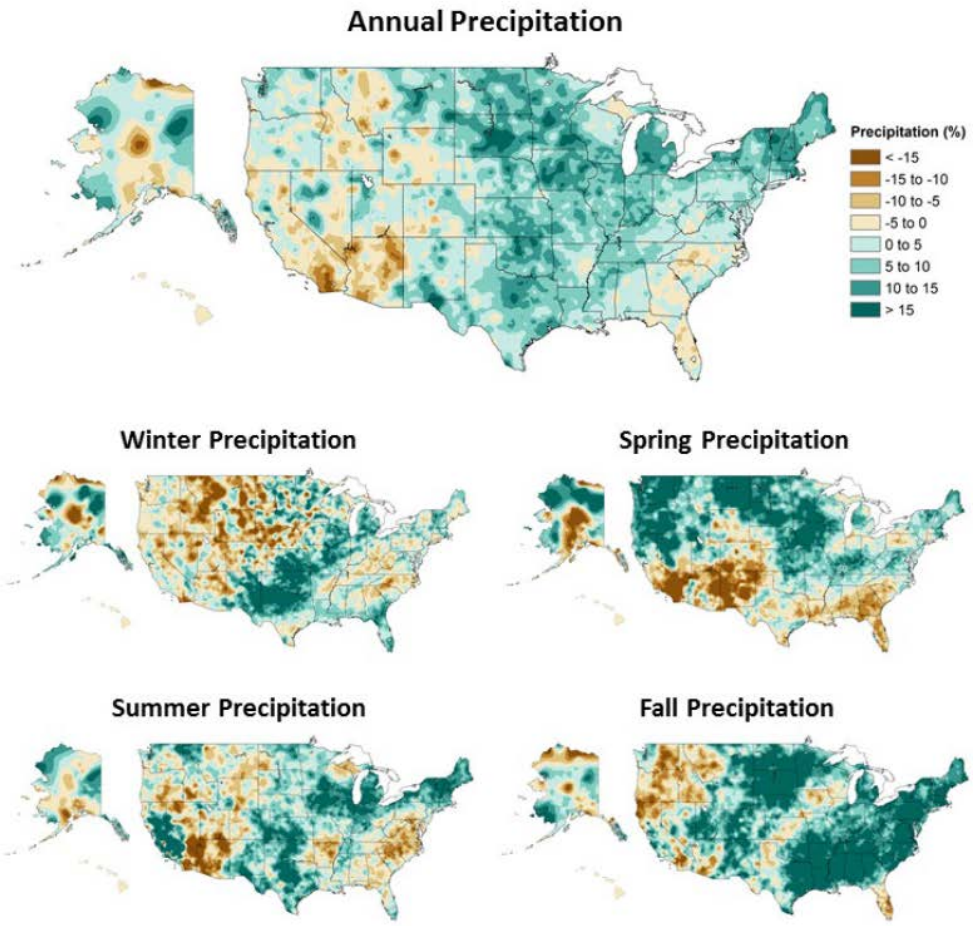

Figure 4-6. Annual and seasonal changes in precipitation over the United States. Changes are the average for present-day (1986–2015) minus the average for the first half of the last century (1901–1960 for the contiguous United States, 1925–1960 for Alaska and Hawai‘i) divided by the average for the first half of the century (Figure source: USGCRP 2017 p. 209).

5 Northern Great Plains Region

5.1 Summary of Climate Projections for the Northern Great Plains Region

5.1.1 Temperature

Over the past 100 years, average temperature has increased across the entire Northern Great Plains (NGP) region (Figure 5-1). The NGP boasts the largest increase in average annual temperature of all regions at 1.69°F (Table 5-1). The largest increases across the region occur in North Dakota and Montana, while increases are limited to 0.5–1.0°F in the southeast portion of the region in Nebraska. Regardless of emissions changes, climate models expect temperatures to increase (Figure 5-2). Temperature increases may range from 4.05–5.10°F across the NGP by mid-century (2036–2065) and 5.44–9.37°F by late-century (2071–2100).

As with the majority of the country, annual maximum temperature has decreased (1.08°F) in the NGP (Table 5-2). The decrease is most prominent in the eastern portion of the region and less prominent in the western part of the region (Montana and Wyoming), where the maximum annual temperature has increased slightly. The entire region has experienced an increase in minimum annual temperature (Figure 5-3). The NGP minimum annual temperature has increased by 4.4°F which is the 2nd greatest increase in the US behind only the Northwest. It is expected that the trends in both annual maximum and annual minimum temperatures will continue, with lower confidence in annual maximum than annual minimum.

According to the CSSR projections, the NGP is forecasted to experience a moderate increase in number of days above 90°F. A projected increase in 90°F days ranges from 0-40 days by the 2036-2065 period based on the higher emissions scenario (RCP8.5) (Figure 5-4). The main exception to this is within the Rocky Mountains on the western edge of the NGP. These areas are unlikely to see more than a few (0–10) days with 90°F temperatures due to elevation, but the rest of the region is likely to increase in 90°F or higher days in the future. CSSR model runs indicate a significant decrease in days below freezing by 2065. The NGP region is expected to see 20-40 fewer days below freezing (Figure 5-4). The western and more mountainous portion of the NGP is projected to have the greatest decrease in days below freezing.

Trends have shown that on average, daily low temperatures have been increasing through time across the majority of the U.S. The number of warm nights is projected to increase in the future under a variety of emissions scenarios (Figure 5-5). The entire region is expected to experience about 20-40 more warm nights per year regardless of emissions scenario (Figure 5-5). At the lower emissions scenario, the eastern portion of the region is expected to see around 20 more warm nights per year, while the western portion of the region should have 25 to 30 more. At the higher emissions scenario, around 25 more warm nights are seen across the eastern portion of the region, with increasing numbers of warm night from east to west across the region. The diurnal temperature range in the NGP should continue to constrict due to a rise in average minimum temperatures and a slower increase in average maximum temperatures.

5.1.2 Precipitation

Most of the region has experienced an increase in annual precipitation (Figure 5-6), except for parts of Wyoming and western Montana that have had modest decreases overall but larger decreases in the highest terrain. During fall and spring, most of the region has experienced an increase in precipitation (~15%) over the past 100 years while winter indicates a significant drying trend with precipitation decreasing by 15%. The CSSR projects an overall increase in precipitation with projected increases in precipitation during winter and spring that are considered large compared to natural variations (Figure 5-7). This is somewhat seasonally contradictory to the trend seen over the last 100 years as winter has seen a drying trend, thus lowering confidence.

Observations from across the region have shown an increase in the 99th percentile of daily precipitation from 1901–2016 and an increase in the frequency of 2-day events that have a precipitation total exceeding the largest 2-day amount that is expected to occur on average once every 5 years for both 1901-2016 and 1958-2016 (Figure 5-8). The fall season has also observed a steady increase in daily 20-year return level precipitation while the other seasons have more modest increases (Figure 5-9). Along with these observational changes, models project heavy precipitation events will continue into the future. Under all scenarios, the number of extreme events that exceed a five-year return period is projected to increase (Figure 5-10).

Research has demonstrated that as temperatures rise, the amount of moisture the atmosphere can hold increases, resulting in more moisture available for storms. The projected change in the 20-year return period amount for daily precipitation is expected to increase by roughly 10% by mid-century under both low and high emissions scenarios, while the late-century is projected to increase by between 10% (lower emissions scenario) and 16% (higher emissions scenario) (Figure 5-11). There are also indications that the number of precipitation days may increase across the region (Figure 5-12).

Finally, the CSSR indicates that mesoscale convective system (MCS) frequency and intensity has increased since 1979 in the central US. MCSs typically bring heavy rainfall in the summer, but this precipitation is often localized. These trends are expected to continue with high confidence over the remainder of the 21st century. This change will be less pronounced over the higher terrain of the region due to terrain influences and because MCSs rarely impact the high terrain.

There have been significant shifts in the seasonality of precipitation across the region. Spring and fall have seen a 15% increase in average precipitation amounts over the last 100 years over most of the region (Figure 5-6). Historical summer precipitation indicates a largely neutral to slightly drying trend and winter exhibits a much more significant drying trend with much of the region showing a 15% decrease in precipitation amounts over the last 100 years. Climate models show the opposite trend going forward in the winter (wetter), and a more significant drying trend in the summer (Figure 5-7). Overall, spring is expected to see the greatest increase in precipitation.

5.1.3 Other Stressors

The increase in heavy rain events would lead to more flood events. In the NGP most of this increased flood risk would occur in the more mountainous areas where water runoff is more rapid, but the rest of the region will still see an increased flood risk. This risk would be enhanced in winter when precipitation is expected to increase. The number of consecutive dry days is expected to decrease across much of the region in the future when compared to historical averages (Figure 5-13). However, if a there is a drying trend in the summer, droughts could become more frequent and more intense.

The NGP is fire-prone during much of the summer and an increasing trend in the number of large fires is already occurring (Figure 5-14). An increase in drier and drought conditions in the summer would directly influence a greater number of wildfires in the region. The NGP is home to many national forests that during dry summers and drought are at extreme risk of wildfires. Areas used for agriculture in the southern or southeastern part of the region may be less susceptible to the threat, but there is ample rangeland throughout the region that is vulnerable to wildfire.

The length of the fire season in the NGP would depend on when the atmospheric wave pattern begins and stops to deliver rain to the region. With the spring and fall projected to be wetter as time progresses, timing of when the rains begin will become critical to determining the length of the wildfire season. Models indicates that if emissions remain high or increase, soil moisture will decrease throughout the year, supporting a longer fire season.

Snowfall will likely increase across the NGP. Trends show that annual snowfall has increased by as much as 1% between 1937 and 2007 (Figure 5-15). Much of the region is expected to experience an increase in winter precipitation which would predominantly fall as snow (Figure 5-7). Further, intensity of winter season precipitation is expected to increase modestly (Figure 5-9). However, this contradicts the historical trend of winter precipitation (Figure 5-6). It is also possible that ice storms could occur more frequently due to the projected increase in precipitation in the fall and spring seasons when the NGP is transitioning to a colder environment.

5.2 Tables and Figures: Northern Great Plains Region

Table 5-1. Change in annual average temperature, annual average maximum temperature, and annual average minimum for various regions of the U.S. Note the largest observed change is in the Northern Great Plains (Source: USGCRP 2017 p. 187).

NCA Region	Change in Annual Average Temperature	Change in Annual Average Maximum Temperature	Change in Annual Average Minimum Temperature
Contiguous U.S.	1.23°F	1.06°F	1.41°F
Northeast	1.43°F	1.16°F	1.70°F
Southeast	0.46°F	0.16°F	0.76°F
Midwest	1.26°F	0.77°F	1.75°F
Great Plains North	1.69°F	1.66°F	1.72°F
Great Plains South	0.76°F	0.56°F	0.96°F
Southwest	1.61°F	1.61°F	1.61°F
Northwest	1.54°F	1.52°F	1.56°F
Alaska	1.67°F	1.43°F	1.91°F
Hawaii	1.26°F	1.01°F	1.49°F
Caribbean	1.35°F	1.08°F	1.60°F

Table 5-2. Observed changes in annual average temperature (°F) for each National Climate Assessment region. Changes are the difference between the average for present-day (1986–2016) and the average for the first half of the last century (1901–1960 for the contiguous United States, 1925–1960 for Alaska, Hawai'i, and the Caribbean). (Source: USGCRP 2017 p. 190).

NCA Region	Change in Coldest Day of the Year	Change in Warmest Day of the Year
Northeast	2.83°F	−0.92°F
Southeast	1.13°F	−1.49°F
Midwest	2.93°F	−2.22°F
Great Plains North	4.40°F	−1.08°F
Great Plains South	3.25°F	−1.07°F
Southwest	3.99°F	0.50°F
Northwest	4.78°F	−0.17°F

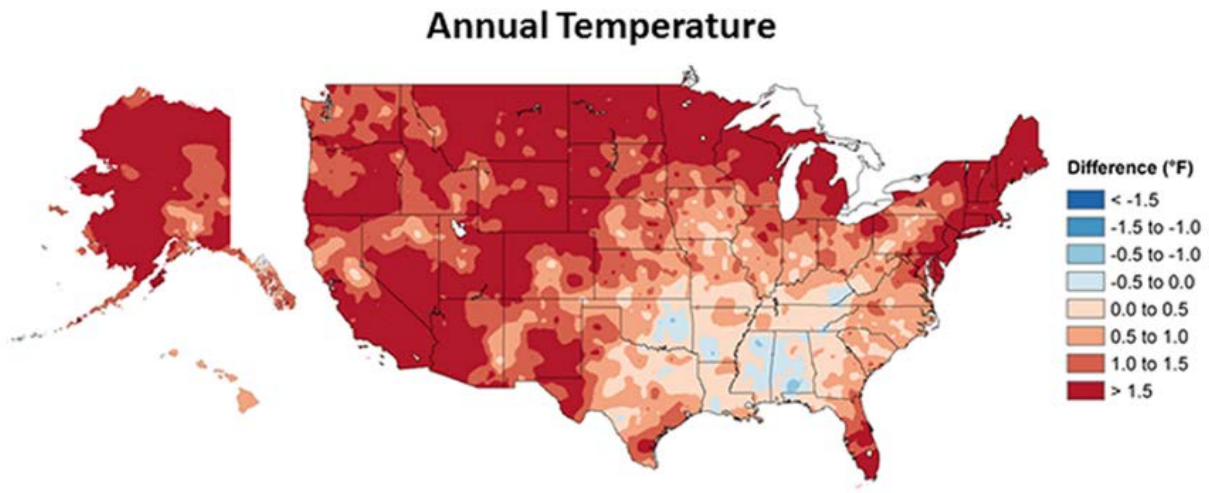

Figure 5-1. Observed change in annual temperatures between the 1986–2016 period and the period 1901–2016 (Figure source: USGCRP 2017 p. 188).

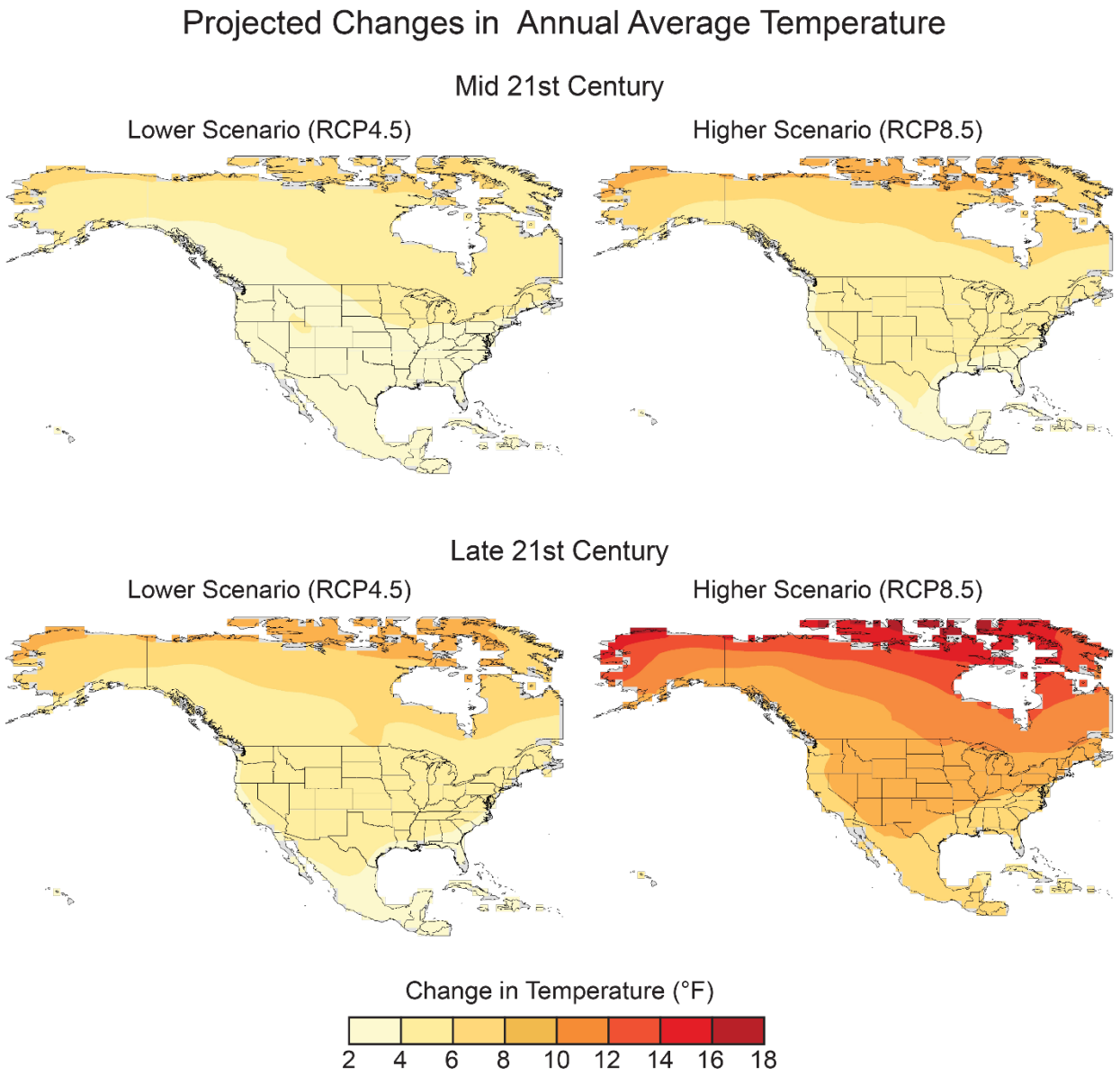

Figure 5-2. Projected changes in annual average temperatures (°F). Changes are the difference between the average for mid-century (2036–2065; top) or late-century (2070-2099; bottom) and the average for near-present (1976–2005). Each map depicts the weighted multi-model mean. Increases are statistically significant in all areas (that is, more than 50% of the models show a statistically significant change, and more than 67% agree on the sign of the change) (Figure source: USGCRP 2017 p. 196).

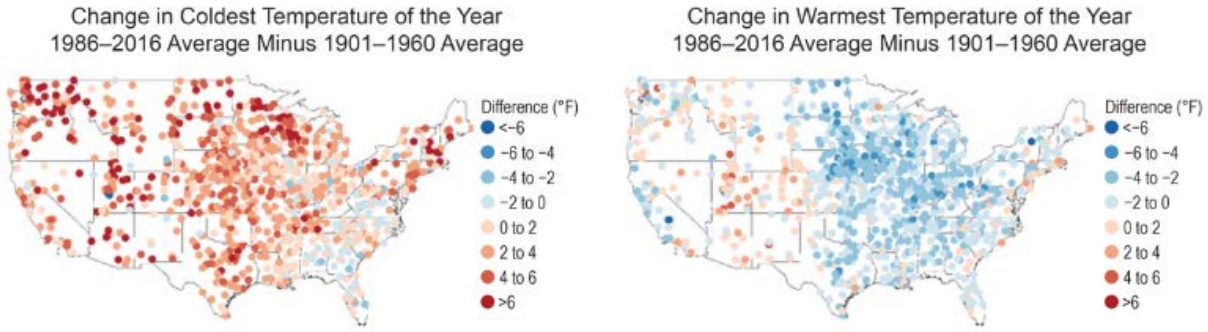

Figure 5-3. Change in the coldest temperature of the year (left) and warmest temperature of the year (right) (Figure source: USGCRP 2017 p. 190).

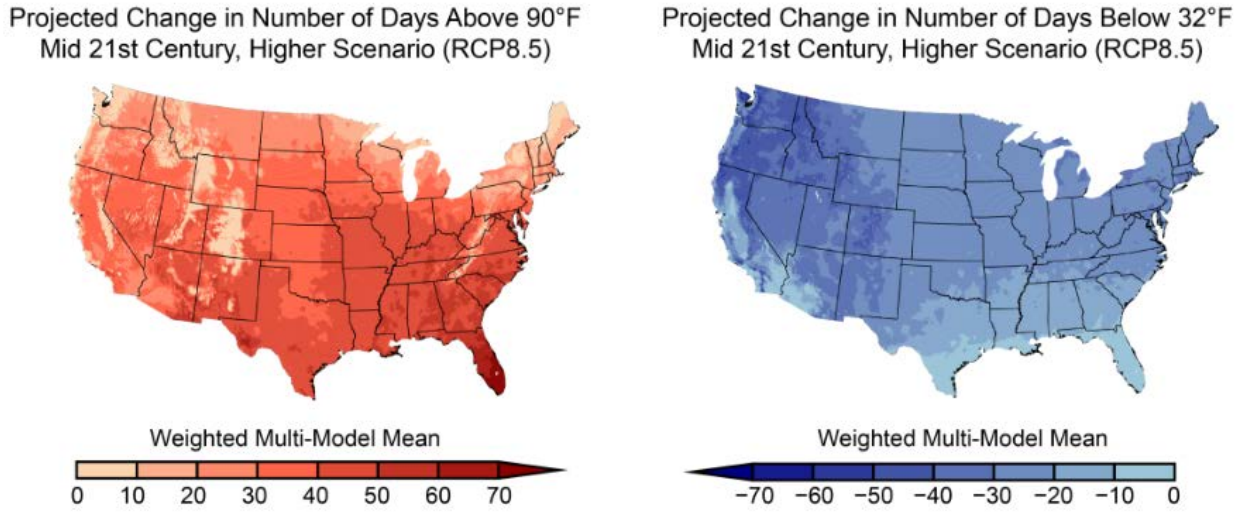

Figure 5-4. Projected change in days above 90°F (left) and projected changes in the number of days below 32°F (right) by mid-century (2040–2060) (Figure source: USGCRP 2017 p. 199).

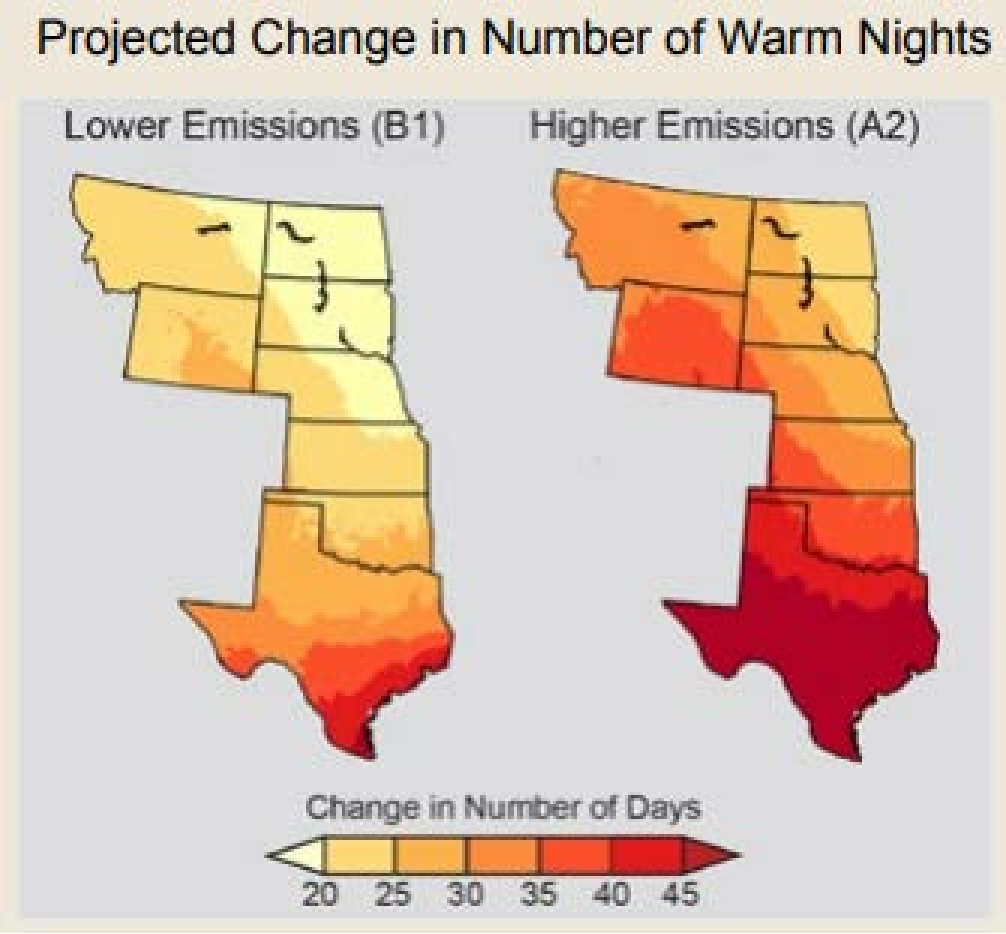

Figure 5-5. Projected change in the number of warm nights by emissions scenario – lower emissions (left) and higher emissions (right) (Figure source: Melillo et al. 2014 p. 444).

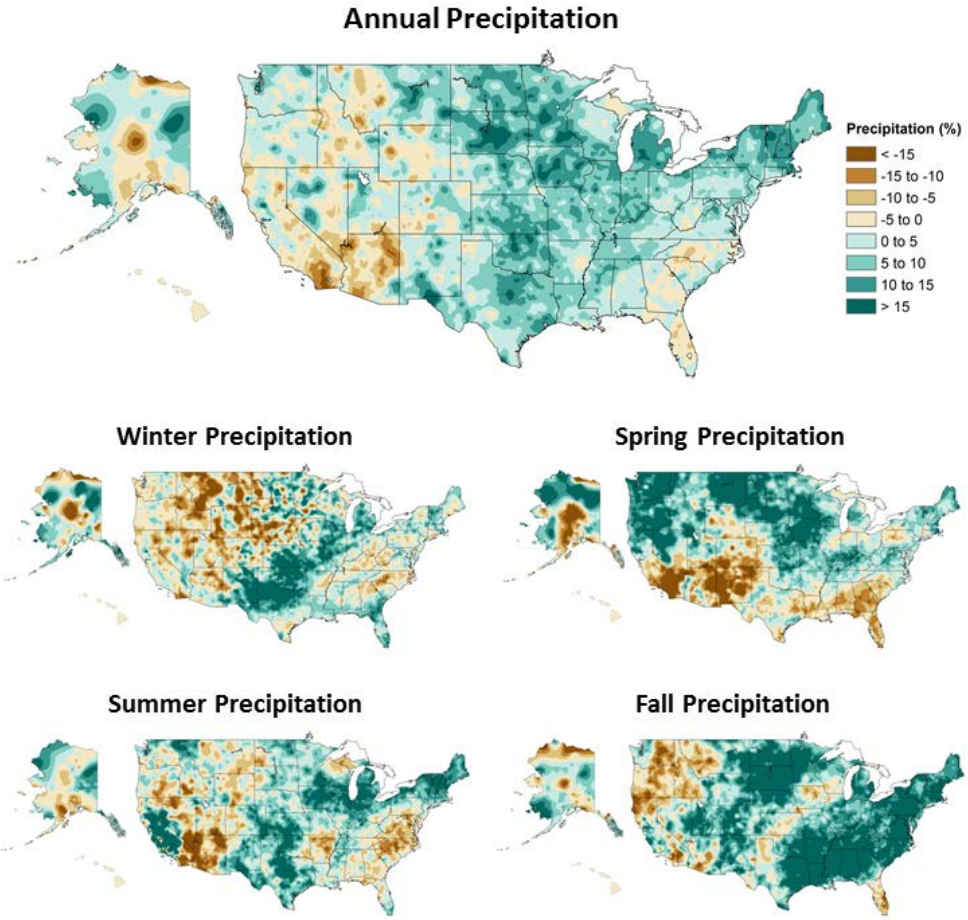

Figure 5-6. Annual and seasonal changes in precipitation of the United States. Changes are the average for the present-day (1986–2015) minus the average for the first half of the last century (1901–1960 for the contiguous U.S. and 1925–1960 for Alaska and Hawai'i) divided by the average for the first half of the century (Figure source: USGCRP 2017 p. 209).

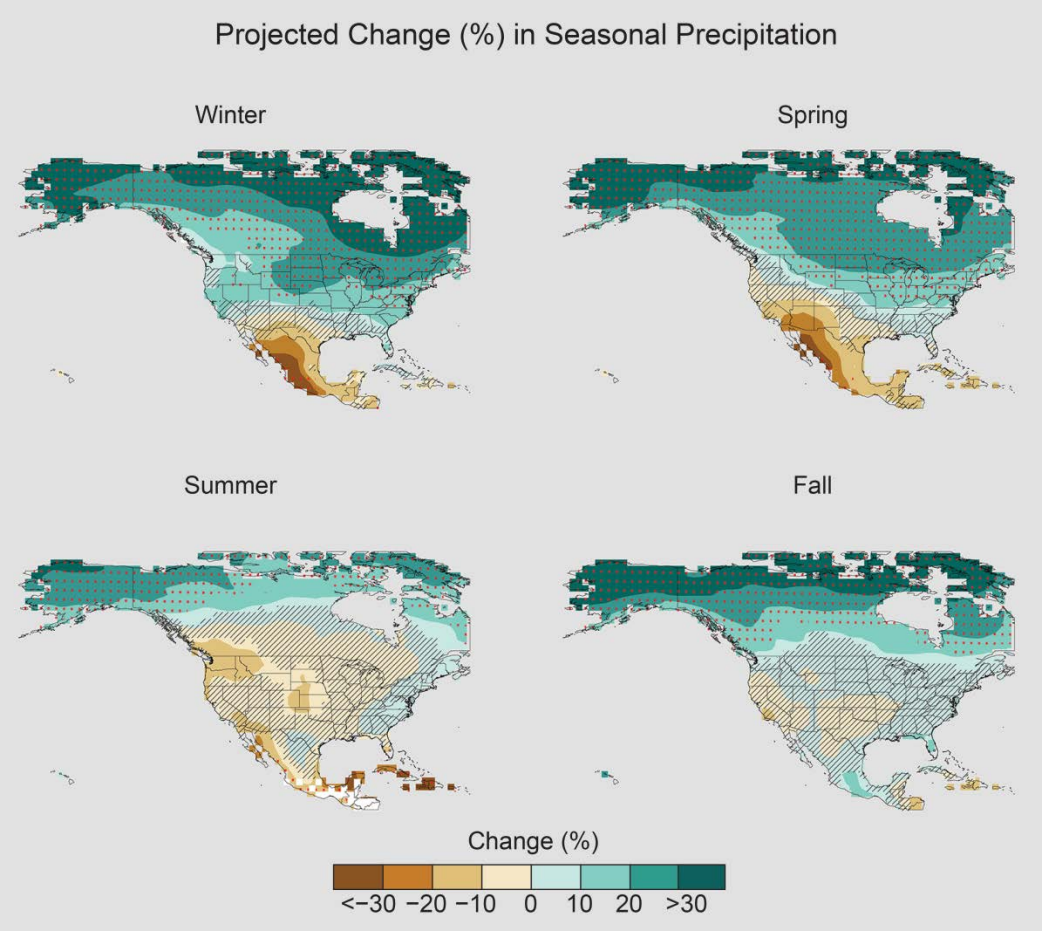

Figure 5-7. Projected change (%) in total seasonal precipitation from CMIP5 simulations for 2070–2099. The values are weighted multi-model means for the higher emissions scenario (RCP 8.5) and expressed as the percent change relative to the 1976–2005 average. Stippling indicates that the changes are large relative to natural variation, while hatching indicates that changes are small relative to natural variations (Figure source: USGCRP 2017 p. 217).

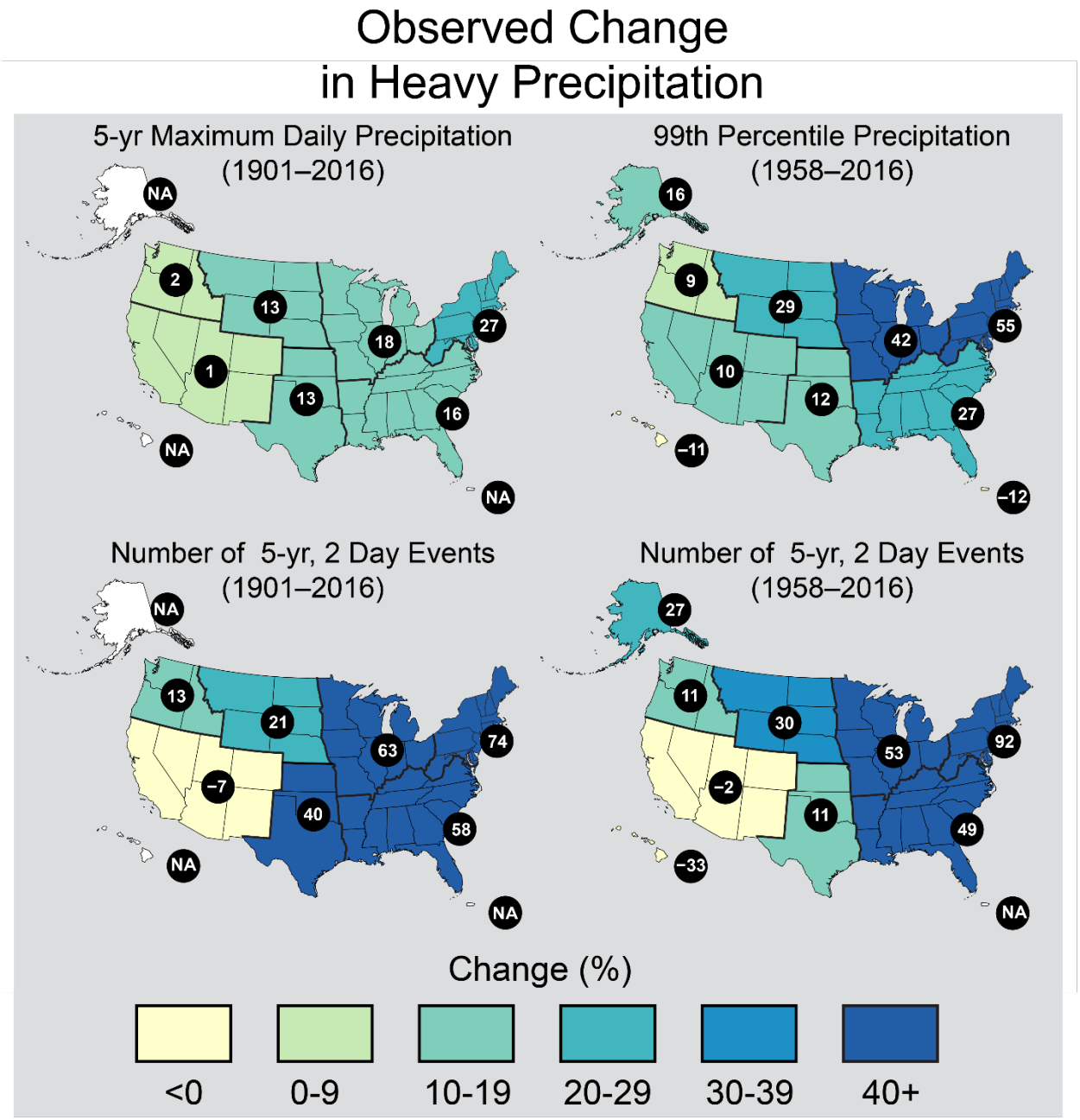

Figure 5-8. Changes in extreme precipitation. The percent change in maximum daily precipitation by 5-year periods (upper left), the percent change in the amount of precipitation falling in daily events that exceed the 99th percentile of precipitation days (upper right), the percent change in number of two day events with a precipitation total exceeding the largest two-day amount that would be expected to occur only once every five years based on data from 1901–2016 (lower left), and the percent change in number of two day events with a precipitation total exceeding the largest two-day amount that would be expected to occur only once every five years based on data from 1958–2016 (lower right) (Figure source: USGCRP 2017 p. 212).

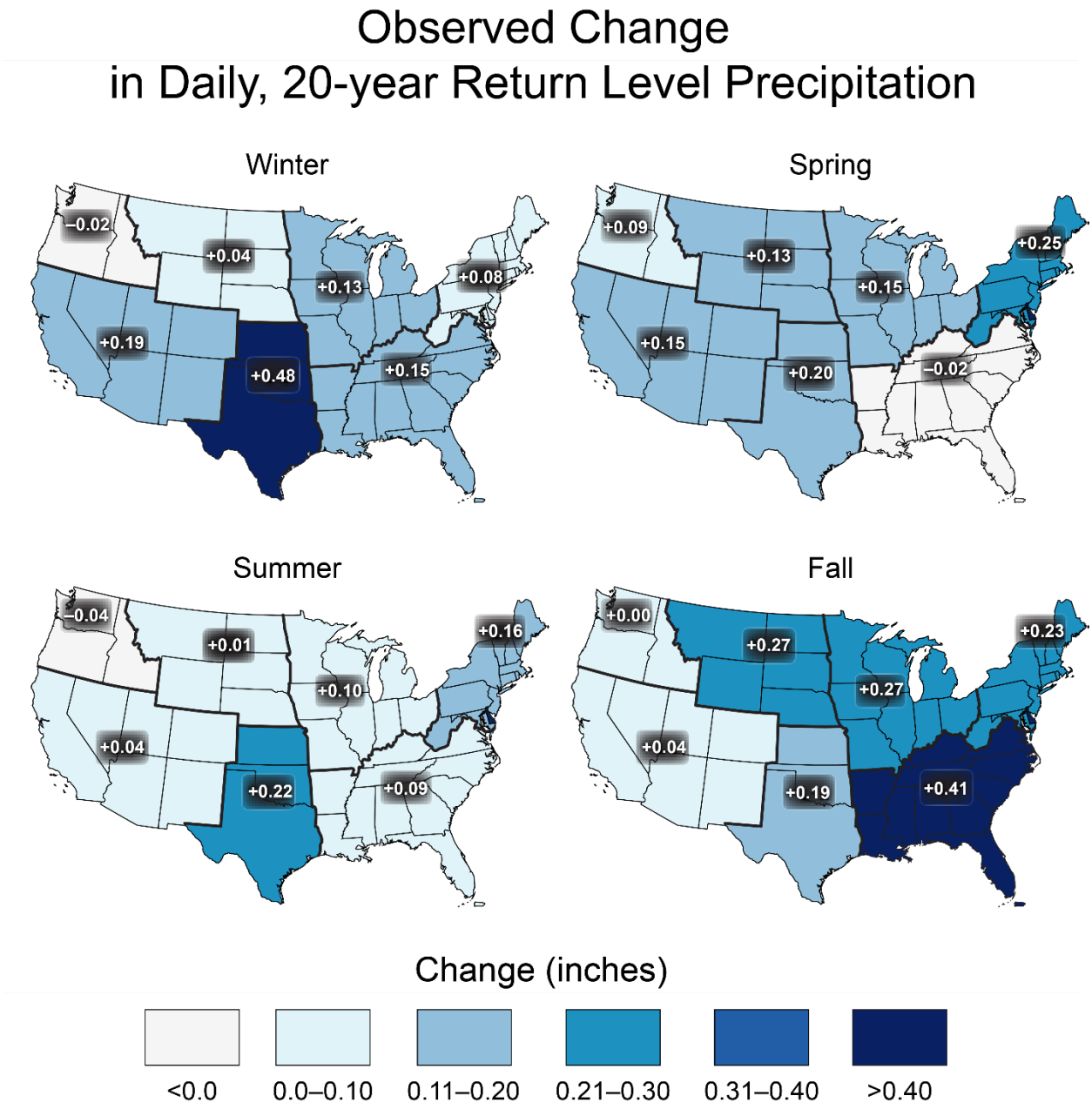

Figure 5-9. Observed changes in the 20-year return value of the seasonal daily precipitation totals for the contiguous U.S. over the period 1948–2015 using data from the Global Historical Climatology Network (GHCN) dataset (Figure source: USGCRP 2017 p. 211).

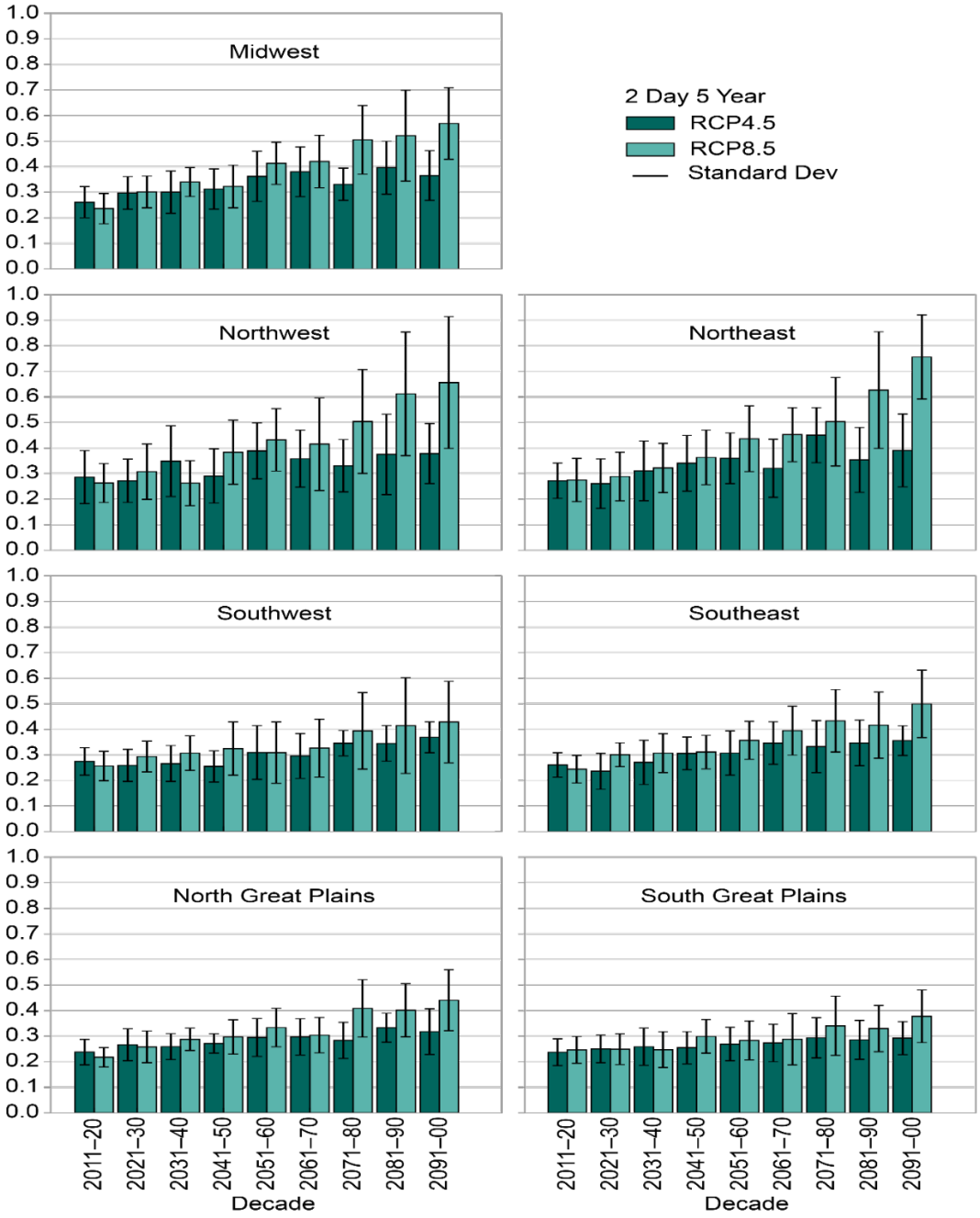

Figure 5-10. Regional extreme precipitation event frequency for a lower scenario (RCP4.5) (green; 16 CMIP5 models) and the higher scenario (RCP8.5) (blue; 14 CMIP5 models) for a 2-day duration and 5-year return. Calculated for 2006–2100 but decadal anomalies begin in 2011. Error bars are ±1 standard deviation; standard deviation is calculated from the 14 or 16 model values that represent the aggregated average over the regions, over the decades, and over the ensemble members of each model. The average frequency for the historical reference period is 0.2 by definition and the values in this graph should be interpreted with respect to a comparison with this historical average value (Figure source: USGCRP 2017 p. 219).

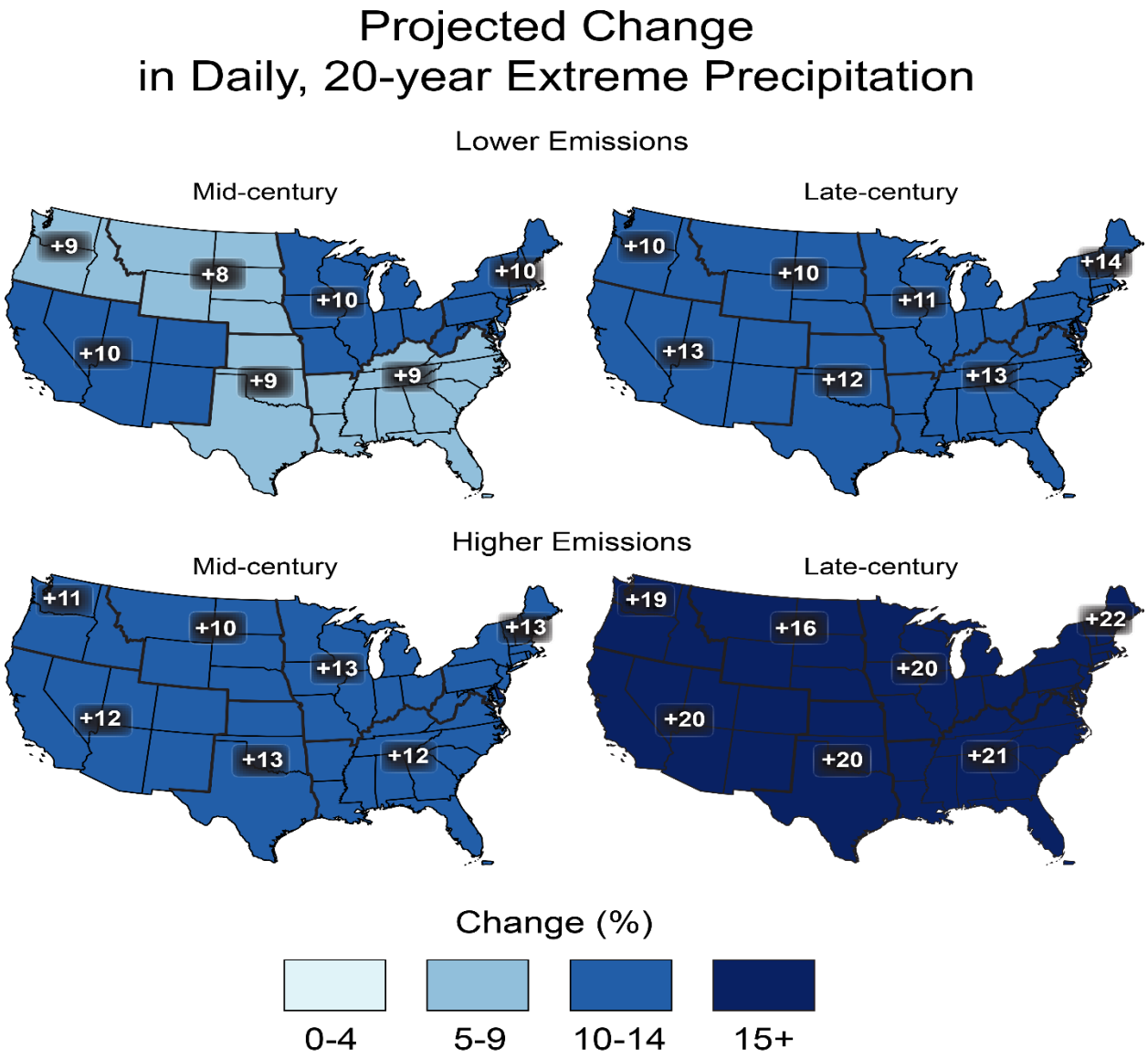

Figure 5-11. Projected change in the 20-year return period amount for daily precipitation for mid- (left maps) and late-21st century (right maps). Results are shown for a lower emissions scenario (top maps; RCP4.5) and for a higher emissions scenario (bottom maps, RCP8.5). These results are calculated from the LOCA downscaled data (Figure source: USGCRP 2017 p. 220).

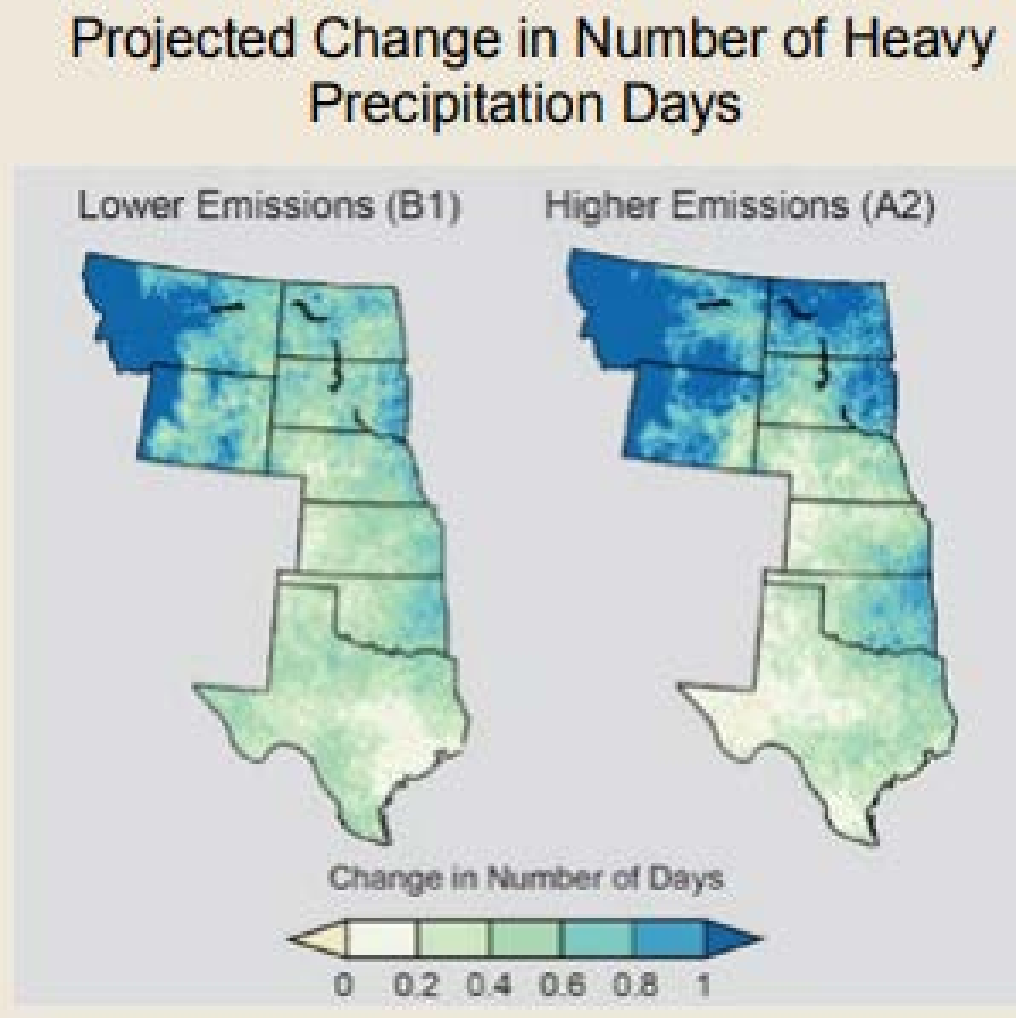

Figure 5-12. Projected change in the number of heavy precipitation days by emissions scenario – lower emissions (left) and higher emissions (right) (Figure source: Melillo et al. 2014 p. 445).

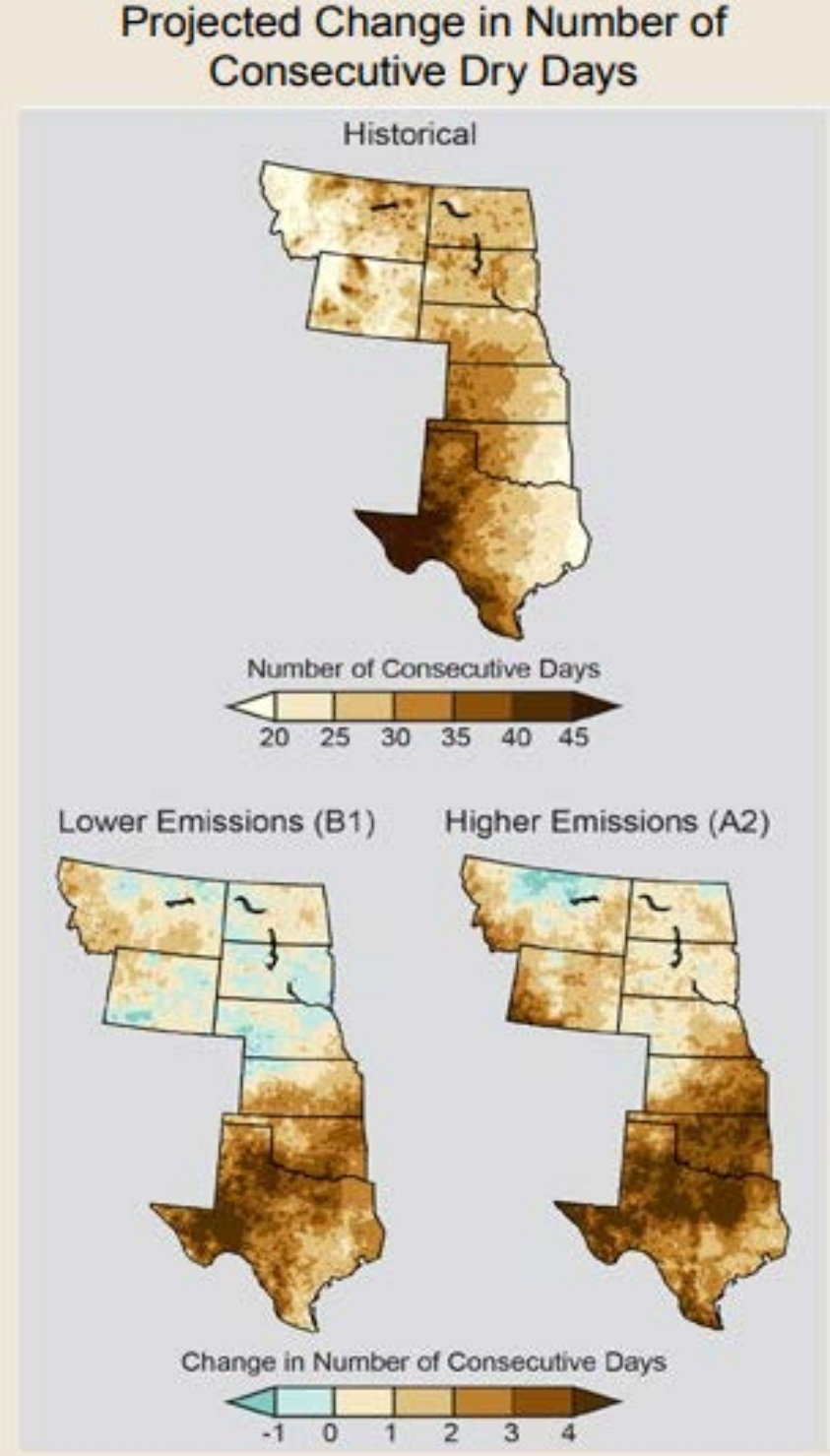

Figure 5-13. Maps showing the maximum annual number of consecutive days in which limited (less than 0.01 inches) precipitation was recorded on average from 1971 to 2000 (top), projected changes in the number of consecutive dry days assuming substantial reductions in emissions (B1), and projected changes if emissions continue to rise (A2). (Figure source: Melillo et al. 2014 p. 445).

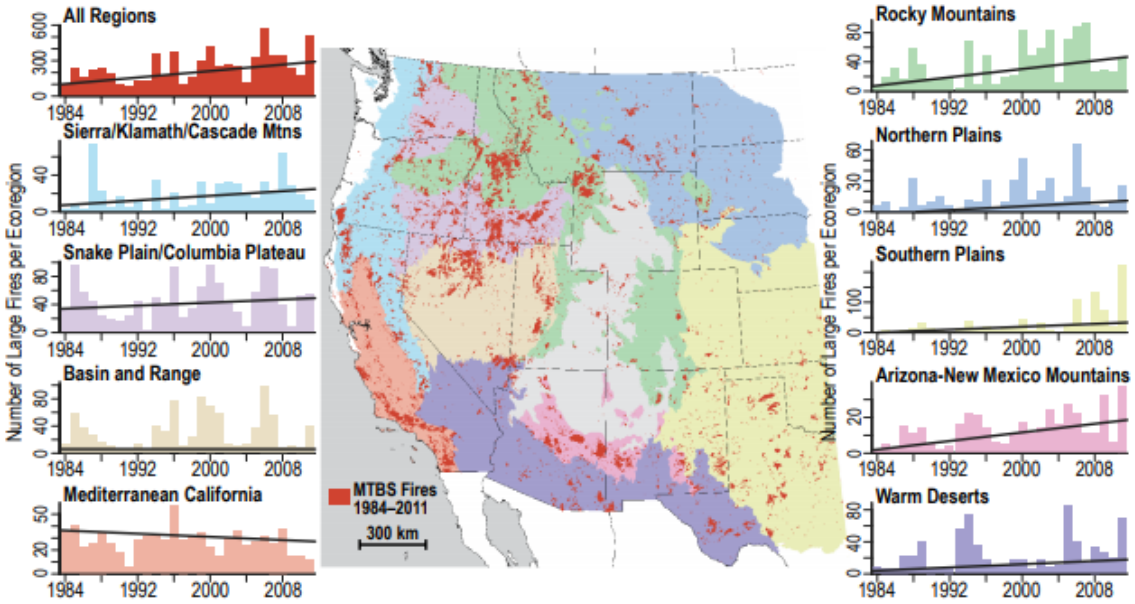

Figure 5-14. Trends in the annual number of large fires in the western U.S. for a variety of ecoregions. The NGP region is highlighted in blue, where a significant upward trend is noted (Figure source: USGCRP 2017 p. 243).

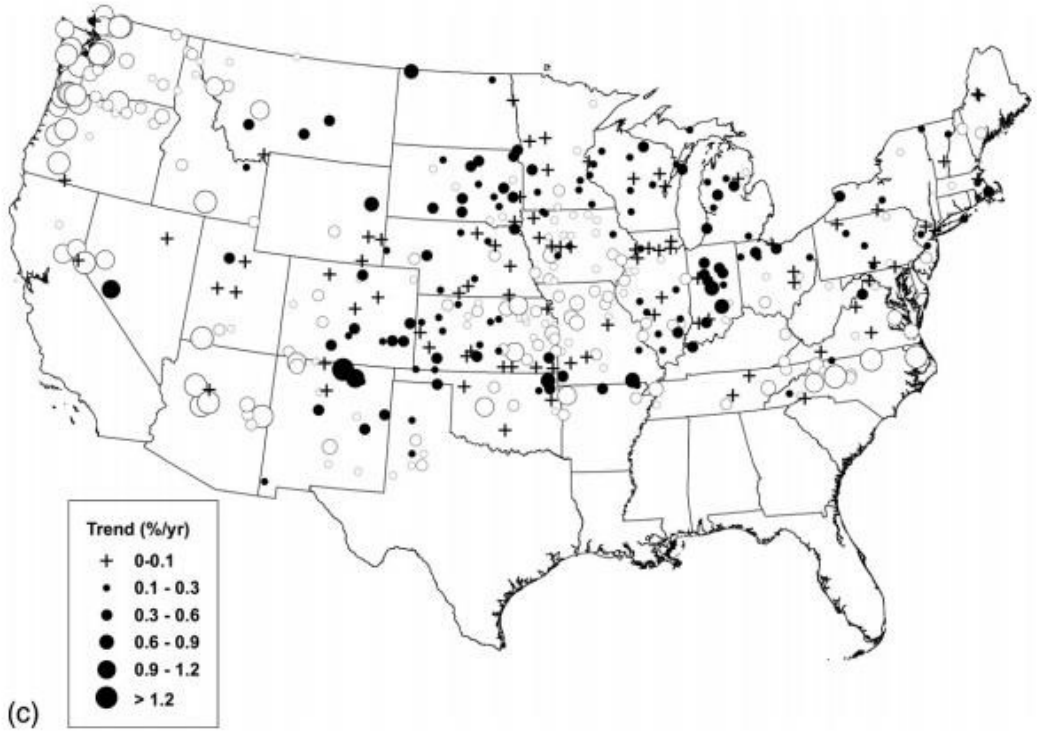

Figure 5-15. Average snowfall trends as determined from individual stations for the period from 1937-2007. White indicates decrease, black indicates increase (Figure source: Kunkel et al. 2009).

6 Southern Great Plains Region

6.1 Summary of Climate Projections for the Southern Great Plains Region

6.1.1 Temperature

Over the past 100 years, the average temperature of the Southern Great Plains (SGP) has increased (Figure 6-1). The SGP has seen the 2nd lowest increase in average temperatures compared to other regions, increasing by only 0.76°F (Table 6-1). Western and southern Texas have increased in average temperature while the rest of the SGP have remained largely neutral even with a small pocket of decreasing temperatures in southeastern Oklahoma. Regardless of emissions scenario, climate models expect temperatures to increase in the future (Figure 6-2).

As with the majority of the country, annual maximum temperature decreased (1.07°F) in the SGP (Table 6-2). Most of the region showed a significant decrease, especially in central Texas (Figure 6-3). However, in western Kansas there has been a minimal increase in maximum annual temperature. The entire region has experienced an increase in minimum annual temperature (Figure 6-3). The SGP minimum annual temperature has increased by 3.25°F. While the entire region has seen an increase in the magnitude of the lowest annual temperature, central Texas has seen the most significant rise in lowest annual temperatures.

According to the Climate Science Special Report (CSSR), the SGP is expected to see an increase in days above 90°F (Figure 6-4) under the higher emissions scenario (RCP8.5). Up to 60 more days above 90°F are expected by mid-21st century based on the higher emissions scenario. There is a low probability the number of days above 90°F decreases in this region, especially considering the projected increase for other regions including the Northern Great Plains. The CSSR indicates a moderate decrease in days below freezing by 2065. It is expected that there will be 10-30 fewer days below freezing across the region (Figure 6-4). Coastal Texas is expected to see a minimal decrease in days below freezing as the area rarely drops below freezing.

Average annual minimum temperatures have increased in the Southern Great Plains by roughly 0.96°F (Table 6-1). This is further supported by the projected change in number of warm nights (Figure 6-5) which, even with lower emissions, is expected to increase by 20-45 warm nights per year over the entire region. The higher emissions scenarios project 30+ more warm nights per year. A strong latitudinal trend is visible in both higher and lower emissions projections, with the smaller increases in warm night as latitude increases (Figure 6-5). The diurnal temperature range in the Southern Great Plains should continue to constrict due to a rise in average minimum temperatures and a slower increase in average maximum temperatures.

6.1.2 Precipitation

The SGP experienced a roughly 5-10% increase in annual precipitation (Figure 6-6) with winter and summer having widespread increases (approximately 15%) during the past ~100 years. The CSSR projects a drying trend in the SGP (Figure 6-7), but determined the change was small compared to natural influences (not outside what naturally occurs). Annually, central Oklahoma and northeastern Texas have seen the greatest increase in precipitation while values decrease westward (Figure 6-6).

The CSSR indicated the frequency of mesoscale convective systems (MCSs) increased since 1979 in the central US. MCSs typically bring intense rainfall to an area and the CSSR indicates these storms are getting more frequent and intense. These trends are expected to continue with high confidence over the remainder of the 21st century. The Texas coastline is also at risk of tropical cyclones during the summer and fall months of the year; however, there is uncertainty on how those events will impact rainfall amounts on rainy days.

Observations from across the region have shown an increase in the 99th percentile of daily precipitation from 1958-2016 and an increase in the frequency of 2-day events that have a precipitation total exceeding the largest 2-day amount that is expected to occur on average once every 5 years for both 1901-2016 and 1958-2016 (Figure 6-8). Winter also observed a steady increase in daily 20-year return level precipitation while the other seasons saw an increase to a slightly lesser extent (Figure 6-9). Under all scenarios, the number of extreme events that exceed a five-year return period is projected to slightly increase (Figure 6-10).

Research has demonstrated that as temperature increases, the amount of moisture the atmosphere can hold increases, resulting in more moisture available for storms. The projected change in the 20-year return period amount for daily precipitation is expected to increase by roughly 10% by mid-century under both low and high emission scenarios, while the late-century is projected to increase by between 12% (lower emissions scenario) and 20% (higher emissions scenario) (Figure 6-11). The NCA indicates about 0.2 more heavy precipitation days per year by midcentury in both lower and higher emissions scenarios (Figure 6-12). Eastern Oklahoma and Kansas show more change in projected heavy precipitation days, whereas western Texas demonstrates a near zero and possible negative change in heavy precipitation days by mid-century (Figure 6-13). This is due to moisture from the Gulf of Mexico propagating into eastern Oklahoma and Kansas but not traveling to western Texas.

Summer, winter and fall have seen a 10-15% increase in average precipitation amounts over the last 100 years over most of the region (Figure 6-7). In winter, southern Texas has seen little change over the last 100 years but the remainder of the region has experienced an increase in precipitation. During fall, eastern Texas has shown a 15% increase in precipitation while the rest of the SGP exhibits a neutral to drying trend (Figure 6-6). Historically, spring precipitation exhibits a slight drying trend in the SGP over the last 100 years. Extreme western parts of the region show significant drying in the spring, but northern Kansas demonstrates an increasing precipitation trend. Climate models indicate a decreasing trend in precipitation across the SGP, with the largest decreases in summer (Figure 6-7).

6.1.3 Other Stressors

If the projected increase in heavy rain events occurs, it will likely lead to more flood events. In the SGP, most of the increasing flood risk is along river basin areas and along the coast. Increased heavy rain events inland and tropical cyclone strikes along the coast bring large amounts of rain and storm surge will contribute to the increase in flooding events.

The NCA report indicates droughts will become more frequent and intense in the future. The SGP is expected to see an increase in precipitation in the winter months but a drying trend in the summer would lead to more intense droughts regionwide. The entire region is expected to see an increase in consecutive dry days regardless of emissions tendencies (Figure 6-12). Much of the region is projected to see two to four or more consecutive dry days. Oklahoma and Northern Texas are expected to see the largest increase in consecutive dry days, while the coastal Texas and Northwestern Kansas are expected to see the smallest increase (Figure 6-13).

The SGP region has seen a recent increase in the number of large wildfires (Figure 6-14). Should areas in the region receive an increasing number of consecutive dry days, wildfire occurrences would likely continue to increase. Most of the fires from 1984-2011 in the SGP have occurred in Texas (Figure 6-14). The length of the fire season in the SGP would depend on possible drought conditions in the region. With the spring and fall project to be wetter as time progresses, timing of when the rains begin will become critical to determining the length of the wildfire season. The CSSR indicates that if emissions remain high or increase, soil moisture will decrease throughout the year, supporting a longer fire season.

6.2 Tables and Figures: Southern Great Plains Region

Table 6-1. Change in annual average temperature, annual average maximum temperature, and annual average minimum for various regions of the U.S. (Source: USGCRP 2017 p. 187).

NCA Region	Change in Annual Average Temperature	Change in Annual Average Maximum Temperature	Change in Annual Average Minimum Temperature
Contiguous U.S.	1.23°F	1.06°F	1.41°F
Northeast	1.43°F	1.16°F	1.70°F
Southeast	0.46°F	0.16°F	0.76°F
Midwest	1.26°F	0.77°F	1.75°F
Great Plains North	1.69°F	1.66°F	1.72°F
Great Plains South	0.76°F	0.56°F	0.96°F
Southwest	1.61°F	1.61°F	1.61°F
Northwest	1.54°F	1.52°F	1.56°F
Alaska	1.67°F	1.43°F	1.91°F
Hawaii	1.26°F	1.01°F	1.49°F
Caribbean	1.35°F	1.08°F	1.60°F

Table 6-2. Observed changes in annual average temperature (°F) for each National Climate Assessment region. Changes are the difference between the average for present-day (1986–2016) and the average for the first half of the last century (1901–1960 for the contiguous United States, 1925–1960 for Alaska, Hawai'i, and the Caribbean). (Source: USGCRP 2017 p. 190).

NCA Region	Change in Coldest Day of the Year	Change in Warmest Day of the Year
Northeast	2.83°F	−0.92°F
Southeast	1.13°F	−1.49°F
Midwest	2.93°F	−2.22°F
Great Plains North	4.40°F	−1.08°F
Great Plains South	3.25°F	−1.07°F
Southwest	3.99°F	0.50°F
Northwest	4.78°F	−0.17°F

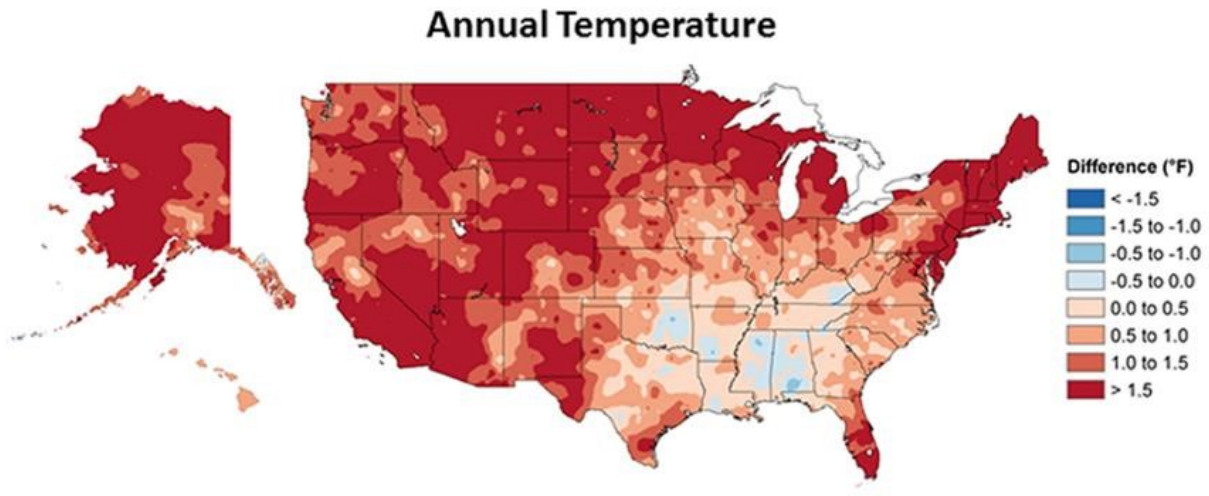

Figure 6-1. Observed change in annual temperatures between the 1986–2016 period and the period 1901–2016. (Figure source: USGCRP 2017 p. 188).

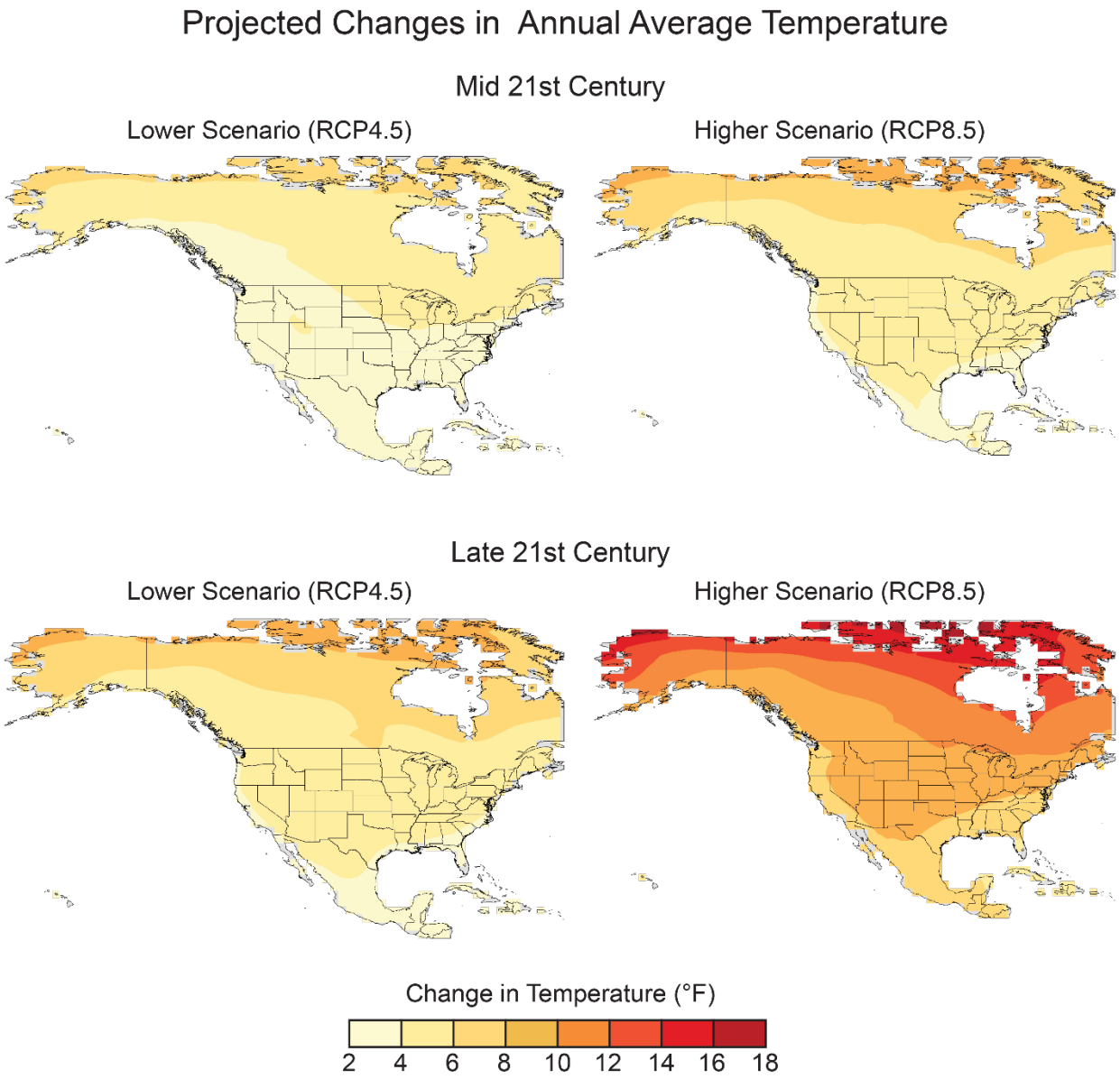

Figure 6-2. Projected changes in annual average temperatures (°F). Changes are the difference between the average for mid-century (2036–2065; top) or late-century (2070-2099; bottom) and the average for near-present (1976–2005). Each map depicts the weighted multi-model mean. Increases are statistically significant in all areas (that is, more than 50% of the models show a statistically significant change, and more than 67% agree on the sign of the change) (Figure source: USGCRP 2017 p. 196).

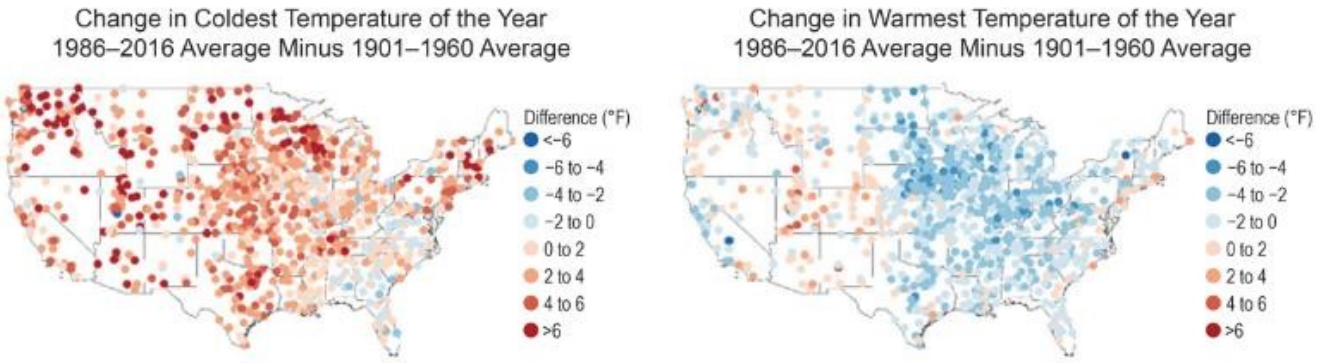

Figure 6-3. Change in the coldest temperature of the year (left) and warmest temperature of the year (right) (Figure source: USGCRP 2017 p. 190).

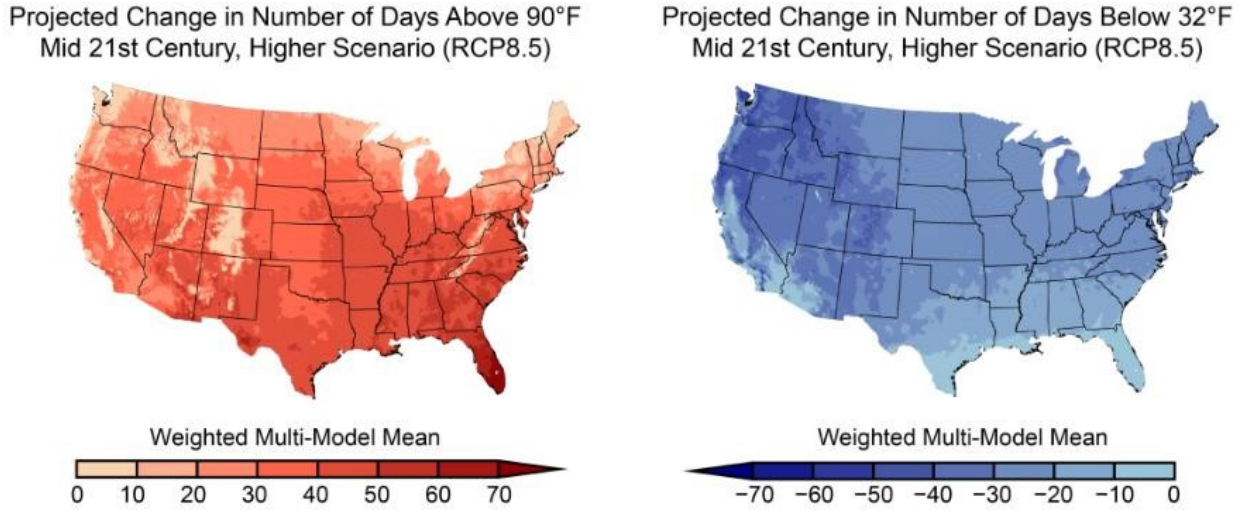

Figure 6-4. Projected change in days above 90°F (left) and projected changes in the number of days below 32°F (right) by mid-century (2040–2060) (Figure source: USGCRP 2017 p. 199).

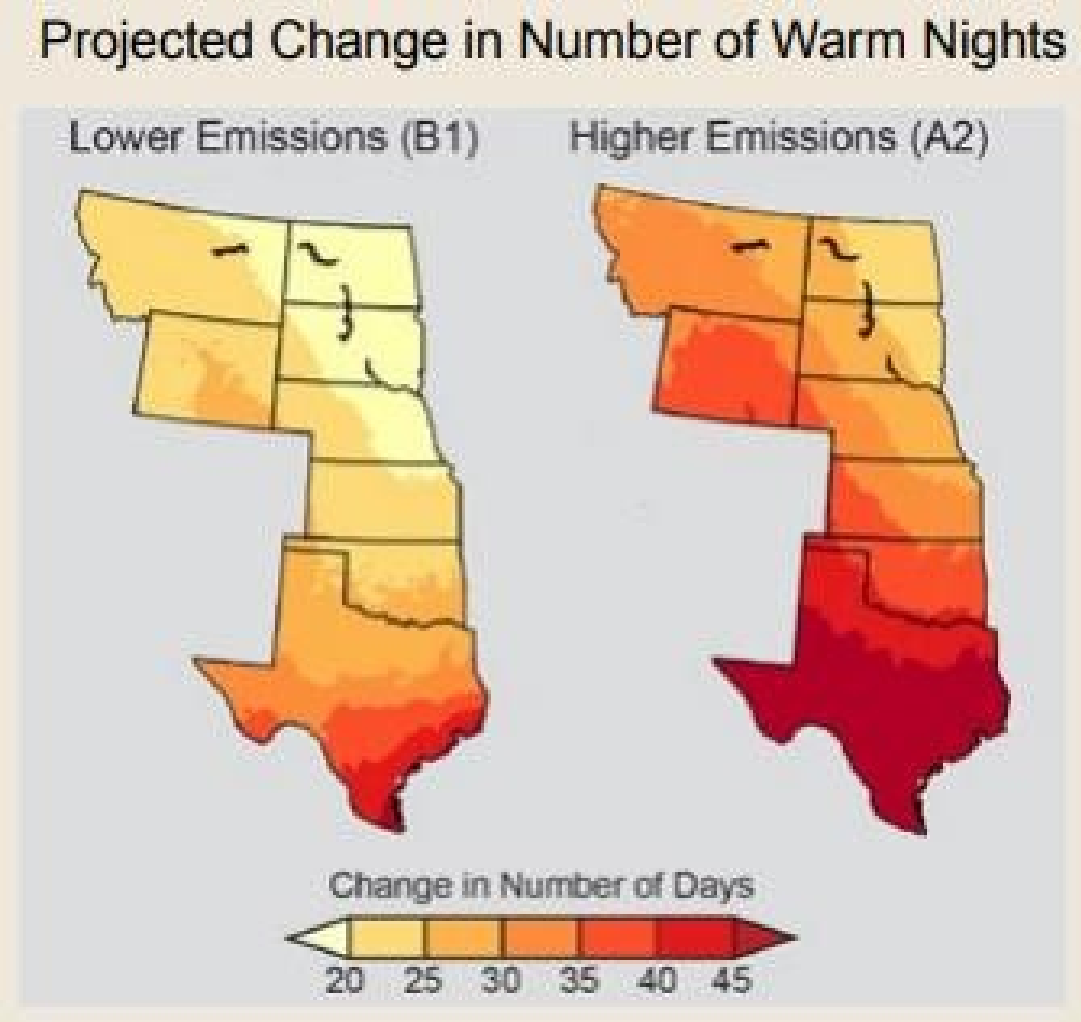

Figure 6-5. Projected change in the number of warm nights by emissions scenario – lower emissions (left) and higher emissions (right) (Figure source: Melillo et al. 2014 p. 444).

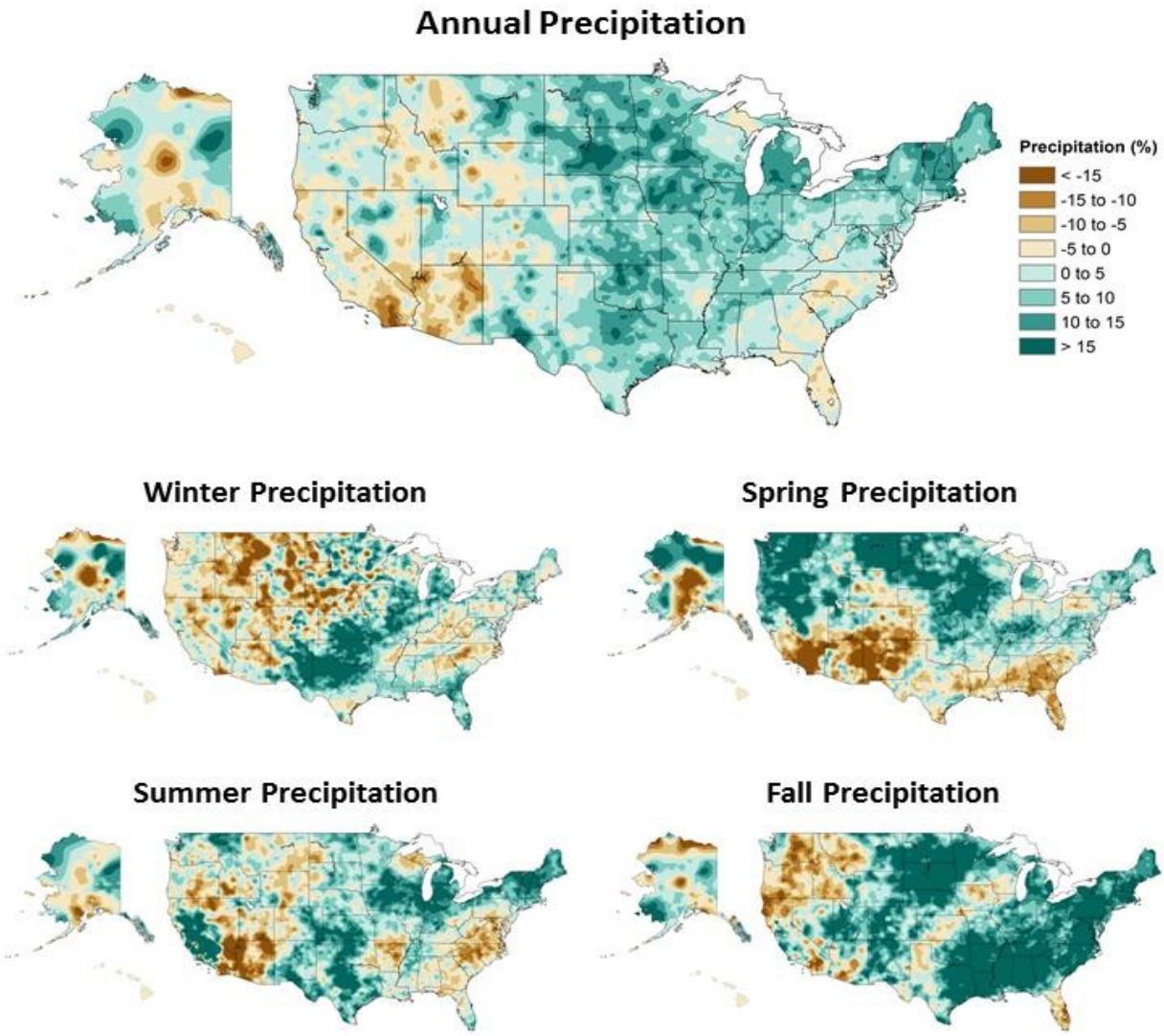

Figure 6-6. Annual and seasonal changes in precipitation of the United States. Changes are the average for the present-day (1986–2015) minus the average for the first half of the last century (1901–1960 for the contiguous U.S. and 1925–1960 for Alaska and Hawai'i) divided by the average for the first half of the century (Figure source: USGCRP 2017 p. 209).

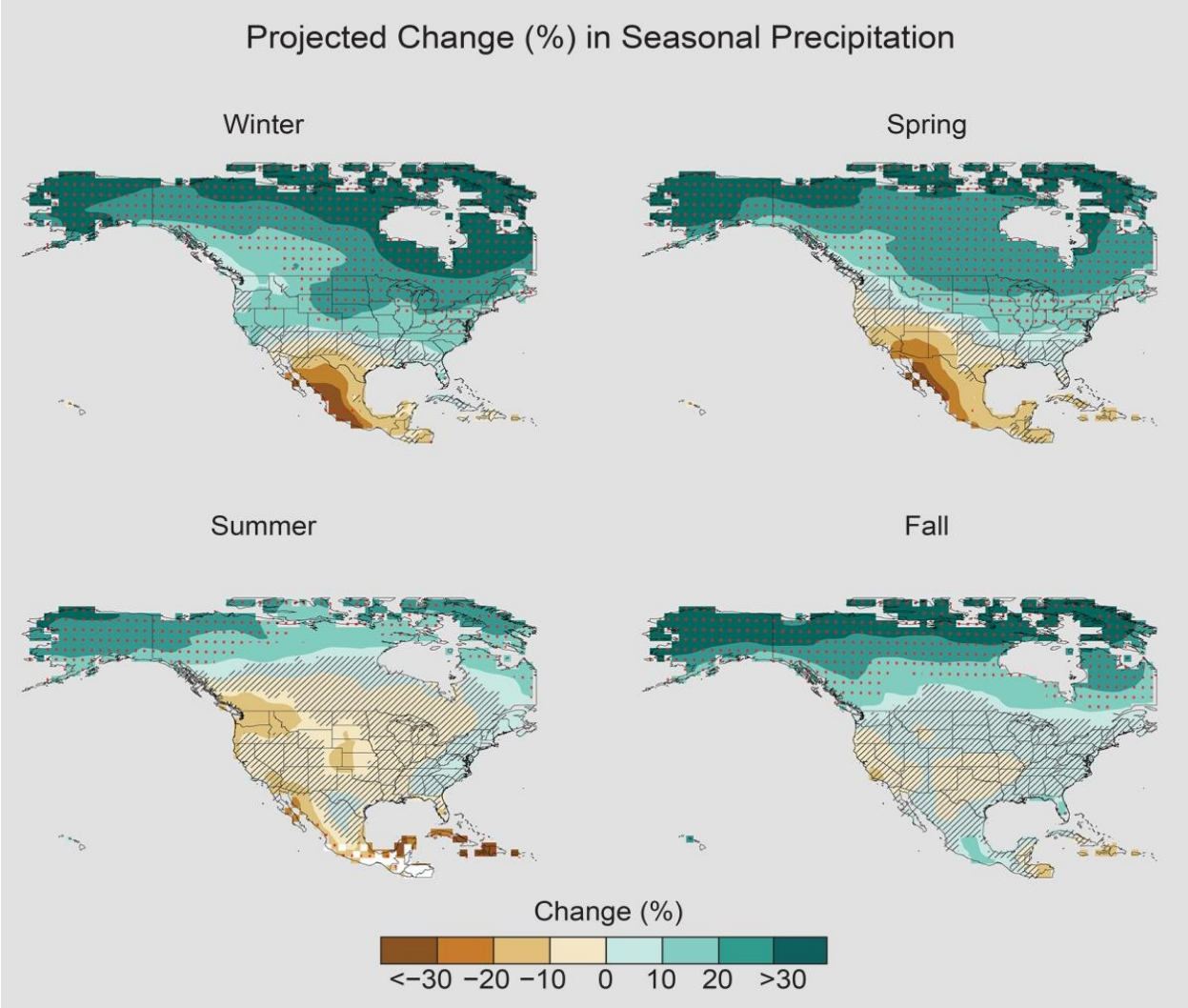

Figure 6-7. Projected change (%) in total seasonal precipitation from CMIP5 simulations for 2070–2099. The values are weighted multi-model means for the higher emissions scenario (RCP 8.5) and expressed as the percent change relative to the 1976–2005 average. Stippling indicates that the changes are large relative to natural variation, while hatching indicates that changes are small relative to natural variations (Figure source: USGCRP 2017 p. 217).

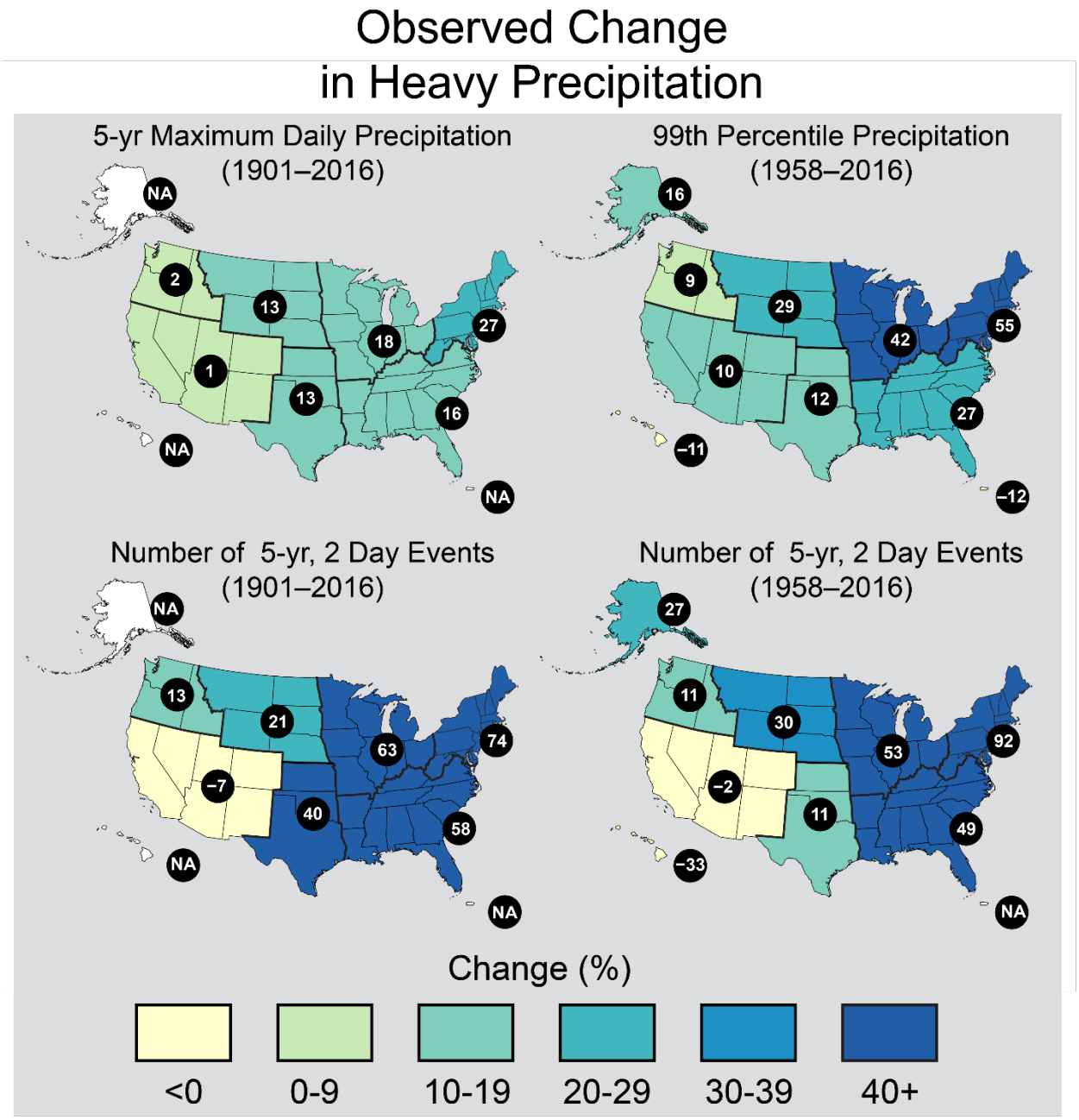

Figure 6-8. Changes in extreme precipitation. The percent change in maximum daily precipitation by 5-year periods (upper left), the percent change in the amount of precipitation falling in daily events that exceed the 99th percentile of precipitation days (upper right), the percent change in number of two day events with a precipitation total exceeding the largest two-day amount that would be expected to occur only once every five years based on data from 1901–2016 (lower left), and the percent change in number of two day events with a precipitation total exceeding the largest two-day amount that would be expected to occur only once every five years based on data from 1958–2016 (lower right) (Figure source: USGCRP 2017 p. 212).

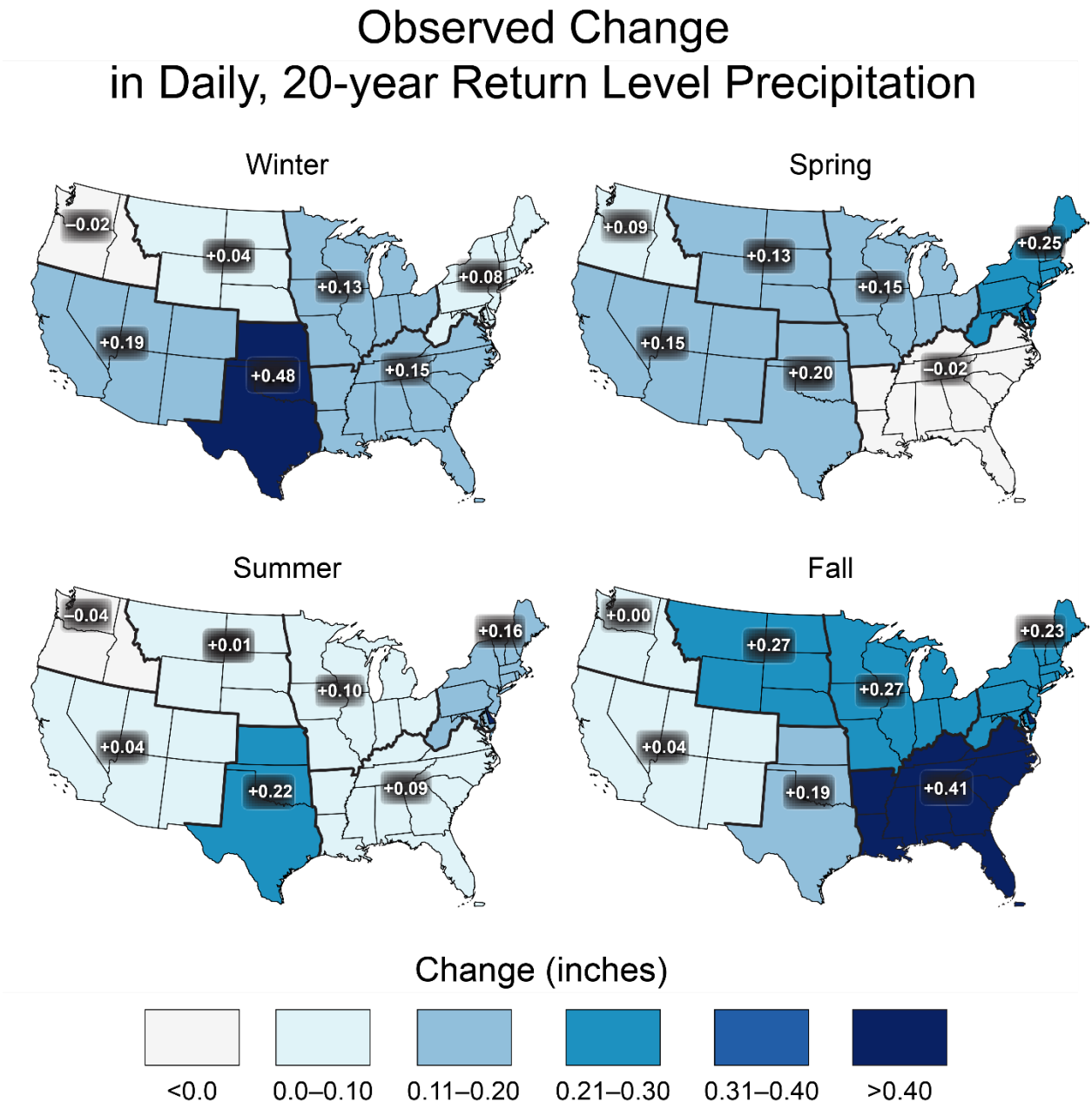

Figure 6-9. Observed changes in the 20-year return value of the seasonal daily precipitation totals for the contiguous U.S. over the period 1948–2015 using data from the Global Historical Climatology Network (GHCN) dataset (Figure source: USGCRP 2017 p. 211).

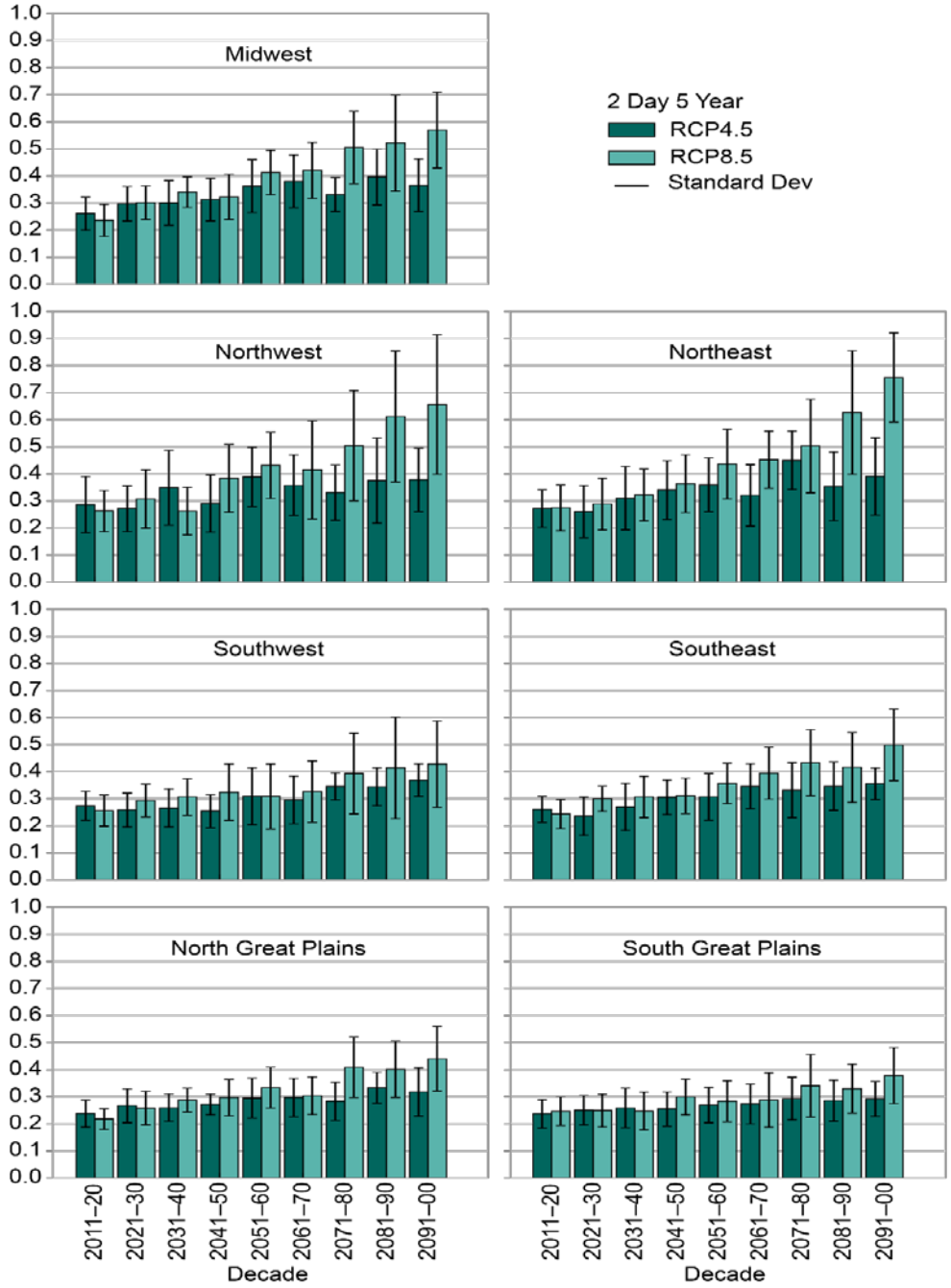

Figure 6-10. Regional extreme precipitation event frequency for a lower scenario (RCP4.5) (green; 16 CMIP5 models) and the higher scenario (RCP8.5) (blue; 14 CMIP5 models) for a 2-day duration and 5-year return. Calculated for 2006–2100 but decadal anomalies begin in 2011. Error bars are ±1 standard deviation; standard deviation is calculated from the 14 or 16 model values that represent the aggregated average over the regions, over the decades, and over the ensemble members of each model. The average frequency for the historical reference period is 0.2 by definition and the values in this graph should be interpreted with respect to a comparison with this historical average value (Figure source: USGCRP 2017 p. 219).

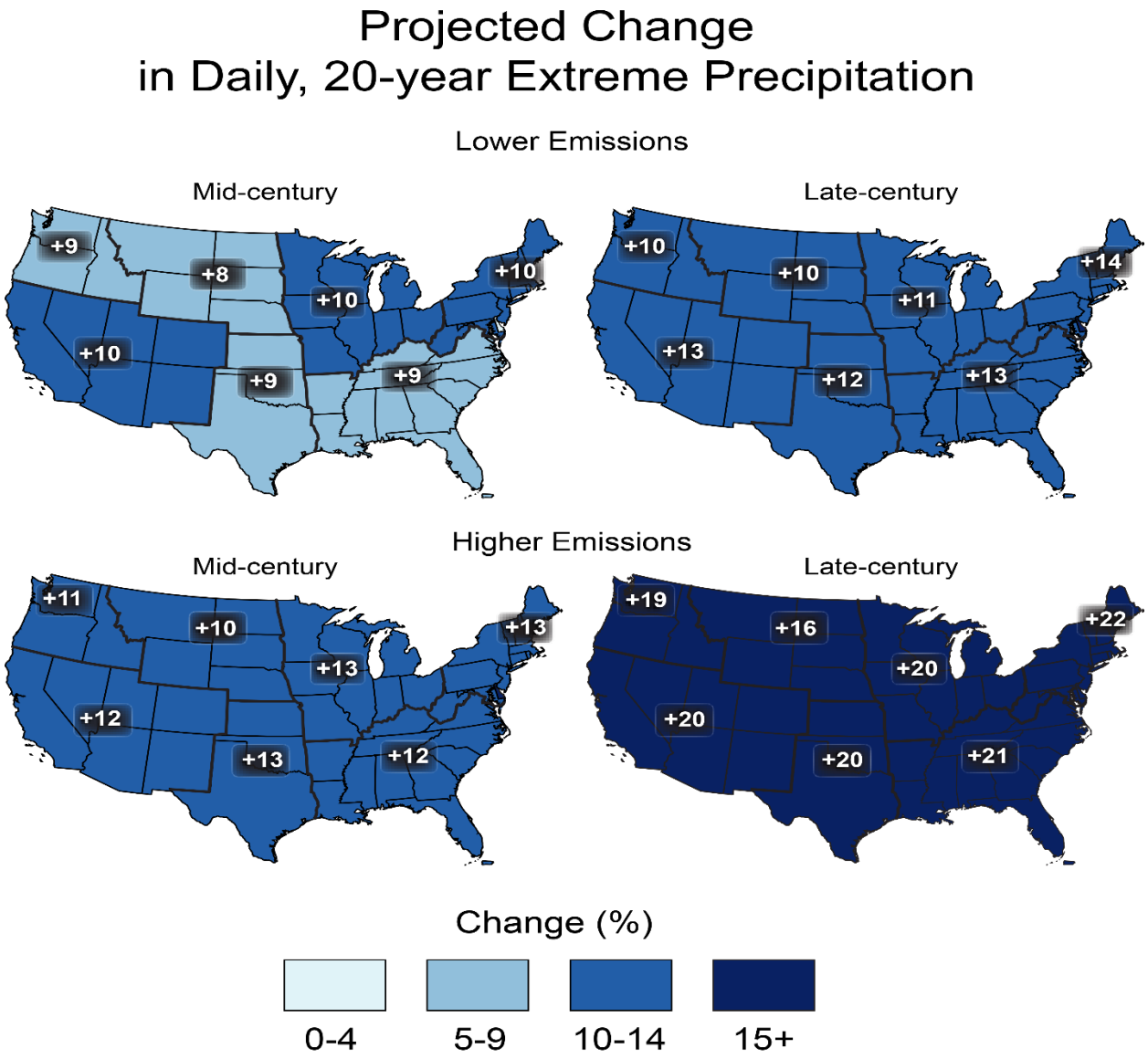

Figure 6-11. Projected change in the 20-year return period amount for daily precipitation for mid- (left maps) and late-21st century (right maps). Results are shown for a lower scenario (top maps; RCP4.5) and for a higher scenario (bottom maps; RCP8.5). These results are calculated from the LOCA downscaled data (Figure source: USGCRP 2017 p. 220).

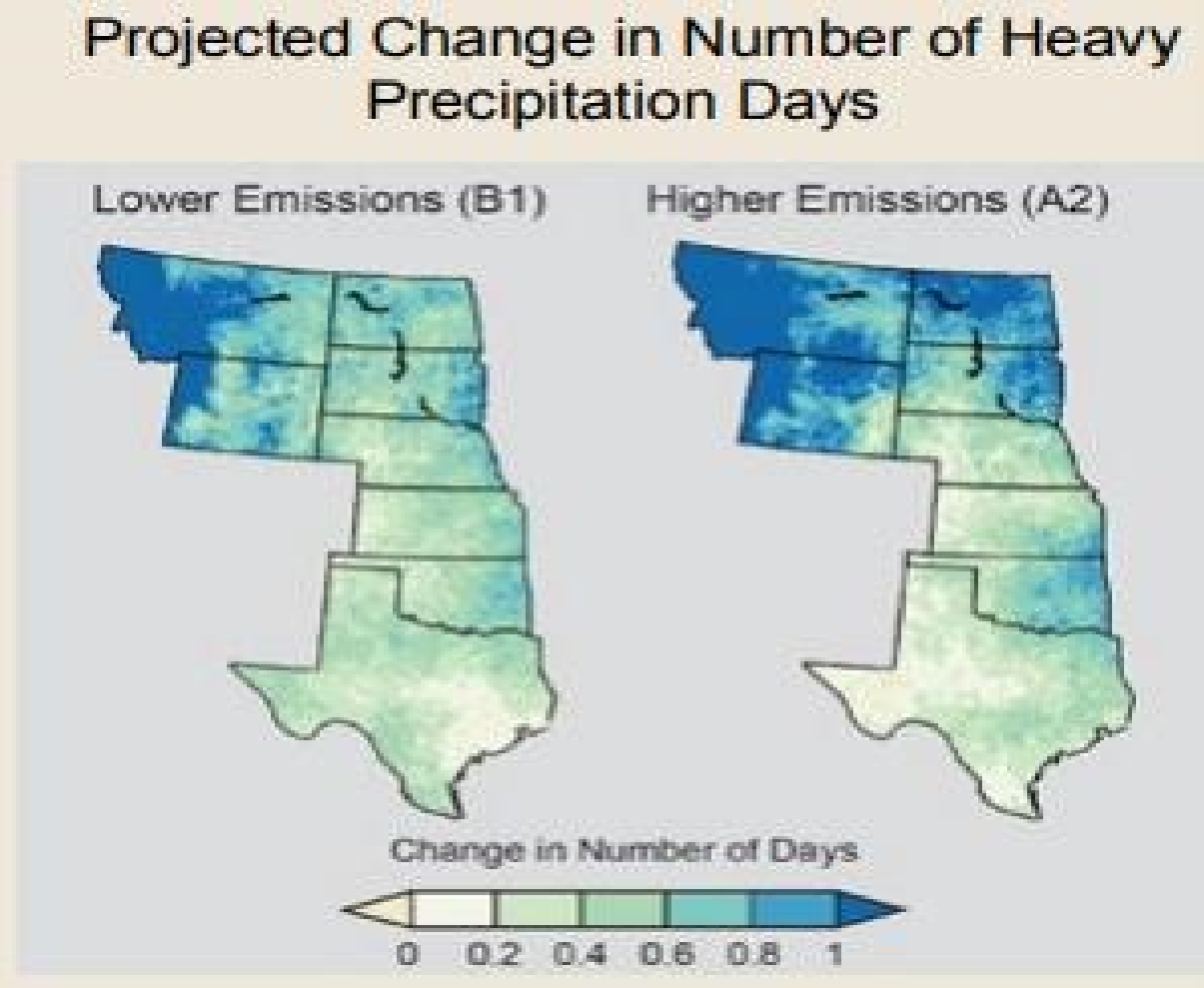

Figure 6-12. Projected change in the number of heavy precipitation days by emissions scenario – lower emissions (left) and higher emissions (right) (Figure source: Melillo et al. 2014 p. 445).

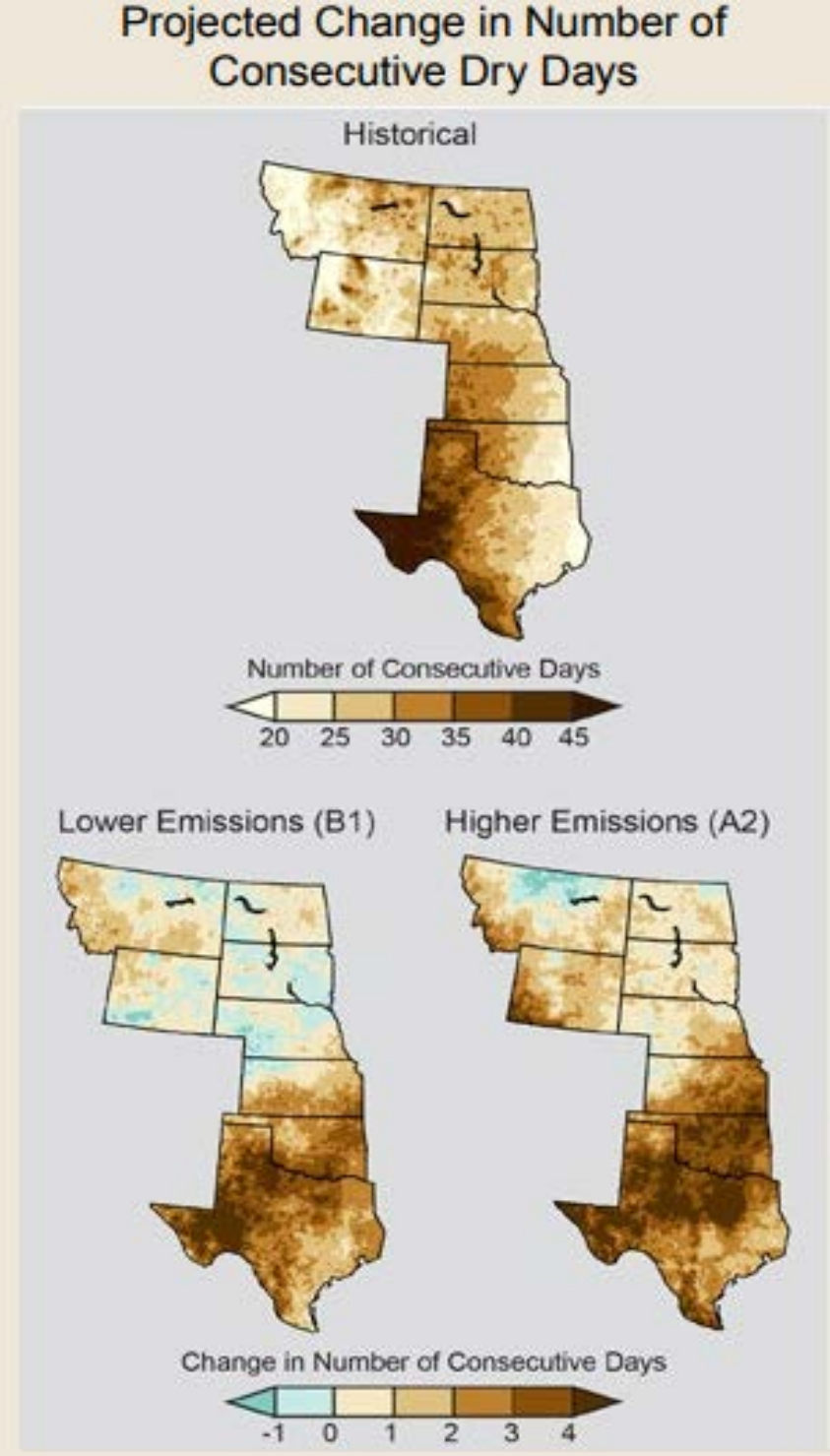

Figure 6-13. Maps showing the maximum annual number of consecutive days in which limited (less than 0.01 inches) precipitation was recorded on average from 1971 to 2000 (top), projected changes in the number of consecutive dry days assuming substantial reductions in emissions (B1), and projected changes if emissions continue to rise (A2) (Figure source: Melillo et al. 2014 p. 445).

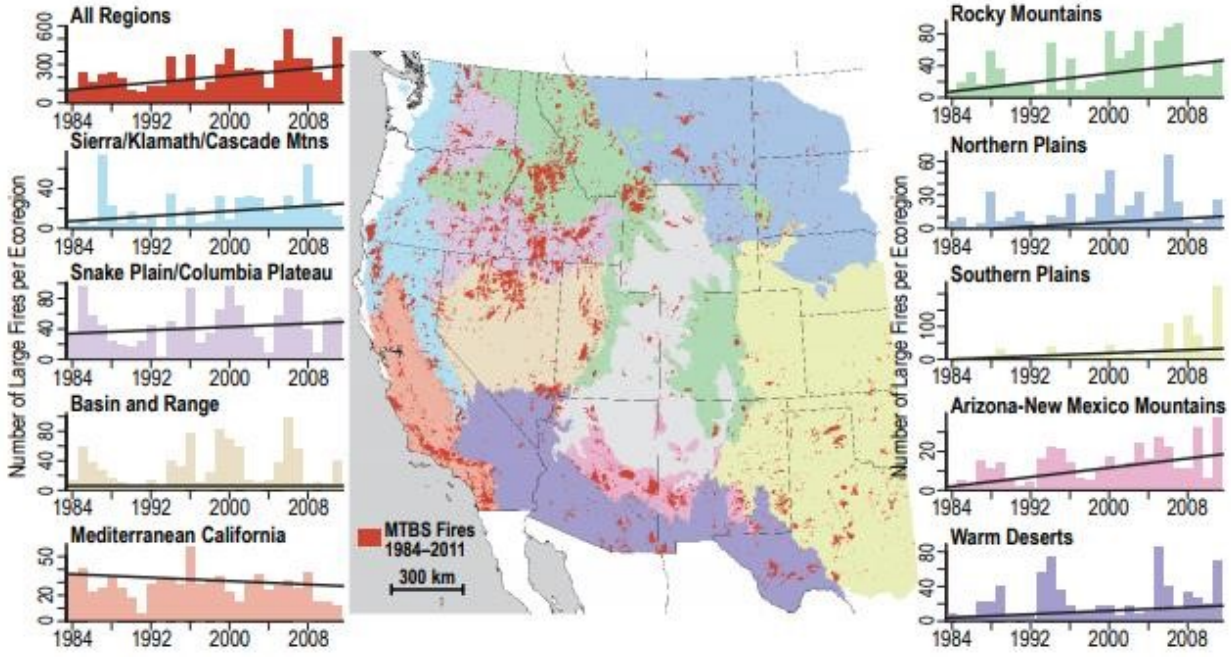

Figure 6-14. Trends in the annual number of large fires in the western U.S. for a variety of ecoregions. The SGP region is highlighted in yellow where a significant upward trend is noted (Figure source: USGCRP 2017 p. 243).

7 Southwest Region

7.1 Summary of Climate Projections for the Southwest Region

7.1.1 Temperature

Observed trends in temperature indicate that temperatures across the Southwest region have increased roughly 0.17°F per decade during the period from 1895-2011. Every state in the region has seen temperatures increase over 1.5°F in some areas, while statistically significant upward trends have been detected from analyzing temperature deviations from the 1901-1960 average (see Figure 7-1 and Figure 7-2). Model simulations project temperature to increase in each future time period (2021-2050, 2041-2070, and 2070-2099, hereafter referred to as near-, mid-, and late-century, respectively), with both high (A2) and low (B1) emissions scenarios from the CMIP3 global climate simulations indicating a statistically significant increase in temperature (see Figure 7-3).

The near century is projected to see annual temperature increases ranging between 1.5 and 3.5°F across both emissions scenarios. The mid-century is projected to see temperature increases range between 2.5 and 4.5°F for the B1 scenario and 2.5 and 5.5°F for the A2 scenario. Late-century temperatures are simulated to increase between 3.5 and 5.5°F for the B1 scenario, but the A2 scenario projects an increase between 5.5 and 9.5°F (note that the temperature increases are relative to the reference period of 1971-1999) (Figure 7-4). Uncertainty increases from near-century to late-century, but annual temperature projections indicate increases in temperature for each time period, even when NARCCAP models are included in the analysis. Coastal areas stand to see slightly smaller increases in temperature due to the moderating influence of the Pacific Ocean. Temperatures vary across the region due to the presence of both the ocean and elevation differences due to mountainous terrain.

With observed temperatures having increased and model projections all indicating temperature increases in the future, there is a very low probability that annual average temperatures will decrease across the region.

The Southwest region has seen an increase in the hottest annual temperature on the magnitude of 0.50°F. There has also been a statistically significant increase in the occurrence of heat waves throughout the region. Model simulations (NARCCAP and Daily CMIP3) suggest that the number of days with temperatures above 90, 95, and 100°F will increase substantially under the high (A2) emissions scenario for the mid-century (2041-2070) time period. Sillmann et al. (2013) utilized a CMIP5 model ensemble with three emission scenarios (RCP2.6, 4.5, and 8.5), and their results suggest an increase in annual maximum temperatures in the late century (2081-2100). However, the magnitude of the increase varies on the emission scenario, with values ranging from roughly 1 to 15°F in western North America, which includes the Southwest region (see Figure 7-5). According to the Fourth National Climate Assessment (NCA4), the RCP8.5 emission scenario for the mid-century (defined as 2036-2065) time period yields an increase in the hottest annual temperature by 5.85°F (See Figure 7-5). While the lower emissions scenarios yield a smaller projected increase, there are no projections that exhibit a decrease in the hottest annual temperature. As such, there is low confidence that the hottest annual temperature will decrease.

The Southwest region has seen an increase in the magnitude of the lowest annual temperature by 3.99°F (See Table 7-1). The region has seen multiple long-term stations exhibit an increase in the lowest annual temperature, with several exhibiting changes on the order of 6°F or greater (see Figure 7-6). Changes in cold extremes are more pronounced than warm extremes, as can be seen in Figure 7-2. Model simulations (NARCCAP and Daily CMIP3) suggest that the number of days with temperatures below 32, 10, and 0°F will decrease substantially under the high (A2) emissions scenario for the mid-century (2041-2070) time period (see Figure 7-7). According to the Fourth National Climate Assessment (NCA4), the RCP8.5 scenario for the mid-century (defined as 2036-2065) time period yields an increase in the lowest annual temperature by 6.13°F (see Figure 7-5). Increases in the magnitude of the lowest annual temperature are projected to be more pronounced in the northern part of the region. Thus, Utah, northeast Nevada, and southwest Colorado have the potential to have greater increases than other parts of the region.

Several model simulations with different time scales and emissions scenarios all predict continued increases in the magnitude of the lowest annual temperature. With observed trends indicating warming and projections suggesting future warming, the probability that the lowest annual temperature will decrease is very low.

Since the 2000s, there have been multiple heat waves (defined as a 4-day period where temperatures are hotter than what is experienced once in five years) throughout the region, a trend that is considered to be statistically significant (see Figure 7-8). Model projections from the NARCCAP and CMIP3 downscaled data sets indicate that the number of consecutive days with temperatures ≥ 95°F and 100°F will increase (see Figure 7-7). Furthermore, the CMIP5 models with both low (RCP4.5) and high (RCP8.5) scenarios predict that days with temperatures ≥ 90°F will increase (see Figure 7-9). Mountainous parts of the region (central Colorado, central Utah, and northern New Mexico) are projected to have smaller increases in the number of 90°F days due to the relative lack of days exceeding that threshold, with projected increases along the Rocky Mountains not considered to be statistically significant. Conversely, interior southern areas of the region could expect the greatest increase.

While direct information pertaining to the trend in days with temperatures ≥ 90°F is not readily available for the Southwest region, model projections using various model ensembles and emissions scenarios all predict an increase in the number of days with temperatures ≥ 90°F, regardless of uncertainty pertaining to the exact number of days. As a result, it is possible that the number of days with temperatures ≥ 90°F could decline, but unlikely.

In recent years, there has been a statistically significant decrease in the number of cold waves (defined as a 4-day period where temperatures are colder than what is typically experienced once every five years) throughout the region. Furthermore, cold extremes have become less severe over the past century.

Model projections using the NARCCAP and CMIP3 downscaled models with both low and high emission scenarios predict the number of days with freezing temperatures (here taken to be temperatures ≤ 32°F) will decrease by mid-century (2041-2070), with the NARCCAP models being considered statistically significant across the whole region. The models also agree that the changes in freezing temperatures will be a decrease across the entire region. The CMIP5 model ensemble also predicted a decrease in the number of days with freezing temperatures by mid-century (2036-2065) for the high emission scenario (see Figure 7-3). As a result, there is low confidence that the number of days with freezing temperatures will increase and high confidence that they will decrease. Coastal California as well as southern California and Arizona are projected to have the smallest decrease in the number of freezing days, primarily due to the relative lack of freezing temperatures those parts of the region experience. Areas of high elevation are predicted to have the largest decrease in the number of days with freezing temperatures.

Minimum temperatures have been observed to have increased at a rate up to 1°F per decade during the period from 1895-2011 (see Figure 7-10). Furthermore, the diurnal temperature range has been observed as having decreased due to the increase in minimum temperatures. Urban areas tend to have warmer nighttime temperatures due to the urban heat island effect (temperatures tend to be warmer on the order of 1.8 to 4.5°F in urban areas compared to rural areas). As a result, urban areas such as Los Angeles, Phoenix, and Denver would stand to have higher minimum nighttime temperatures. Projections indicate nighttime temperatures will increase predominantly inland, with Coastal California and the Rocky Mountains serving as buffers where increases are less pronounced.

The daily temperature range exhibits a decreasing trend in the region from the period of 1911-2012, with the daily temperature range having decreased almost 2°F during this span (see Figure 7-11). Minimum temperatures (which more often than not occur at night) have increased during the period from 1895-2011. Since model projections (with different emissions scenarios) have minimum temperatures continuing to increase (see Figure 7-12), especially at a rate greater than daily maximum temperatures, it is highly likely that the daily temperature range will continue to decrease as well.

7.1.2 Precipitation

Precipitation across the region did not exhibit a consistent pattern, with increases balanced by decreases (see Figure 7-13). To further reinforce this, there is no statistically significant trend in precipitation throughout the region, as determined from the 1901-1960 averages (see Figure 7-14). CMIP3 models with low (B1) and high (A2) emissions scenarios each predicted decreases in precipitation for the near, mid, and late century time scales. However, the emissions scenarios yielded different results. The B1 scenario does not begin to exhibit statistically significant changes until the mid-century (2055) time period. The A2 emissions scenario was similar to the B1 scenario in that the near century would not exhibit a statistically significant change. However, the A2 models were in agreement that significant decreases in precipitation would occur starting in the near century, with the greatest decreases located in the southern part of the region (see Figure 7-15). The NARCCAP regional climate model ensemble with the A2 emissions scenario predicted decreases in precipitation by mid-century (2041-2070) across much of the region, with increases in northern Nevada and Utah (see Figure 7-16). However, the range of model-simulated changes is quite large, which reduces confidence. Since precipitation

estimates have such large uncertainties, and the potential for both increases and decreases in precipitation are possible, there exists an equal chance that precipitation will either increase or decrease through time.

Rainfall intensity in the Southwest has seen very slight increases, depending on the metric used to define intensity. The daily 20-year return level definition (the amount of rain that falls in a day that a location might experience once every 20 years) shows very slight increases in summer and fall (0.04 inches for both seasons) and moderate increases in winter and spring (0.19 and 0.15 inches, respectively), which combine to a 0.42 inch annual increase (see Figure 7-17). There has also been a noted increase in the value of the 5-year maximum daily precipitation (1% increase from 1901-2016) and a 10% increase in 99th percentile precipitation (see Figure 7-18).

LOCA downscaled data predict an increase in the 20-year return period amount for daily precipitation for both low and high emission scenarios. For the low emissions scenario, the 20-year return period amount is projected to increase 10% by mid-century and 13% by late-century, while the high emissions scenario calls for increases of 12% by mid-century and 20% by late century.

For the period from 1901-2016, the region has seen a 7% decrease in the number of 2-day rainfall events that would normally be expected to occur once every five years. The number of 1-day rainfall events that would normally be expected to occur once every five years has seen a decrease in recent years, but the trend is not considered to be statistically significant.

Simulations involving NARCCAP regional climate models using a high emissions scenario predicted an increase in the number of days with rainfall totals exceeding 1-inch. Increases in the number of days with rainfall amounts greater than 2, 3, and 4 inches are also predicted. However, the standard deviation exceeds the projected mean with respect to 1-inch days, with the mean gradually exceeding the standard deviation as rainfall totals increase. This introduces an element of uncertainty. LOCA downscaled data using both low and high emission scenarios predict an increase in the number of 2-day, 5-year events (2-day rain events with totals expected once every 5-years) as the decades progress. However, these increases are gradual.

With respect to seasonality, the region has seen an increase in fall precipitation while winter, spring, and summer precipitation has decreased, calculated as the difference between the 1901-1960 average and the 1986-2015 average. However, there has not been a statistically significant trend in precipitation per season throughout the region, as determined from the 1901-1960 average.

NARCCAP model simulations using a high emissions scenario indicated increases in precipitation for fall, winter, and spring, and a decrease in precipitation for summer by midcentury (2041-2070). However, the only portions of these predictions that were statistically significant were decreases in parts of Arizona in spring and parts of Colorado in summer. No significant trend was identified in the fall or winter (see Figure 7-16). The CMIP5 simulations for late century (2075-2099) with high emissions predicted a decrease in summer precipitation and an increase in winter precipitation across most of the region. Much like the NARCCAP simulations, however, very few of the projected changes were considered statistically significant (see Figure 7-19).

The observed seasonality varies for each season. Winter precipitation saw decreases across much of the region except for New Mexico, which experienced an increase. Spring precipitation increased in northern California and Nevada but decreased everywhere else. Summer precipitation increased in California, New Mexico, and eastern Colorado, but strongly decreased in Arizona and southern Nevada. Fall precipitation decreased in northern California and southern Arizona but increased everywhere else. Projected changes in seasonality appear to have a north/south gradient, with increased precipitation in the north and decreased precipitation in the south.

7.1.3 Other Stressors

The Southwest region is prone to experiencing flooding, with winter storms, the North American monsoon, East Pacific tropical cyclones, and atmospheric rivers contributing to heavy rain and snowfall events along the region. Furthermore, coastal flooding due to sea level rise is an issue to consider, as sea level has risen roughly 0.5 inches per decade for the period from 1993-2015 (see Figure 7-20). Sea level changes along the California coast have been projected to increase 3-4 feet by 2100, according to the Interagency Intermediate Scenario (see Figure 7-21). Extreme precipitation is projected to increase, both in terms of the number of days as well as the amount of precipitation (see precipitation stressors for more information), Atmospheric rivers are also projected to become more frequent and intense along the West Coast in the future. However, peak streamflow rates have declined across the region for the period from 1901-2008, which reduces confidence.

Sea level rise, as the name implies, would have a greater impact in coastal regions as opposed to locations inland. The presence of mountains (and thus orthographic enhancement of precipitation) also contributes to a greater risk of floods on the windward side of mountain ranges, especially those closer to the coast. The North American monsoon contributes to flooding in southern Arizona and New Mexico.

Drought is most pronounced in the region when winter precipitation is deficient, although summer precipitation deficits can play a role. Drought can also be exacerbated by lack of snowpack, as snowmelt can help mitigate drought in future seasons. Despite decreases in New Mexico, California, and Colorado, multiple climate divisions throughout the region have seen increasing drought, as defined by the Palmer Drought Severity Index, with significant trends present in Arizona and Nevada (although it should be mentioned that Colorado has seen one climate division experience a statistically significant decrease in drought; see Figure 7-22).

NARCCAP model projections using a high (A2) emissions scenario suggest that the number of consecutive days with precipitation less than a tenth of an inch will increase by mid-century, with much of the increases considered to be statistically significant (see Figure 7-23). Furthermore, the CMIP5 model ensemble with a high (RCP8.5) scenario also predicted significant increases in the number of consecutive dry days (defined as days with less than 0.04 inches of rain) by end of the century (see Figure 7-24). Another potential cause of drought is the projected decrease in snowpack atop the various mountains located throughout the region, as predicted by the CAM5 model with the RCP8.5 scenario.

Drought characteristics are not uniform across the region, according to Kunkel et al. (2013). Colorado, for instance, can receive precipitation via multiple sources, which reduces lengthy

droughts. The Colorado River Basin is projected with high confidence to experience more frequent and intense drought, while the northern Sierra Nevada watersheds have potential to become wetter, thus mitigating drought. Projected increases in consecutive days with low rainfall totals are greatest in the southern part of the region.

There has been an increase in the number of large wildfires (area burned ≥ 405 hectares) per year for the period of record from 1984-2011, with most increases in the region statistically significant (see Figure 7-25). This increase in wildfires has been driven in part by warmer and drier conditions. In fact, warmer and drier conditions contributed to increasing burned area in mid-elevation conifer forests by 650%.

Model simulations project wildfires to increase in occurrence, with one model simulation predicting increases in burn areas across much of the region if temperatures were to rise 1.8°F (see Figure 7-26). The major causes for uncertainty in these projections are the lack of studies focusing on other regions, projections tending to focus on limited areas, and other factors of climate change (water deficits, insect infestations) reducing fuel loads, which inhibit wildfire development. The sensitivity of fuel to climate conditions and fuel availability are the main causes for sub-regional variability. Areas of great vulnerability throughout the region include the conifer forests of California and the sky islands of Arizona. Areas not projected to see increases include coastal California and eastern New Mexico.

In the last 40 years, the first wildfires of the year have been observed to start earlier, while the last fires start later. As a result, the length of fire season has been observed as having increased. Since temperature and soil moisture are among the more important aspects of the relationship between fire frequency and ecosystems, and projections for the region involve increased temperature and reductions in soil moisture, it stands to reason that the length of the fire season in the region will continue to increase.

The Southwest region experiences large-scale winter storms during the winter. These storms bring rain, snow, and high winds to the region, decreasing in frequency from north to south. Some studies have found changes in winter storm tracks, but overall very few studies have examined this change. Studies exploring arctic amplification of winter storms have returned mixed results, and projections for future winter storms yielded large model-to-model differences. As a result, there is low confidence in predicting if winter storm intensity will increase or decrease in the future.

Migration of winter storm tracks have been northward, but there is considerable uncertainty about how this will impact winter storm intensity in the future. The El Nino Southern Oscillation influences winter storm tracks, moving tracks further south (north) when in a strong warm (cold) phase. Due to the presence of multiple mountain ranges, winter storm precipitation type varies across the region due to elevation.

According to Kunkel et al. (2009), snowfall has seen an increase in the eastern half of the region, while the southern and western parts of the region have seen a decrease, using the period from 1937-2007 (see Figure 7-27). These increases and decreases range in magnitude from 0.1% per decade to 1.2% or greater. Furthermore, there has been an observed change in precipitation type throughout the region as systems that used to be predominately snow have transitioned to rain.

Both the CMIP3 and CMIP5 model suites predict that snowpack will decrease in the future, with both models using a high emissions scenario. In both cases, snowpacks face reductions up to 40%. Furthermore, snowpacks in southernmost mountains are projected to disappear by the end of the 21st century, regardless of emissions scenario. Precipitation changes at high elevations (a naturally cold environment) introduce more uncertainty, so mountainous terrain throughout the region could experience increases in snowfall totals.

Since the decade from 1966-1977, there has been a decrease in the number of ice storms throughout the northern portion of the region (see Figure 7-28). As mentioned in the snowfall stressor report, there has been an observed change in precipitation type throughout the region as systems that used to be predominately snow have transitioned to rain. This, coupled with the relatively confident projections that temperature will increase in the future regardless of emissions, enforces the notion that ice storms and freezing rain will decrease throughout the region, as precipitation regimes change to become predominately rain. According to the Second National Climate Assessment, knowledge of ice storms is relatively limited, making it difficult to ascertain both observed trends and projected changes. However, having observed changes in ice storms helps raise confidence in this projection.

The decreasing trend in ice storms was detected mainly in Utah, with slight decreases noted in central California, eastern Nevada, northern Arizona, eastern Colorado, and eastern New Mexico. Mountainous terrain will have a greater chance of seeing freezing rain and ice storms.

7.2 Tables and Figures: Southwest Region

Table 7-1. Observed changes in the coldest and warmest daily temperatures (°F) of the year for each National Climate Assessment region in the contiguous United States. Changes are the difference between the average for present-day (1986–2016) and the average for the first half of the last century (1901–1960). Estimates are derived from long-term stations with minimal missing data in the Global Historical Climatology Network–Daily dataset (Source: USGCRP 2017 p. 190).

NCA Region	Change in Coldest Day of the Year	Change in Warmest Day of the Year
Northeast	2.83°F	−0.92°F
Southeast	1.13°F	−1.49°F
Midwest	2.93°F	−2.22°F
Great Plains North	4.40°F	−1.08°F
Great Plains South	3.25°F	−1.07°F
Southwest	3.99°F	0.50°F
Northwest	4.78°F	−0.17°F

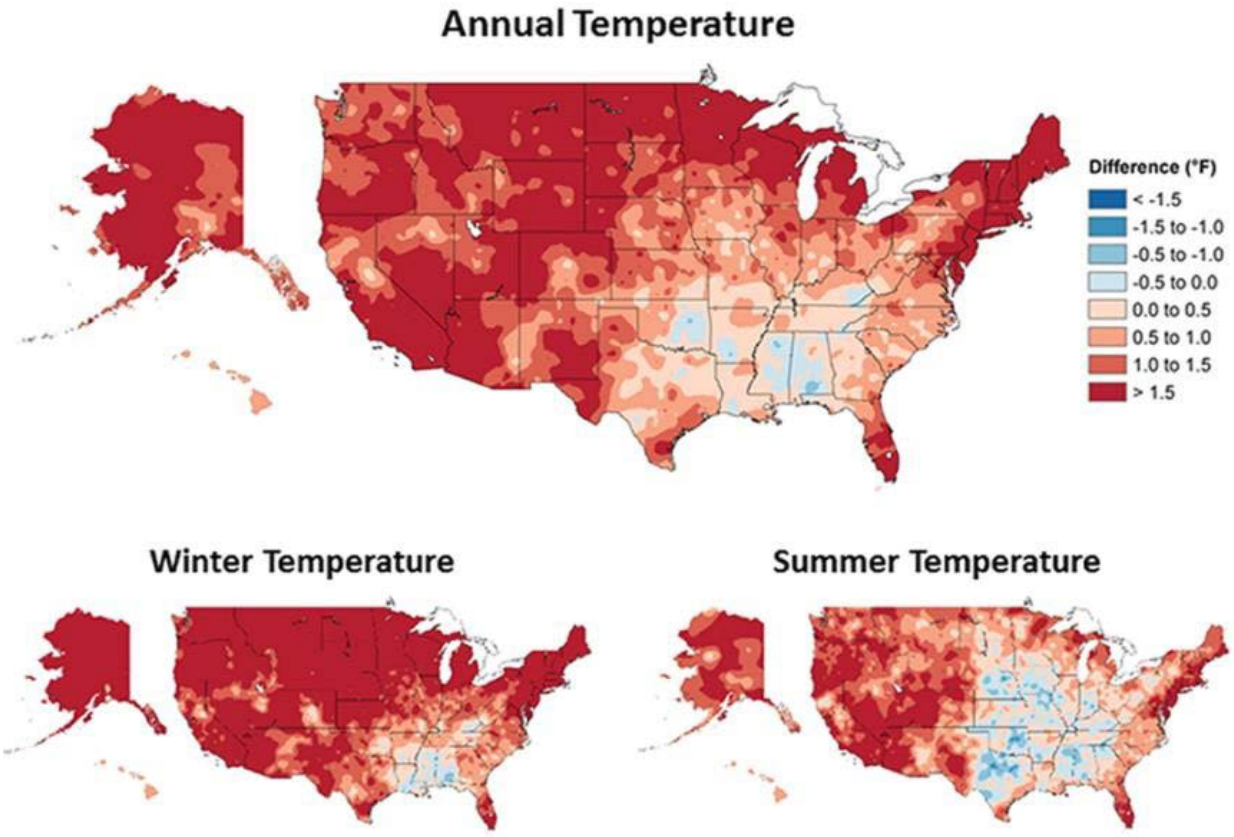

Figure 7-1. Observed changes in annual, winter, and summer temperature (°F) between present-day (1986–2016) averages and 1901–1960 (continental United States)/1925–1960 (Alaska & Hawai'i) averages. Estimates are derived from the nClimDiv dataset (Figure and caption adapted from USGCRP 2017 p. 188).

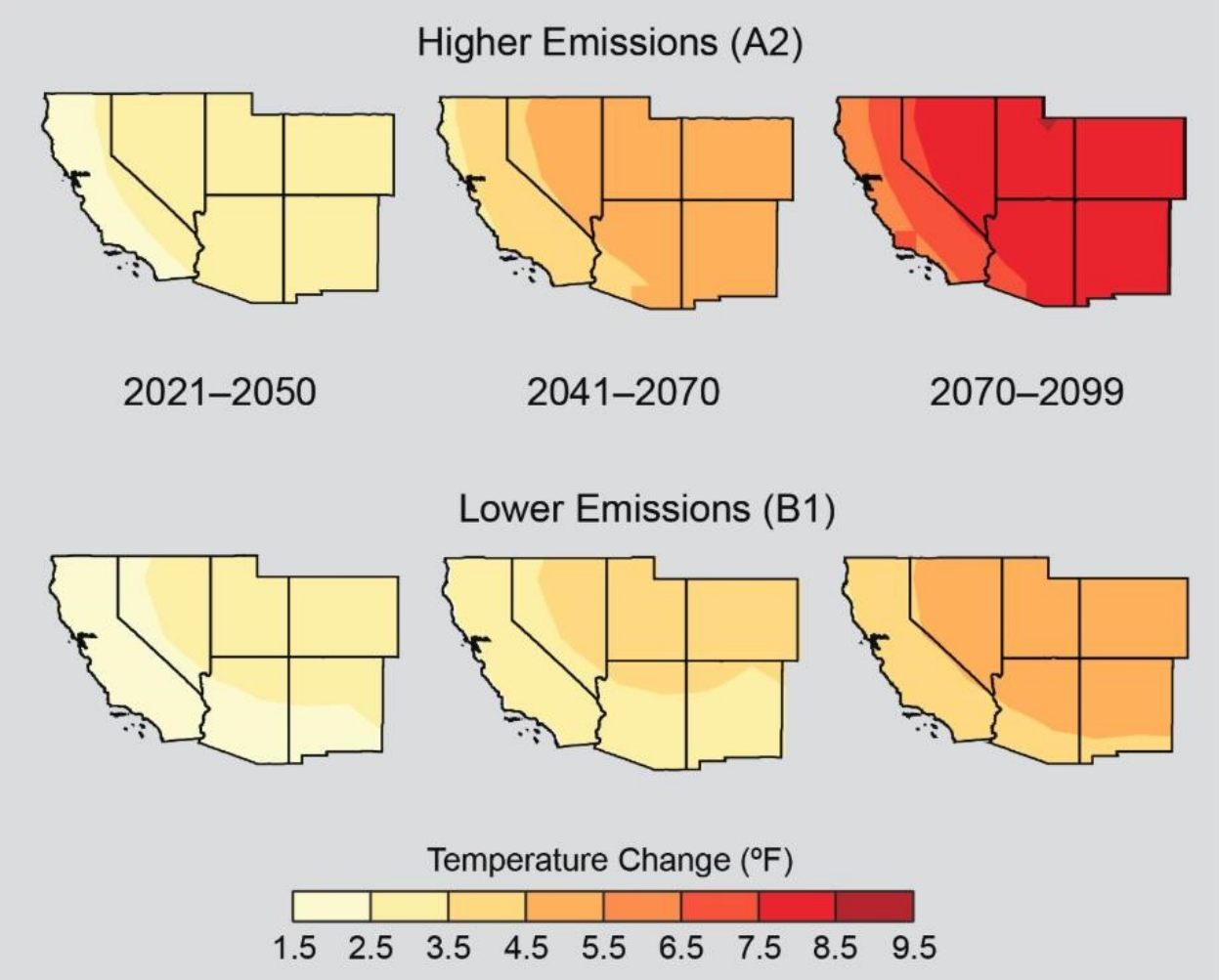

Figure 7-2. Maps showing projected changes in average temperature, as compared to 1971-1999. Top row shows projections assuming heat-trapping gas emissions continue to rise (A2). Bottom row shows projections assuming substantial reductions in emissions (B1) (Figure source: Melillo et al. 2014 p. 464).

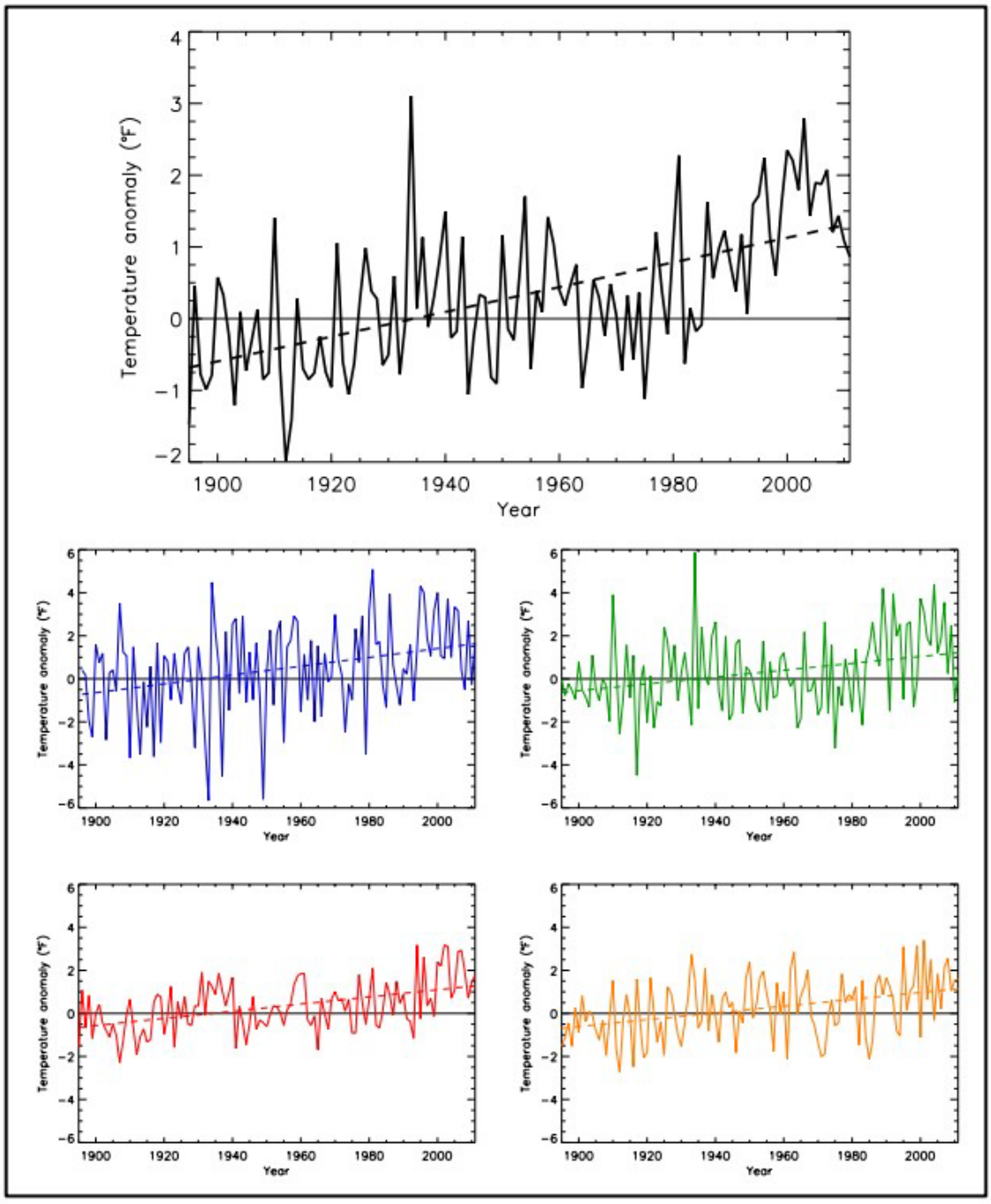

Figure 7-3. Temperature anomaly (deviations from the 1901–1960 average in °F) for annual (black), winter (blue), spring (green), summer (red) and fall (orange), for the Southwest U.S. Dashed lines indicate the best fit trend. Trends are upward and statistically significant on an annual basis for all seasons (Figure source: Kunkel et al. 2013, part 5).

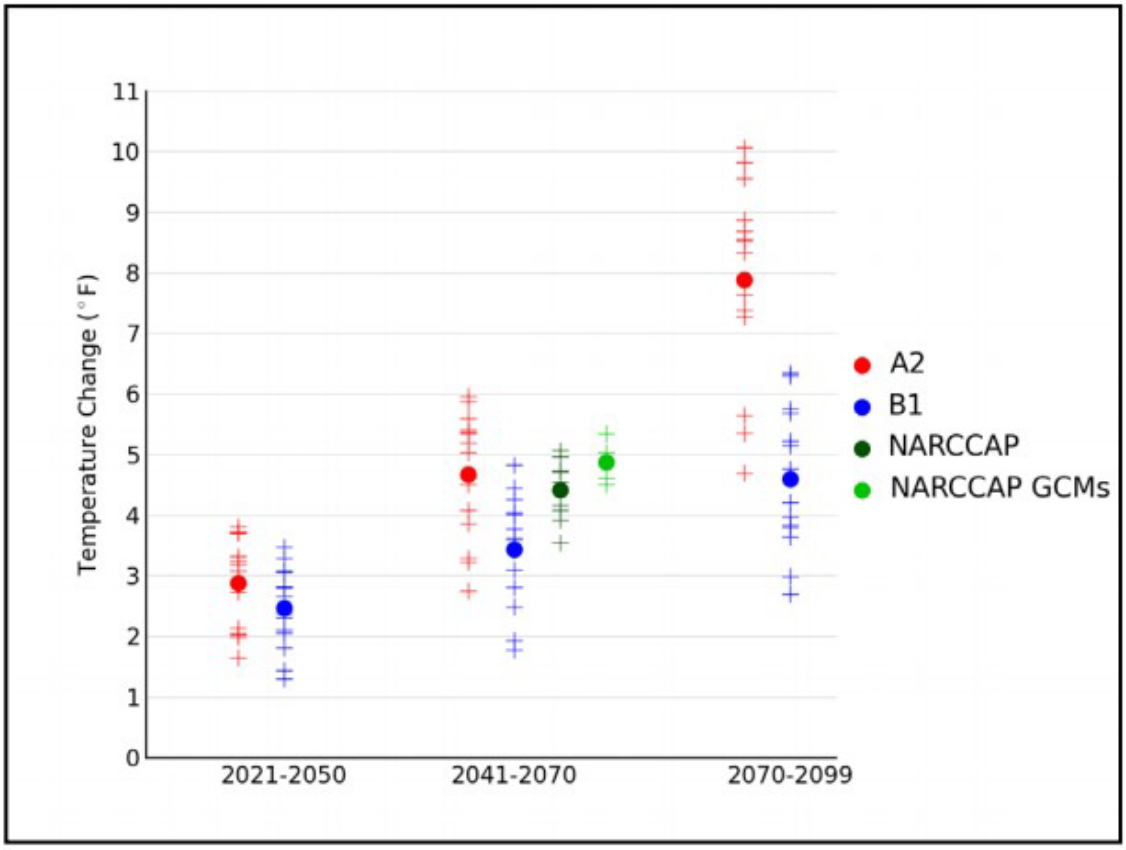

Figure 7-4. Simulated annual temperature change (°F) for the Southwest region, for each future time period (2021–2050, 2041–2070, and 2070–2099) with respect to the reference period of 1971–1999 for the CMIP3 models (A2 and B1) and 1971–2000 for the NARCCAP models (Figure source: Kunkel et al. 2013, part 5).

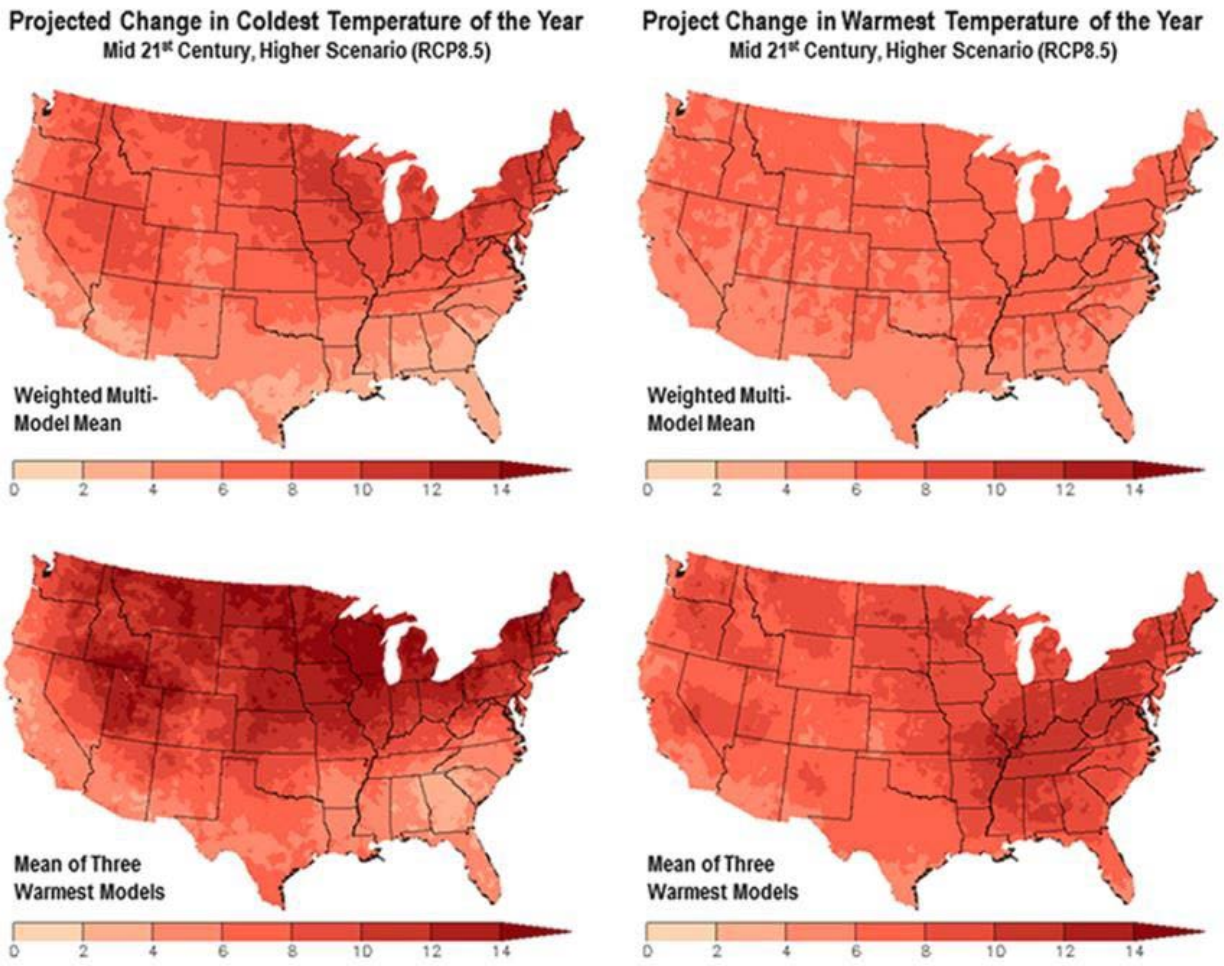

Figure 7-5. Projected changes in the coldest and warmest daily temperatures (°F) of the year in the contiguous United States. Changes are the difference between the average for mid-century (2036–2065) and the average for near-present (1976–2005) under the higher scenario (RCP8.5). Maps in the top row depict the weighted multi-model mean whereas maps on the bottom row depict the mean of the three warmest models (that is, the models with the largest temperature increase). Maps are derived from 32 climate model projections that were statistically downscaled using the Localized Constructed Analogs technique. Increases are statistically significant in all areas (that is, more than 50% of the models show a statistically significant change, and more than 67% agree on the sign of the change) (Source: USGCRP 2017 p. 198).

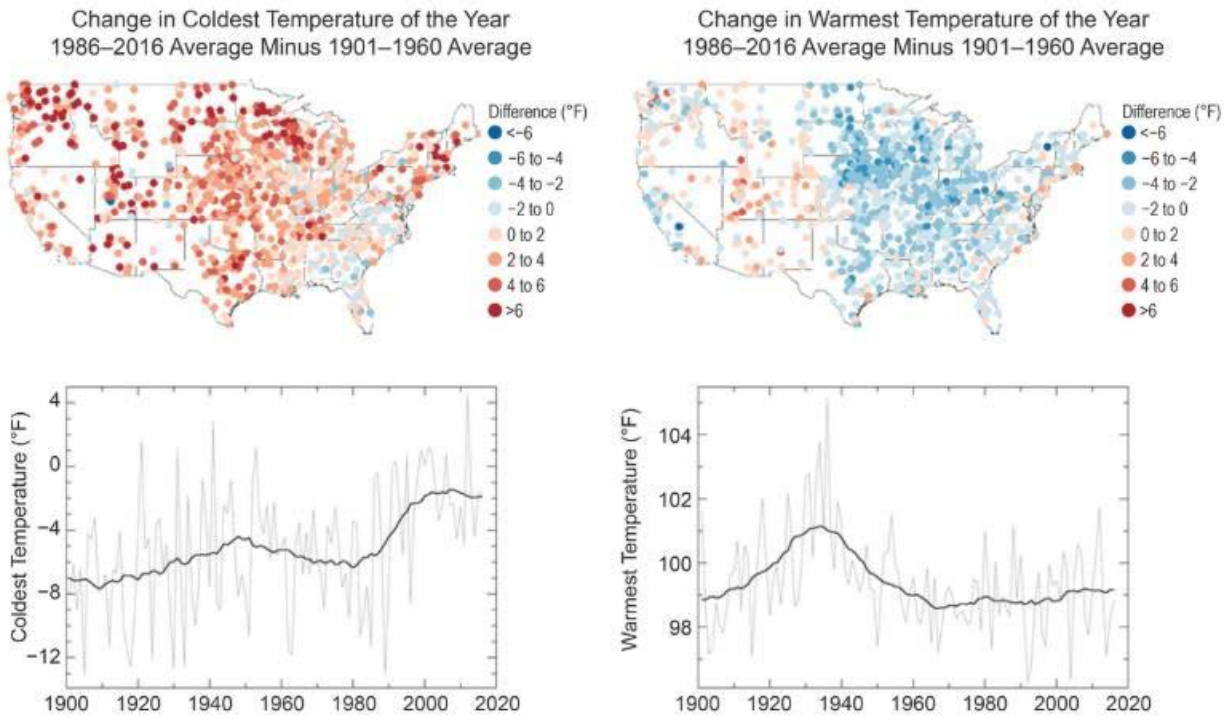

Figure 7-6. Observed changes in the coldest and warmest daily temperatures (°F) of the year in the contiguous United States. Maps (top) depict changes at stations; changes are the difference between the average for present-day (1986–2016) and the average for the first half of the last century (1901–1960). Time series (bottom) depict the area-weighted average for the contiguous United States. Estimates are derived from long-term stations with minimal missing data in the Global Historical Climatology Network–Daily dataset (Source: USGCRP 2017 p. 190).

Temperature Variable	NARCCAP Mean	NARCCAP Standard Deviation	Daily_CMIP3 Mean
Freeze-free period	+30 days	3 days	+31 days
#days T_{max} > 90°F	+24 days	4 days	+31 days
#days T_{max} > 95°F	+20 days	7 days	+24 days
#days T_{max} > 100°F	+15 days	9 days	+14 days
#days T_{min} < 32°F	-29 days	3 days	-29 days
#days T_{min} < 10°F	-11 days	5 days	-8 days
#days T_{min} < 0°F	-5 days	3 days	-3 days
Consecutive #days > 95°F	+82%	44%	+114%
Consecutive #days > 100°F	+103%	74%	+158%
Heating degree days	-18%	1%	-19%
Cooling degree days	+64%	19%	+65%
Growing degree days (base 50°F)	+34%	5%	+34%

Figure 7-7. Multi-Model means and standard deviations of the simulated annual mean change in select temperature variables from 9 NARCCAP simulations for the Southwest region. Multi-model means from the 8 daily CMIP3 simulations are also shown for comparison. Analyses are for the 2041-2070 time period with respect to the reference period of 1971-2000, for the high (A2) emission scenario (Figure source: Vose et al. 2017).

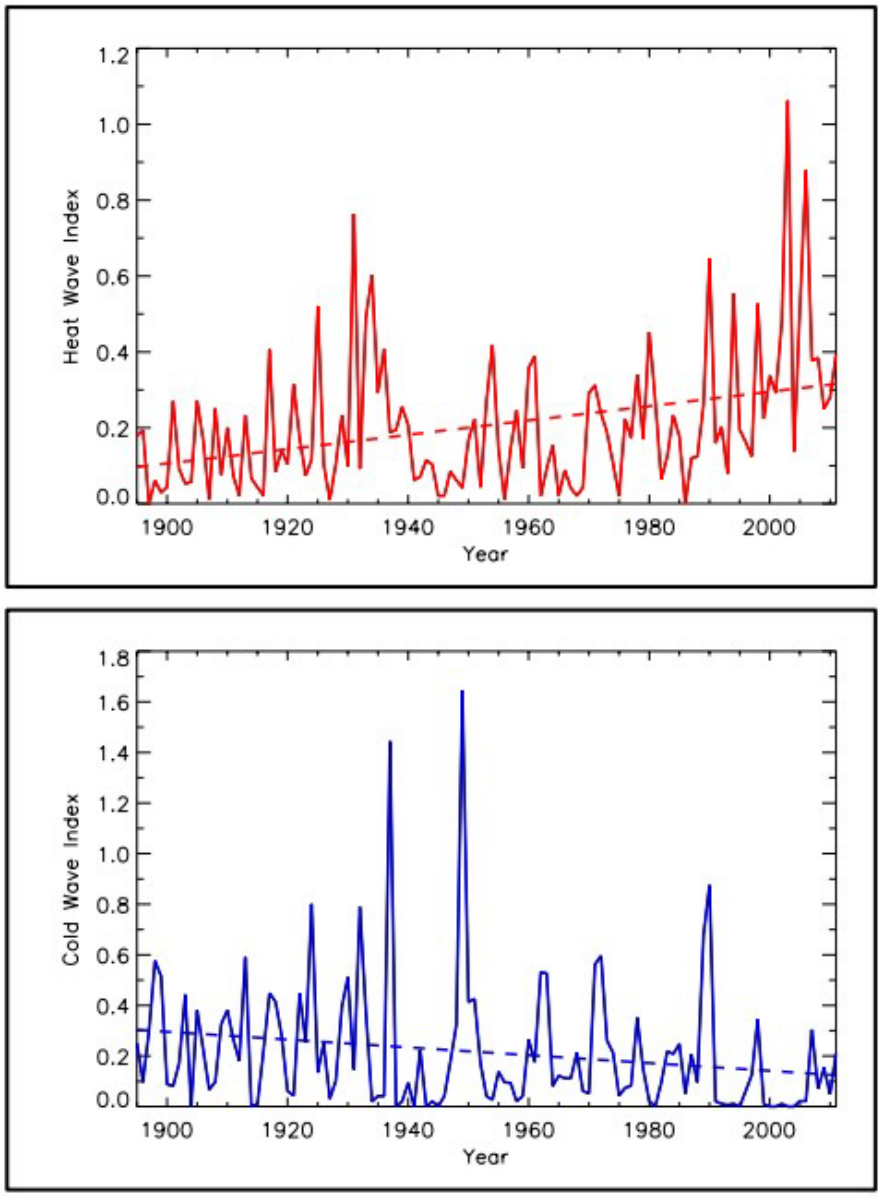

Figure 7-8. Time series of an index for the occurrence of heat waves (top) and cold waves (bottom), defined as 4-day periods that are hotter and colder, respectively, than the threshold for a 1 in 5-year occurrence for the Southwest Region. There is a statistically significant upward trend in heat waves and a statistically significant downward trend in cold waves (Figure source: Kunkel et al. 2013, part 5).

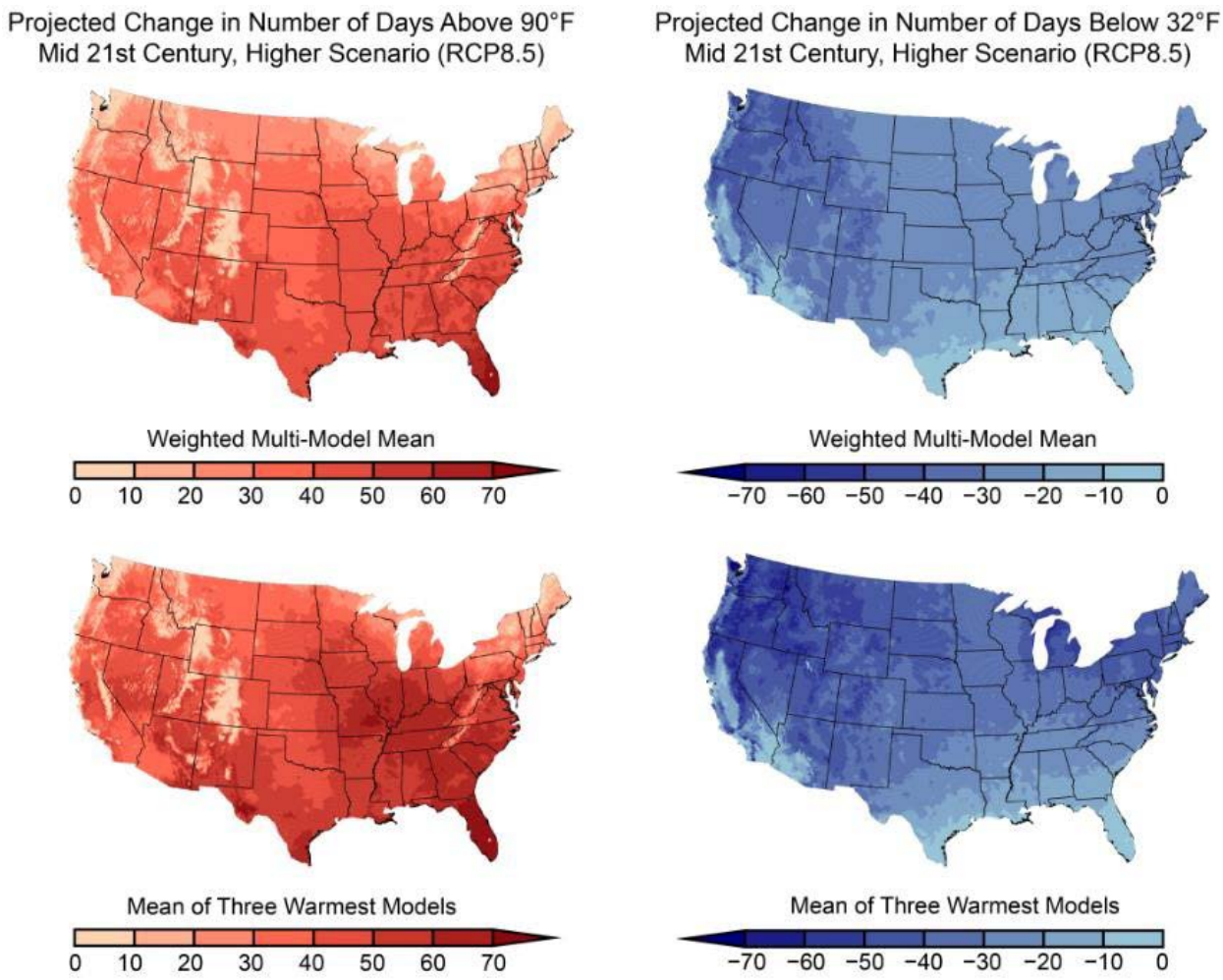

Figure 7-9. Projected changes in the number of days per year with a maximum temperature above 90°F and a minimum temperature below 32°F in the contiguous United States. Changes are the difference between the average for mid-century (2036–2065) and the average for near-present (1976–2005) under the higher scenario (RCP8.5). Maps in the top row depict the weighted multi-model mean whereas maps on the bottom row depict the mean of the three warmest models (that is, the models with the largest temperature increase). Maps are derived from 32 climate model projections that were statistically downscaled using the Localized Constructed Analogs technique. Changes are statistically significant in all areas (that is, more than 50% of the models show a statistically significant change, and more than 67% agree on the sign of the change) (Source: USGCRP 2017 p. 199).

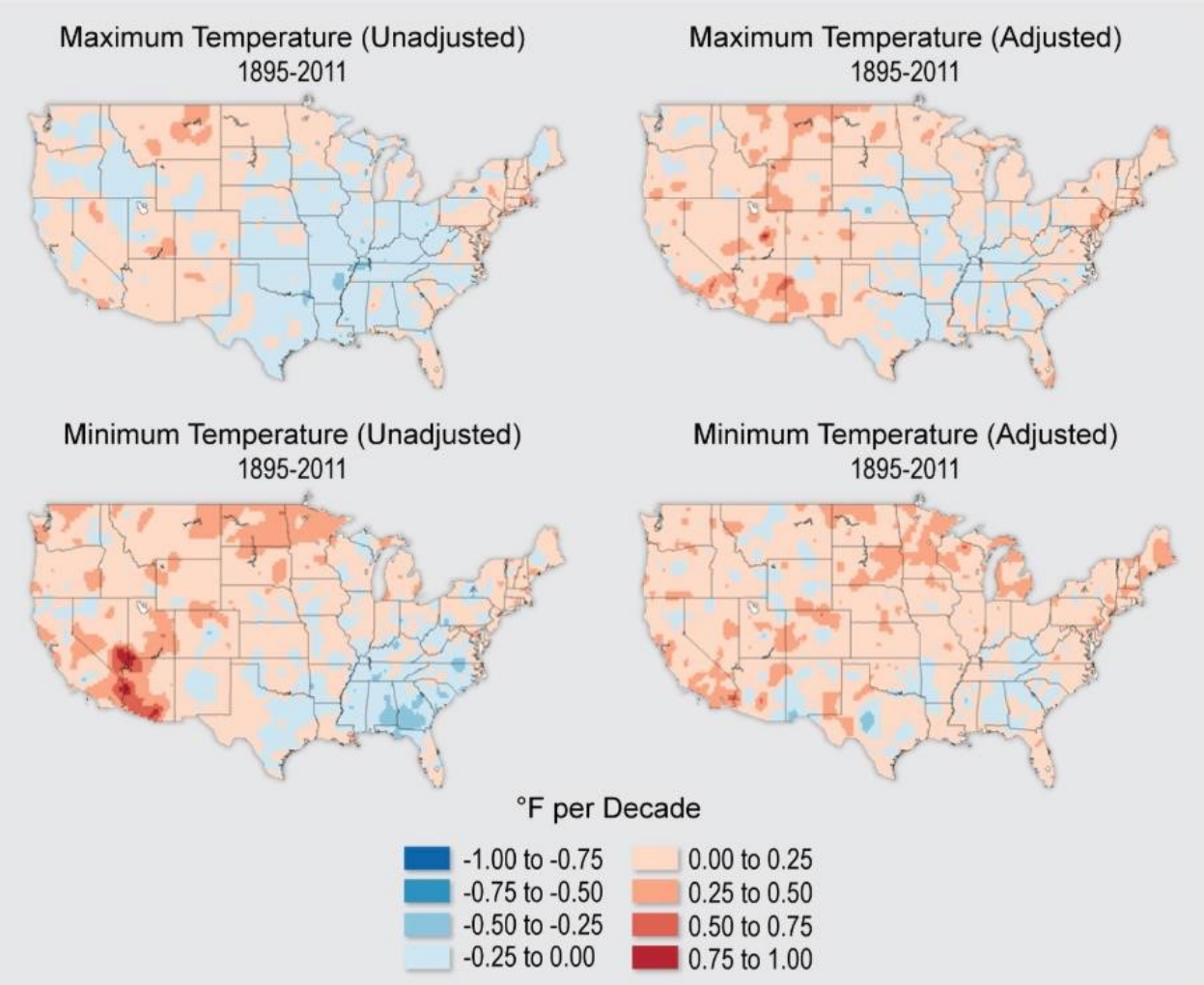

Figure 7-10. Geographic distribution of linear trends in the U.S. Historical Climatology Network for the period 1895-2011 (Figure source: Melillo et al. 2014 p. 765).

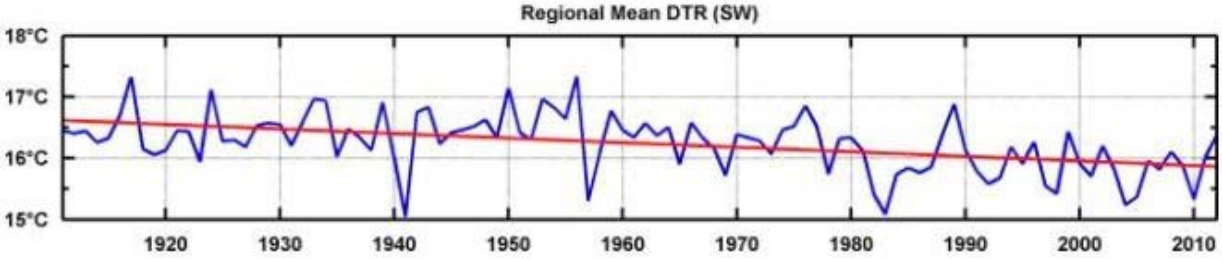

Figure 7-11. Regional average diurnal temperature range (high temperature minus low temperature) for the Southwest region (Figure source: Hibbard et al. 2017).

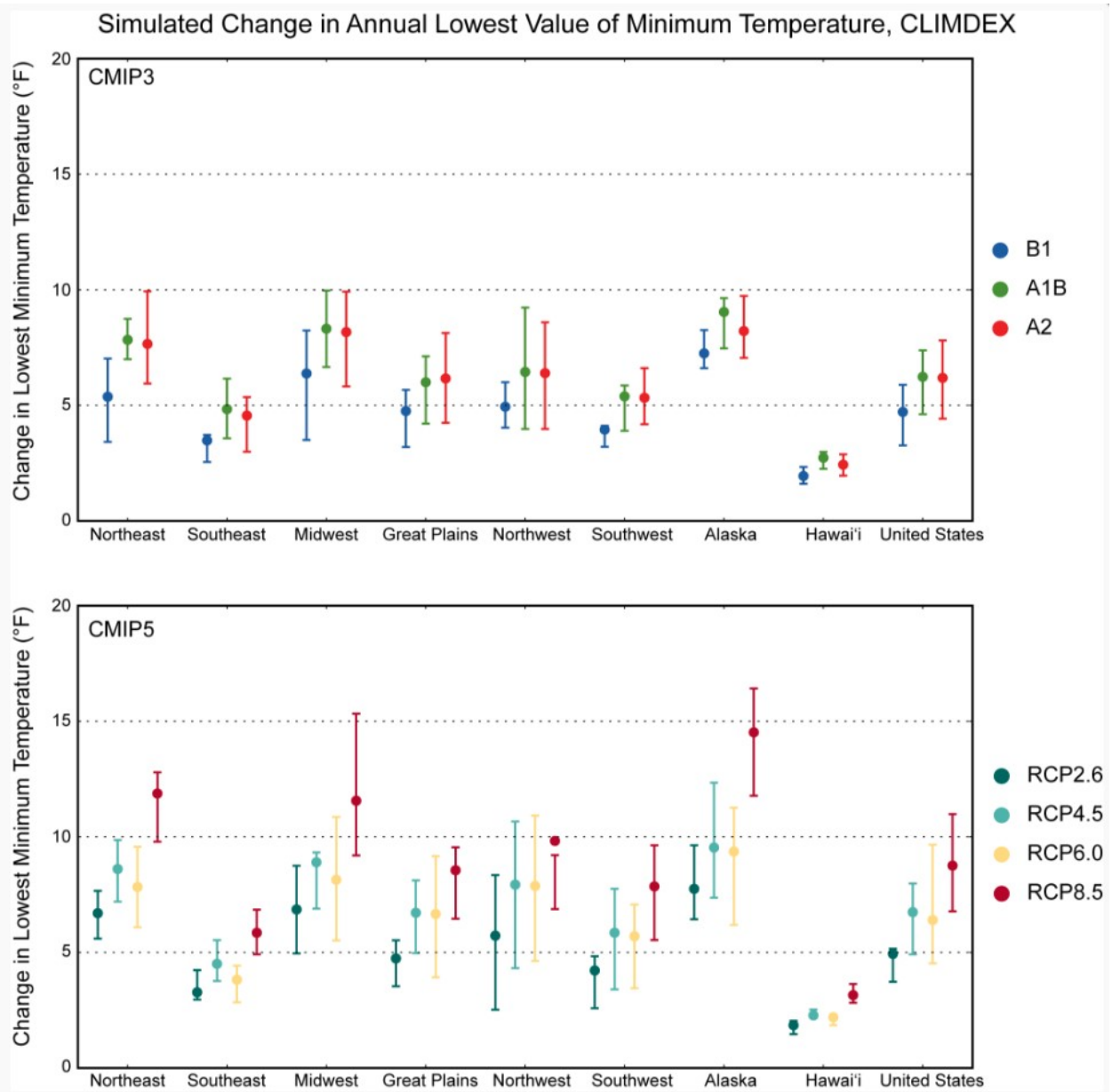

Figure 7-12. Simulated change in annual lowest value of minimum temperature. Lowest annual minimum temperature is expected to increase between approximately 4 and 8°F (Figure source: Qu et al. 2014).

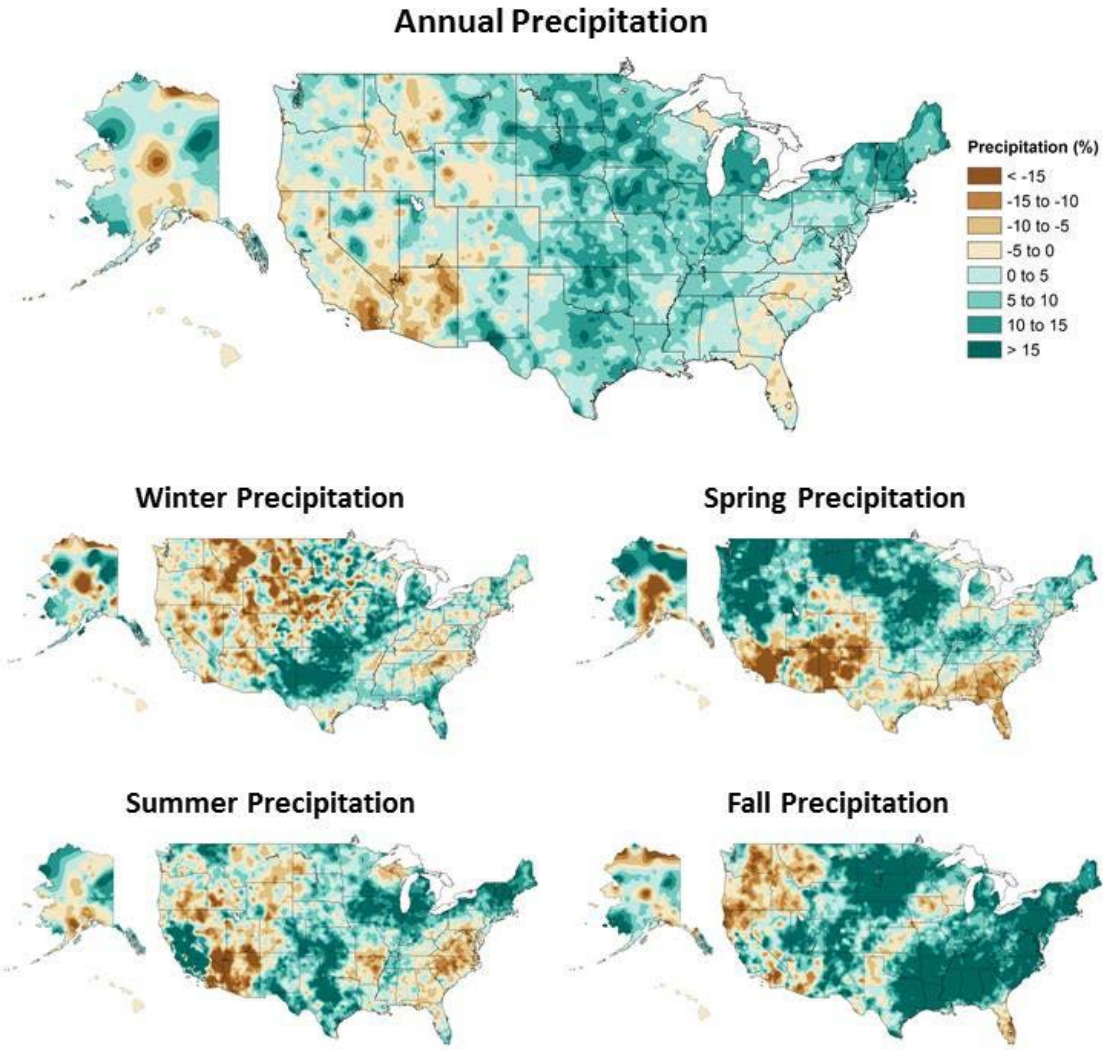

Figure 7-13. Projected change (%) in total seasonal precipitation from CMIP5 simulations for 2070–2099. The values are weighted multi-model means for the higher scenario (RCP 8.5) and expressed as the percent change relative to the 1976–2005 average. Stippling indicates that the changes are large relative to natural variation, while hatching indicates that changes are small relative to natural variations (Source: USGCRP 2017 p. 209).

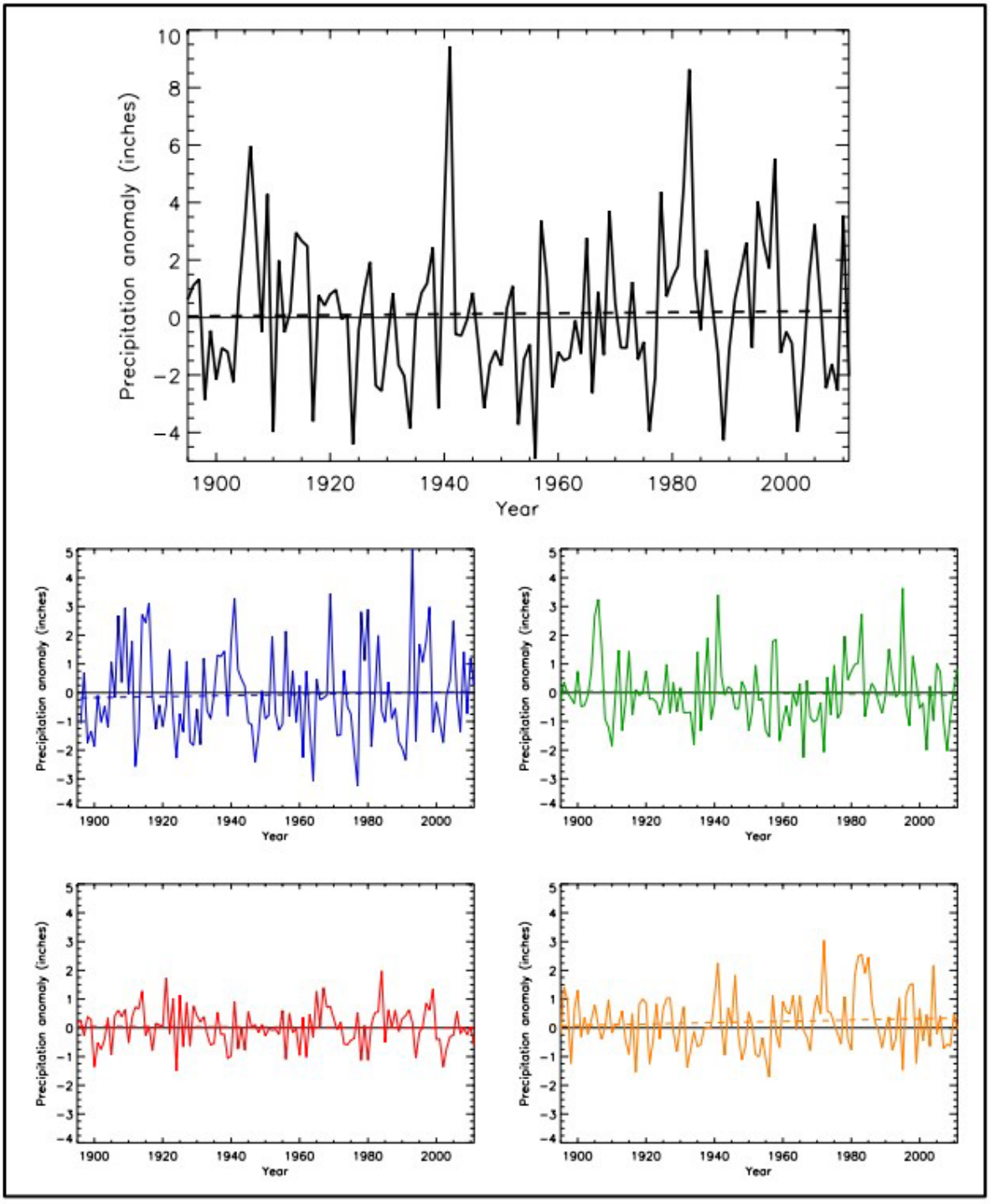

Figure 7-14. Precipitation anomaly (deviation from the 1901-1960 averages, inches) for annual (black) winter (blue) spring (green) and fall (orange) for the Southwest United States. Dashed lines indicate the best fit by minimizing the chi-square error statistic. Based on a new gridded version of COOP data from the National Climatic Data Center, the CDDv2 dataset (R. Vose, personal communication, July 27, 2012). No significant trends in any of the seasons (Figure source: Easterling et al. 2017)

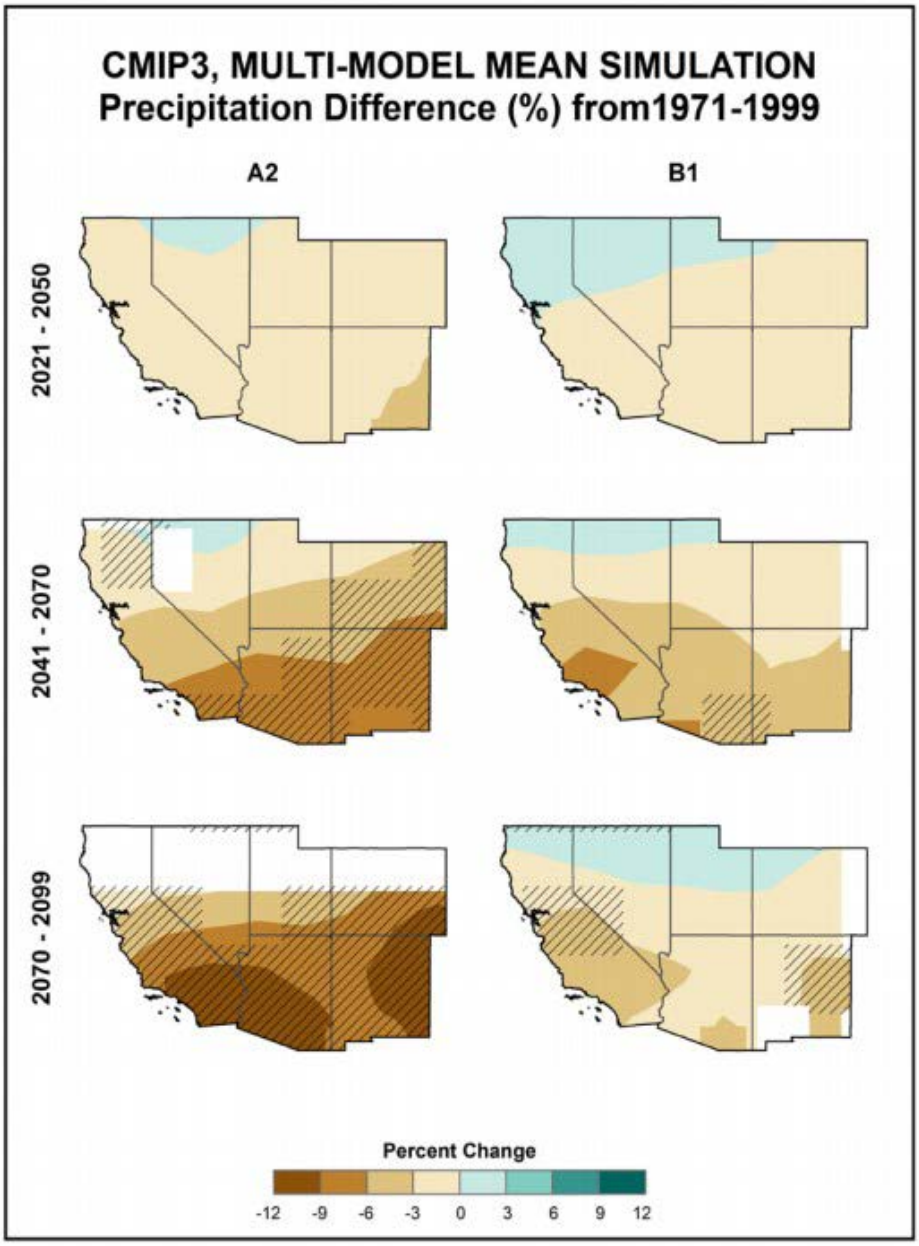

Figure 7-15. Simulated difference in annual mean precipitation (%) for the Southwest region for each future time period (2021-2050, 2041-2070, and 2070-2099) with respect to the reference period of 1971-1999. These are multi-model means for the high (A2) and low (B1) emissions scenarios from the 14 (B1) or 15 (A2) CMIP3 global climate simulations. Color only (category 1) indicates that less than 50% of the models show a statistically significant change. Color with hatching (category 3) indicates that more than 50% of the models show a statistically significant change in precipitation, and more than 67% agree on the sign of the change. Whited out areas (category 2) indicate that more than 50% of the models show a statistically significant change in precipitation but less than 67% agree on the sign of the change. Generally, the models simulate increases in the far north, but decreases in the majority of the region (Figure source: Kunkel et al. 2013, part 5).

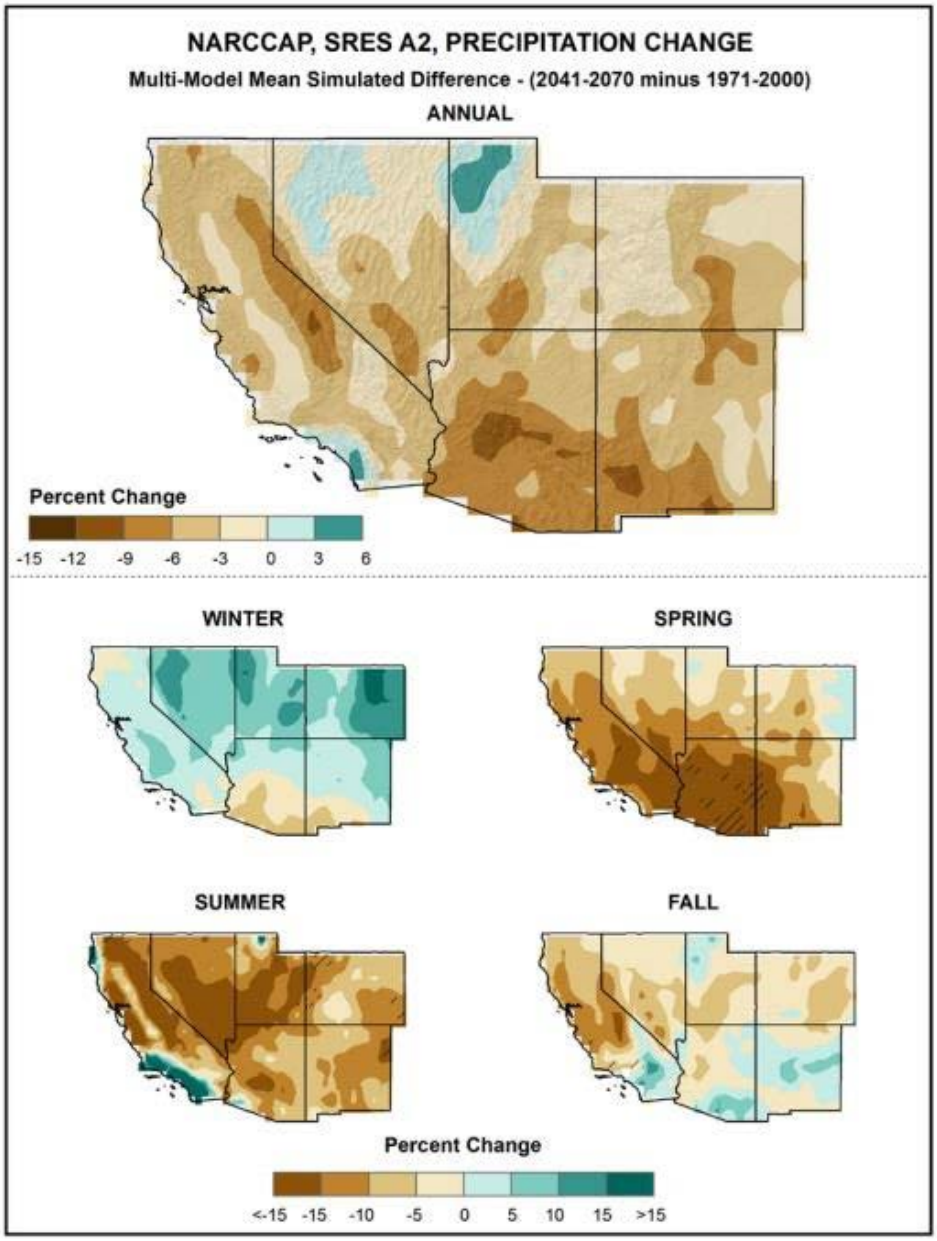

Figure 7-16. Simulated difference in seasonal mean precipitation (%) for the Southwest region for 2041-2070 with respect to the reference period of 1971-2000. There are multi-model means from 11 NARCCAP regional climate simulations for the high (A2) emissions scenario. Color only (category 1) indicates that less than 50% of the models show a statistically significant change in precipitation. Color with hatching (category 3) indicates that more that 50% of the models show a significant change in precipitation and more than 67% agree on the sign of the change. The annual change is upward in the far north and downward throughout the remainder of the region. Changes are mostly upward in winter, and downward in the other seasons (Figure source: Kunkel et al. 2013, part 5).

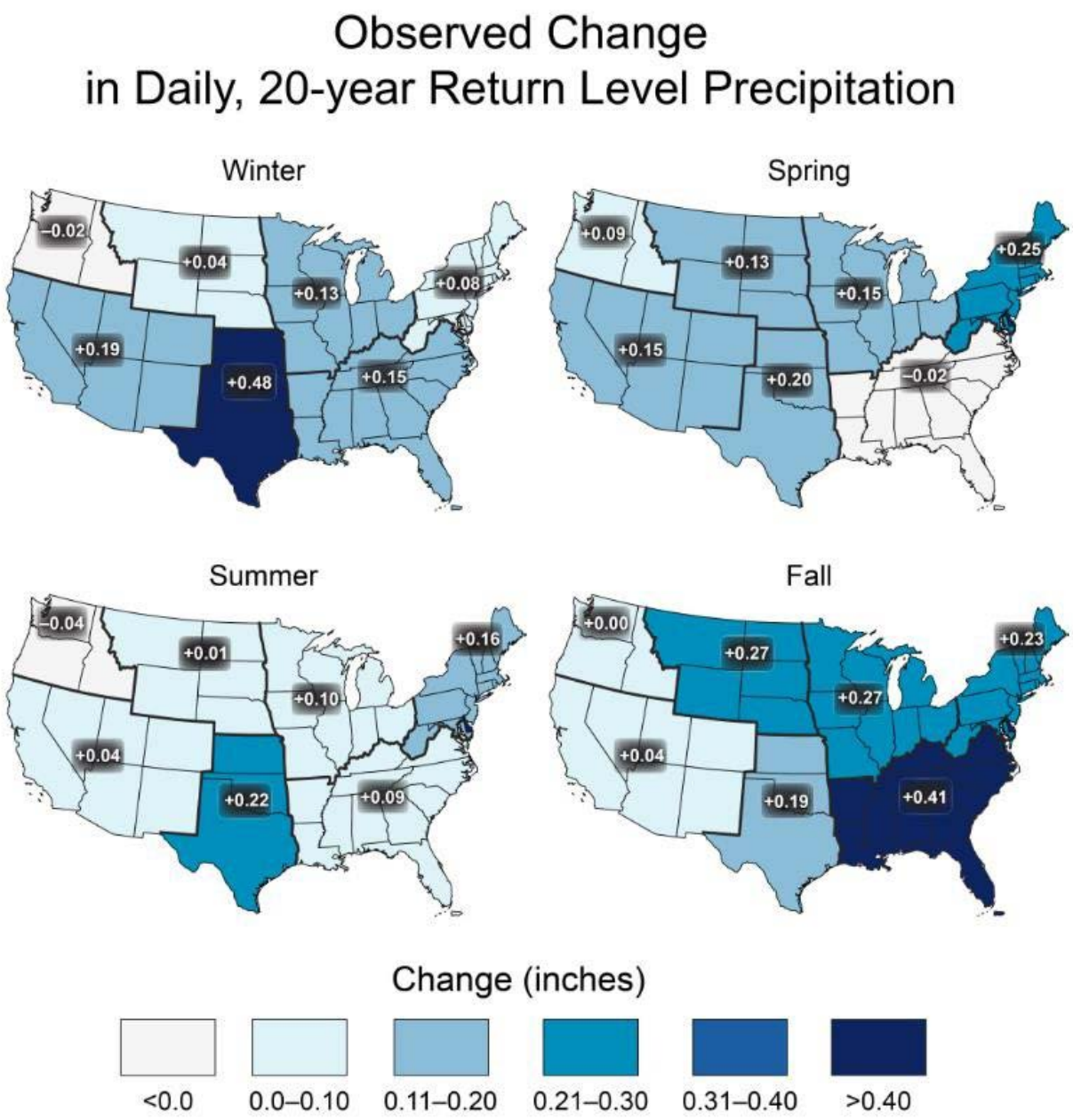

Figure 7-17. Observed changes in the 20-year return value of the seasonal daily precipitation totals for the contiguous United States over the period 1948 to 2015 using data from the Global Historical Climatology Network (GHCN) dataset (Source: USGCRP 2017 p. 211).

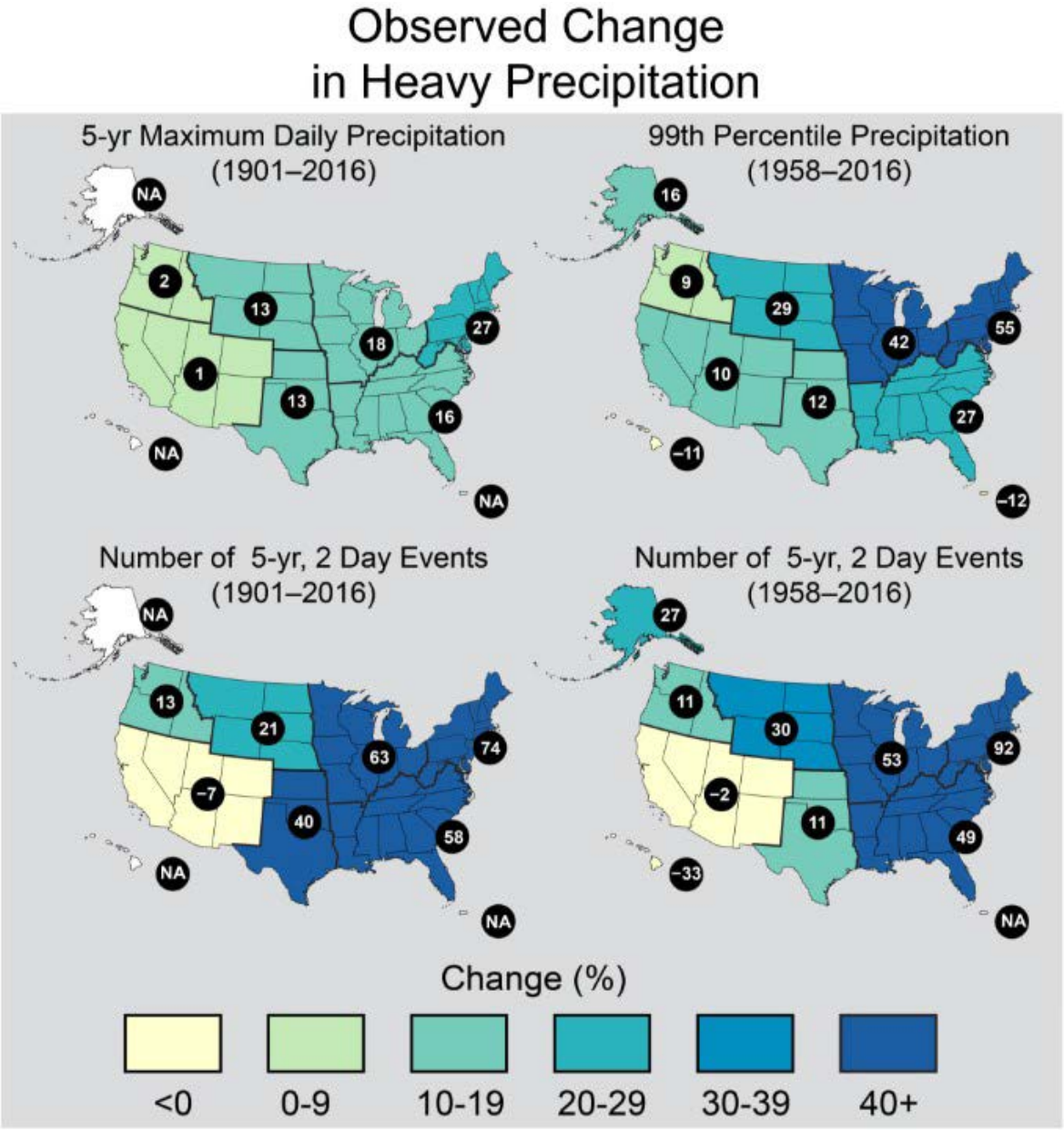

Figure 7-18. Changes in extreme precipitation. The percent change in maximum daily precipitation by 5-year periods (upper left), the percent change in the amount of precipitation falling in daily events that exceed the 99th percentile of precipitation days (upper right), the percent change in number of two day events with a precipitation total exceeding the largest two-day amount that would be expected to occur only once every five years based on data from 1901–2016 (lower left), and the percent change in number of two day events with a precipitation total exceeding the largest two-day amount that would be expected to occur only once every five years based on data from 1958–2016 (lower right) (Source: USGCRP 2017 p. 212).

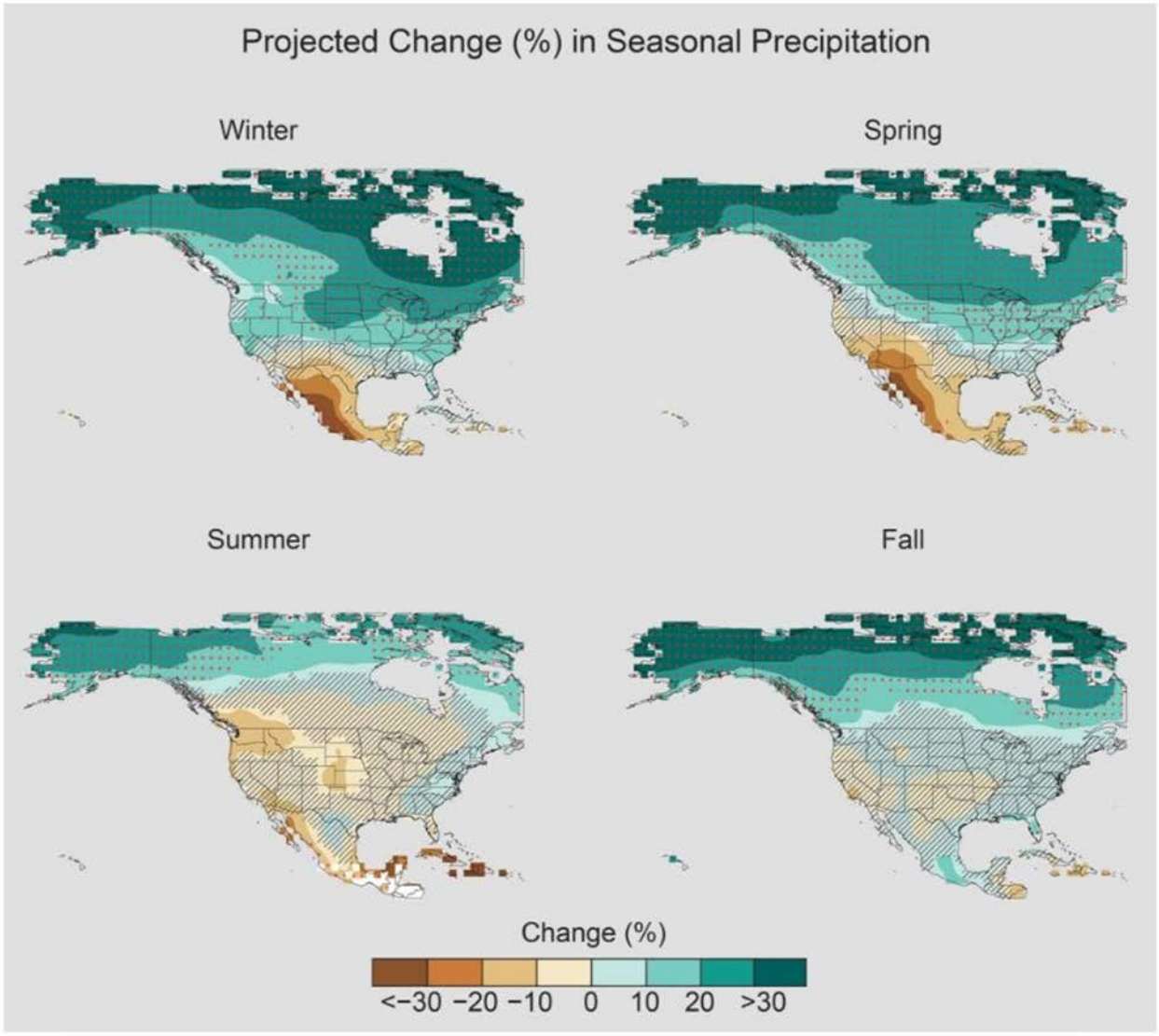

Figure 7-19. Projected change (%) in total seasonal precipitation from CMIP5 simulations for 2070–2099. The values are weighted multi-model means and expressed as the percent change relative to the 1976–2005 average. These are results for the higher scenario (RCP8.5). Stippling indicates that changes are assessed to be large compared to natural variations. Hatching indicates that changes are assessed to be small compared to natural variations. Blank regions (if any) are where projections are assessed to be inconclusive. Data source: World Climate Research Program's (WCRP's) Coupled Model Intercomparison Project (Figure source: USGCRP 2017 p. 217).

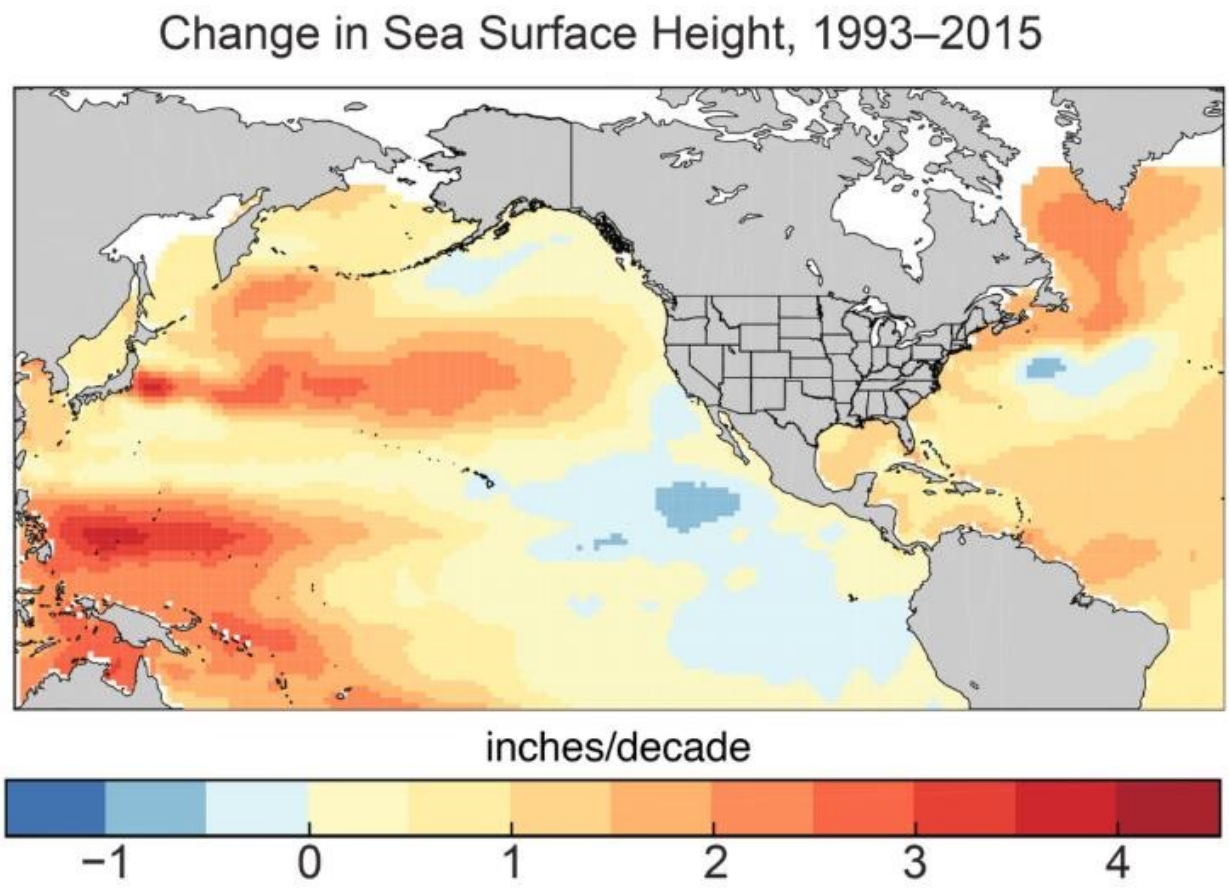

Figure 7-20. Rates of change from 1993 to 2015 in sea surface height from satellite altimetry data; updated from Kopp et al. using data updated from Church and White (Figure source: USGCRP 2017 p. 340).

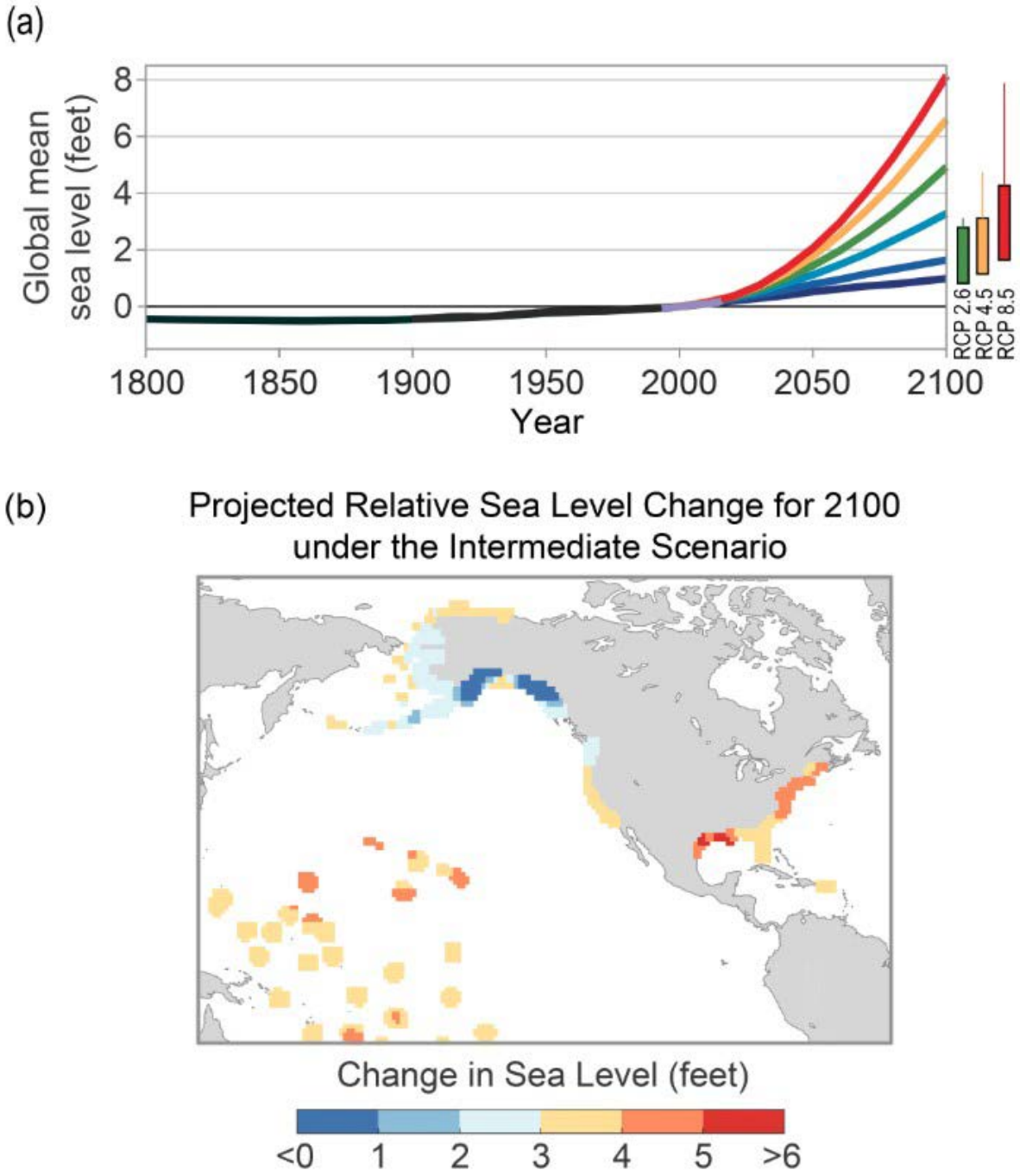

Figure 7-21. (a) Global mean sea level (GMSL) rise from 1800 to 2100, based on Figure 12.2b from 1800 to 2015, the six Interagency GMSL scenarios (navy blue, royal blue, cyan, green, orange, and red curves), the very likely ranges in 2100 for different RCPs (colored boxes), and lines augmenting the very likely ranges by the difference between the median Antarctic contribution of Kopp et al. and the various median Antarctic projections of DeConto and Pollard. (b) Relative sea level (RSL) rise (feet) in 2100 projected for the Interagency Intermediate Scenario (1-meter [3.3 feet] GMSL rise by 2100) (Figure source: USGCRP 2017 p. 342).

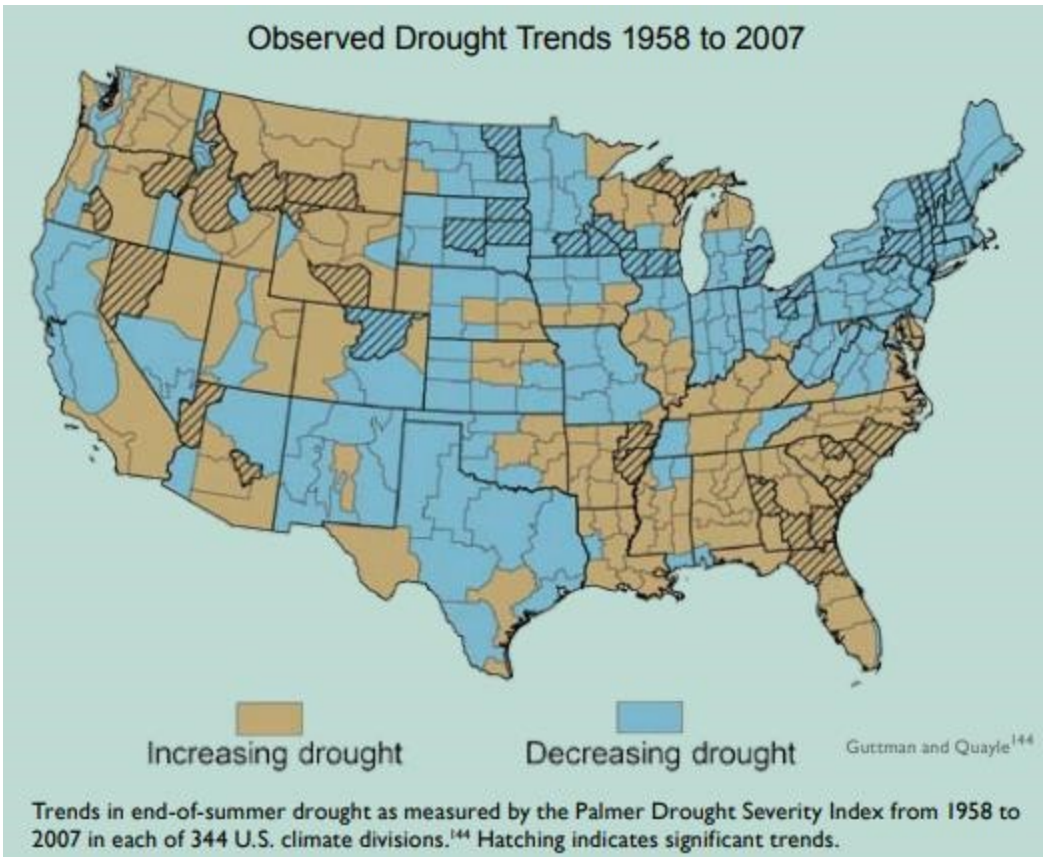

Figure 7-22. Trends in end-of-summer drought as measured by the Palmer Drought Severity Index from 1958 to 2007 in each of 344 U.S. climate divisions. Hatching indicates significant trends (Figure source: Sweet et al. 2017).

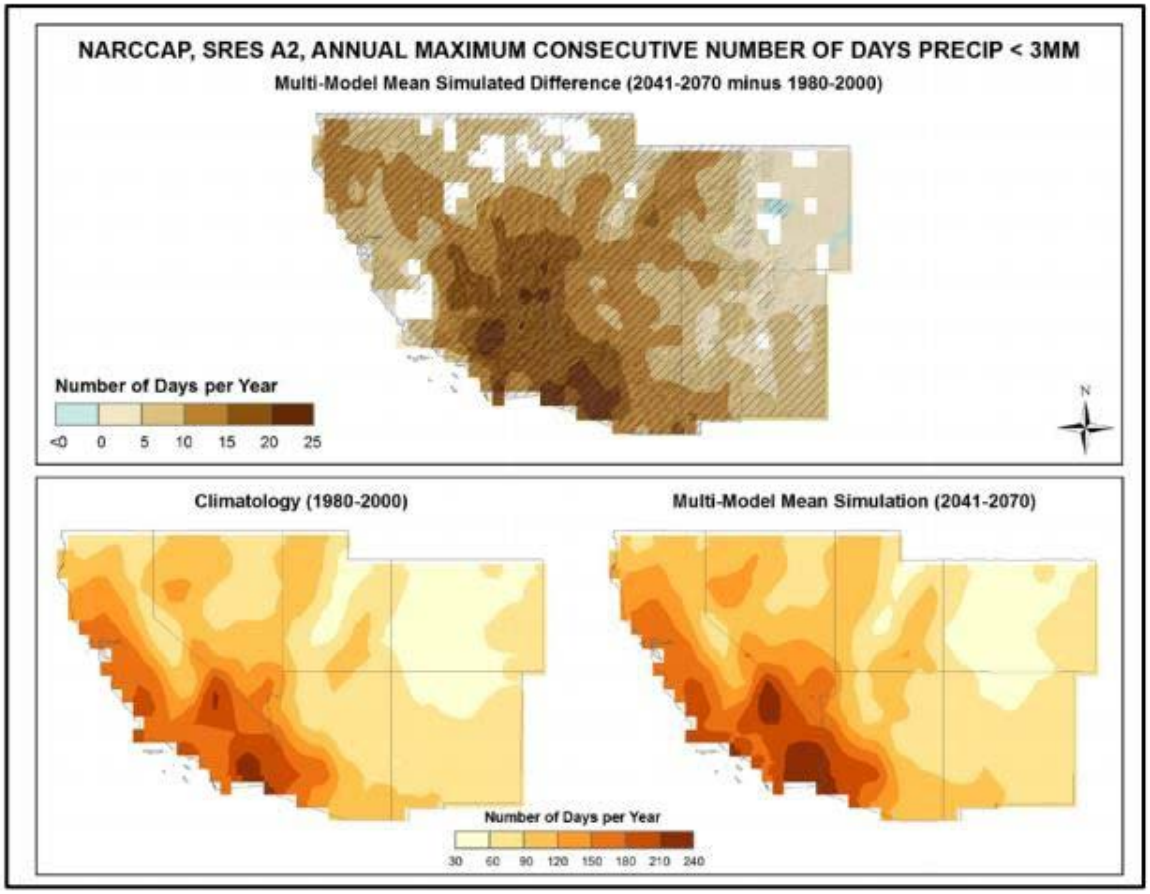

Figure 7-23. Simulated difference in the mean annual maximum number of consecutive days with precipitation of less than .1 inches (3mm) for the Northwest Region for the 2041-2070 time period with respect to the reference period 1980-2000 (top). Color only (category1) indicates that less than 50% of the models show a statistically significant change in the number of consecutive dry days. Color with hatching (category 3) indicates that more than 50% of the models show a statistically significant change in the number of consecutive dry days, and more than 67% agree on the sign of the change. Whited out areas (category 2) indicate that more than 50% of the models show a statistically significant change in the number of consecutive dry days but less than 67% agree on the sign of the change. Mean annual maximum number of consecutive days with precipitation less than 0.10 inches for the 1980-2000 reference period is shown bottom left. Simulated mean annual maximum number of consecutive days with precipitation less than 0.1 inches for the 2041-2070 future time period is shown bottom right. These are multi-model means from 8 NARCCAP regional climate simulations for the high (A2) emissions scenario. The models simulate increases over the majority of the region, with the greatest changes in the south (Figure source: Sweet et al. 2017).

.

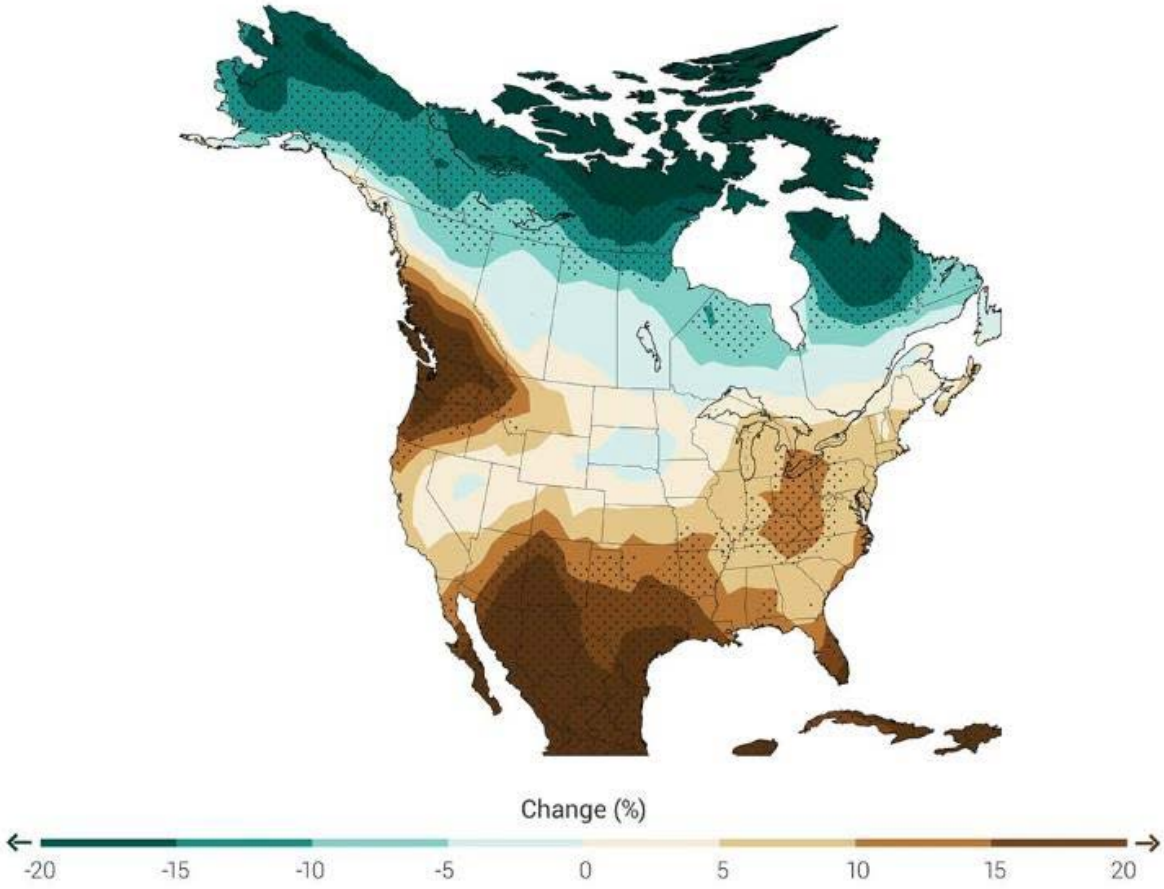

Figure 7-24. Change in the number of consecutive dry days (less than 0.04 inches (1mm) of precipitation) at the end of this century (2070-2099) relative to the end of the last century (1971-2000) under the higher scenario, RCP 8.5. Stippling indicates area where changes are consistent among at least 80% of the 25 models used in this analysis (Figure source: Melillo et al. 2014 p. 33).

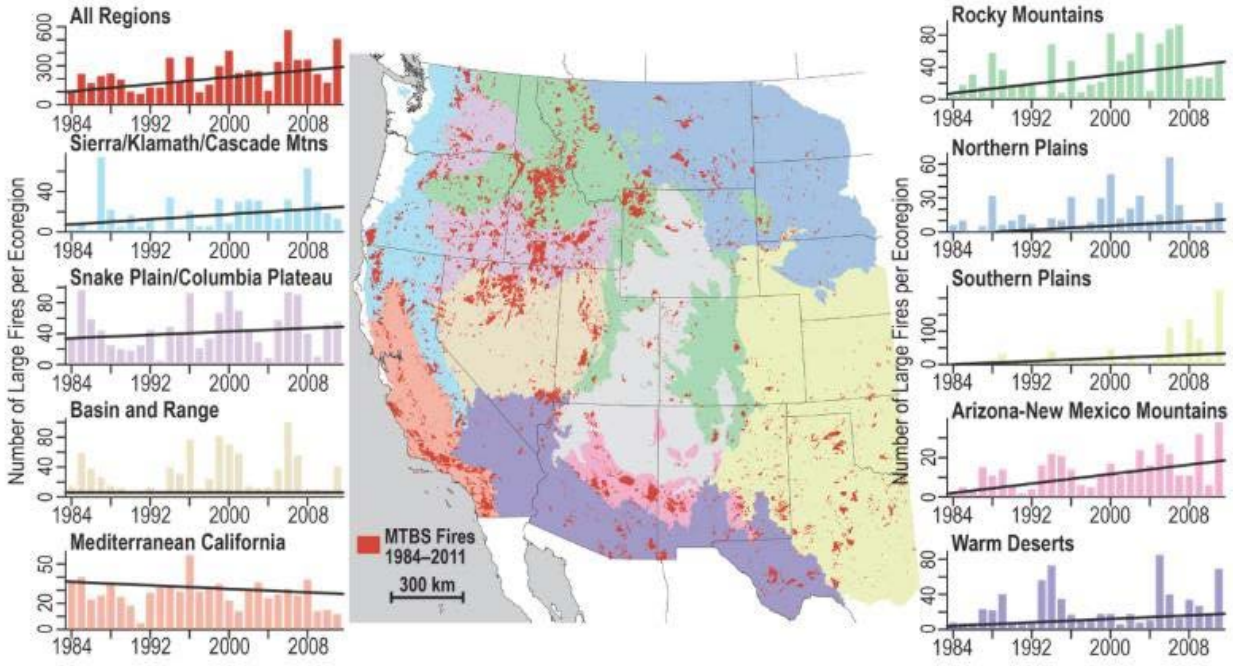

Figure 7-25. Trends in the annual number of large fires in the western United States for a variety of ecoregions. The black lines are fitted trend lines, statistically significant at a 10% level for all regions except the Snake Plain/Columbia Plateau, Basin and Range, and Mediterranean California regions (Figure source: USGCRP 2017 p. 243).

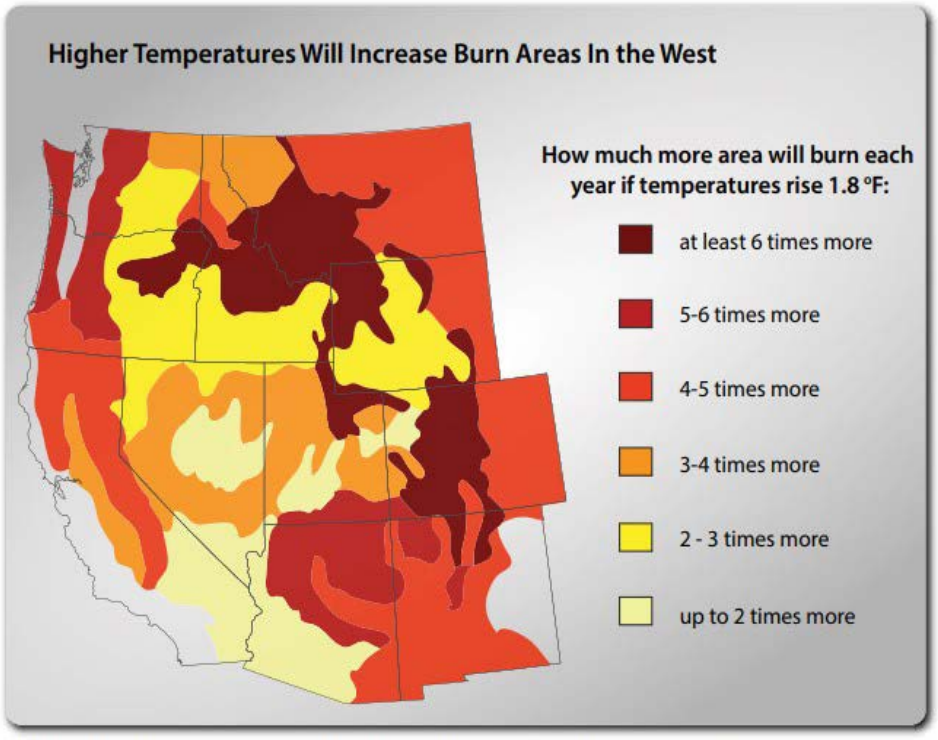

Figure 7-26. Projected increases in the area burned each year by wildfire assuming a 1.8°F rise in temperature (Figure source: Climate Central 2012, p. 9).

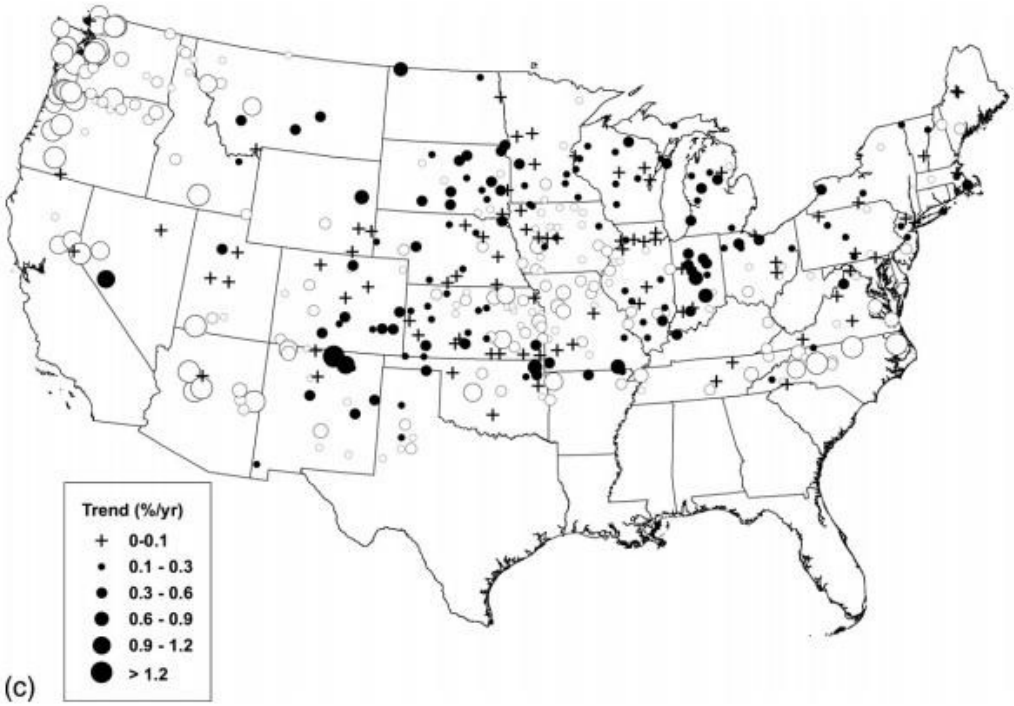

Figure 7-27. Average snowfall trends as determined from individual stations for the period from 1937-2007. White indicates decrease, black indicates increase (Figure source: Kunkel et al. 2009).

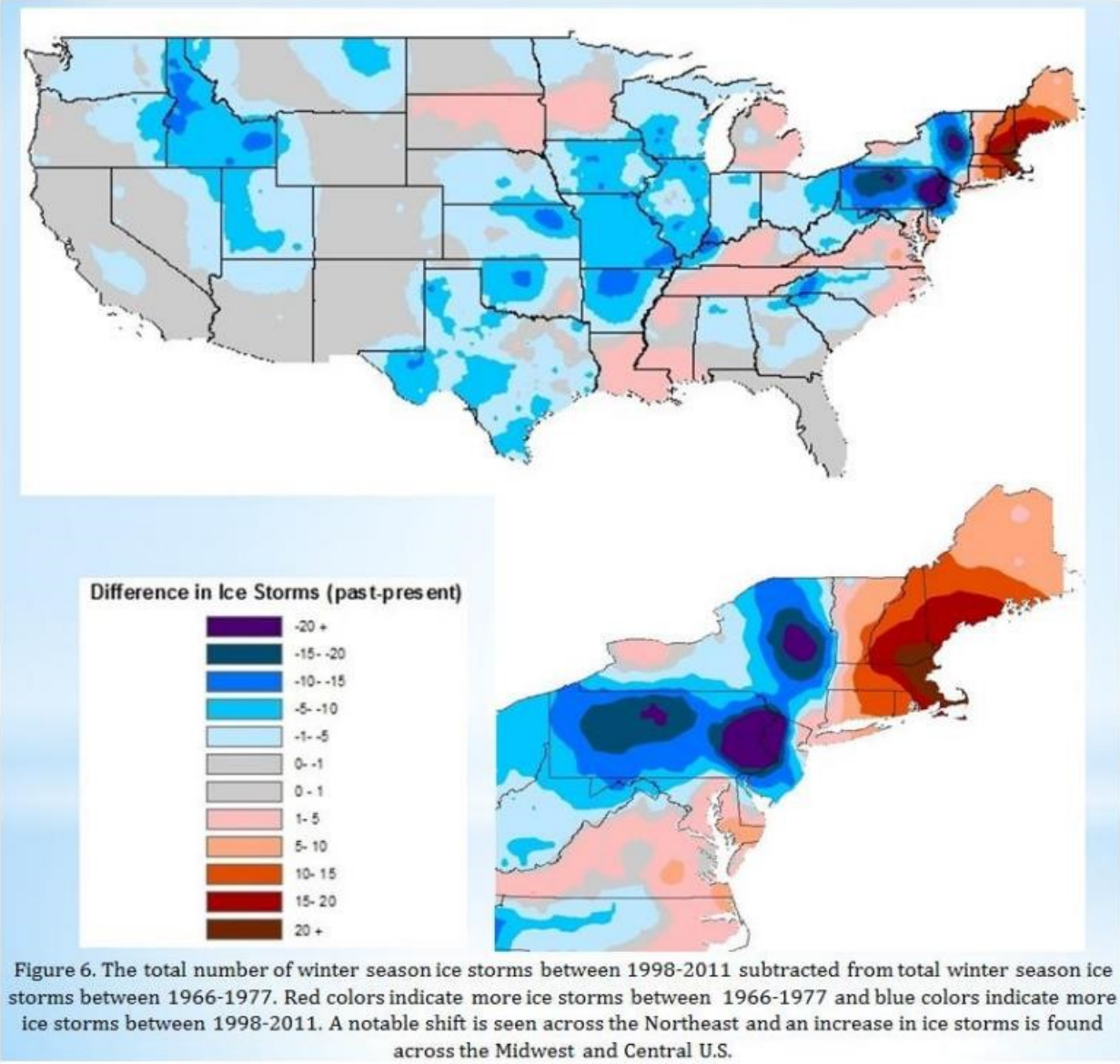

Figure 6. The total number of winter season ice storms between 1998-2011 subtracted from total winter season ice storms between 1966-1977. Red colors indicate more ice storms between 1966-1977 and blue colors indicate more ice storms between 1998-2011. A notable shift is seen across the Northeast and an increase in ice storms is found across the Midwest and Central U.S.

Figure 7-28. The total number of winter season ice storms between 1998–2011 subtracted from total winter season ice storms between 1966–1977. Red colors indicate more ice storms between 1966–1977 and blue colors indicate more ice storms between 1998–2011. Notably, ice storms are decreasing across portions of Utah, Nevada, and Arizona (Figure source: Kovacik et al. 2014).

8 Northwest Region

8.1 Summary of Climate Projections for the Northwest Region

8.1.1 Temperature

Observed trends indicate that temperatures across the Northwest region have increased roughly 0.13°F per decade from 1895-2011. Portions of the region have seen temperatures increase over 1.5°F (determined from the difference between the 1986-2016 temperature average and the 1901-1960 temperature average), while statistically significant upward trends have been detected from analyzing temperature deviations from the 1901-1960 average (see Figure 8-1 and Figure 8-2).

Model simulations project temperature to increase in each future time period (2021-2050, 2041-2070, and 2070-2099, hereafter referred to as near-, mid-, and late-century, respectively), with both high (A2) and low (B1) emissions scenarios from the CMIP3 global climate simulations indicating a statistically significant increase in temperature (see Figure 8-3). The near century is projected to see annual temperature increases ranging between 1.5 and 3.5°F across both emissions scenarios. The mid-century is projected to see temperature increases range between 2.5 and 4.5°F for the B1 scenario and 2.5 and 5.5°F for the A2 scenario. Late-century temperatures are estimated to increase between 3.5 and 5.5°F for the B1 scenario, but the A2 scenario projects an increase between 5.5 and 8.5°F (note that the temperature increases are relative to the reference period of 1971-1999). Uncertainty increases from near-century to late-century, but annual temperature projections indicate increases in temperature for each time period, even when NARCCAP models are included in the analysis (see Figure 8-4).

The southeastern portion of the region (southern Idaho, southeastern and eastern Oregon) is projected to have the highest temperature increases, while the west coasts of Washington and Oregon are projected to experience less intense increases. This is due to the moderating influence of the Pacific Ocean, whereas the southeastern portion of the region is situated far enough inland to avoid moderation. With observed temperatures having increased and model projections all indicating temperature increases in the future, there is a very low probability that annual average temperatures will decrease across the region.

The Northwest region has seen a decrease in the hottest annual temperature on the magnitude of -0.17°F (value determined by calculating the difference between the 1986-2016 average and the 1901-1960 average). There has been an increase in the occurrences of heat waves throughout the region, according to Kunkel et al., 2013, but the increase is not considered statistically significant.

Model simulations (NARCCAP and Daily CMIP3) suggest the number of days with temperatures above 90°F, 95°F, and 100°F will increase substantially under the high (A2) emissions scenario for the mid-century (2041-2070) time period. The NARCCAP standard deviation, however, exceeds the multi-model mean for the days above 95°F and 100°F, which reduces confidence (see Figure 8-5). Sillmann et al. (2013) utilized a CMIP5 model ensemble with three emission scenarios (RCP2.6, 4.5, and 8.5), and their results suggest an increase in annual maximum temperatures in the late century (2081-2100). However, the magnitude of the

increase varies with the emission scenario, with values ranging from roughly 1 to 15°F in western North America, which includes the Northwest region (see Figure 8-6). According to the Third National Climate Assessment (NCA3), the RCP8.5 scenario for the mid-century (defined as 2036-2065) time period yields an increase in the hottest annual temperature by 6.25°F (See Figure 8-7). While the lower emission scenarios yield a smaller projected increase, there are no projections that exhibit a decrease in the hottest annual temperature. As such, there is low confidence that the hottest annual temperature will decrease.

The Northwest region has seen an increase in the magnitude of the lowest annual temperature by 4.78°F (See Figure 8-8). The region has seen multiple long-term stations exhibit an increase in the lowest annual temperature, with several exhibiting changes on the order of 6°F or greater (see Figure 8-9). Changes in cold extremes are more pronounced than warm extremes, as can be seen in Figure 8-2.

Model simulations (NARCCAP and Daily CMIP3) suggest that the number of days with temperatures below 32°F, 10°F, and 0°F will decrease substantially under the high (A2) emissions scenario for the mid-century (2041-2070) time period. Sillmann et al. (2013) utilized a CMIP5 model ensemble with three scenarios (RCP2.6, 4.5, and 8.5), and their results suggest an increase in annual minimum temperatures in the late century (2081-2100). However, the magnitude of the increase varies by emissions scenario, with values ranging from roughly 2 to 27°F in western North America, which includes the Northwest region. According to the Third National Climate Assessment (NCA3), the RCP8.5 scenario for the mid-century (defined as 2036-2065) time period yields an increase in the lowest annual temperature by 7.33°F.

Several model simulations with different time scales and emissions scenarios all predict continued increases in the magnitude of the lowest annual temperature. With observed trends indicating warming and projections suggesting future warming, the probability that the lowest annual temperature will decrease is very low.

Since the 2000s, there have been multiple heat waves (defined as a 4-day period where temperatures are hotter than what is experienced once in five years) throughout the region. However, this is not considered to be a statistically significant trend. Model projections from the NARCCAP and CMIP3 downscaled data sets indicate that the number of days with temperatures ≥ 90°F will increase. Furthermore, the CMIP5 model ensemble with both low (RCP4.5) and high (RCP8.5) scenarios predict that days with temperatures ≥ 90°F will increase (see Figure 8-10). Places further away from the coast (Idaho, southeast Oregon) could see a greater increase in the number of days with temperatures ≥ 90°F. Areas of high elevation and regions where this temperature is not regularly reached (western Washington, Idaho) did not exhibit statistically significant increases. However, these regions would more than likely experience at least the same number of days with temperatures ≥ 90°F, as opposed to a decrease.

In recent years, there has been a relative lack of cold waves (defined as a 4-day period where temperatures are colder than what is typically experienced once every five years) in the region. However, this is not considered a statistically significant trend. Furthermore, cold extremes have become less severe over the past century. Model projections using the NARCCAP and CMIP3 downscaled models with both low and high emissions scenarios predict the number of days with freezing temperatures (here taken to be temperatures ≤ 32°F) will decrease by mid-century

(2055), with the NARCCAP models being considered statistically significant across the whole region (see Figure 8-11). The CMIP5 model ensemble also predicted a decrease in the number of days with freezing temperatures by mid-century (2036-2065) for the high emissions scenario (see Figure 8-10). As a result, there is low confidence that the number of days with freezing temperatures will increase. With three different model suites predicting decreases in the number of days with freezing temperatures, there is a high likelihood that the number of freezing temperature days will decrease. Areas of high elevation are predicted to have the largest decrease in the number of days with freezing temperatures, while the smallest change is simulated along the Pacific coast due to the lack of freezing days throughout the historical period.

Minimum temperatures have been observed to have increased at a rate between 0 to 0.50°F per decade during the period from 1895-2011. Furthermore, the diurnal temperature range has decreased due to increases in minimum temperatures. Using CMIP5 projections with three scenarios (RCP2.6, 4.5, and 8.5), frost days are projected to decrease by late century (2081-2100) for all emissions scenarios. Tropical nights are projected to increase for all emissions scenarios, but increases are much less than frost day decreases. This suggests that nighttime temperatures will be increasing.

Urban areas tend to have warmer nighttime temperatures due to the urban heat island effect (temperatures tend to be warmer on the order of 1.8 to 4.5°F in urban areas compared to rural areas). As a result, urban areas such as Seattle, Portland, and Boise would likely have higher minimum nighttime temperatures. Projections indicate nighttime temperatures will increase predominately inland, with the Pacific coast and the Rocky Mountains serving as buffers where increases are less pronounced.

The daily temperature range exhibits a decreasing trend in the region from 1911-2012, with the daily temperature range having decreased almost 2°F during this period. Minimum temperatures (which more often than not occur at night) have increased during the period 1895-2011. Since model projections (with different emission scenarios) have minimum temperatures continuing to increase, especially at a rate greater than daily maximum temperatures, it is highly likely that the daily temperature range will continue to decrease as well.

8.1.2 Precipitation

Overserved precipitation across the region did not exhibit a consistent pattern, with increases balanced by decreases (see Figure 8-12). To further reinforce this, there is no statistically significant trend in precipitation throughout the region, as determined from the 1901-1960 averages (see Figure 8-13).

CMIP3 models with low (B1) and high (A2) emissions scenarios each predicted increases in precipitation for the near-, mid-, and late-century time scales. However, the emissions scenarios yielded different results. The B1 scenario does not begin to exhibit statistically significant changes until the mid-century (2055) time period, with individual model runs differing on how precipitation would change in the southwestern portion of the region. The A2 emission scenario was similar to the B1 scenario in that the near century would not exhibit a statistically significant change. However, the A2 models were in agreement that significant increases in precipitation would occur starting in the near century, with the greatest increases located in the northern part of the region before migrating southward (see Figure 8-14). The NARCCAP regional climate

model ensemble with the A2 emissions scenario predicted increases in precipitation by mid-century (2041-2070) in central Washington, but decreases in central Idaho and southwestern Oregon (see Figure 8-15).

The range of model simulated changes is quite large, which reduces confidence (see Figure 8-16). Since precipitation estimates have such large uncertainties, and the potential for both increases and decreases in precipitation are possible, there exists an equal chance that precipitation will either increase or decrease through time. Model estimates tended to have the greatest increase in precipitation in the northern parts of the region (northern Washington and Idaho) while southwest Oregon and central Idaho experienced decreases in precipitation.

Rainfall intensity in the Northwest has seen very slight increases, depending on the metric used to define intensity. The daily 20-year return level definition (the amount of rain that falls in a day that a location might experience once every 20 years) shows very slight decreases in winter and summer (0.02 and 0.04 inches, respectively) and a slight increase in spring (0.09 inches), which combine to a 0.03 annual increase (see Figure 8-17). There has also been a noted increase in the value of the 5-year maximum daily precipitation (2% increase from 1901-2016) and a 9% increase in 99th percentile precipitation (see Figure 8-18).

LOCA downscaled data predict an increase in the 20-year return period amount for daily precipitation for both low and high emissions scenarios (see Figure 8-19). For the low emissions scenario, the 20-year return period amount is projected to increase 9% by mid-century and 10% by late-century, while the high emissions scenario calls for increases of 11% by mid-century and 19% by late-century.

For the period from 1901-2016, the region has seen a 13% increase in the number of 2-day rainfall events that would normally be expected to occur once every five years. The number of 1-day rainfall events that would normally be expected to occur once every five years has seen an increase in recent years, but the trend is not considered to be statistically significant. Simulations involving NARCCAP regional climate models using a high emissions scenario predicted an increase in the number of days with rainfall totals exceeding 1-inch (see Figure 8-20). Increases in the number of days with rainfall amounts greater than 2, 3, and 4 inches are also predicted. However, the standard deviation is just as large if not larger than the projected average increase, which introduces uncertainty. LOCA downscaled data using both low and high emissions scenarios predict an increase in the number of 2-day, 5-year events (2-day rain events with totals expected once every 5-years) as the decades progress (see Figure 8-21).

Increases in the number of days with rainfall totals over 1 inch were not considered to be statistically significant in most of the region (with respect to the NARCCAP predictions). However, increases were statistically significant in eastern Washington, eastern Oregon, and northern Idaho, which suggests these areas stand to see increases in days with heavy rainfall.

With respect to seasonality, the region has seen an increase in spring precipitation while fall and winter precipitation has decreased, calculated as the difference between the 1901-1960 average and the 1986-2015 average. However, there has not been a statistically significant trend in precipitation per season throughout the region, as determined from the 1901-1960 average. NARCCAP model simulations using a high emissions scenario indicated increases in

precipitation for fall, winter, and spring, and a decrease in precipitation for summer by midcentury (2041-2070). However, the only portions of these predictions that were statistically significant were decreases in parts of Oregon in spring and summer, part of Idaho in summer, and increases in northeast Washington/north Idaho in fall. No significant trend was identified in winter (see Figure 8-15). The CMIP5 simulations for late century (2075-2099) with high emissions predicted a decrease in summer precipitation and an increase in winter precipitation across most of the region. Much like the NARCCAP simulations, however, very few of the projected changes were considered statistically significant (see Figure 8-22).

This region is prone to experiencing flooding from extreme precipitation events, with winter storms and atmospheric rivers contributing to heavy rain and snowfall events along the Coast and Cascades mountain ranges. Furthermore, coastal flooding due to sea level rise is an issue to consider, as sea level has risen roughly 0.5 inches per decade for the period from 1993-2015 (see Figure 8-23).

Sea level changes along the northwest coast (coastal Washington and Oregon) have been projected to increase 2-4 feet by 2100, according to the Interagency Intermediate Scenario (see Figure 8-24). Extreme precipitation is projected to increase, both in terms of the number of days as well as the amount of precipitation (see precipitation stressors for more information). Atmospheric rivers are also projected to become more frequent and intense along the West Coast in the future. As a result, it is unlikely that flooding will decrease.

Sea level rise, as the name implies, would have a greater impact in coastal regions as opposed to locations inland. The presence of mountains (and thus orthographic enhancement of precipitation) also contributes to a greater risk of floods on the windward side of mountain ranges, especially those closer to the coast such as the Coast and Cascades ranges.

Drought is most pronounced in the region when winter precipitation is deficient. However, drought can develop further inland during other seasons due to less concentrated precipitation further away from the Cascades. Drought can also be exacerbated by snowpack, as snowmelt can help mitigate drought in future seasons. Multiple climate divisions throughout the region have seen increasing drought, as defined by the Palmer Drought Severity Index, with significant trends present in Idaho and Oregon.

NARCCAP model projections using a high (A2) emissions scenario suggest that the number of consecutive days with precipitation less than a tenth of an inch will increase by midcentury, with much of the increases considered to be statistically significant (see Figure 8-25). Furthermore, the CMIP5 model ensemble with a high (RCP8.5) scenario also predicted significant increases in the number of consecutive dry days (defined as days with less than 0.04 inches of rain) by end of the century (see Figure 8-26). Snowpack atop the various mountains located throughout the region is projected to decrease, as predicted by the CAM5 model with the RCP8.5 scenario (see Figure 8-27).

Regions further inland (on the leeward side of mountain ranges) do not have concentrated precipitation regimes, and thus can have drought throughout the year, as opposed to areas that receive greater amounts of rain/snow, which feel drought when precipitation is lacking.

8.1.3 Other Stressors

There has been an increase in the number of large wildfires (area burned ≥ 405 hectares) per year for the period of record from 1984-2011, with most increases in the region statistically significant (see Figure 8-28). This increase in wildfires has been driven in part by warmer and drier conditions.

Model simulations project wildfires to increase in occurrence, with one model simulation using the A1B emissions scenario predicting the median annual area burned in the region to quadruple in size relative to the 1916-2007 period by the 2080s, increasing the likelihood that the region as a whole would have a 50% chance of having 2.2 million acres burn every year. The major causes for uncertainty in these projections are the lack of studies focusing on other regions, projections tending to focus on limited areas, and other factors of climate change (water deficits, insect infestations) reducing fuel loads, which inhibit wildfire development. The sensitivity of fuel to climate conditions and fuel availability are the main causes for sub-regional variability. For instance, the western Cascades in Washington experience year-to year variability that cannot easily be attributed to climate conditions, while the eastern Cascades and other vegetation zones throughout the region are responsive to climate.

In the last 40 years, the first wildfires of the year have been observed to start earlier, while the last fires start later. As a result, the length of fire season has been observed as having increased. Since temperature and soil moisture are among the more important aspects of the relationship between fire frequency and ecosystems, and projections for the region involve increased temperature and reductions in soil moisture, it stands to reason that fire season in the region will continue to increase.

The Northwest region experiences large-scale winter storms during the period from late October to the beginning of April. These storms bring rain, snow, and high winds to the region. Winter storm tracks have been observed as having changed, but these studies are limited. Studies exploring arctic amplification of winter storms have returned mixed results, and projections for future winter storms yielded large model-to-model differences. As a result, there is low confidence in predicting if winter storm intensity will increase or decrease in the future.

According to Kunkel et al. (2009), snowfall has been decreasing throughout the region, using the period from 1937-2007. These decreases range in magnitude from 0.1% per decade to 1.2% or greater. Furthermore, there has been an observed change in precipitation type throughout the region as systems that used to be predominantly snow have transitioned to rain. Both the CMIP3 and CMIP5 model suites predict that snowpack will decrease in the future, with both models using a high emissions scenario. In both cases, snowpack faces reductions up to 40%. By the end of the century, many places currently receiving snow in the cold season are projected to be rain-dominated.

Cold air entrapment by the Cascades can evolve into major ice storms, given sufficient precipitation. Northwest Washington also experiences ice storms, and the middle Columbia basin has received freezing rain events in the past. Since 1966-1977, there has been a decrease in the number of ice storms throughout the eastern portion of the region. Furthermore, freezing rain has decreased throughout most of the region, with slight increases present in the northwest and southeast. As mentioned in the snowfall stressor report, there has been an observed change in

precipitation type throughout the region as systems that used to be predominantly snow have transitioned to rain. This, coupled with the relatively confident projections that temperature will increase in the future regardless of emissions, enforces the notion that ice storms and freezing rain will decrease throughout the region, as precipitation regimes change to become predominantly rain. According to the Third National Climate Assessment, knowledge of ice storms is relatively limited, making it difficult to ascertain both observed trends and projected changes. However, observed changes in ice storms helps raise confidence in this projection.

8.2 Tables and Figures: Northwest Region

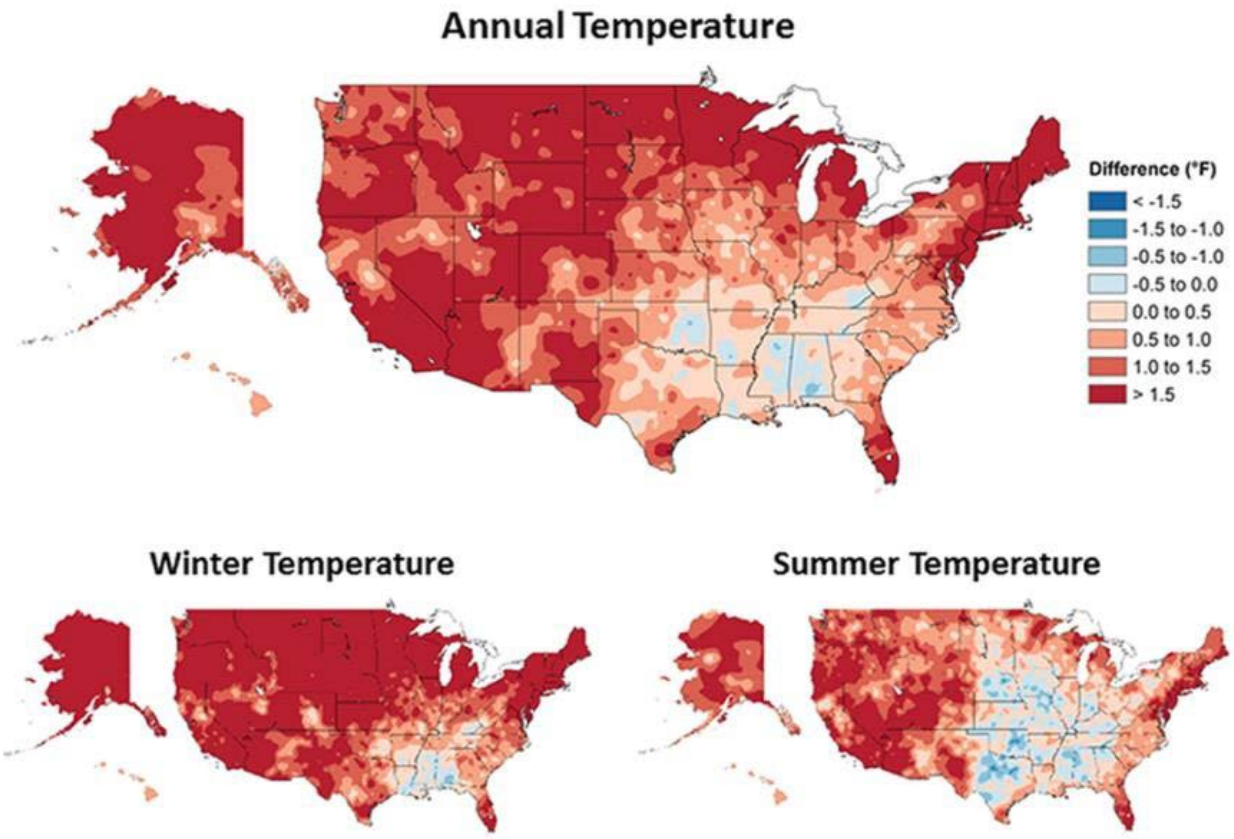

Figure 8-1. Observed change in annual (top), winter (bottom left), and summer (bottom right) temperatures between the 1986–2016 period and the period 1901–2016. Changes are the differences between the average for present day (1986–2016) and the average for the first half of the last century (1901–1960 for the contiguous United States, 1925–1960 for Alaska and Hawaii) (Figure source: USGCRP 2017 p. 188).

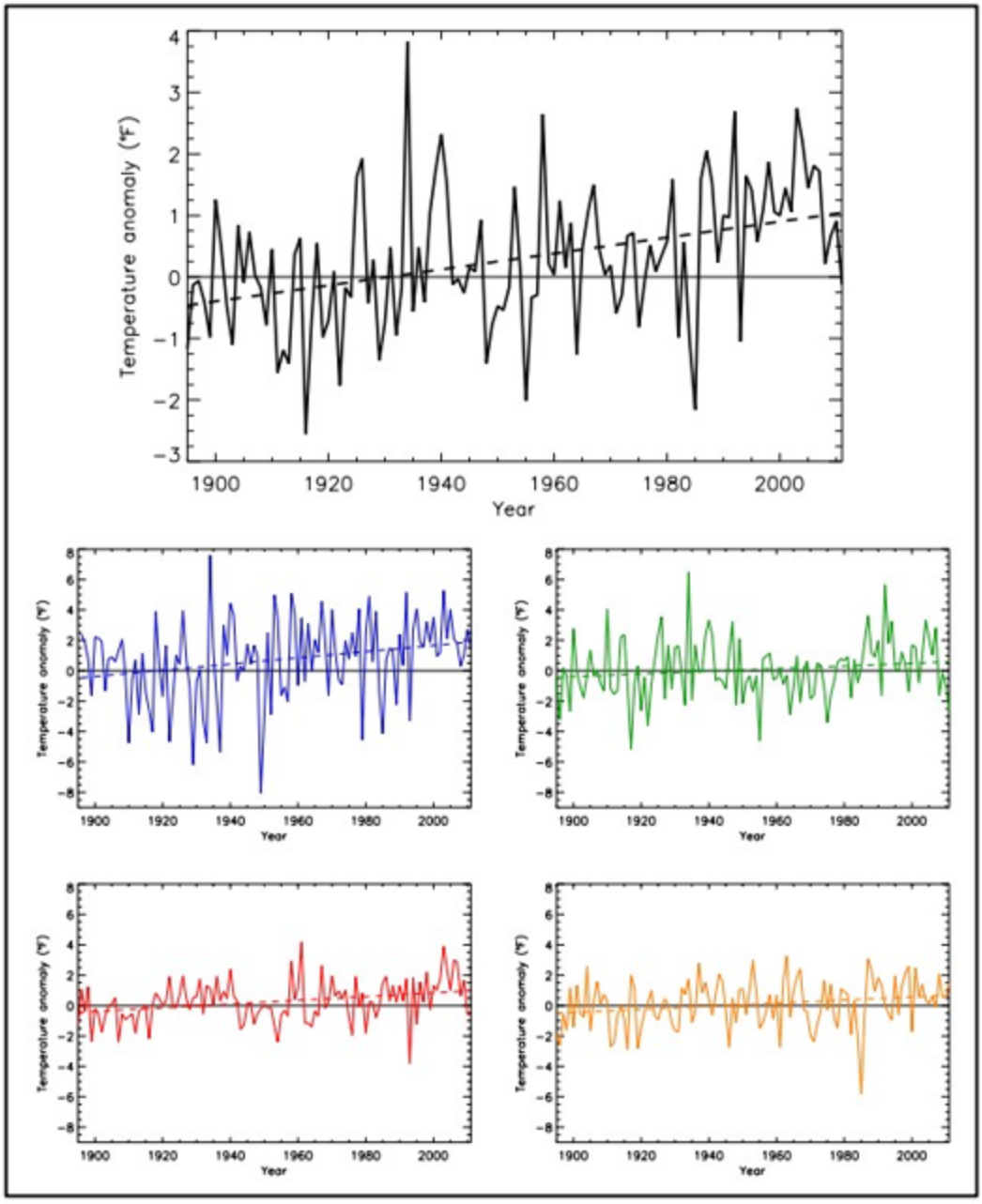

Figure 8-2. Temperature anomaly (deviations from the 1901-1960 average, °F) for annual (black), winter (blue), spring (green), summer (red), and fall (orange), for the Northwest U.S. Dashed lines indicate the best fit by minimizing the chi-square error statistic. Based on a new gridded version of COOP data from the National Climatic Data Center, the CDDv2 data set (R. Vose, personal communication, July 27, 2012). Note that the annual time series is on a unique scale. Trends are upward and statistically significant annually and for all seasons (Figure source: Kunkel et al. 2013, part 6).

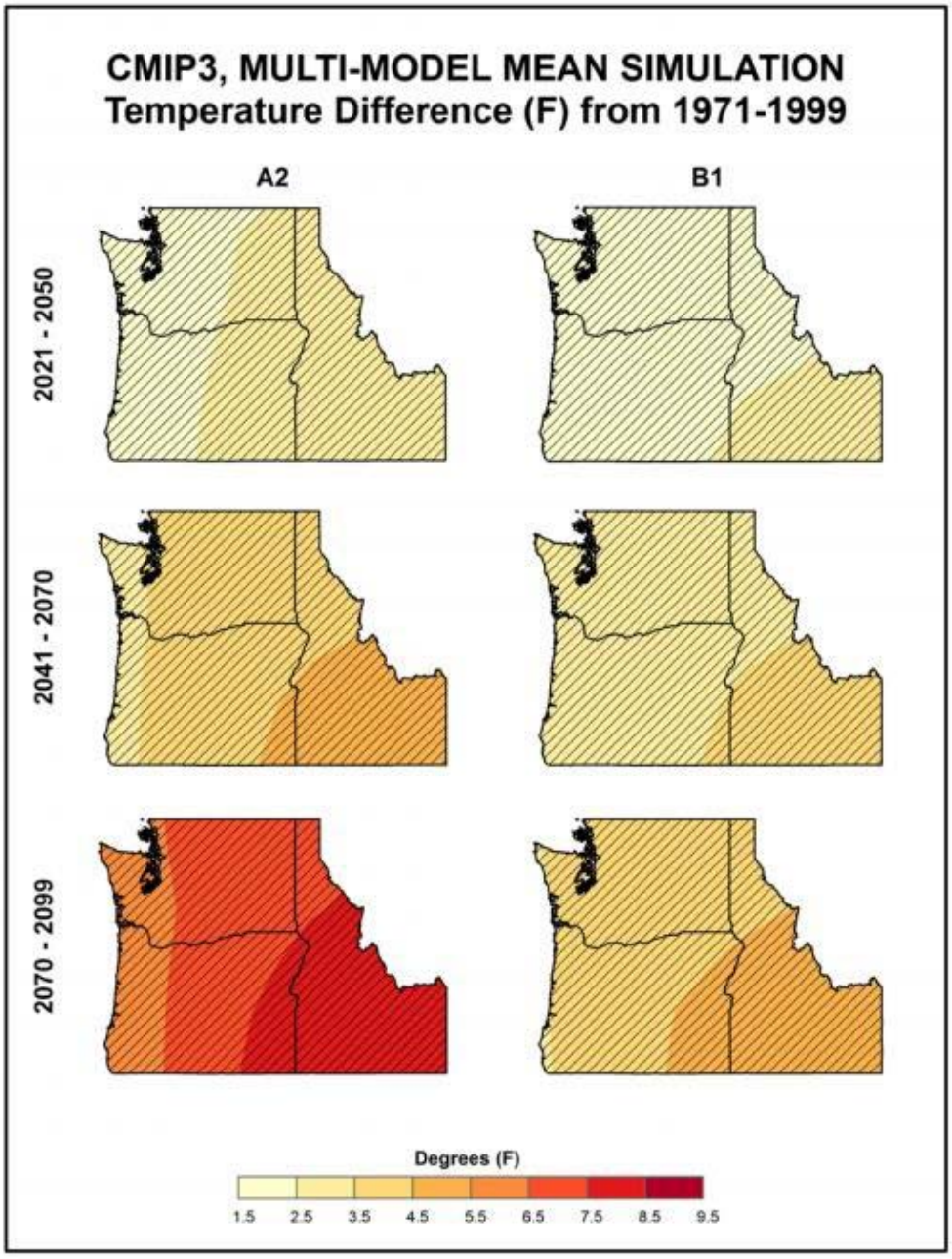

Figure 8-3. Simulated difference in annual mean temperature (°F) for the contiguous United States, for each future time period (2021-2050, 2041-2070, and 2070-2099) with respect to the reference period of 1971-1999. These are multi-model means for the high (A2) and low (B1) emissions scenarios from the 14 (B1) or 15 (A2) CMIP3 global climate simulations. Color with hatching (category 3) indicates that more than 50% of the models show a statistically significant change in temperature, and more than 67% agree on the sign of the change (see text). Temperature changes increase throughout the 21st century, more rapidly for the high emissions scenario (Figure source: Kunkel et al. 2013, part 6).

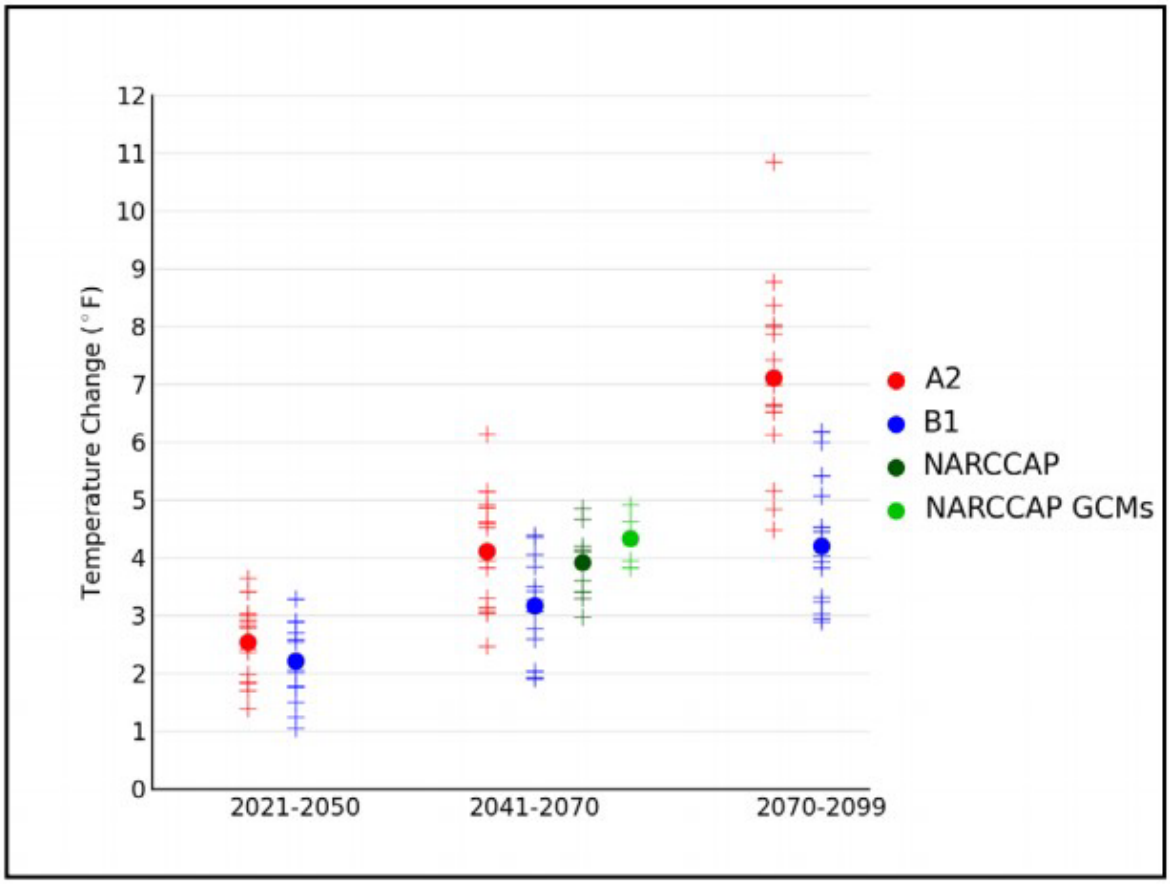

Figure 8-4. Simulated annual mean temperature change (°F) for the Northwestern United States, for each future time period (2021-2050, 2041-2070, and 2070-2099) with respect to the reference period of 1971-1999 for the CMIP3 models and 1971-2000 for the NARCCAP models. Values are given for the high (A2) and low (B1) emissions scenarios for the 14 (B1) or 15 (A2) CMIP3 models. Also shown for 2041-2070 (high emissions scenario only) are values for 9 NARCCAP models, as well as for the 4 GCMs used to drive the NARCCAP simulations. The small plus signs (+) indicate each individual model and the circles depict the multi-model means. The range of model-simulated changes is large compared to the mean differences between A2 and B1 in the early and middle 21st century. By the end of the 21st century, the difference between A2 and B1 is comparable to the range of B1 simulations (Figure source: Kunkel et al. 2013, part 6).

Temperature Variable	NARCCAP Mean	NARCCAP Standard Deviation	Daily_CMIP3 Mean
Freeze-free period	+35 days	6 days	+33 days
#days $T_{max} > 90°F$	+8 days	7 days	+18 days
#days $T_{max} > 95°F$	+5 days	7 days	+10 days
#days $T_{max} > 100°F$	+3 days	6 days	+4 days
#days $T_{min} < 32°F$	-35 days	6 days	-35 days
#days $T_{min} < 10°F$	-15 days	7 days	-9 days
#days $T_{min} < 0°F$	-8 days	5 days	-4 days
Consecutive #days > 95°F	+134%	206%	+225%
Consecutive #days > 100°F	+163%	307%	+439%
Heating degree days	-15%	2%	-16%
Cooling degree days	+105%	98%	+147%
Growing degree days (base 50°F)	+51%	14%	+49%

Figure 8-5. Multi-model means and standard deviations of the simulated annual mean change in select temperature variables from 9 NARCCAP simulations for the Northwest region. Multi-model means from the 8 daily CMIP3 simulations are also shown for comparison. Analyses are for the 2041-2070 time period with respect to the reference period of 1971-2000, for the high (A2) emissions scenario (Figure source: Kunkel et al. 2013, part 6).

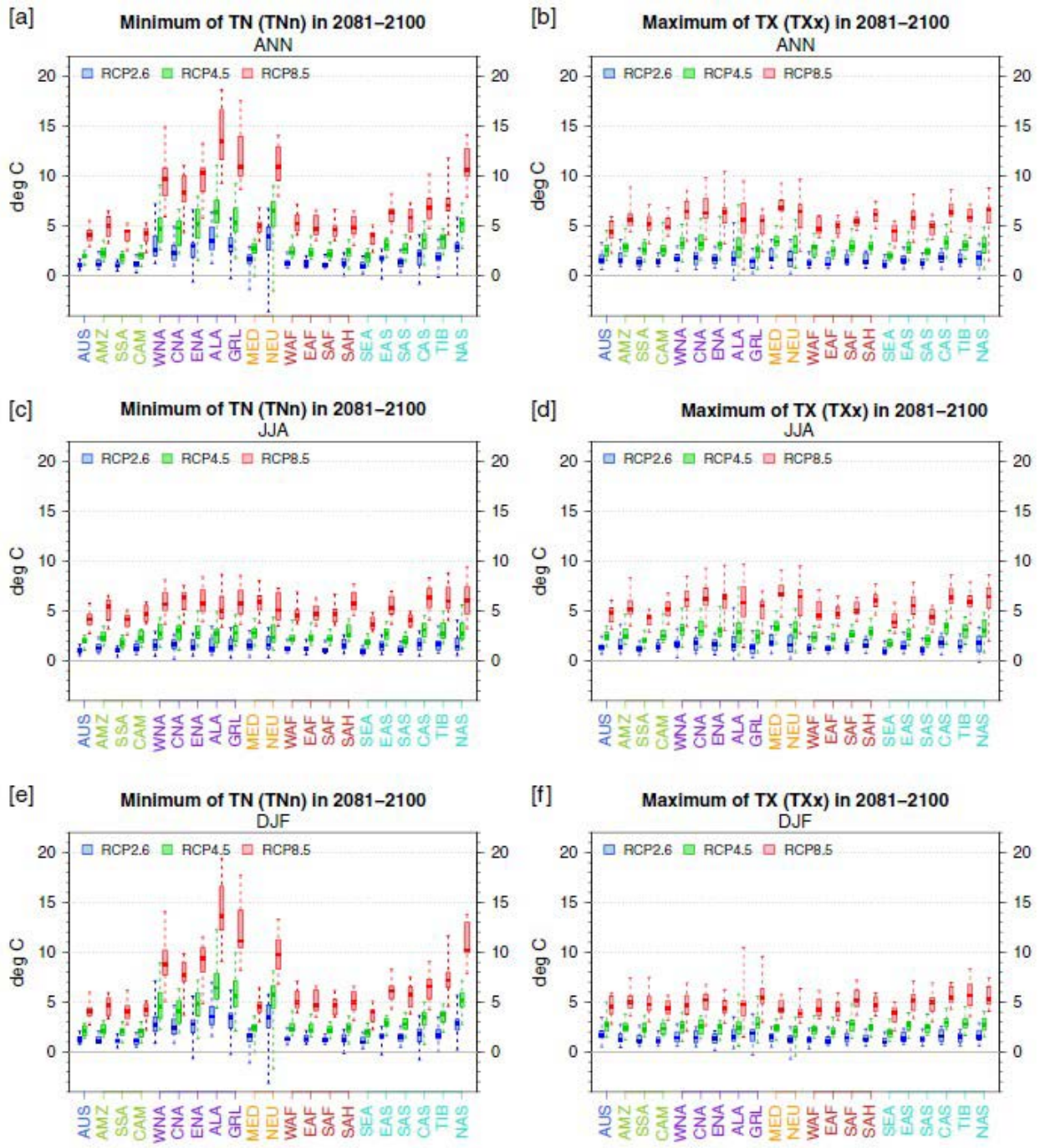

Figure 8-6. Projected changes in annual (ANN), JJA and DFJ minima of TN (TNn, left) and maximum TX (TXx, right) over the time period 2081-2100 as difference relative to the reference period (1981-2000) for RCP2.6 (blue) RCP4.5 (green) and RCP8.5 (red). Regional mean changes are shown for each of the 21 sub regions (cf figure 2) Boxes indicate the interquartile model spread (25th and 75th quantiles) with the horizontal line indicating the ensemble median and the whiskers showing the extreme range of the CMIP5 ensemble (Figure source: Sillmann et al. 2013, part 2).

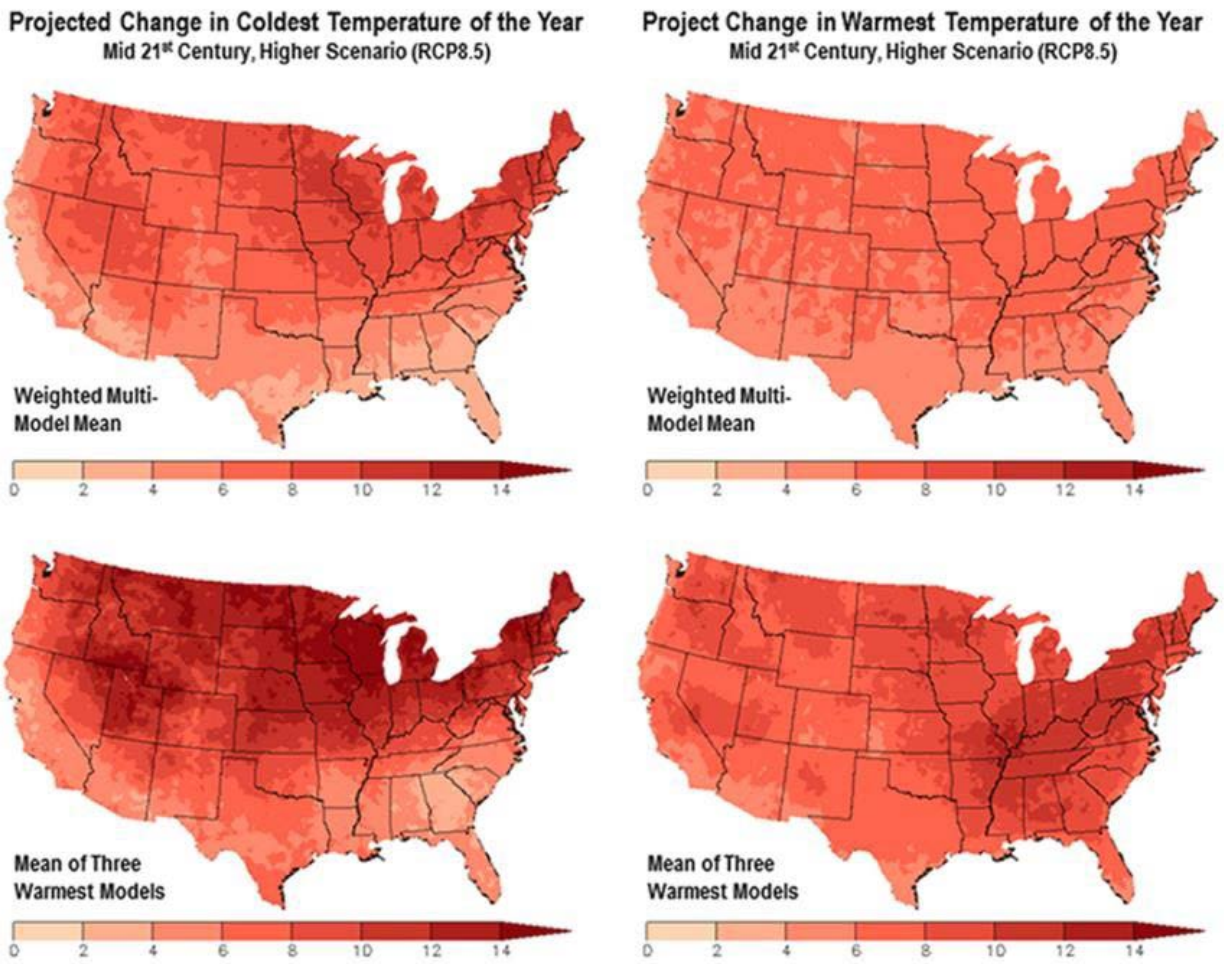

Figure 8-7. Projected changes in the coldest and warmest daily temperatures (°F) of the year in the contiguous United States. Changes are the difference between the average for mid-century (2036–2065) and the average for near-present (1976–2005) under the higher scenario (RCP8.5). Maps in the top row depict the weighted multi-model mean whereas maps on the bottom row depict the mean of the three warmest models (that is, the models with the largest temperature increase). Maps are derived from 32 climate model projections that were statistically downscaled using the Localized Constructed Analogs technique. Increases are statistically significant in all areas (that is, more than 50% of the models show a statistically significant change, and more than 67% agree on the sign of the change) (Figure source: USGCRP 2017 p. 198).

NCA Region	Change in Coldest Day of the Year	Change in Warmest Day of the Year
Northeast	2.83°F	−0.92°F
Southeast	1.13°F	−1.49°F
Midwest	2.93°F	−2.22°F
Great Plains North	4.40°F	−1.08°F
Great Plains South	3.25°F	−1.07°F
Southwest	3.99°F	0.50°F
Northwest	4.78°F	−0.17°F

Figure 8-8. Observed changes in the coldest and warmest daily temperatures (°F) of the year for each National Climate Assessment region in the contiguous United States. Changes are the difference between the average for present-day (1986–2016) and the average for the first half of the last century (1901–1960). Estimates are derived from long-term stations with minimal missing data in the Global Historical Climatology Network–Daily dataset (Figure source: USGCRP 2017 p. 190).

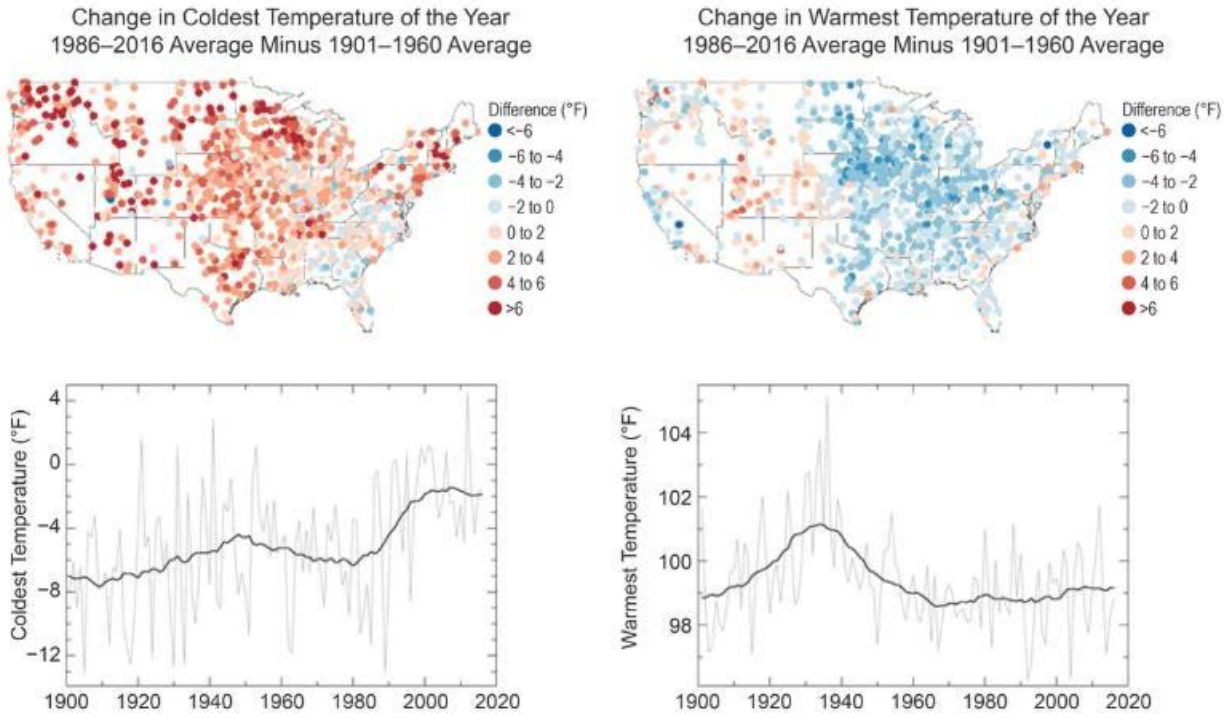

Figure 8-9. Observed changes in the coldest and warmest daily temperatures (°F) of the year in the contiguous United States. Maps (top) depict changes at stations; changes are the difference between the average for present-day (1986–2016) and the average for the first half of the last century (1901–1960). Time series (bottom) depict the area-weighted average for the contiguous United States. Estimates are derived from long-term stations with minimal missing data in the Global Historical Climatology Network–Daily dataset (Figure source: USGCRP 2017 p. 190).

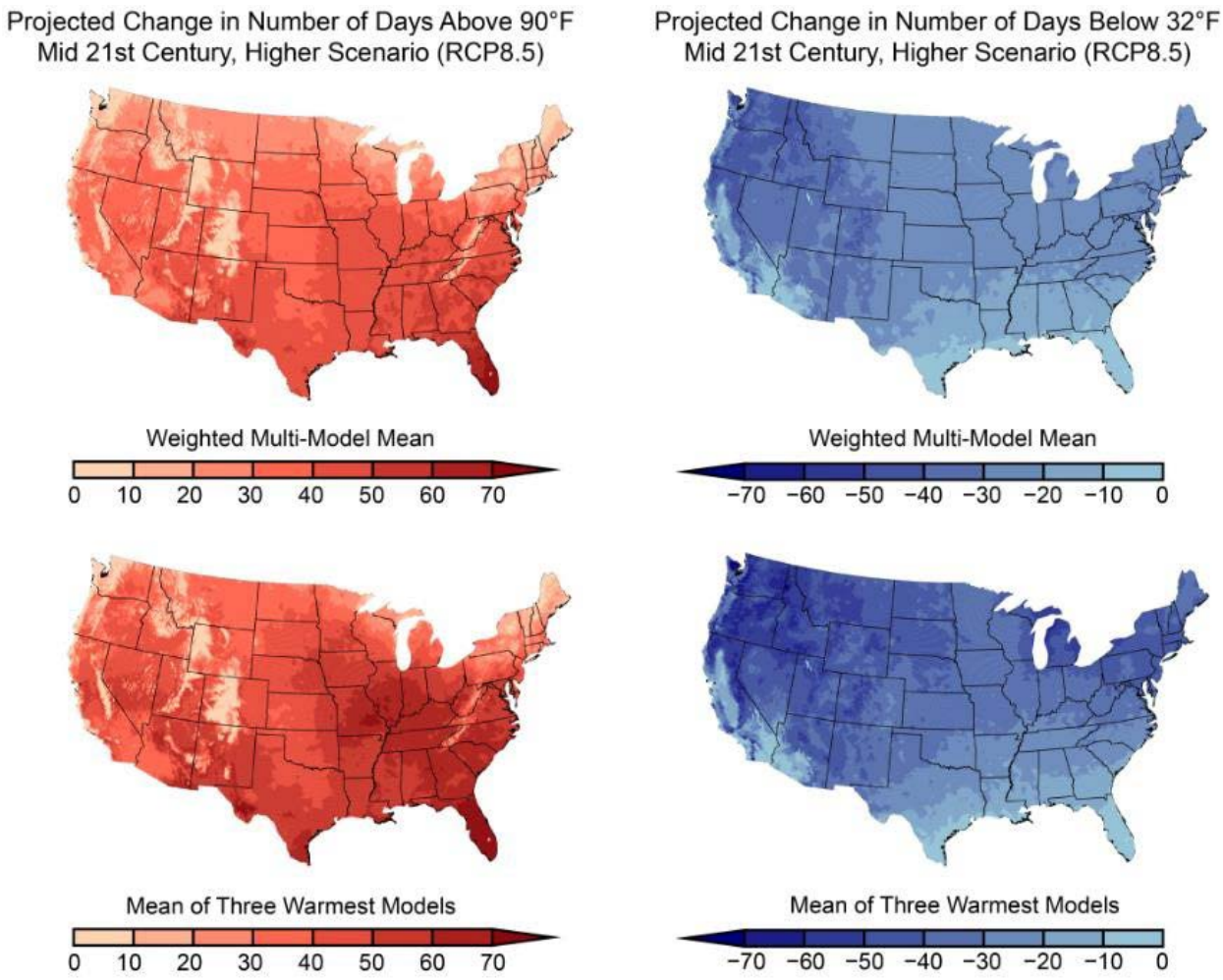

Figure 8-10. Projected changes in the number of days per year with a maximum temperature above 90°F and a minimum temperature below 32°F in the contiguous United States. Changes are the difference between the average for mid-century (2036–2065) and the average for near-present (1976–2005) under the higher scenario (RCP8.5). Maps in the top row depict the weighted multi-model mean whereas maps on the bottom row depict the mean of the three warmest models (that is, the models with the largest temperature increase). Maps are derived from 32 climate model projections that were statistically downscaled using the Localized Constructed Analogs technique. Changes are statistically significant in all areas (that is, more than 50% of the models show a statistically significant change, and more than 67% agree on the sign of the change) (Figure source: USGCRP 2017 p. 199).

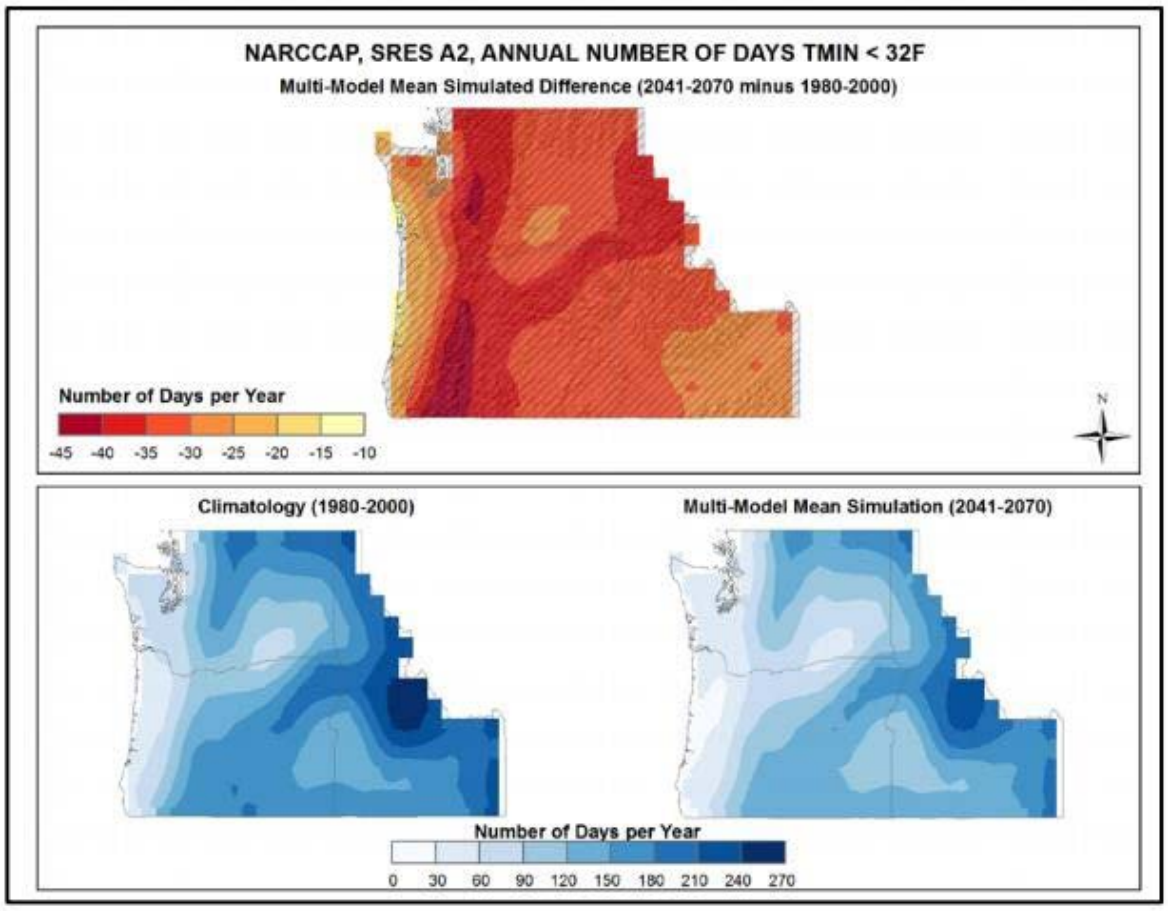

Figure 8-11. Simulated difference in the mean annual number of days with a minimum temperature less than 32°F for the Northwest region for 2041-2010 with respect to the reference period 1980-2000 (top). Color with hatching (category 3) indicated that more than 50% of the models show a statistically significant change in the number of days, and more than 67% agree on the sign of the change (Figure source: Kunkel et al. 2013, part 6).

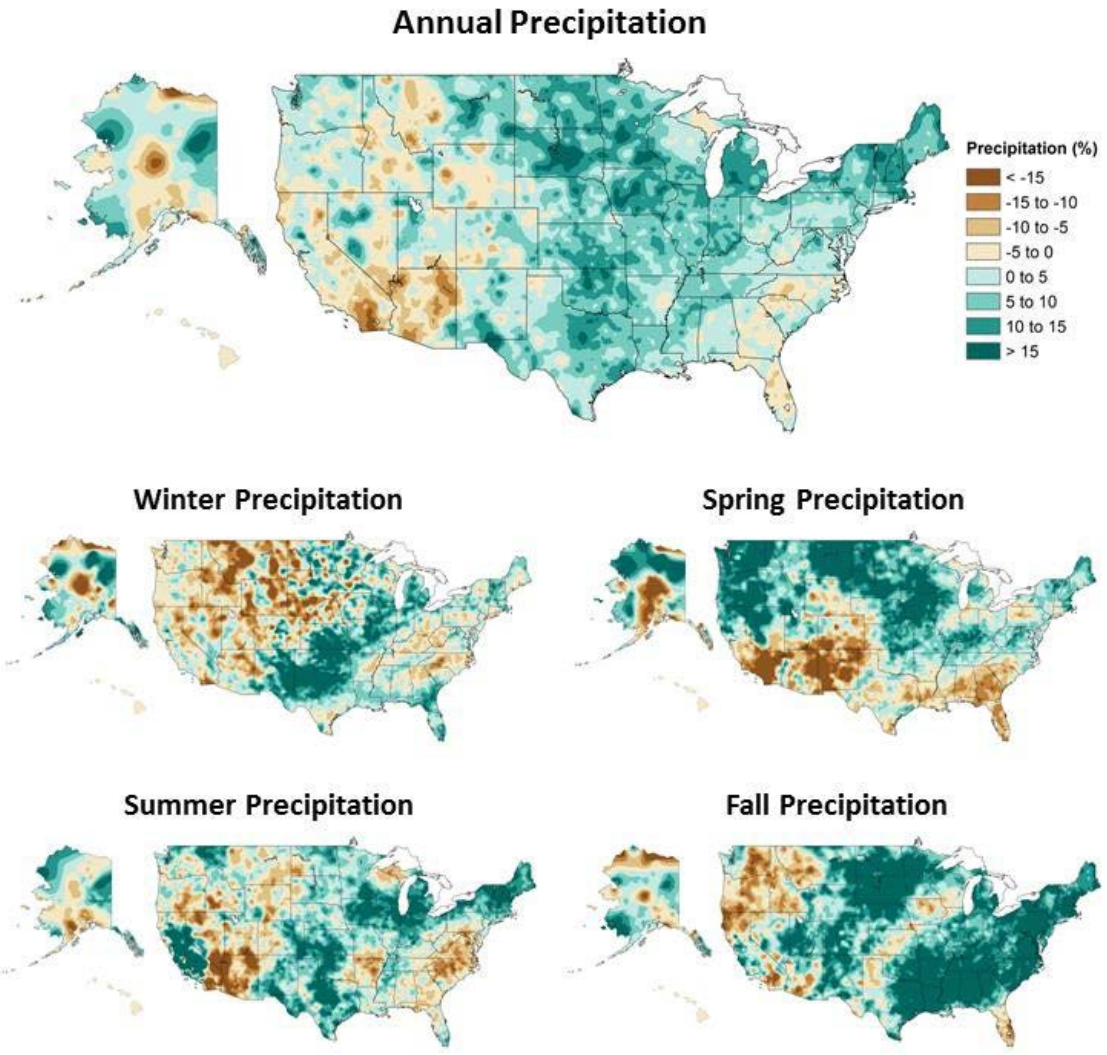

Figure 8-12. Annual and seasonal changes in precipitation over the United States. Changes are the average for present-day (1986–2015) minus the average for the first half of the last century (1901–1960 for the contiguous United States, 1925–1960 for Alaska and Hawai'i) divided by the average for the first half of the century (Figure source: USGCRP 2017 p. 209).

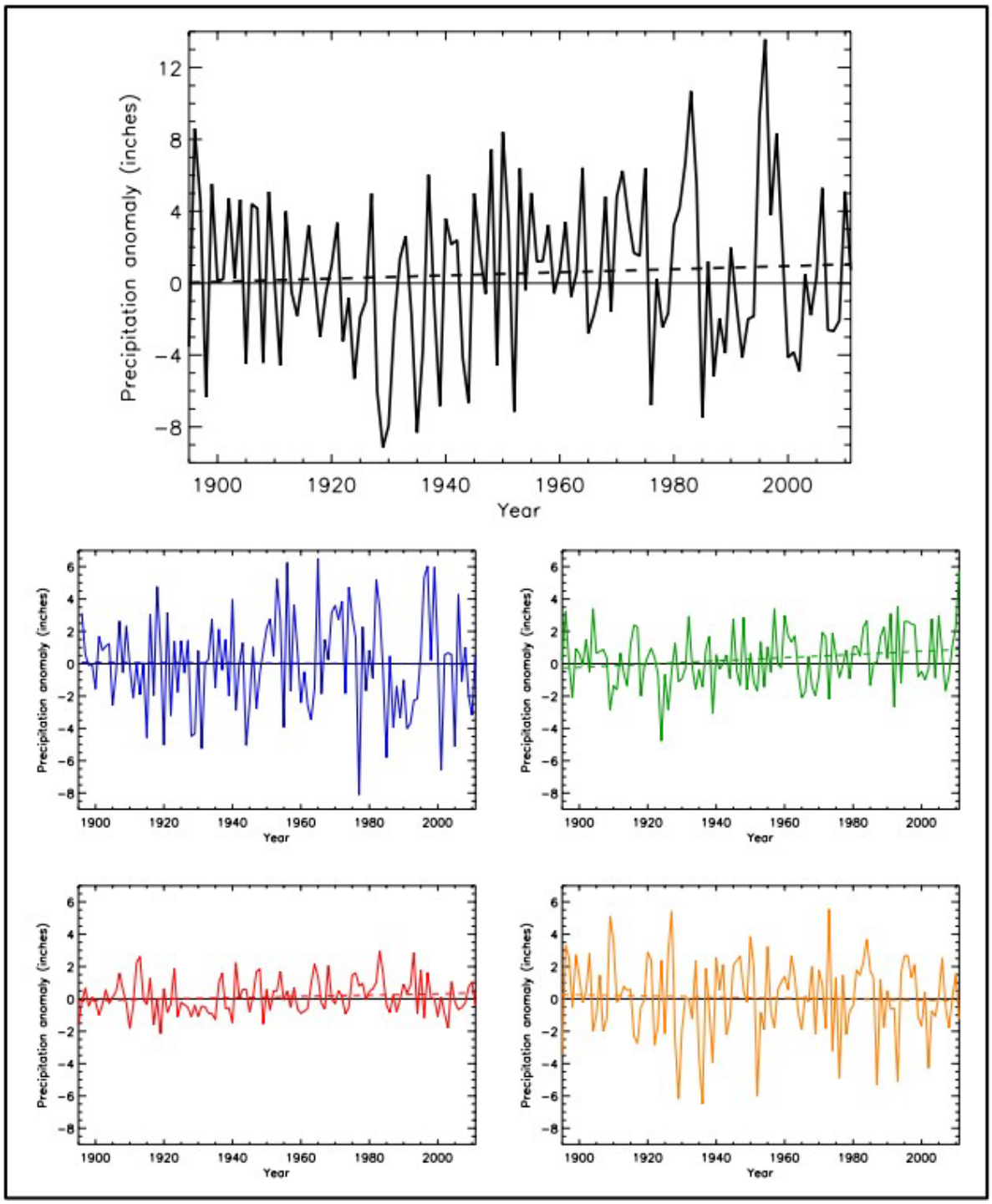

Figure 8-13. Precipitation anomaly (deviation from the 1901-1960 averages, inches) for annual (black) winter (blue) spring (green) and fall (orange) for the Northwest United States. Dashed lines indicate the best fit by minimizing the chi-square error statistic. Based on a new gridded version of COOP data from the National Climatic Data Center, the CDDv2 dataset (R. Vose, personal communication, July 27, 2012). No significant trends in any of the seasons (Figure source: Kunkel et al. 2013, part 6).

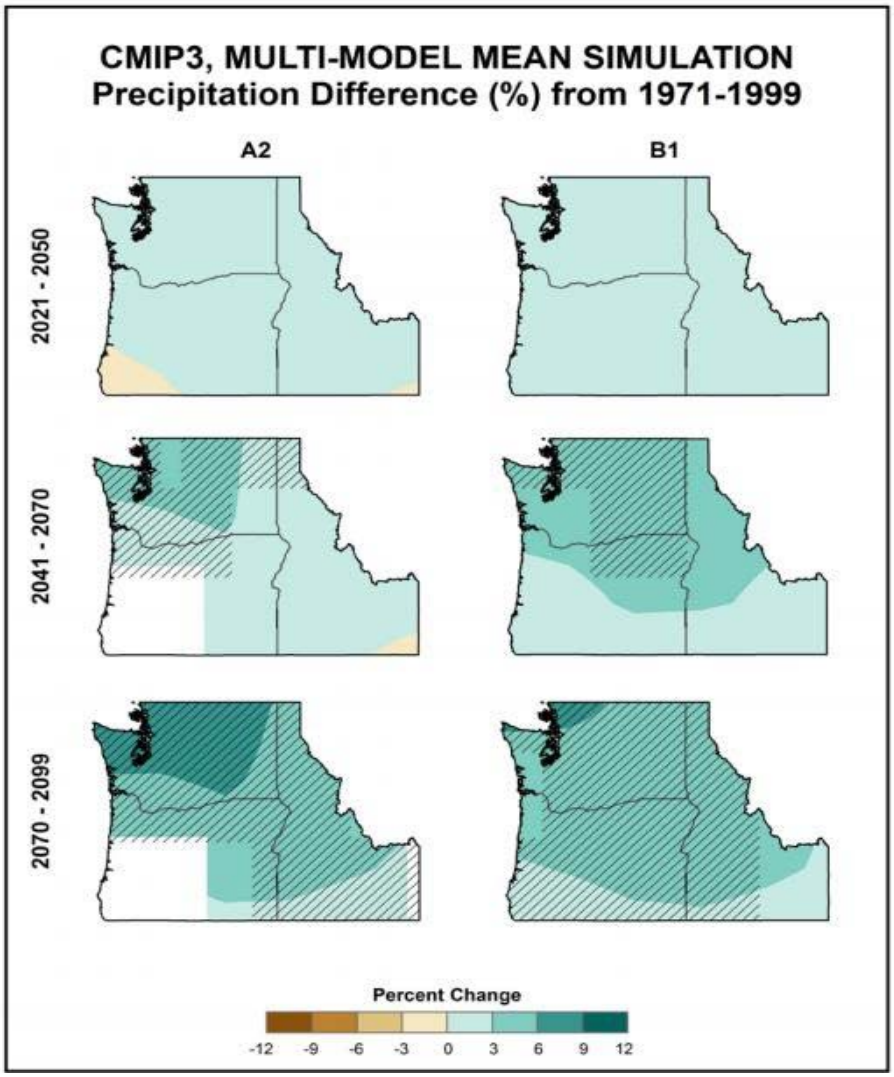

Figure 8-14. Simulated difference in annual mean precipitation (%) for the Northwest region for each future time period (2021-2050, 2041-2070, and 2070-2099) with respect to the reference period of 1971-1999. These are multi-model means for the high (A2) and low (B1) emissions scenarios from the 14 (B1) or 15 (A2) CMIP3 global climate simulations. Color only (category1) indicates that less than 50% of the models show a statistically significant change in precipitation. Color with hatching (category 3) indicates that more than 50% of the models show a statistically significant change in precipitation, and more than 67% agree on the sign of the change. Whited out areas (category 2) indicate that more than 50% of the models show a statistically significant change in precipitation but less than 67% agree on the sign of the change. Models simulate increases almost everywhere and the change generally becomes larger moving northward (Figure source: Kunkel et al. 2013, part 6).

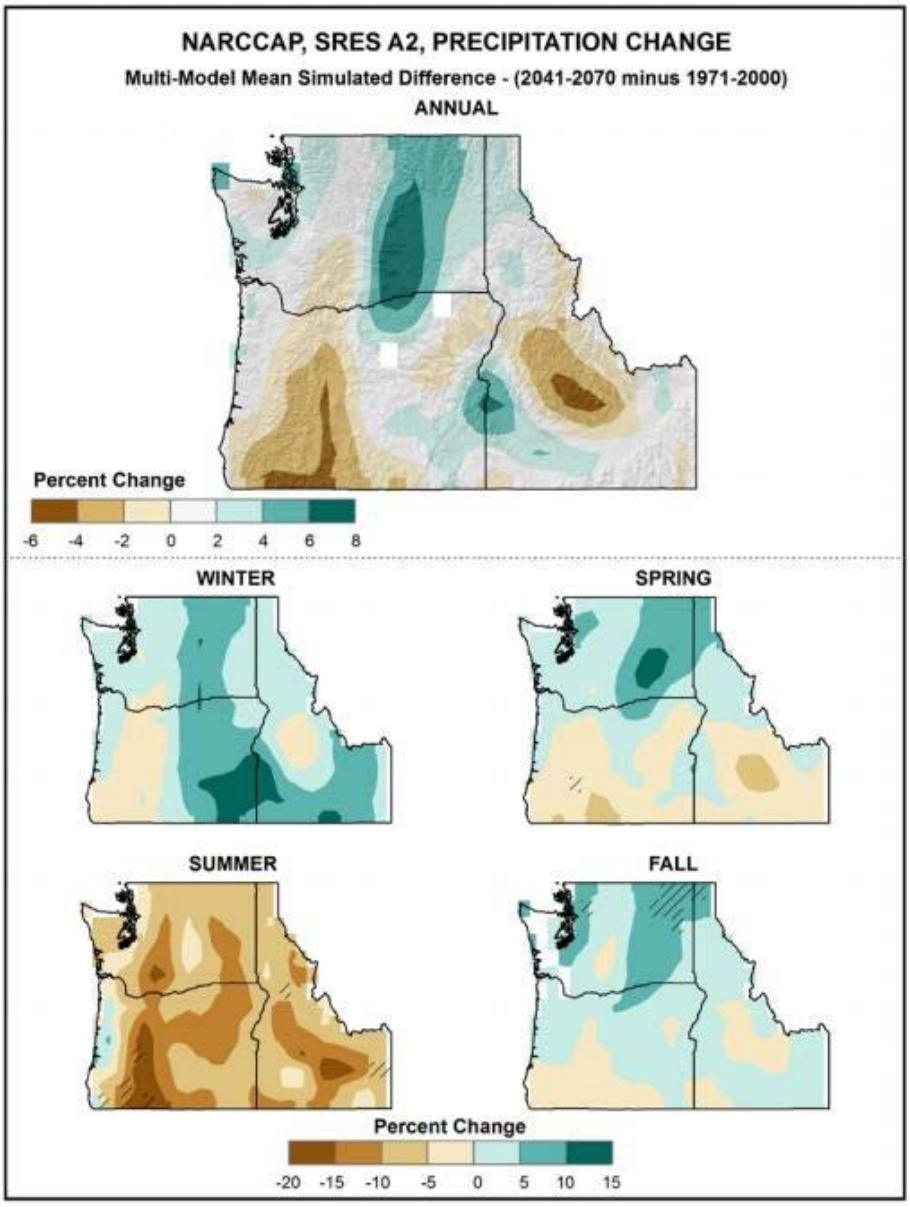

Figure 8-15. Simulated difference in seasonal mean precipitation (%) for the Northwest region for 2041-2070 with respect to the reference period of 1971-2000. There are multi-model means from 11 NARCCAP regional climate simulations for the high (A2) emissions scenario. Color only (category 1) indicates that less than 50% of the models show a statistically significant change in precipitation. Color with hatching (category 3) indicates that more that 50% of the models show a significant change in precipitation and more than 67% agree on the sign of the change. Whited out areas (category 2) indicate that more than 50% of the models show a statistically significant change in precipitation, but less than 67% agree on the sign of the change (Figure source: Kunkel et al. 2013, part 6).

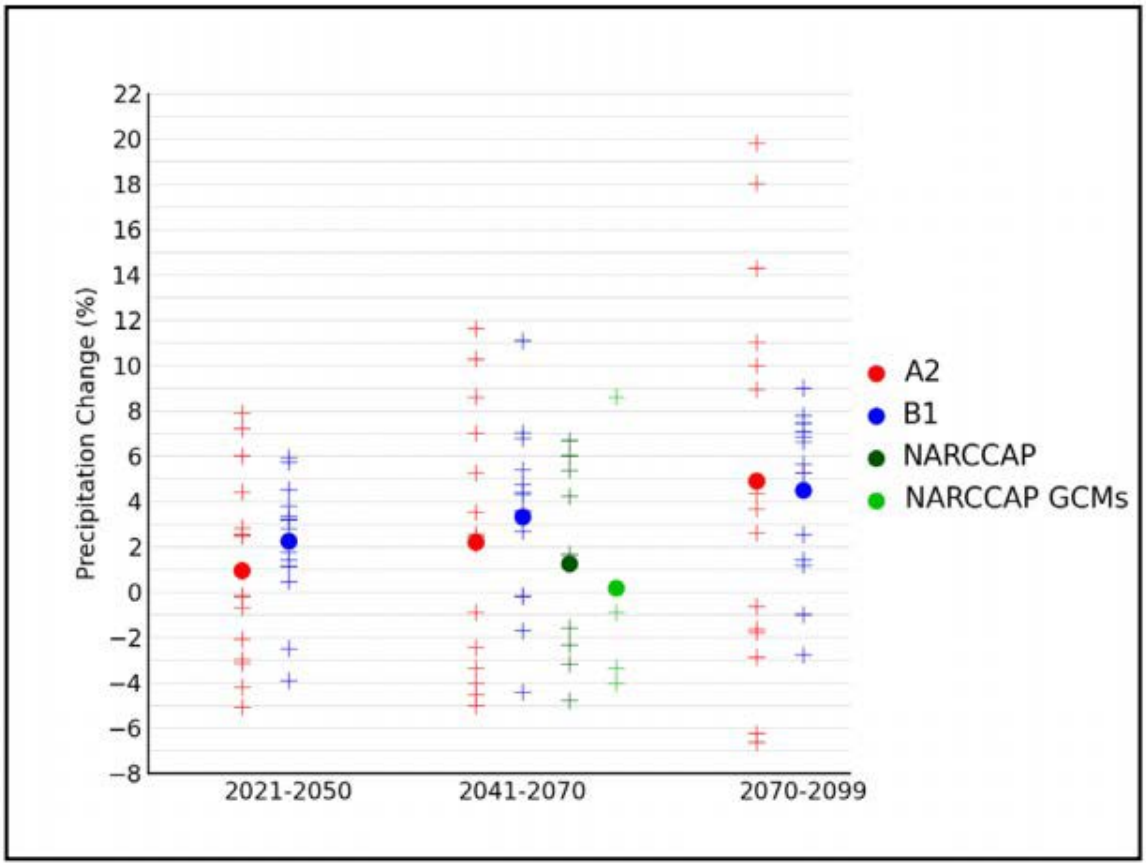

Figure 8-16. Simulated annual mean precipitation change (%) for the Northwestern United States, for each future time period (2021-2050, 2041-2070, and 2070-2099) with respect to the reference period of 1971-1999 for the CMIP3 models and 1971-2000 for the NARCCAP models. Values are given for the high (A2) and low (B1) emissions scenarios for the 14 (B1) or 15 (A2) CMIP3 models. Also shown for 2041-2070 (high emissions scenario only) are values for 9 NARCCAP models, as well as for the 4 GCMs used to drive the NARCCAP simulations. The small plus signs (+) indicate each individual model and the circles depict the multi-model means. The range of model-simulated changes is large compared to the mean differences between A2 and B1 in the early and middle 21st century (Figure source: Kunkel et al. 2013, part 6).

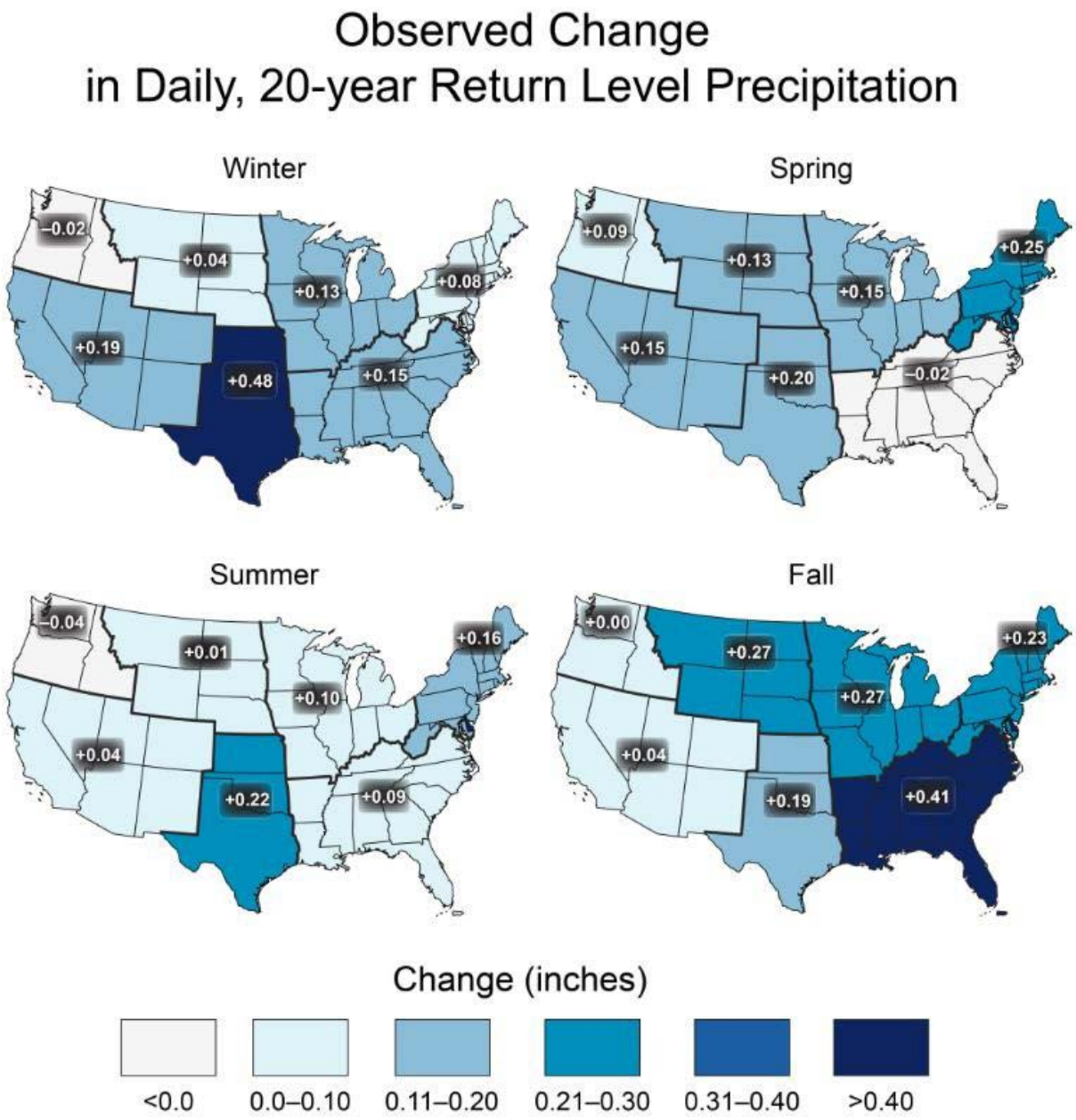

Figure 8-17. Observed changes in the 20-year return value of the seasonal daily precipitation totals for the contiguous United States over the period 1948 to 2015 using data from the Global Historical Climatology Network (GHCN) dataset (Figure source: USGCRP 2017 p. 211).

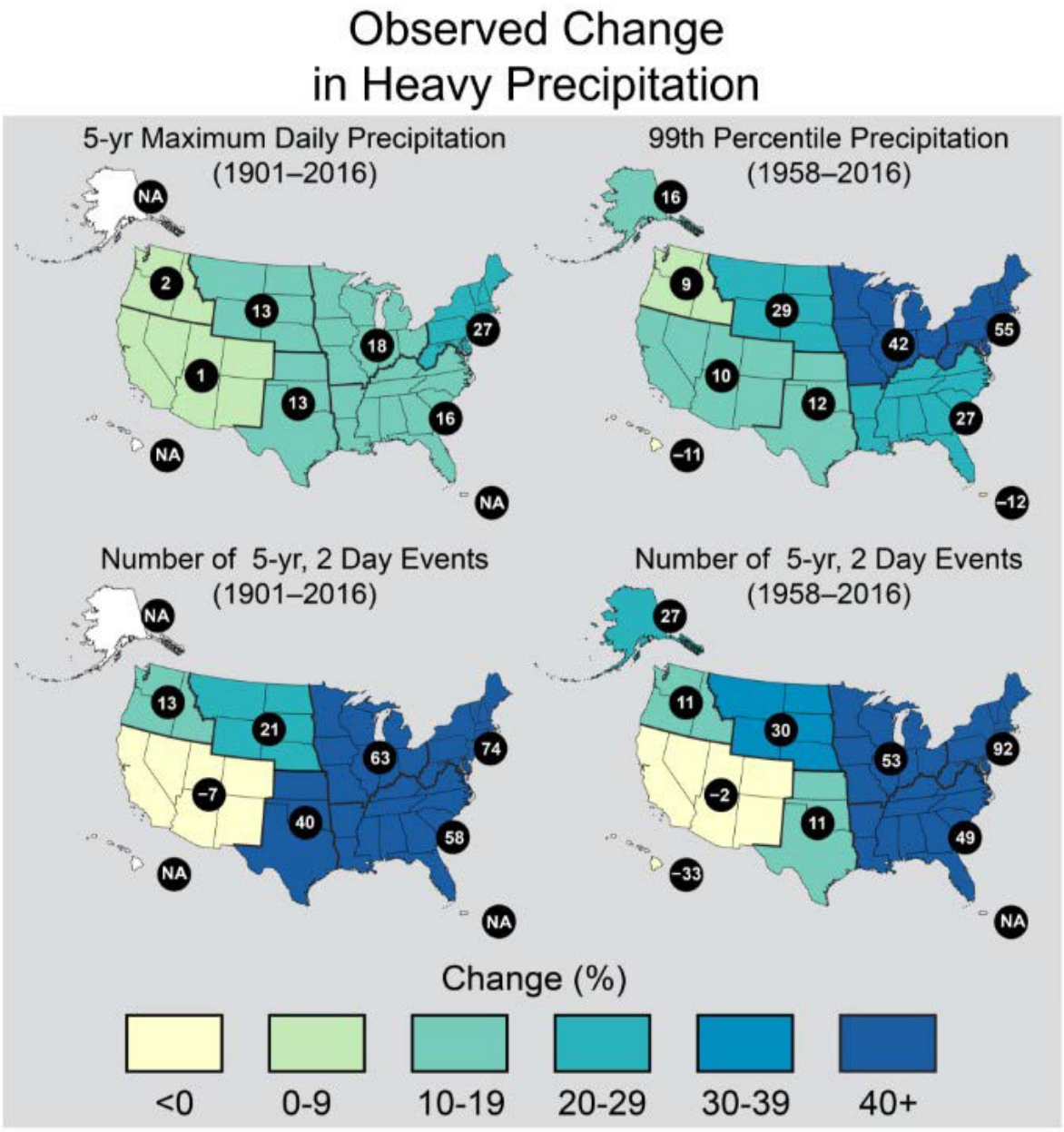

Figure 8-18. Changes in extreme precipitation. The percent change in maximum daily precipitation by 5-year periods (upper left), the percent change in the amount of precipitation falling in daily events that exceed the 99th percentile of precipitation days (upper right), the percent change in number of two day events with a precipitation total exceeding the largest two-day amount that would be expected to occur only once every five years based on data from 1901–2016 (lower left), and the percent change in number of two day events with a precipitation total exceeding the largest two-day amount that would be expected to occur only once every five years based on data from 1958–2016 (lower right) (Figure source: USGCRP 2017 p. 212).

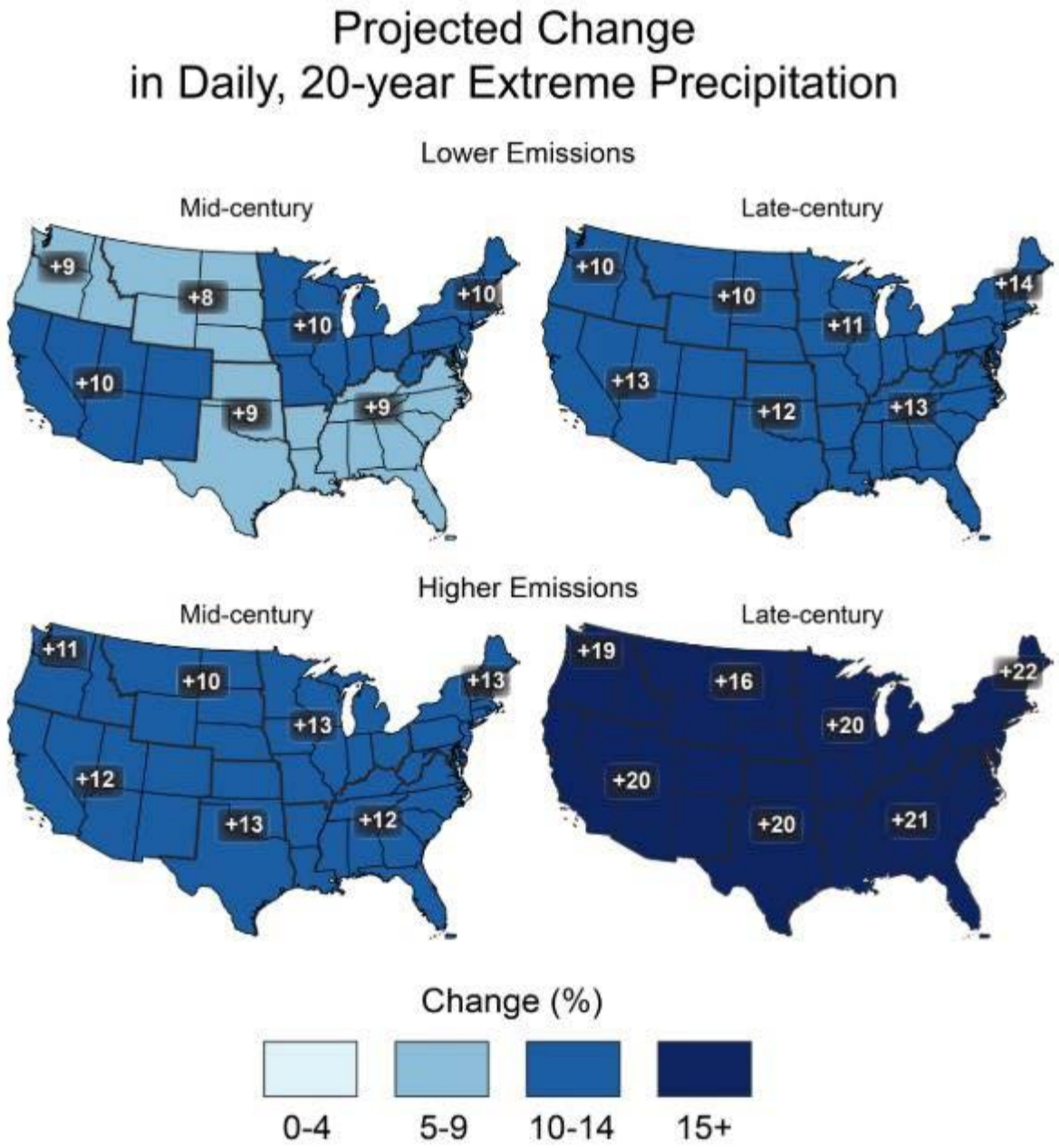

Figure 8-19. Projected change in the 20-year return period amount for daily precipitation for mid- (left maps) and late-21st century (right maps). Results are shown for a lower scenario (top maps; RCP4.5) and for a higher scenario (bottom maps; RCP8.5). These results are calculated from the LOCA downscaled data (Figure source: USGCRP 2017 p. 220).

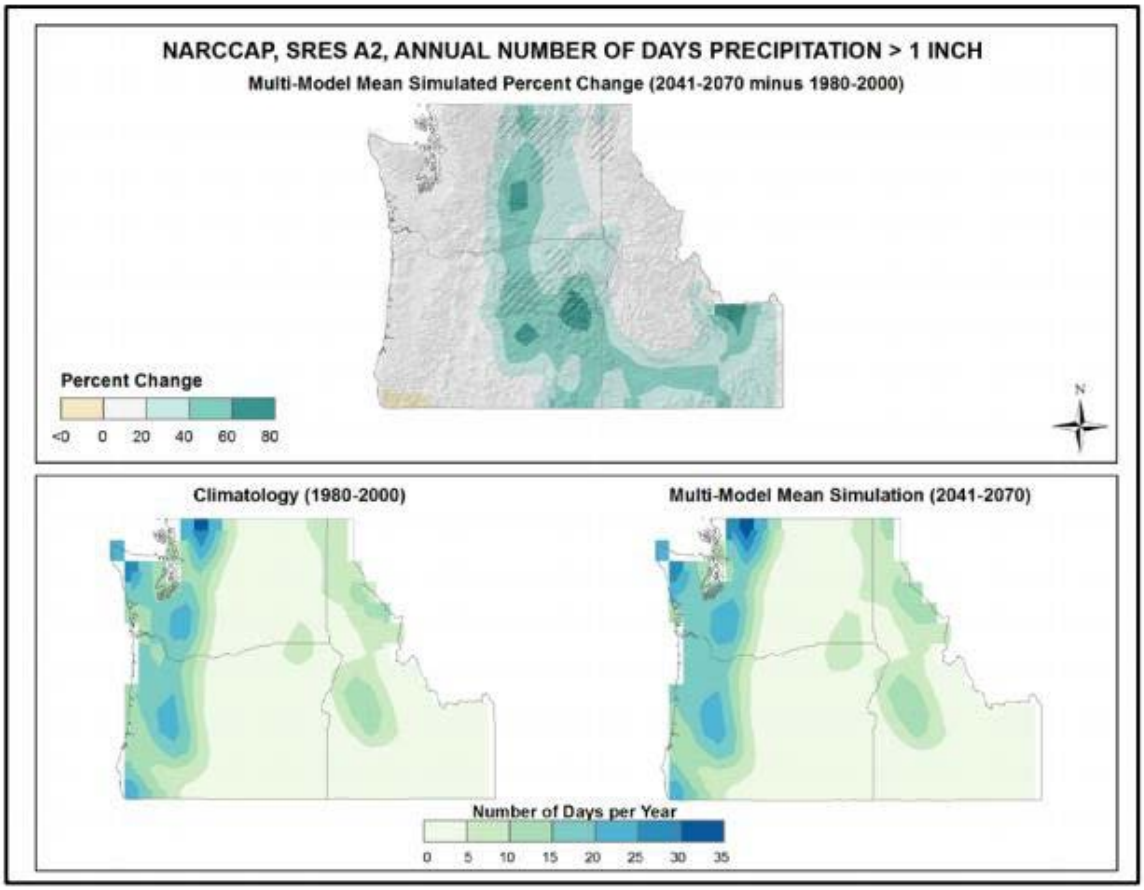

Figure 8-20. Simulated percentage difference in the mean annual number of days with precipitation of greater than once inch for the Northwest region for the 2041-2070 time period with respect to the reference period of 1980-2000 (top). Color only (category 1) indicates that less than 50% of the models show a statically significant change in the number of days. Color with hatching (category 3) indicates that more that 50% of the models show a significant change in number of days and more than 67% agree on the sign of the change. Mean annual number of days with precipitation of greater than one inch for the 1980-2000 reference period is shown bottom left. Simulated mean annual number of days with precipitation of greater than one inch for the 2041-2070 future time period is shown bottom right. These are multi-model means from NARCCAP regional climate simulations for the high (A2) emissions scenario. Models simulate increases over most of the region (Figure source: Kunkel et al. 2013, part 6).

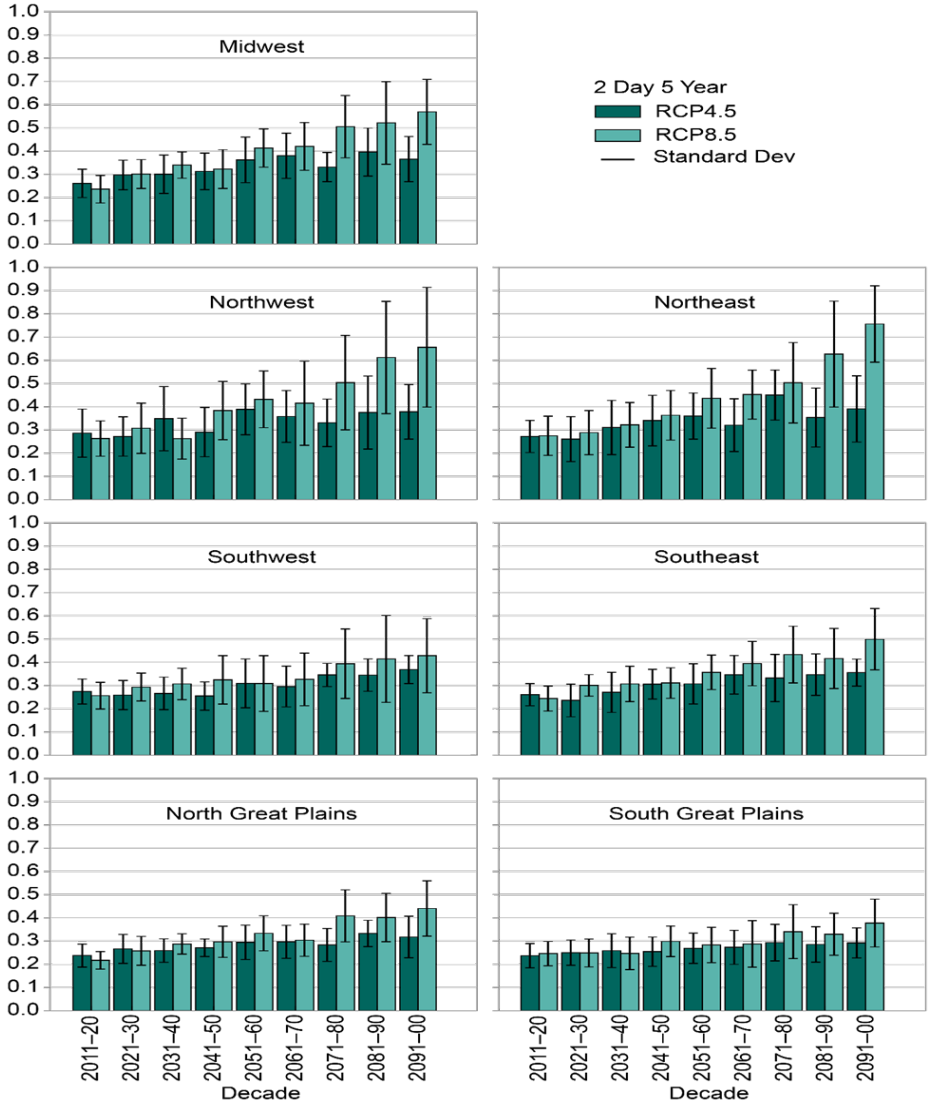

Figure 8-21. Regional extreme precipitation event frequency for a lower scenario (RCP4.5) (green; 16 CMIP5 models) and the higher scenario (RCP8.5) (blue; 14 CMIP5 models) for a 2-day duration and 5-year return. Calculated for 2006–2100 but decadal anomalies begin in 2011. Error bars are ±1 standard deviation; standard deviation is calculated from the 14 or 16 model values that represent the aggregated average over the regions, over the decades, and over the ensemble members of each model. The average frequency for the historical reference period is 0.2 by definition and the values in this graph should be interpreted with respect to a comparison with this historical average value (Figure source: USGCRP 2017 p. 219).

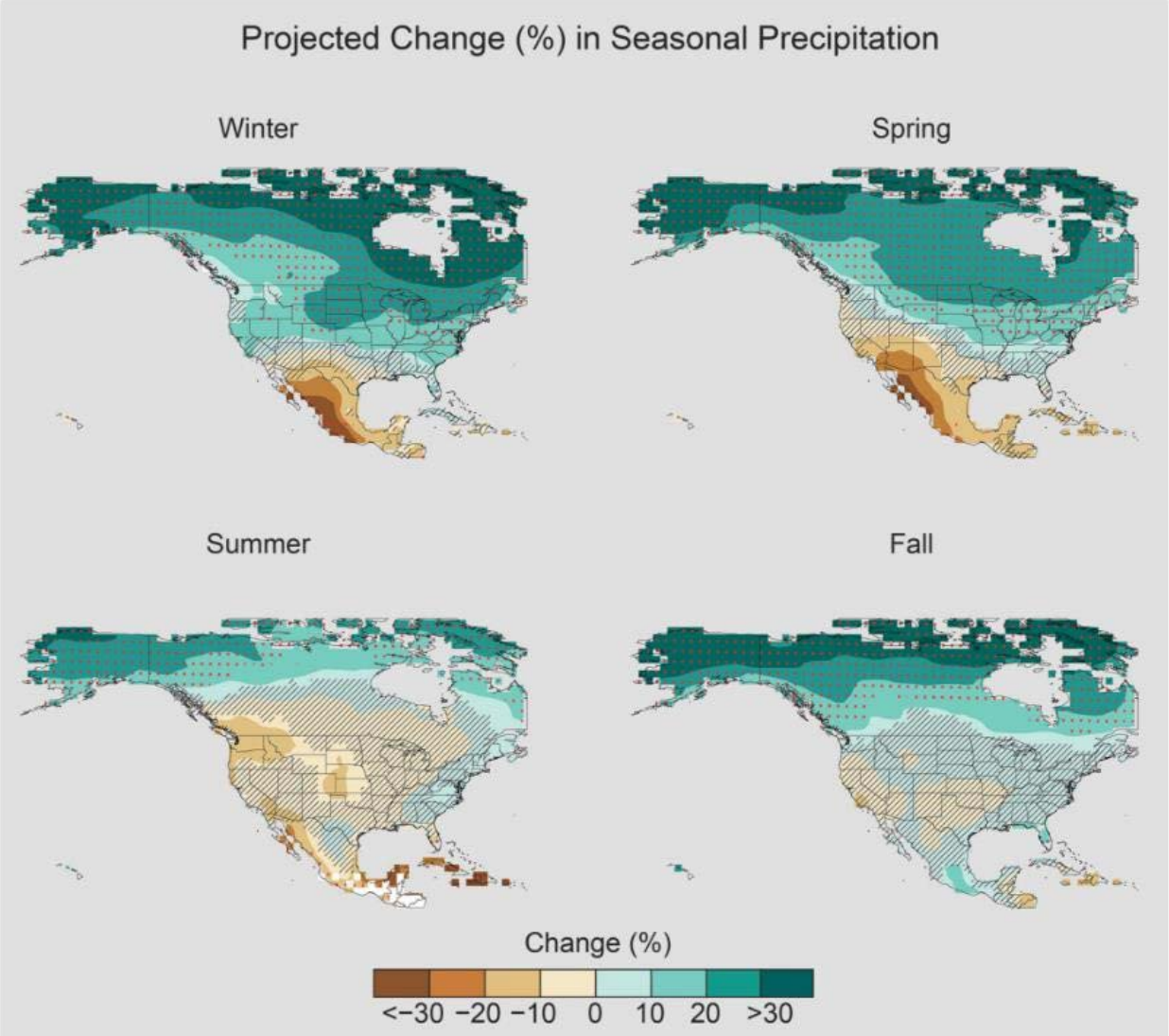

Figure 8-22. Projected change (%) in total seasonal precipitation from CMIP5 simulations for 2070–2099. The values are weighted multi-model means and expressed as the percent change relative to the 1976–2005 average. These are results for the higher scenario (RCP8.5). Stippling indicates that changes are assessed to be large compared to natural variations. Hatching indicates that changes are assessed to be small compared to natural variations. Blank regions (if any) are where projections are assessed to be inconclusive. Data source: World Climate Research Program's (WCRP's) Coupled Model Intercomparison Project (Figure source: USGCRP 2017 p. 217).

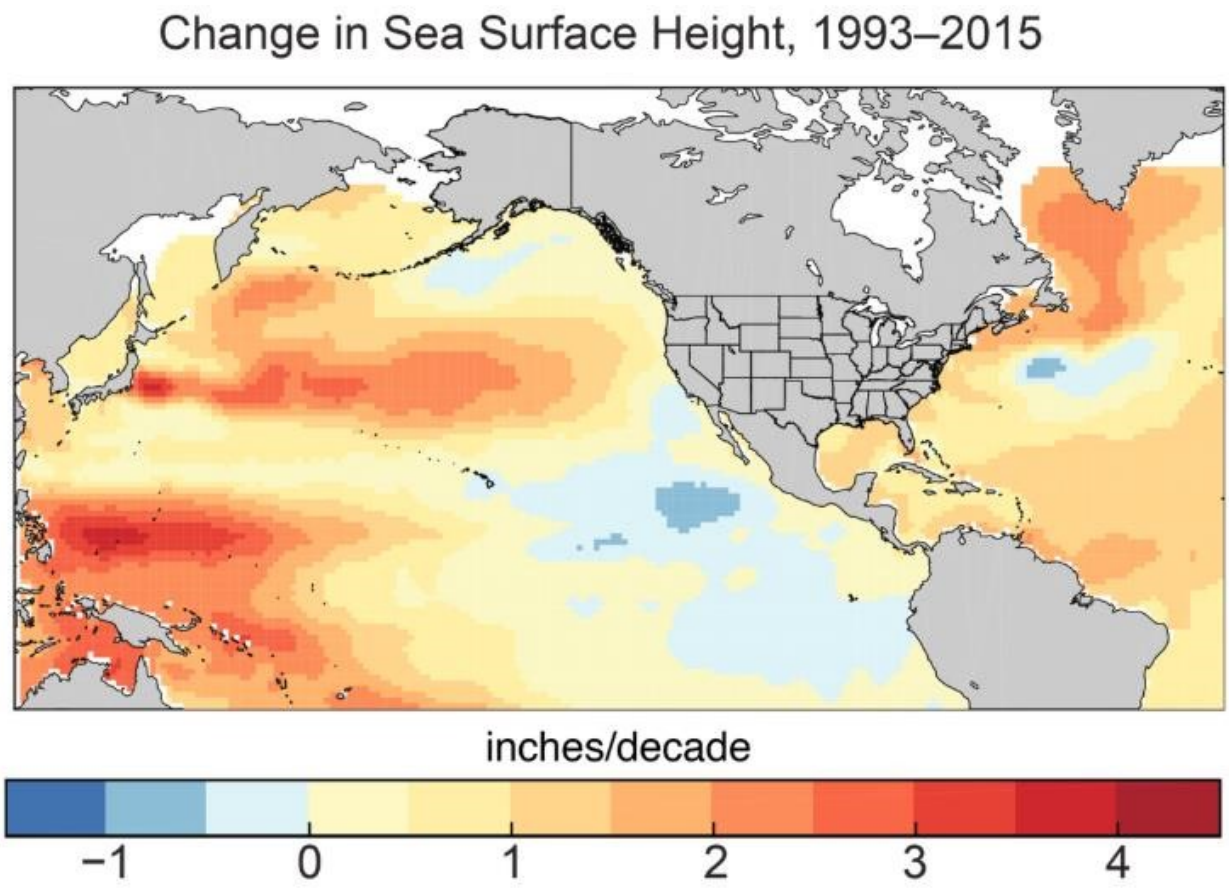

Figure 8-23. Rates of change from 1993 to 2015 in sea surface height from satellite altimetry data; updated from Kopp et al. using data updated from Church and White. (Figure source: USGCRP 2017 p. 340).

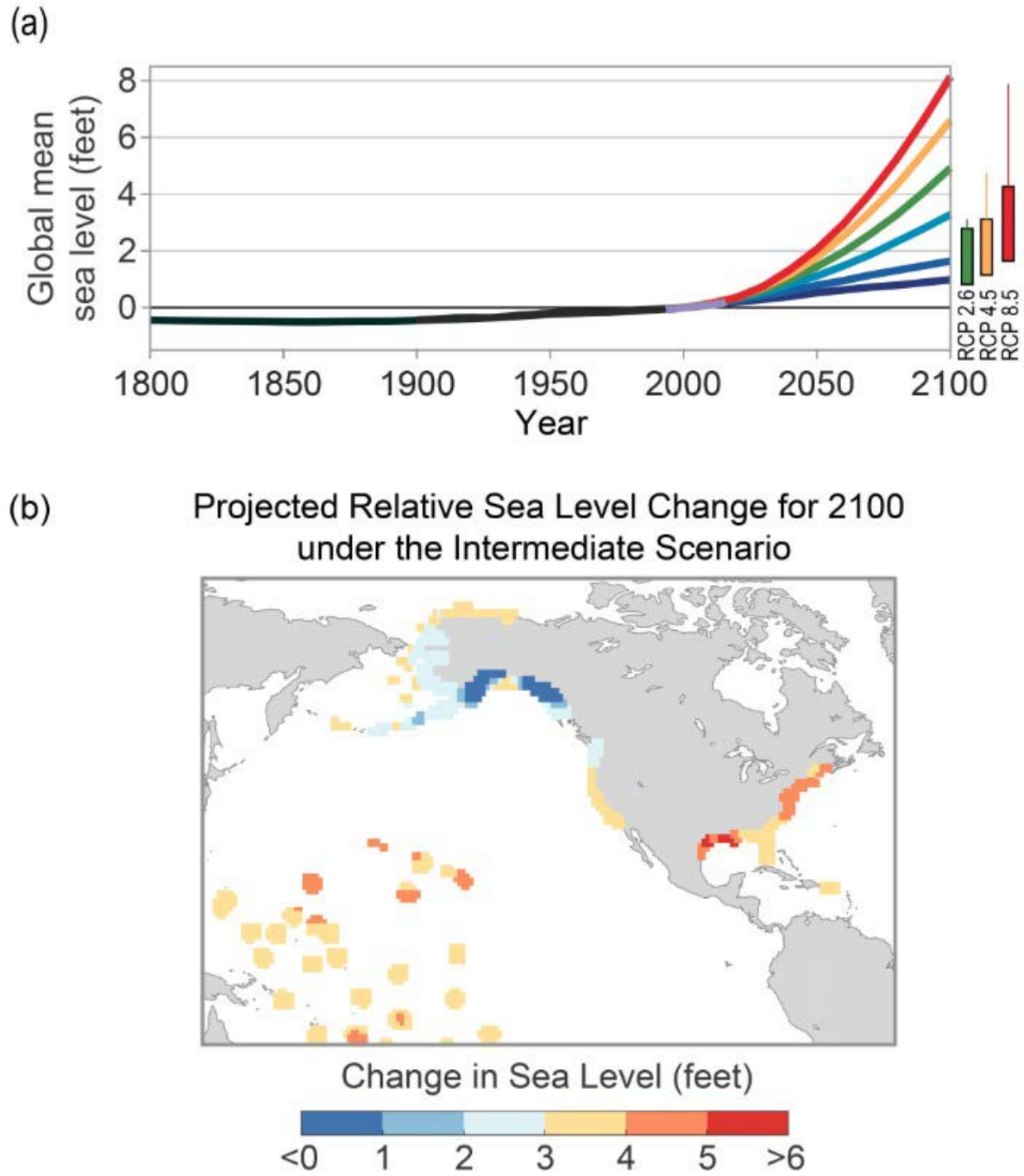

Figure 8-24. (a) Global mean sea level (GMSL) rise from 1800 to 2100, based on Figure 12.2b from 1800 to 2015, the six Interagency GMSL scenarios (navy blue, royal blue, cyan, green, orange, and red curves), the very likely ranges in 2100 for different RCPs (colored boxes), and lines augmenting the very likely ranges by the difference between the median Antarctic contribution of Kopp et al. and the various median Antarctic projections of DeConto and Pollard. (b) Relative sea level (RSL) rise (feet) in 2100 projected for the Interagency Intermediate Scenario (1-meter [3.3 feet] GMSL rise by 2100) (Figure source: USGCRP 2017 p. 342).

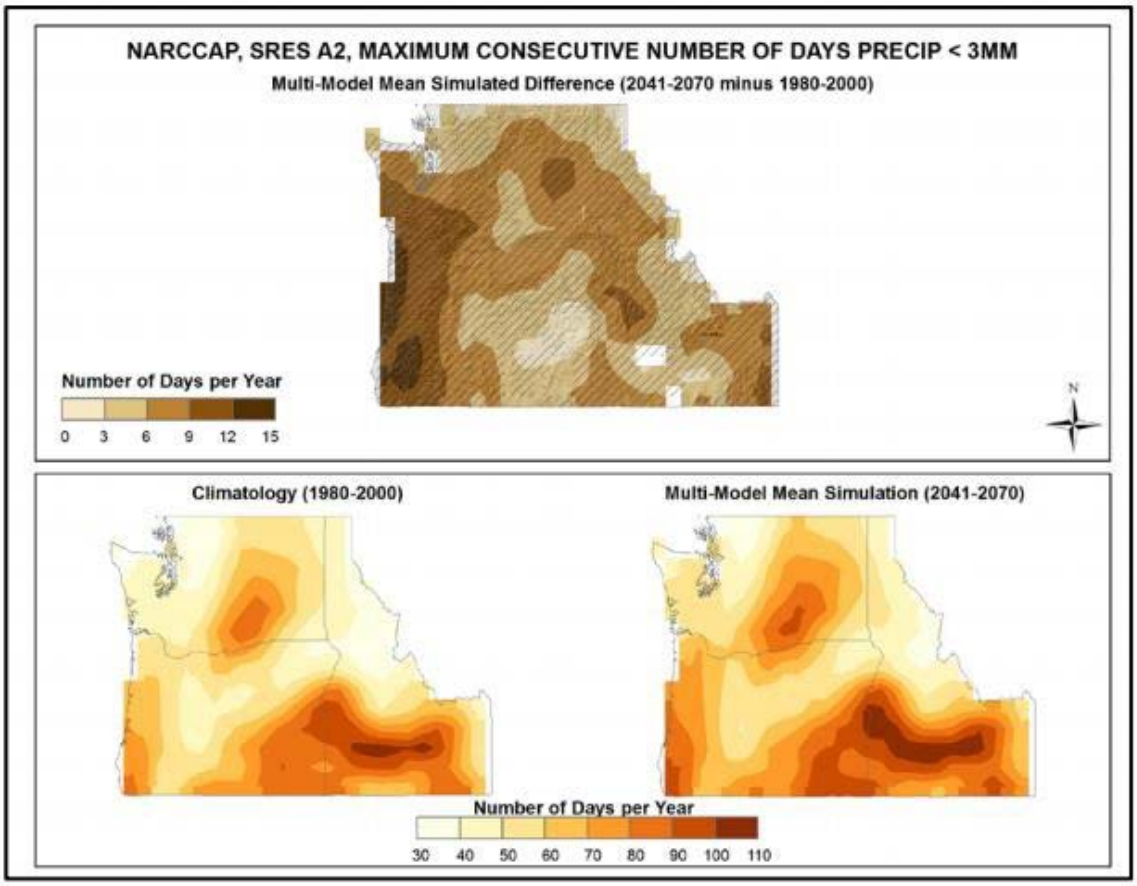

Figure 8-25. Simulated difference in the mean annual maximum number of consecutive days with precipitation of less than .1 inches (3mm) for the Northwest Region for the 2041-2070 time period with respect to the reference period 1980-2000 (top). Color only (category 1) indicates that less than 50% of the models show a statistically significant change in the number of consecutive dry days. Color with hatching (category 3) indicates that more than 50% of the models show a statistically significant change in the number of consecutive dry days, and more than 67% agree on the sign of the change. Whited out areas (category 2) indicate that more than 50% of the models show a statistically significant change in the number of consecutive dry days but less than 67% agree on the sign of the change. Mean annual maximum number of consecutive days with precipitation less than 0.10 inches for the 1980-2000 reference period is shown bottom left. Simulated mean annual maximum number of consecutive days with precipitation less than 0.1 inches for the 2041-2070 future time period is shown bottom right. These are multi-model means from 8 NARCCAP regional climate simulations for the high (A2) emissions scenario. The models simulate increases throughout the region, with the greatest increase occurring in western Oregon (Figure source: Kunkel et al. 2013, part 6).

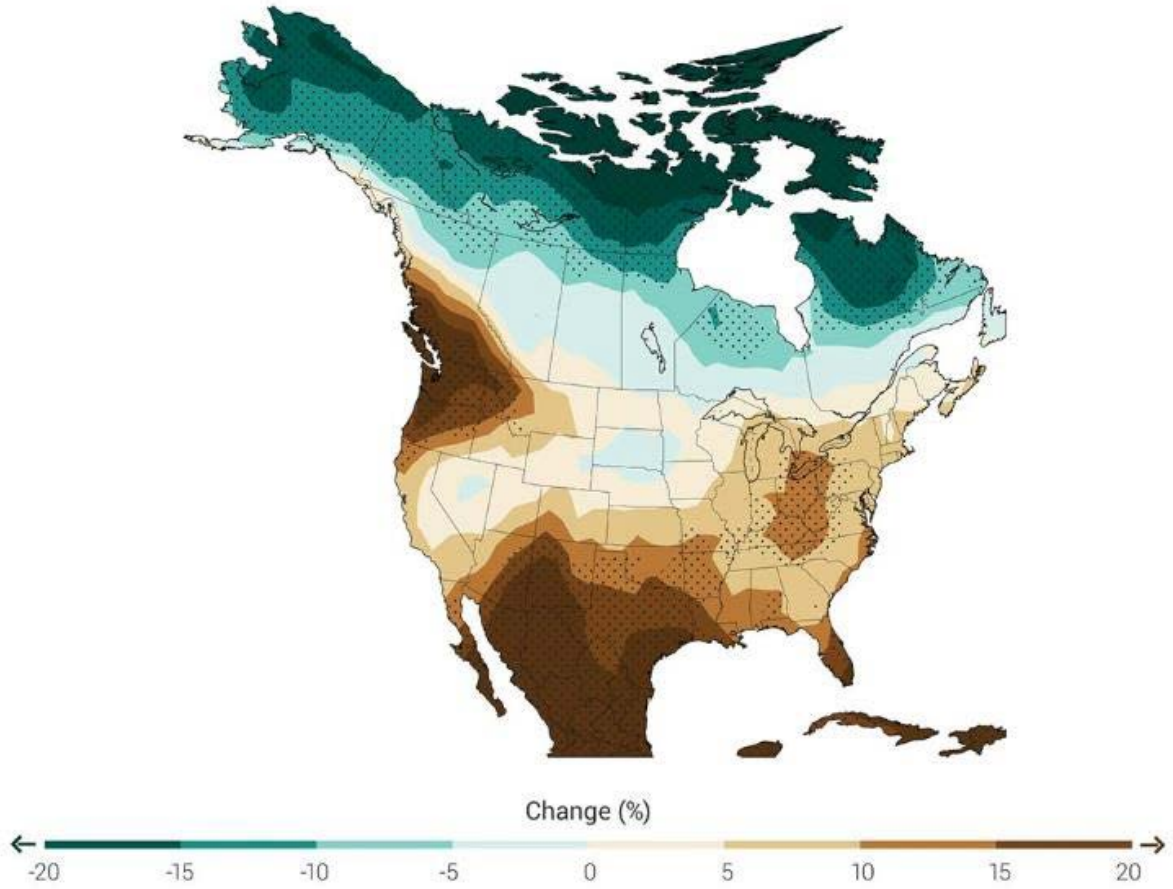

Figure 8-26. Change in the number of consecutive dry days (less than 0.04 inches (1mm) of precipitation) at the end of this century (2070-2099) relative to the end of the last century (1971-2000) under the higher scenario, RCP 8.5. Stippling indicates area where changes are consistent among at least 80% of the 25 models used in this analysis (Figure source: Melillo et al. 2014 p. 33).

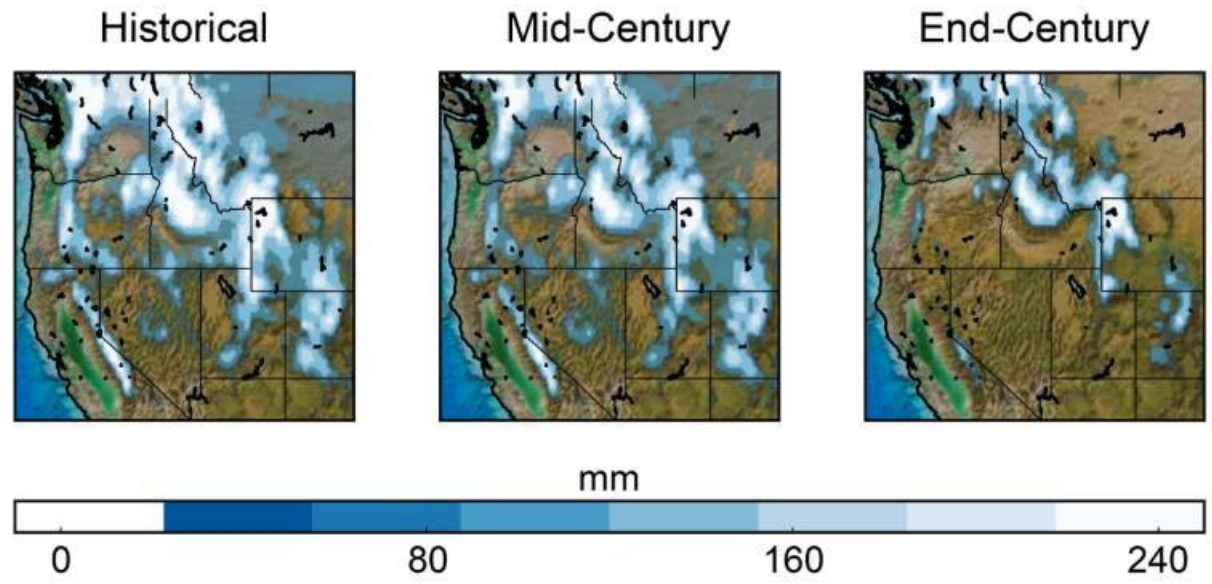

Figure 8-27. Projected changes in winter (DJF) snow water equivalent at the middle and end of this century under the higher scenario (RCP8.5) from a high-resolution version of the Community Atmospheric Model, CAM5 (Figure source: USGCRP 2017 p. 239).

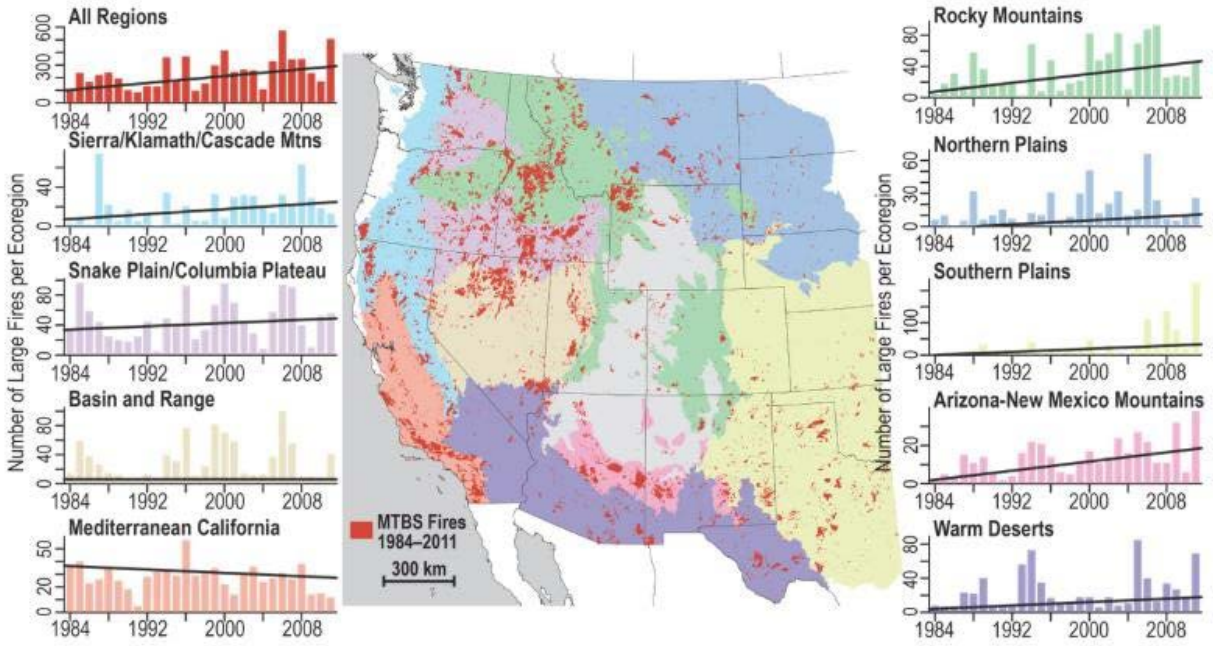

Figure 8-28. Trends in the annual number of large fires in the western United States for a variety of ecoregions. The black lines are fitted trend lines. Statistically significant at a 10% level for all regions except the Snake Plain/Columbian Plateau, Basin and Range, and Mediterranean California regions (Figure source: USGCRP 2017 p. 243).

9 Alaska

9.1 Summary of Climate Projections for Alaska

9.1.1 Temperature

Observed trends indicate that temperatures across Alaska have increased drastically, with the state warming over twice as rapidly as the rest of the United States. The state-wide average annual temperature has increased by 3°F over the last 60 years, with the majority of warming occurring during the winter and spring.

Model simulations project temperature to increase in each future time period (2021-2050, 2041-2070, and 2070-2099, hereafter referred to as near-, mid-, and late-century, respectively), with high (A2), balanced (A1B), and low (B1) emissions scenarios from the CMIP3 global climate simulations as well as the RCP2.6, 4.5, 6.0, and 8.5 emission scenarios from the CMIP5 global climate simulations indicating a statistically significant increase in temperature (see Figure 9-1, Figure 9-2, and Figure 9-3). Individual CMIP3 model runs vary considerably by the late century, but both the A2 and B1 scenarios predict an increase in annual temperature (see Figure 9-4). With observed temperatures having increased and model projections all indicating temperature increases in the future, there is a very low probability that annual average temperatures will decrease across the region.

The interior of Alaska is projected to have the highest temperature increases, while the Inside Passage is projected to experience less intense increases. This is due to the moderating influence of the Pacific Ocean whereas the interior is situated far enough inland to avoid any moderation. Temperature increases are also projected to be higher along the northern coast, forming a north-south gradient.

Determining observed trends in the hottest annual temperature for Alaska is complicated by the fact that the state lacks a sufficient number of long-term stations for a century-long analysis. However, Stewart (2011) found that maximum temperature extremes in Alaska have increased during all seasons across the state.

Sillmann et al. (2013) utilized a CMIP5 model ensemble with three emissions scenarios (RCP2.6, 4.5, and 8.5), and their results suggest an increase in annual maximum temperatures in the late century (2081-2100). However, the magnitude of the increase varies by emissions scenario, with values ranging from roughly -1 to 17°F in Alaska. The CLIMDEX SRES B1, A1B, and A2 scenarios project an increase in the hottest annual temperature in the midcentury (2046-2065), but the increase is slight (~ 2.5°F). The CMIP5 models with the RCP2.6, 4.5, 6.0, and 8.5 scenarios also project an increase by the mid-century, with increases between approximately 2.5 and 6°F. In particular, the RCP8.5 scenario has the hottest annual temperature increasing between 5 and 6°F (see Figure 9-5). The region as a whole is projected to see its hottest annual temperature increase, but small pockets on the eastern coast as well as the Inside Passage are projected to have slightly less of an increase, while an area in southwestern Alaska (but not in the Inside Passage) is projected to have the greatest increase. As such, there is low confidence that the hottest annual temperature will decrease.

CMIP5 model ensemble results with three scenarios (RCP2.6, 4.5, and 8.5) suggest an increase in annual minimum temperatures in the late century (2081-2100). However, the magnitude of the increase varies by emissions scenario, with values ranging from roughly 2 to 34°F in Alaska. According to the CMIP3 simulations (A2, A1B, and B1 emissions scenarios), the lowest annual temperature is projected to increase between 7-10°F by mid-century (2046-2065), while the CMIP5 simulations (RCP2.6, 4.5, 6.0, and 8.5 scenarios) predict the lowest annual temperature to increase between 6-17°F. The RCP8.5 scenario has most of Alaska's minimum temperature increase by more than 12°F, with the Inside Passage and the Aleutian Islands experiencing smaller increases (see Figure 9-6).

There is difficulty in ascertaining how the number of days with temperatures ≥ 90°F has changed in Alaska due to the lack of long-term reporting stations. However, Stewart (2011) found that maximum temperature extremes in Alaska have increased during all seasons across the state. Using the Warm Spell Duration Index (WSDI, defined as the annual count of days with at least 6 consecutive days when daily maximum temperatures are > 90th percentile), model projections from the CMIP3 and CMIP5 downscaled data sets indicate that the number of days with temperatures > 90th percentile will increase by mid-century (2046-2065; see Figure 9-7). These increases are projected regardless of emissions scenario, but the range varies from an increase of just under 20 days to over 100 days. The CMIP5 model ensemble with high (RCP8.5) emissions scenario predicts that the WSDI will increase, with the increase considered statistically significant (see Figure 9-8).

While direct information regarding 90°F days is not readily available, projected increases in the 90th percentile daily maximum temperature brings some confidence that the number of days with temperatures ≥ 90°F will increase. However, the lack of observed trends introduces substantial uncertainty. The Aleutian Islands stand to see the greatest increase in the number of days with maximum temperatures > 90th percentile. While the entire state is projected to see an increase, the smallest increase is projected in Alaska's interior.

There is difficulty in ascertaining how the number of days with freezing temperatures has changed in Alaska due to the lack of long-term reporting stations. However, Stewart (2011) found that minimum temperature extremes in Alaska have decreased in frequency during all seasons across the state. Also, Stewart et al. (2013) observed a decrease in the number of cold waves (defined as 4-day and 7-day periods where temperatures are colder than what is expected once every five years).

Using the Cold Spell Duration Index (CSDI, defined as the annual count of periods with at least 6 consecutive days when daily maximum temperatures are < 10th percentile), model projections from both CMIP3 and CMIP5 indicate that the number of days with freezing temperatures will decrease by mid-century (2046-2065). These decreases are projected regardless of emissions scenario, but the range varies from a decrease of roughly 3 days to almost 10 days. The CMIP5 model ensemble with high (RCP8.5) emissions scenario predicts that the CSDI will decrease, with the decrease considered statistically significant (see Figure 9-9). While direct information regarding freezing temperature days is not readily available, projected decreases in the frequency of 10th percentile daily maximum temperature brings some confidence that the number of days with freezing temperatures will decrease.

However, the lack of observed trends introduces substantial uncertainty, and the lack of direct projections of freezing temperature days further increases uncertainty. The greatest decrease in number of days with temperatures < 10th percentile is expected along the coast, especially in the eastern Aleutian Islands. Assuming the RCP8.5 projection holds, the Inside Passage appears to be the only part of Alaska that will experience cold spells.

Information pertaining to minimum nighttime temperatures in Alaska is difficult to come by. Globally, cold nights have decreased over 74% of the global land area sampled, with warm nights having increased (statistically significantly) over 73% of the area, according to the IPCC Fourth Assessment Report. This implies that cold nights are decreasing. Sillman et al. (2013) explored temperatures using various metrics, and they utilized metrics called frost days (minimum temperature < 32°F) and tropical nights (minimum temperatures > 68°F), which can be used here. Using CMIP5 projections with three scenarios (RCP2.6, 4.5, and 8.5), the authors found that frost days are projected to decrease by late century (2081-2100) for all emissions scenarios, while tropical nights are only projected to increase during the same time period for RCP4.5 and 8.5 scenarios, and even then the increases are miniscule (on the order of 1 night a year). This implies that minimum temperatures will be increasing, but not to the extent that Alaskan nights will be greater than 68°F. This also gives confidence that nighttime temperatures will not decrease in the future.

The daily temperature range exhibits a decreasing trend in Alaska, with the average annual minimum temperature having increased almost 0.5°F more than the annual maximum temperature (calculated as the difference between 1986-2016 average temperatures and 1925-1960 average temperatures). According to Stafford et al. (2000), for the period from 1949-1998, the daily temperature range decreased just under 2°F. The IPCC in 2001 predicted that it was very likely that the daily temperature range would be reduced over most land areas, and the observed data support this. Since model projections (with different emissions scenarios) have minimum temperatures continuing to increase (see Figure 9-10), especially at a rate greater than daily maximum temperatures, it is highly likely that the daily temperature range will continue to decrease as well. There is a low probability the daily temperature range expands given current observed and projected conditions. Decreases in the daily temperature range will be greater in urban areas, since the urban heat island effect increases minimum temperatures. Since the urban heat island effect is more pronounced at night, daily maximum temperatures would not be affected enough to overpower this effect.

9.1.2 Precipitation

Precipitation increased across Alaska by a factor of 10% during the period from 1949-2005 compared to the long-term average. However, this trend has only occurred recently, as 1949-1965 exhibited near normal precipitation before transitioning into a period of 15 years of below-average totals, with recent decades exhibiting an increase (see Figure 9-11). CMIP3 models with low (B1) and high (A2) emissions scenarios as well as CMIP5 models with four emissions scenarios (RCP2.6, 4.5, 6.0, and 8.5) all predicted increases in precipitation for the near, mid, and late century time scales (see Figure 9-12, Figure 9-13, and Figure 9-14). The CMIP3 models exhibit differing levels of uncertainty, with the B1 emissions scenario having a smaller model spread compared to the A2 scenario (see Figure 9-15). Thus, it is unlikely precipitation will decrease across Alaska. Model estimates tended to have the greatest increase in precipitation in the northwestern part of the state, while the Inside Passage is projected to experience the smallest

increases. Even with these increases, the southern part of the state is still projected to receive the most precipitation compared to the rest of the state.

Rainfall intensity in Alaska has increased. In particular, 99th percentile events (the amount of rain that falls in a day that exceeds 99th percent of all non-zero precipitation days, or the top 1% of precipitation days) have increased by 16% from 1958-2016 (see Figure 9-16). The CMIP3 and CMIP5 models (using the A2, A1B and B1 scenarios as well as the RCP2.6, 4.5, 6.0, and 8.5 scenarios) predict that the maximum 1-day and 5-day precipitation amounts will increase by mid-century (2046-2065), with increases ranging from roughly 9 to 25% for the 1-day maximum and roughly 9 to 22% for the 5-day maximum (see Figure 9-17 and Figure 9-18). The RCP8.5 scenario in particular indicates both the maximum 1-day and 5-day precipitation will increase significantly, with the maximum 1-day precipitation significantly increasing across the entire state. The maximum 5-day precipitation was significant everywhere except for southeastern Alaska and part of the Inside Passage (see Figure 9-19 and Figure 9-20).

Furthermore, both model ensembles predict substantial increases in the amount of precipitation that occurs during days that exceed the 99th percentile, with increases ranging from 49 to 150% (see Figure 9-21). The RCP8.5 scenario in particular yields statistically significant increases across the entire state, with only parts of the Aleutians and Inside Passage exhibiting increases less than 90% of current amounts (see Figure 9-22). With rainfall amounts having increased in the past, and multiple model projections indicating rainfall amounts will increase in the future, there is low confidence that rainfall amounts (therefore, intensity) will decrease.

Alaska has seen a 27% (1958-2016) increase in the number of 2-day rainfall events that would normally be expected to occur once every five years (see Figure 9-16). Stewart (2011) found that multiple stations indicated an increase in the number of days with heavy rainfall (in the form of the top 1% of 3-day precipitation events), but this trend was not statistically significant. Sillmann et al. (2013) utilized a parameter called very wet days, which described the amount of precipitation that fell on days when daily precipitation was greater than the 95th percentile (determined from 1961-1990). In other words, this can be used as a proxy for the number of days with heavy rainfall. They found that in both the mid and late century (2046-2065 and 2081-2100, respectively), the number of very wet days was projected to increase, with the magnitude of the increase determined by the emission scenario (RCP2.6, 4.5, and 8.5). Each scenario projected an increase, with ranges of roughly 10 to 110% for mid-century and roughly 10 to 220% for late century.

With respect to seasonality, Alaska has seen a relative balance in seasonal precipitation, with an annual increase of only 1.5%, calculated as the difference between the 1901-1960 average and the 1986-2015 average (see Figure 9-11). However, precipitation in Alaska is considered to be highly variable and spatially dependent. CMIP3 projections under the low (B1) and high (A2) emissions scenarios predict that precipitation will increase across Alaska during the next century, but the model spread is quite large (see Figure 9-23 and Figure 9-24). As a result, there is substantial uncertainty in predicting how precipitation seasonality will change.

With respect to observed precipitation seasonality, central Alaska shows a decrease in every season, while the Inside Passage and the eastern part of the state show an increase every season. Precipitation regimes vary across season, with the Aleutian low providing precipitation to the

southern part of the state during late-fall/early-winter, while storm tracks across ice free waters and convective precipitation impact most of the state during the summer.

9.1.3 Other Stressors

Alaska is prone to flooding from various sources; for example, glacial and snow melt, high wind events in conjunction with the lack of a sea-ice barrier, and ice jams all contribute to flooding. Sea level rise is not considered as an important flooding factor due to the presence of strong regional variability (sea level fall and sea level rise are both occurring along Alaska's coast). Furthermore, lack of data due to the absence of tide gauges complicates observed trends in sea level rise and thus any flooding induced (see Figure 9-25).

Sea level changes along the northern coast have been projected to increase 3-4 feet by 2100, according to the Interagency Intermediate Scenario (see Figure 9-26). Extreme precipitation is projected to increase, both in terms of the number of days as well as the amount of precipitation, while annual precipitation is also projected to increase across all seasons. For these reasons, flooding is expected to increase and there is a lower probability for a decrease in flooding events.

According to Dai (2011), both the Palmer Drought Severity Index and soil moisture models indicate that Alaska has experienced a drying trend for the period from 1950 to 2008. Due to increasing temperatures, snow cover extent has been decreasing as precipitation shifts from snow to rain. Furthermore, warming has begun to occur earlier in the year, which has the potential to influence changes in hydrology. Even though precipitation is projected to increase across all seasons, with extreme precipitation events projected to increase as well, changes in evaporation are expected to lead to drier conditions with reduced soil moisture. This could exacerbate drought conditions. Conversely, the CMIP5 model ensemble with a high (RCP8.5) emissions scenario predicts significant decreases in the number of consecutive dry days (defined as days with less than 0.04 inches of rain) by the end of the century (see Figure 9-27).

Conditions that would alleviate drought are projected to be counteracted by conditions that exacerbate drought, so there is low confidence in making a definitive claim on whether drought will increase or decrease. With respect to precipitation, central and northeastern Alaska have experienced decreases in precipitation across all seasons, suggesting drought could be more pronounced in those parts of the state.

Alaska has experienced more wildfires, in particular large fires (area > 386 square miles), in the last decade than in any decade since recordkeeping began in the 1940s, according to Kasischke et al. (2010). Even so, Alaskan wildfires tend to be less frequent and of smaller extent than the rest of the globe, occurring in both the boreal forest and the arctic tundra. Due to expected warmer and drier conditions, model simulations project wildfires to increase in occurrence, with one model simulation using the B1 emissions scenario predicting the annual burn area in Alaska to double by mid-century and triple by the end of the century. The major causes for uncertainty in these projections are the lack of studies focusing on other regions, projections tending to focus on limited areas, and other factors of climate change (water deficits, insect infestations) reducing fuel loads, which inhibit wildfire development.

Since the 1950s, the first wildfires of the year have been observed to start earlier, while the last fires start later (an expansion of the burning season). As a result, the length of fire season has

been observed as having increased. Specifically, the first fires have been observed to have occurred roughly 14 days earlier on average, while the last fires have started roughly 20 days later on average. Since temperature and soil moisture are among the more important aspects of the relationship between fire frequency and ecosystems, and projections for the region involve increased temperature and reductions in soil moisture, it stands to reason that fire season in the region will continue to increase. There is a lack of evidence to suggest that the fire season would decrease, unless the projected increase in precipitation is enough to dampen forest fire fuel.

There has been an observed increase in the frequency of high-latitude (60-90°N) cold season (November to March) storms, but intensity does not appear to have significantly increased. Winter storm tracks have been observed as having changed, but these studies are limited. Studies exploring arctic amplification of winter storms have returned mixed results, and projections for future winter storms yielded large model-to-model differences. As a result, there is low confidence in predicting if winter storm intensity will increase or decrease in the future. Winter precipitation is project to increase across the entire state, with the greatest changes projected to occur on the northern and western coast (see Figure 9-28).

A study by Winski et al. (2017) found that snow accumulation in the Alaska Range has doubled since 1840, with the increase attributed to a strengthening of the Aleutian Low. In non-mountainous terrain, coastal areas still see substantial snow accumulations. However, projected increases in temperature threaten to reduce snow events at low elevations as precipitation regimes transition into rain dominant. Furthermore, Alaska has seen some of the lowest May statewide snow coverage in the last three years. Both the CMIP3 and CMIP5 model suites predict that snowpack will decrease in the future, with both models using a high emissions scenario. In both cases, snowpack faces reductions up to 40%.

However, high elevation areas could see increases in snowfall in the future, coinciding with projected increases in precipitation. Despite the uncertainty, there exists slightly more confidence that snowfall totals for the region as a whole will decrease. Precipitation changes at high elevations (a naturally cold environment) introduce more uncertainty, so mountainous terrain throughout the region could experience increases in snowfall totals. Coastal areas stand to receive less snowfall due to projected temperature increases.

Freezing rain has exhibited both increases and decreases across the state (calculated as the change in frequency between 2005-2014 and 1975-2004), with slight increases present in the north, extreme southwest and southeastern part of the state while decreases were detected in the south-central part of the state. According to the Third National Climate Assessment, knowledge of ice storms is limited, making it difficult to know how they have changed and how they might change. This introduces substantial uncertainty. Considering the relatively confident projections that temperature will increase in the future regardless of emissions, it is plausible that ice storms and freezing rain will decrease throughout the region, as precipitation regimes change to become predominantly rain. However, there is too much uncertainty to be able to confidently predict such a change. More observed data are needed in Alaska.

9.2 Tables and Figures: Alaska

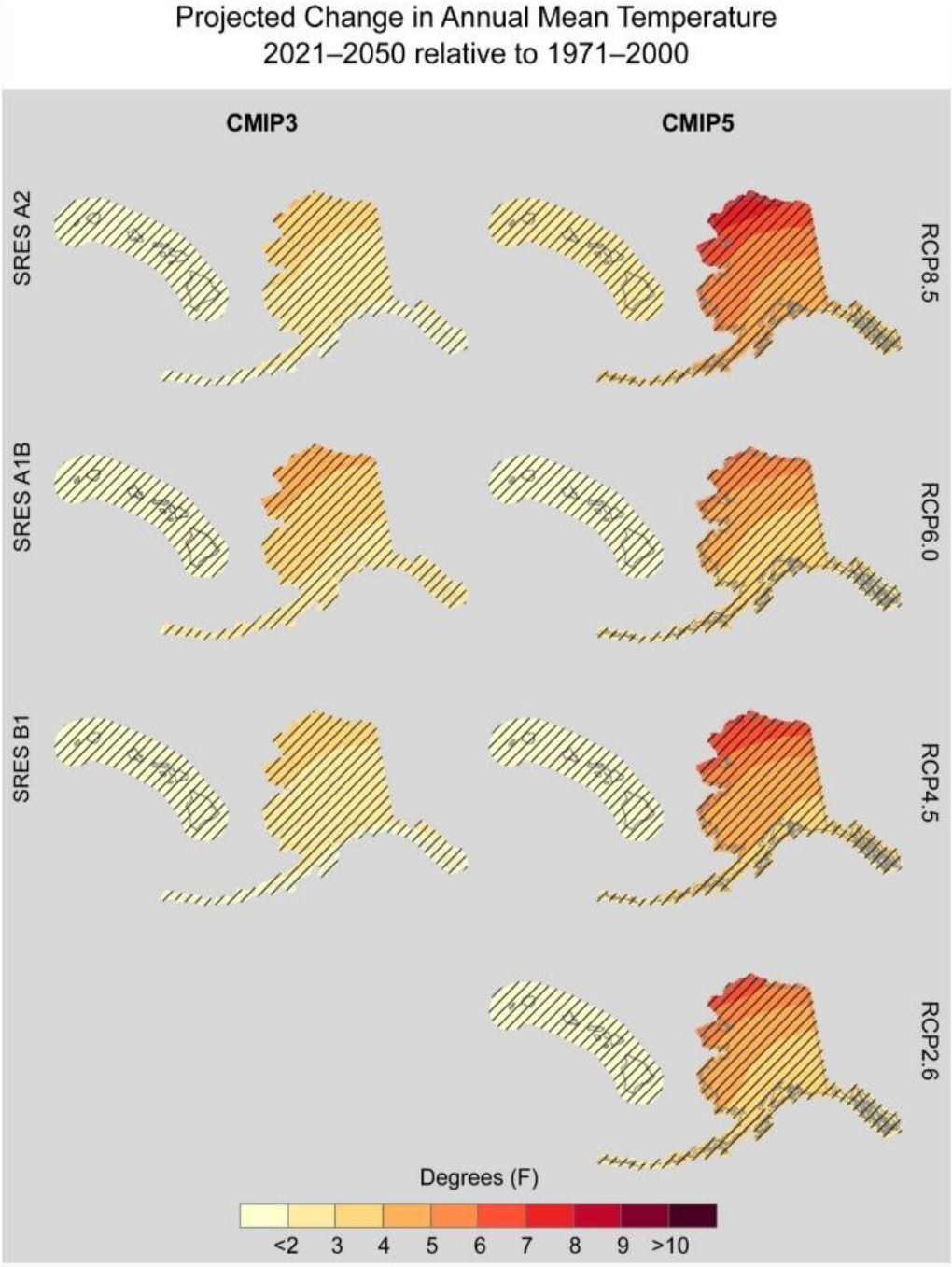

Figure 9-1. Projected change in annual mean temperature (°F) for Alaska and Hawai'i, for 2021–2050 with respect to the reference period of 1971–2000. These are multi-model means using CMIP3 SRES A2, A1B, and B1 scenarios (left column), and CMIP5 RCP8.5, 6.0, 4.5, and 2.6 scenarios (right column). Color with hatching (category 3) indicates that more than 50% of the models show a statistically significant change, and more than 67% agree on the sign of the change (Figure source: Sun et al. 2015).

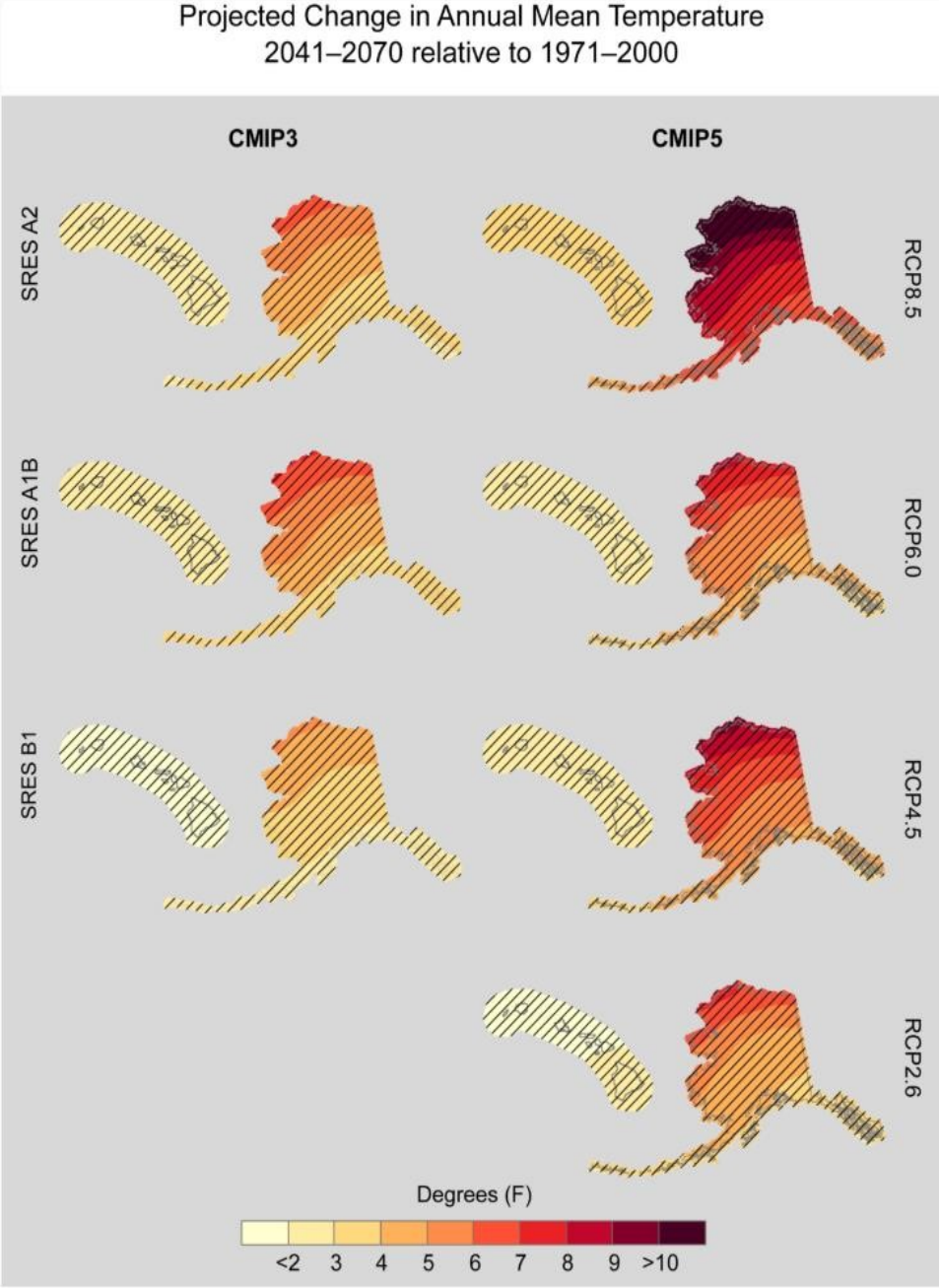

Figure 9-2. Projected change in seasonal mean temperature (°F) for Alaska and Hawai'i, for 2041–2070 with respect to the reference period of 1971–2000. These are multi-model means using CMIP3 SRES A2 (left column) and CMIP5 RCP8.5 (right column). Color with hatching (category 3) indicates that more than 50% of the models show a statistically significant change, and more than 67% agree on the sign of the change (Figure source: Sun et al. 2015).

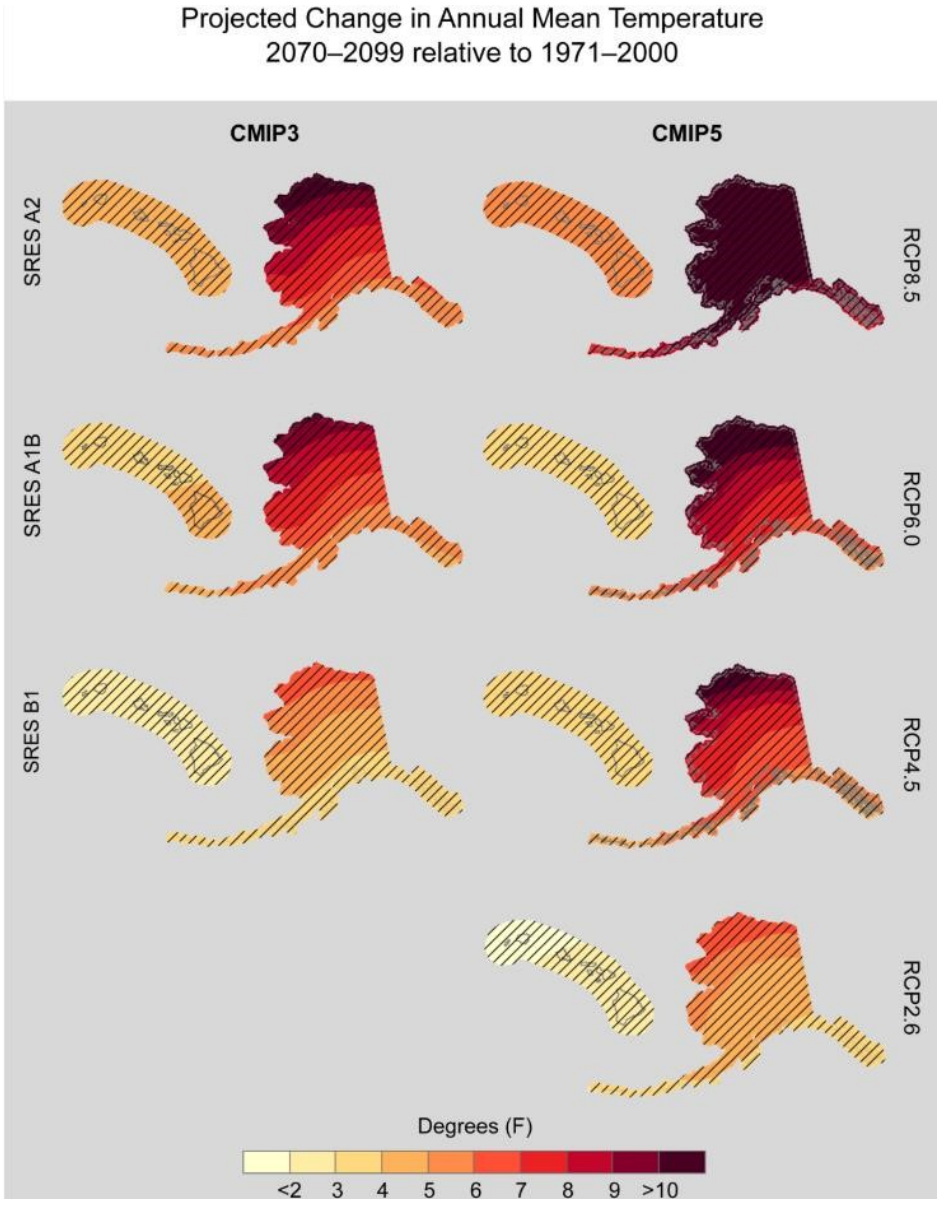

Figure 9-3. Projected change in annual mean temperature (°F) for Alaska and Hawai'i, for 2070–2099 with respect to the reference period of 1971–2000. These are multi-model means using CMIP3 SRES A2, A1B, and B1 scenarios (left column), and CMIP5 RCP8.5, 6.0, 4.5, and 2.6 scenarios (right column). Color with hatching (category 3) indicates that more than 50% of the models show a statistically significant change, and more than 67% agree on the sign of the change (Figure source: Sun et al. 2015).

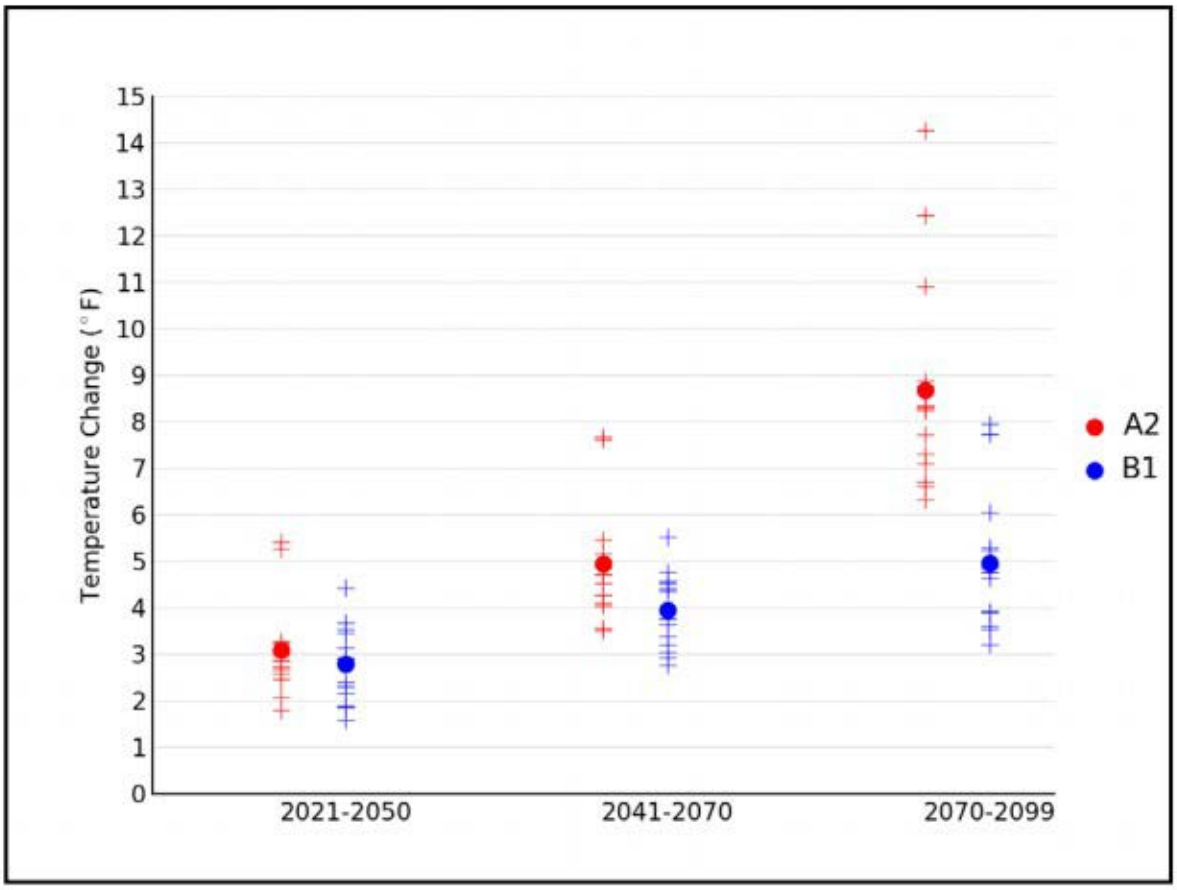

Figure 9-4. Simulated annual mean temperature change (°F) for Alaska for each future time period (2021-2050, 2041-2070, and 2070-2099 with respect to the reference period of 1971-1999. Values are given for the high (A2) and low (B1) emissions scenarios for the 14 (B1) and 15 (A2) CMIP3 models. The small plus signs indicate each individual model and the circles depict the multi-model means. The range of the model simulated change is large compared to the mean difference between A2 and B1 in the early and middle 21st century. By the end of the 21st century, the difference between the A2 and B1 is comparable to the range of B1 simulations (Figure source: Stewart et al. 2013).

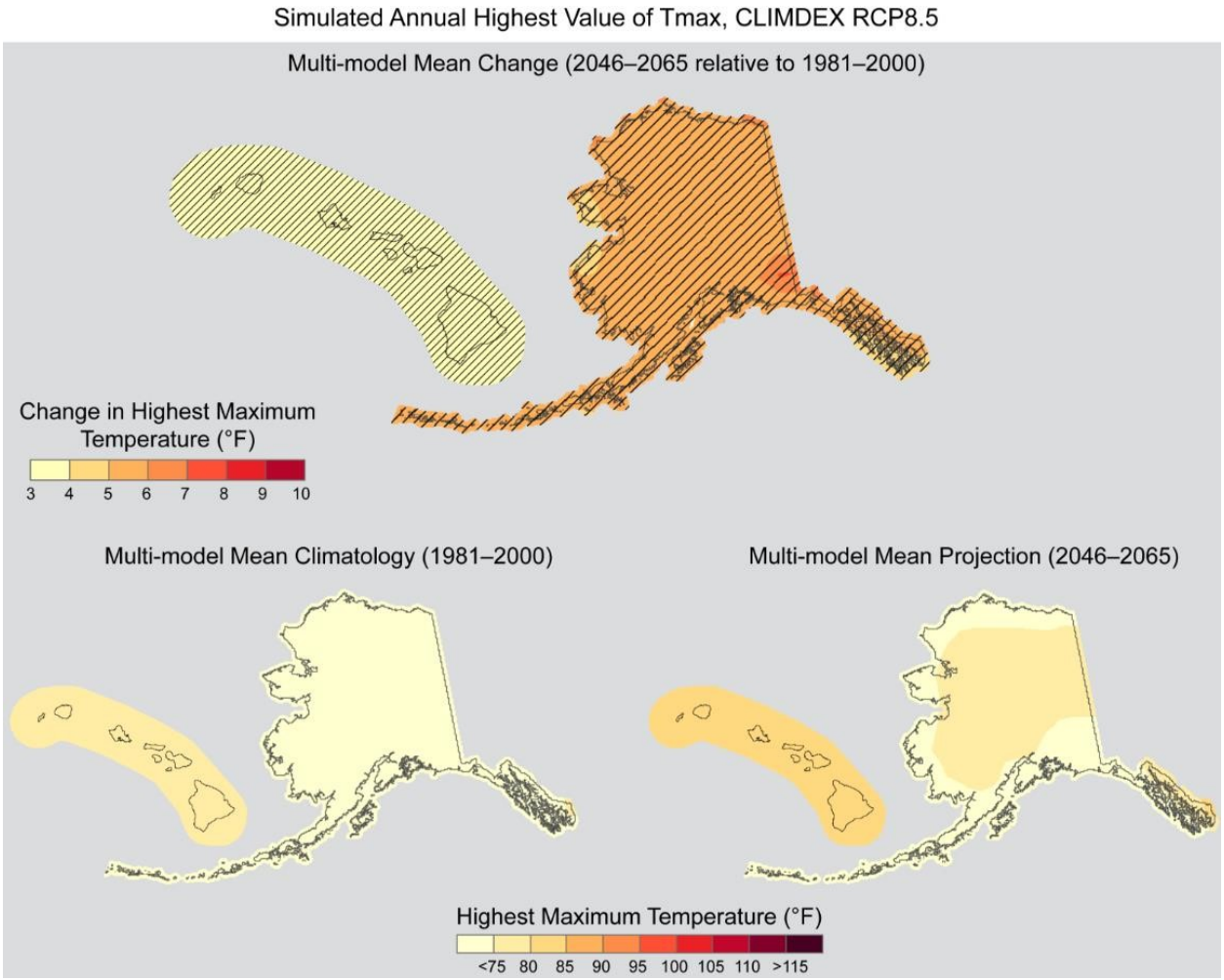

Figure 9-5. Simulated multi-model mean change in the annual highest value of daily maximum temperature (TXx) for Alaska and Hawai‘i, for 2046–2065 with respect to the reference period of 1981–2000, using the CLIMDEX RCP8.5 scenario (top). Color with hatching (category 3) indicates that more than 50% of the models show a statistically significant change, and more than 67% agree on the sign of the change. Multi-model mean climatology indicating the TXx for 1981–2000 is shown bottom left. Multi-model mean projection indicating the TXx for 2046–2065 is shown bottom right (Figure source: Sun et al. 2015).

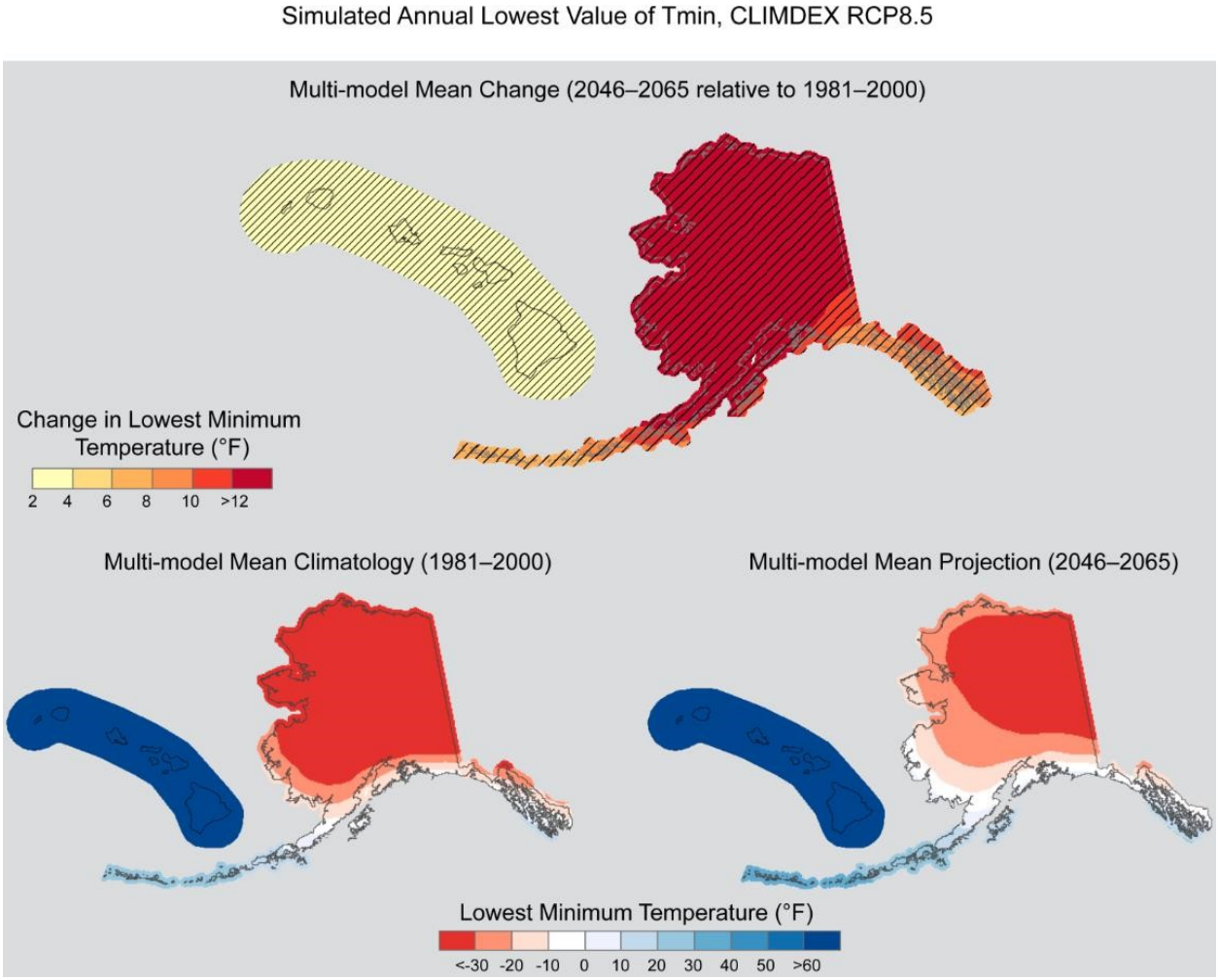

Figure 9-6. Simulated multi-model mean change in the annual lowest value of daily minimum temperature (TNn) for Alaska and Hawai'i, for 2046–2065 with respect to the reference period of 1981–2000, using the CLIMDEX RCP8.5 scenario (top). Color with hatching (category 3) indicates that more than 50% of the models show a statistically significant change, and more than 67% agree on the sign of the change. Multi-model mean climatology indicating the TNn for 1981–2000 is shown bottom left. Multi-model mean projection indicating the TNn for 2046–2065 is shown bottom right (Figure source: Sun et al. 2015).

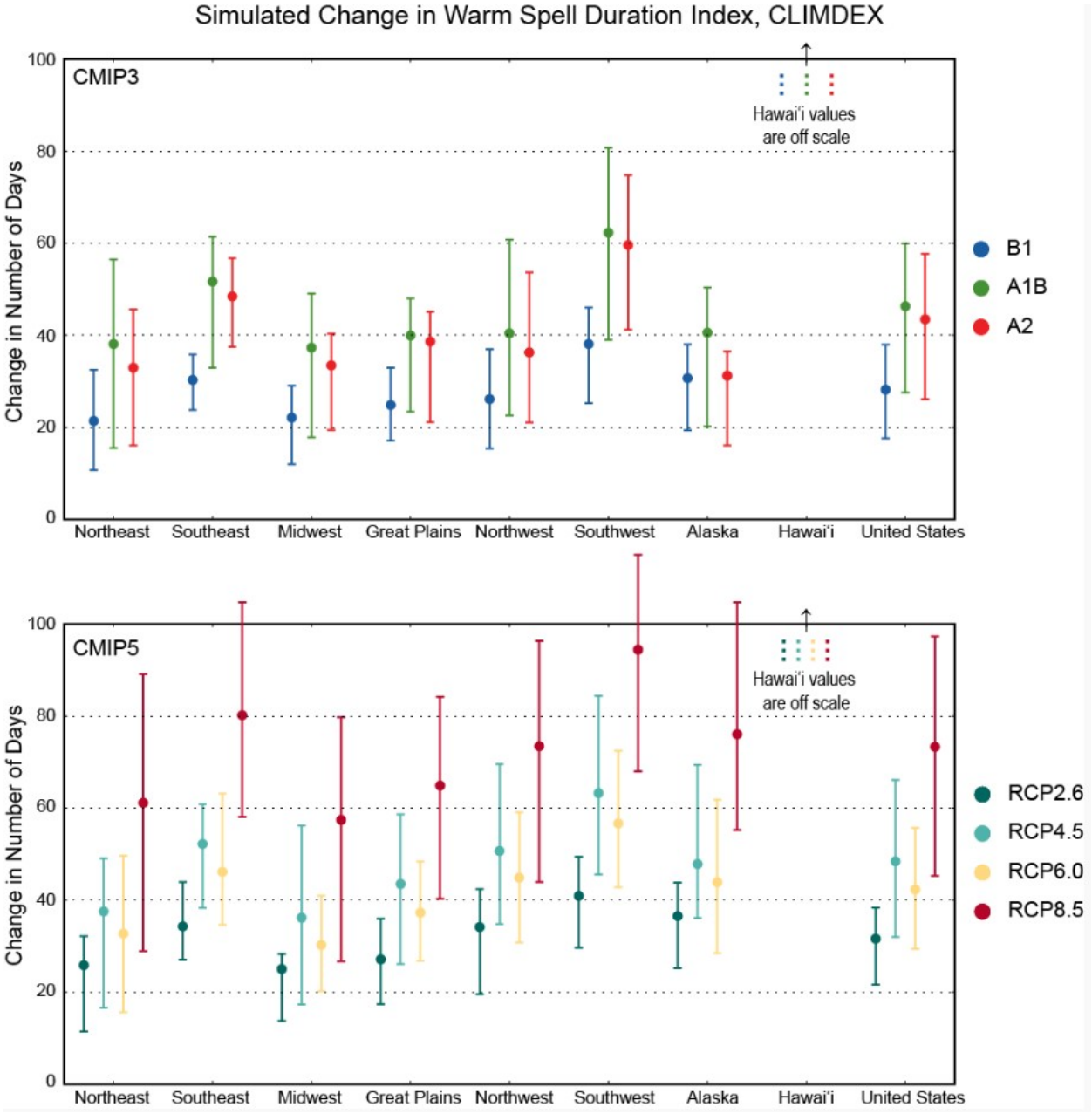

Figure 9-7. Simulated change in warm spell duration index (WSDI) for each region and the contiguous United States, for 2046–2065 with respect to the reference period of 1981–2000. The upper panel shows values for the CLIMDEX SRES B1 (blue), A1B (green), and A2 (red) scenarios. The lower panel shows values for the CLIMDEX RCP2.6 (dark teal), 4.5 (light teal), 6.0 (yellow), and 8.5 (dark red) scenarios. Bars indicate the interquartile ranges of model values and circles depict the multi-model means. Note: values for Hawai'i lie off the scale, with multi-model means ranging from 184.4 days for the RCP2.6 scenario, to 271.3 days for RCP8.5 (Figure source: Sun et al. 2015).

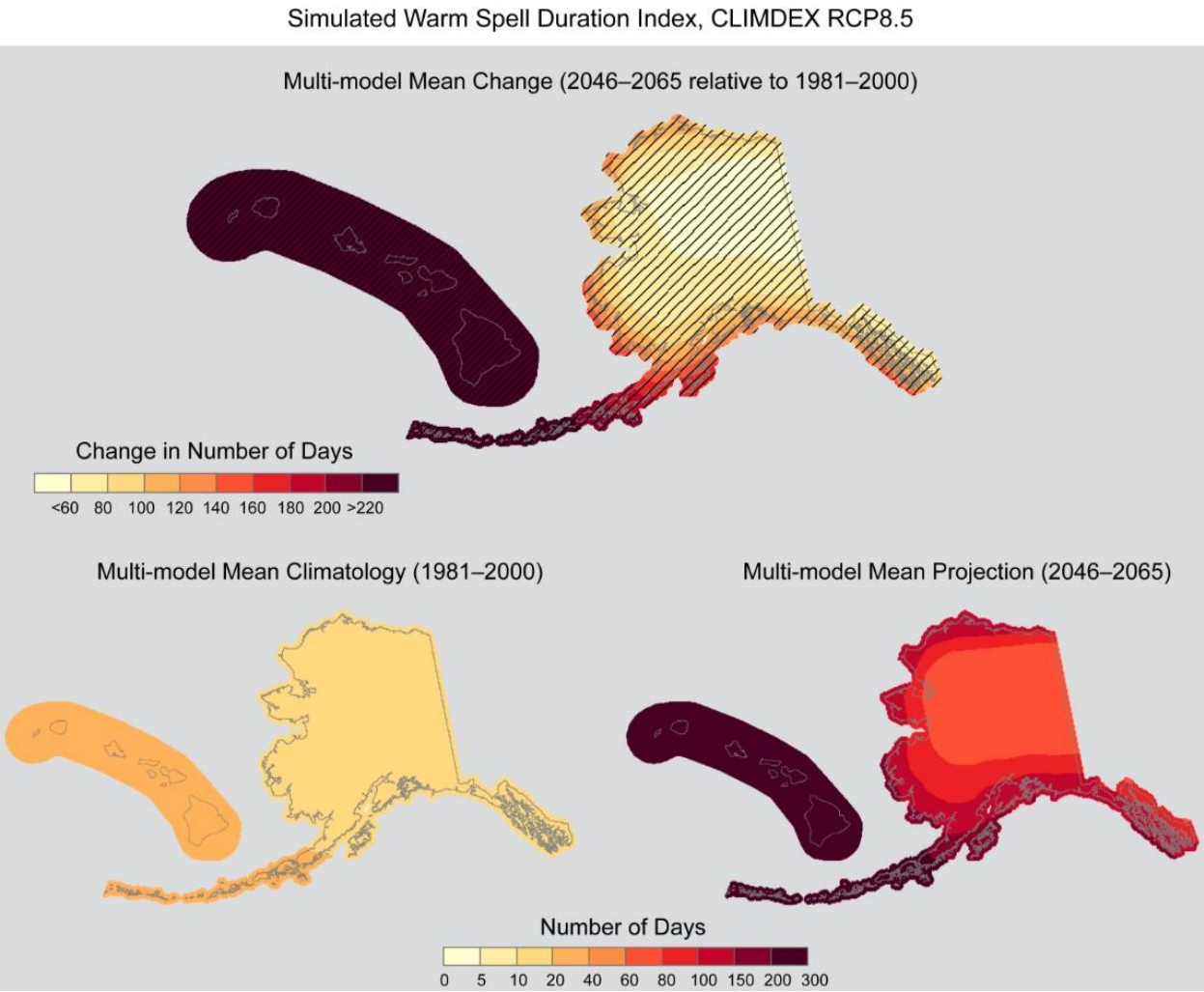

Figure 9-8. Simulated multi-model mean change in warm spell duration index (WSDI) for Alaska and Hawai'i, for 2046–2065 with respect to the reference period of 1981–2000, using the CLIMDEX RCP8.5 scenario (top). Color with hatching (category 3) indicates that more than 50% of the models show a statistically significant change, and more than 67% agree on the sign of the change. Multi-model mean climatology indicating the WSDI for 1981–2000 is shown bottom left. Multi-model mean projection indicating the WSDI for 2046–2065 is shown bottom right (Figure source: Sun et al. 2015).

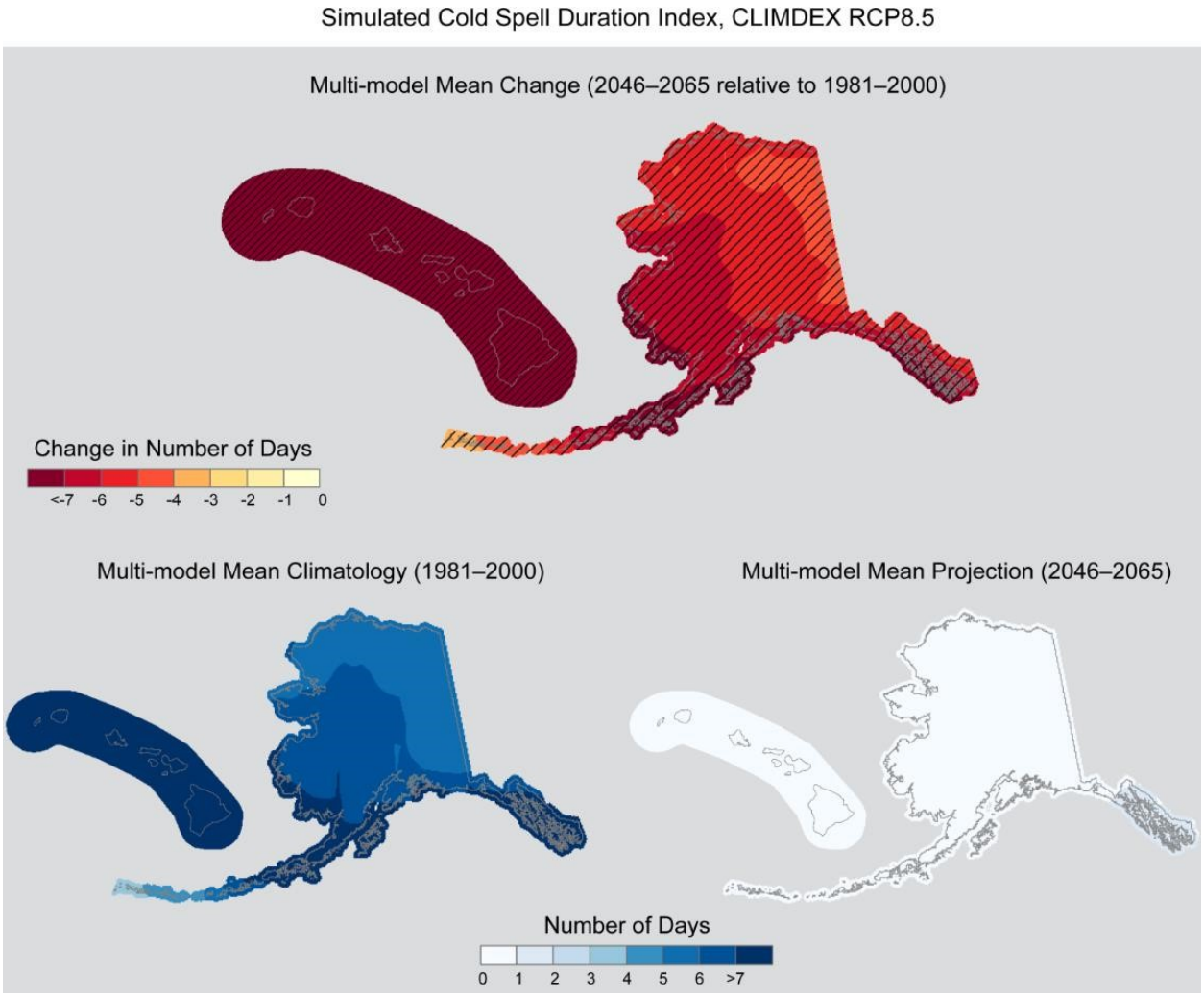

Figure 9-9. Simulated multi-model mean change in cold spell duration index (CSDI) for Alaska and Hawai'i, for 2046–2065 with respect to the reference period of 1981–2000, using the CLIMDEX RCP8.5 scenario (top). Color with hatching (category 3) indicates that more than 50% of the models show a statistically significant change, and more than 67% agree on the sign of the change. Multi-model mean climatology indicating the CSDI for 1981–2000 is shown bottom left. Multi-model mean projection indicating the CSDI for 2046–2065 is shown bottom right (Figure source: Sun et al. 2015).

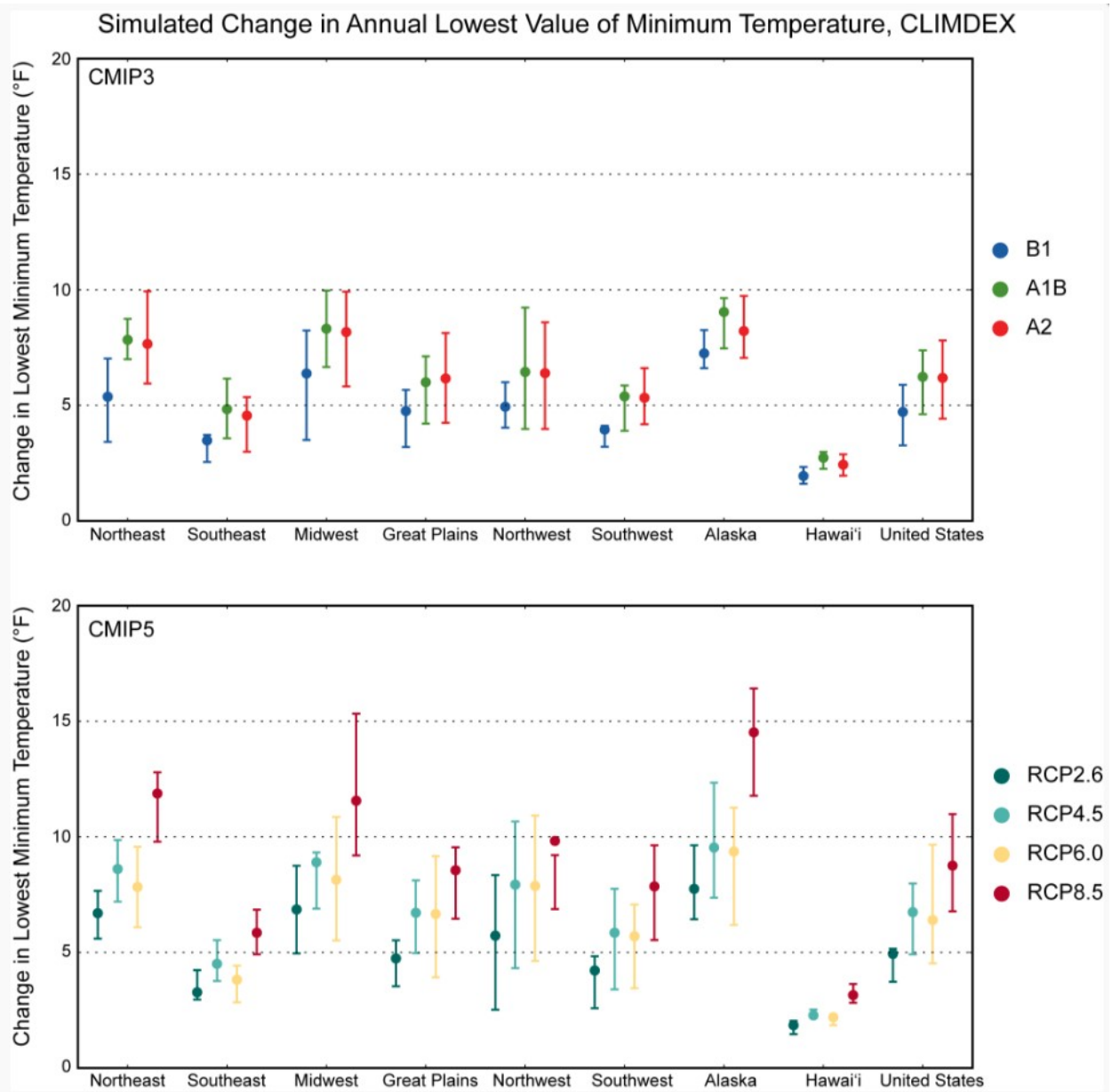

Figure 9-10. Simulated change in the annual lowest value of daily minimum temperature (TNn) for each region and the contiguous United States, for 2046–2065 with respect to the reference period of 1981–2000. The upper panel shows values for the CLIMDEX SRES B1 (blue), A1B (green), and A2 (red) scenarios. The lower panel shows values for the CLIMDEX RCP2.6 (dark teal), 4.5 (light teal), 6.0 (yellow), and 8.5 (dark red) scenarios. Bars indicate the interquartile ranges of model values and circles depict the multi-model means (Figure source: Sun et al. 2015).

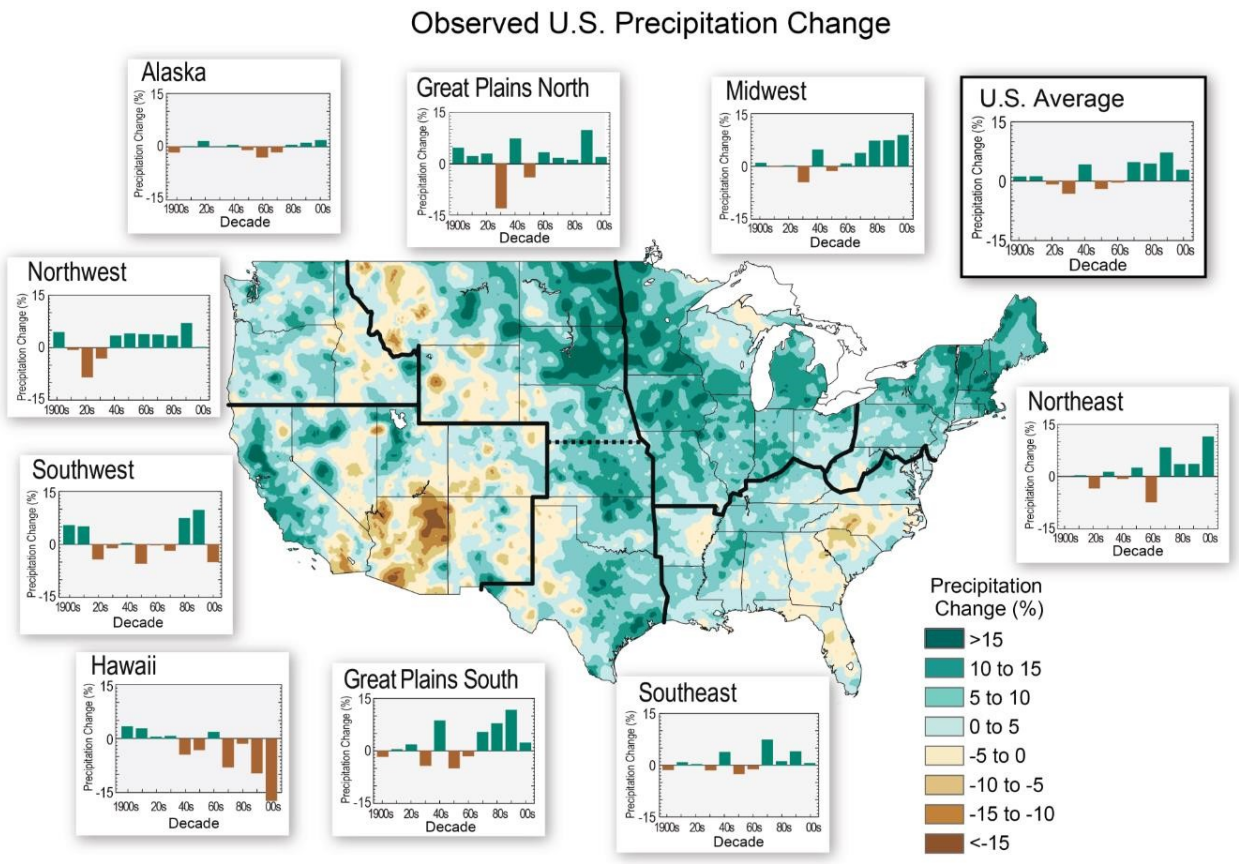

Figure 9-11. The colors on the map show annual total precipitation changes for 1991-2012 compared to the 1901-1960 average and show wetter conditions in most areas. The bars on the graphs show average precipitation differences by decade for 1901-2012 (relative to the 1901-1960 average) for each region. The far-right bar in each graph is for 2001-2012 (Figure source: Melillo et al. 2014 p. 32).

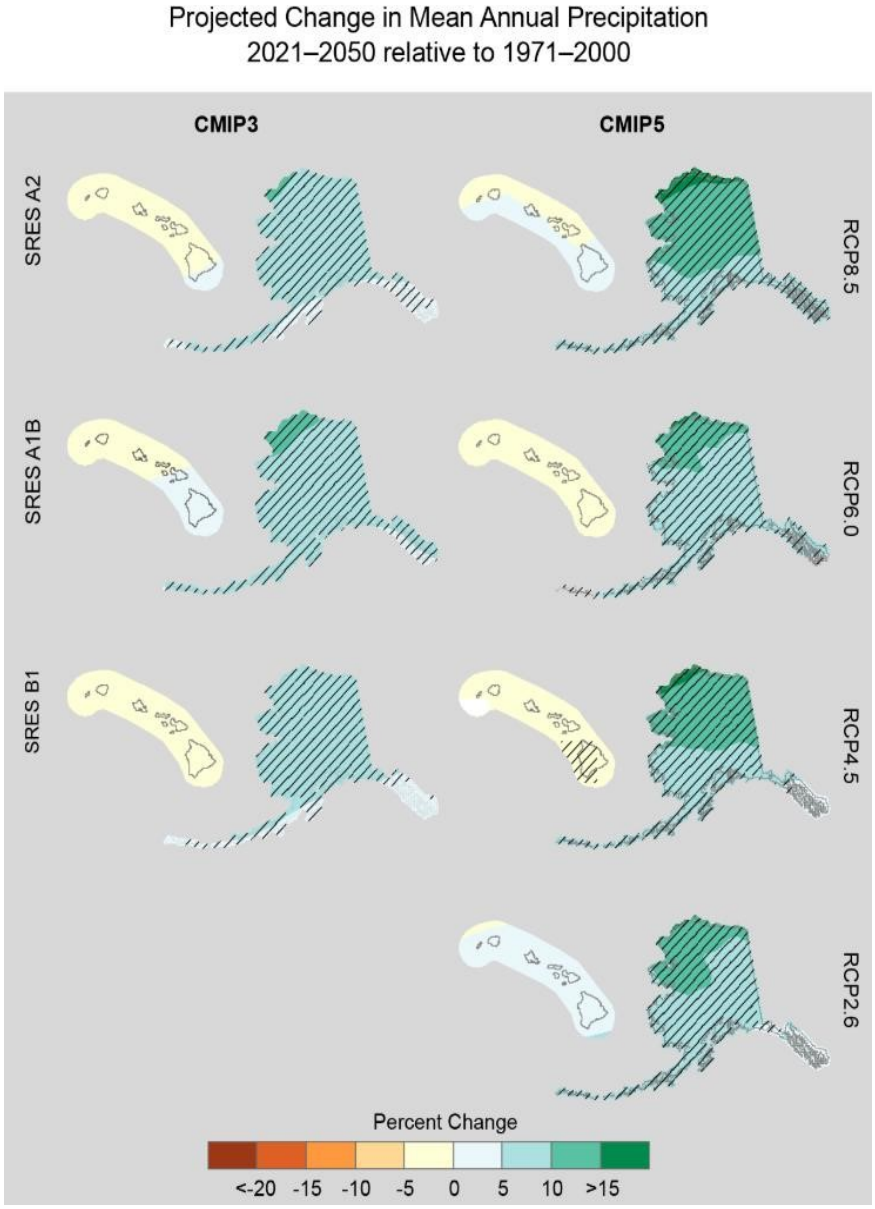

Figure 9-12. Projected change in mean annual precipitation (%) for Alaska and Hawai'i, for 2021–2050 with respect to the reference period of 1971–2000. These are multi-model means using CMIP3 SRES A2, A1B, and B1 scenarios (left column), and CMIP5 RCP8.5, 6.0, 4.5, and 2.6 scenarios (right column). Color only (category 1) indicates that less than 50% of the models show a statistically significant change. Whited out areas (category 2) indicate that more than 50% of the models show a statistically significant change, but less than 67% agree of the sign of the change. Color with hatching (category 3) indicates that more than 50% of the models show a statistically significant change, and more than 67% agree on the sign of the change (Figure source: Sun et al. 2015).

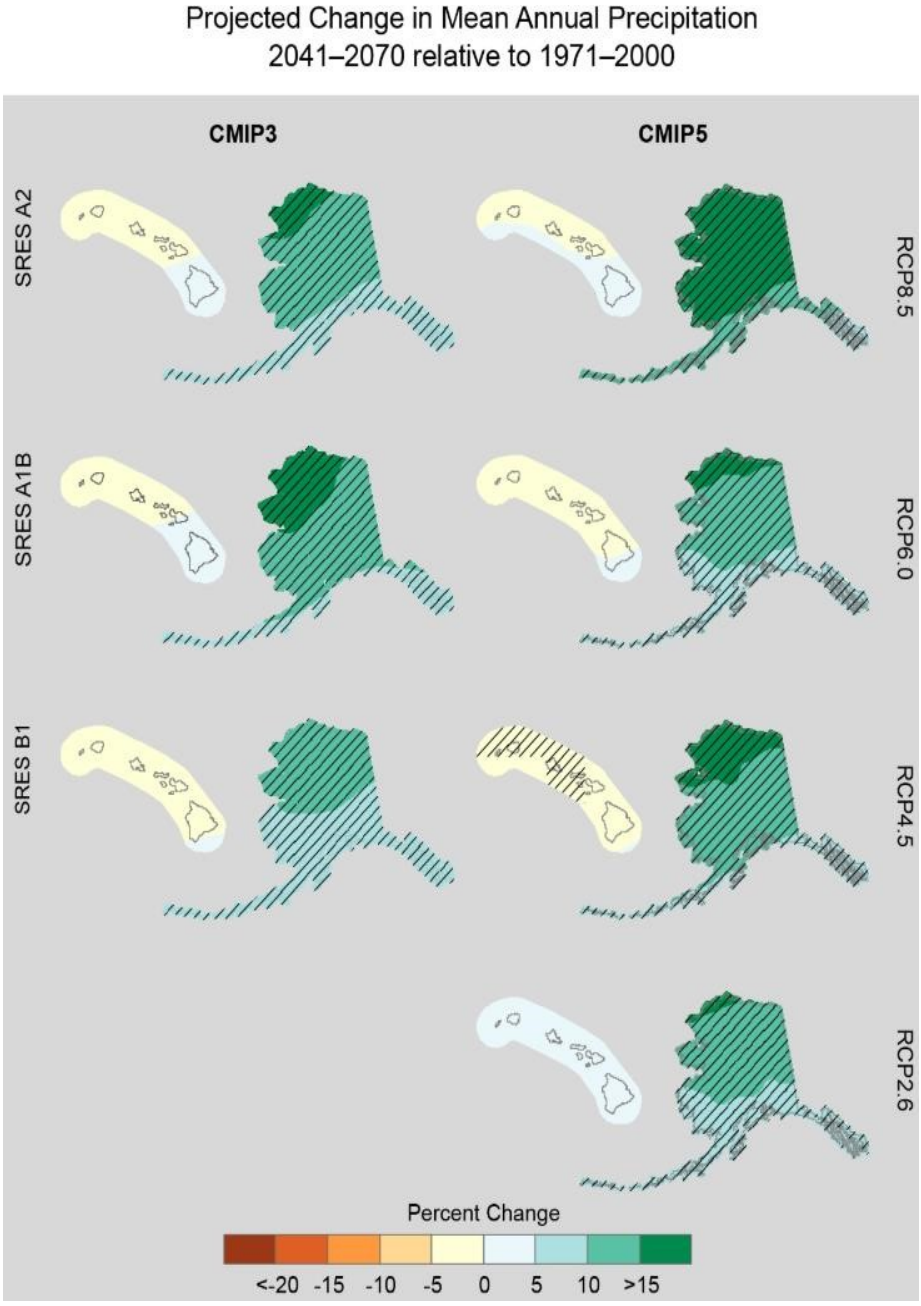

Figure 9-13. Projected change in mean annual precipitation (%) for Alaska and Hawai'i, for 2041–2070 with respect to the reference period of 1971–2000. These are multi-model means using CMIP3 SRES A2, A1B, and B1 scenarios (left column), and CMIP5 RCP8.5, 6.0, 4.5, and 2.6 scenarios (right column). Color only (category 1) indicates that less than 50% of the models show a statistically significant change. Color with hatching (category 3) indicates that more than 50% of the models show a statistically significant change, and more than 67% agree on the sign of the change (Figure source: Sun et al. 2015).

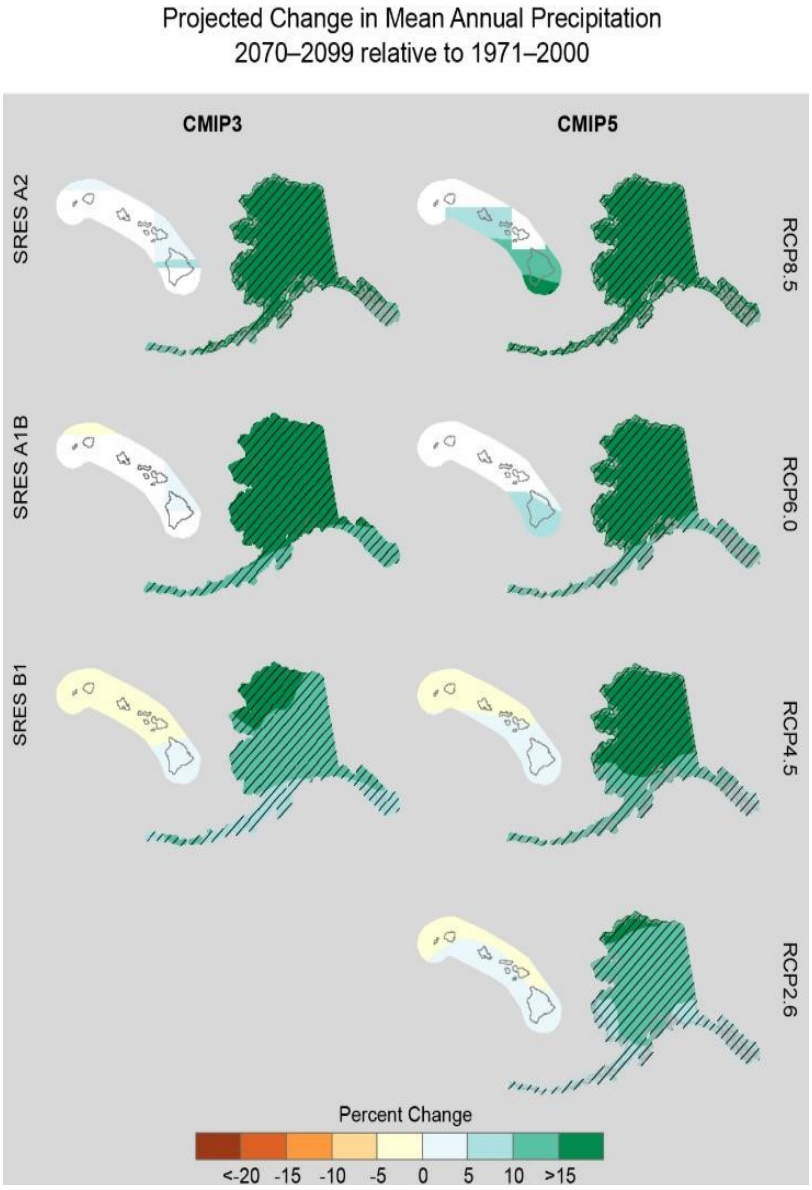

Figure 9-14. Projected change in mean annual precipitation (%) for Alaska and Hawai'i, for 2070–2099 with respect to the reference period of 1971–2000. These are multi-model means using CMIP3 SRES A2, A1B, and B1 scenarios (left column), and CMIP5 RCP8.5, 6.0, 4.5, and 2.6 scenarios (right column). Color only (category 1) indicates that less than 50% of the models show a statistically significant change. Whited out areas (category 2) indicate that more than 50% of the models show a statistically significant change, but less than 67% agree of the sign of the change. Color with hatching (category 3) indicates that more than 50% of the models show a statistically significant change, and more than 67% agree on the sign of the change (Figure source: Sun et al. 2015).

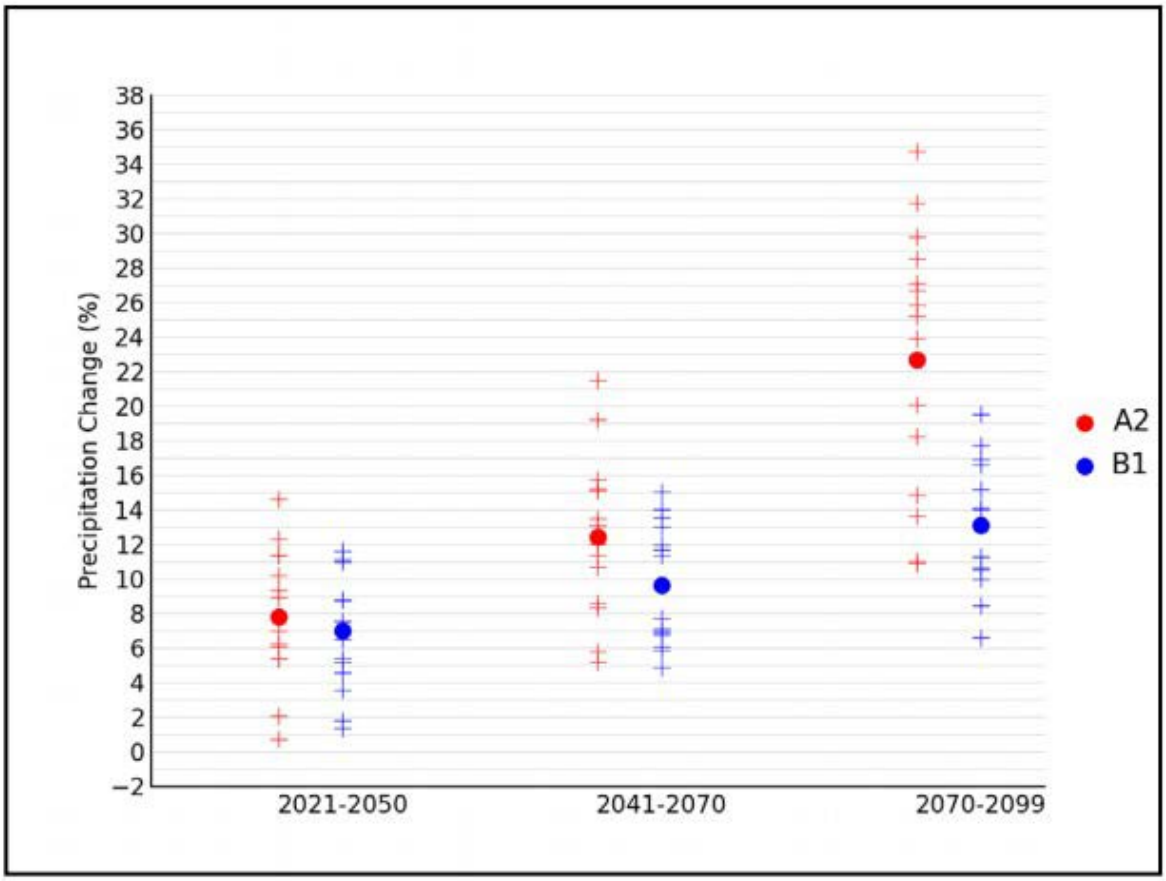

Figure 9-15. Simulated annual mean precipitation change (%) for Alaska for each of the future time periods (2021-2050, 2041-2070, and 2070-2099) with respect to the reference period of 1971-1999. Values are given for the high (A2) and the low (B1) emissions scenarios for the 14 (B1) or 15 (A2) CMIP3 models. The small plus signs indicate each individual model and the circles depict the multi-model means. The ranges of the model simulated changes are very large compared to the mean changes and the differences between the A2 and B1 emissions scenarios (Figure source: Stewart et al. 2013).

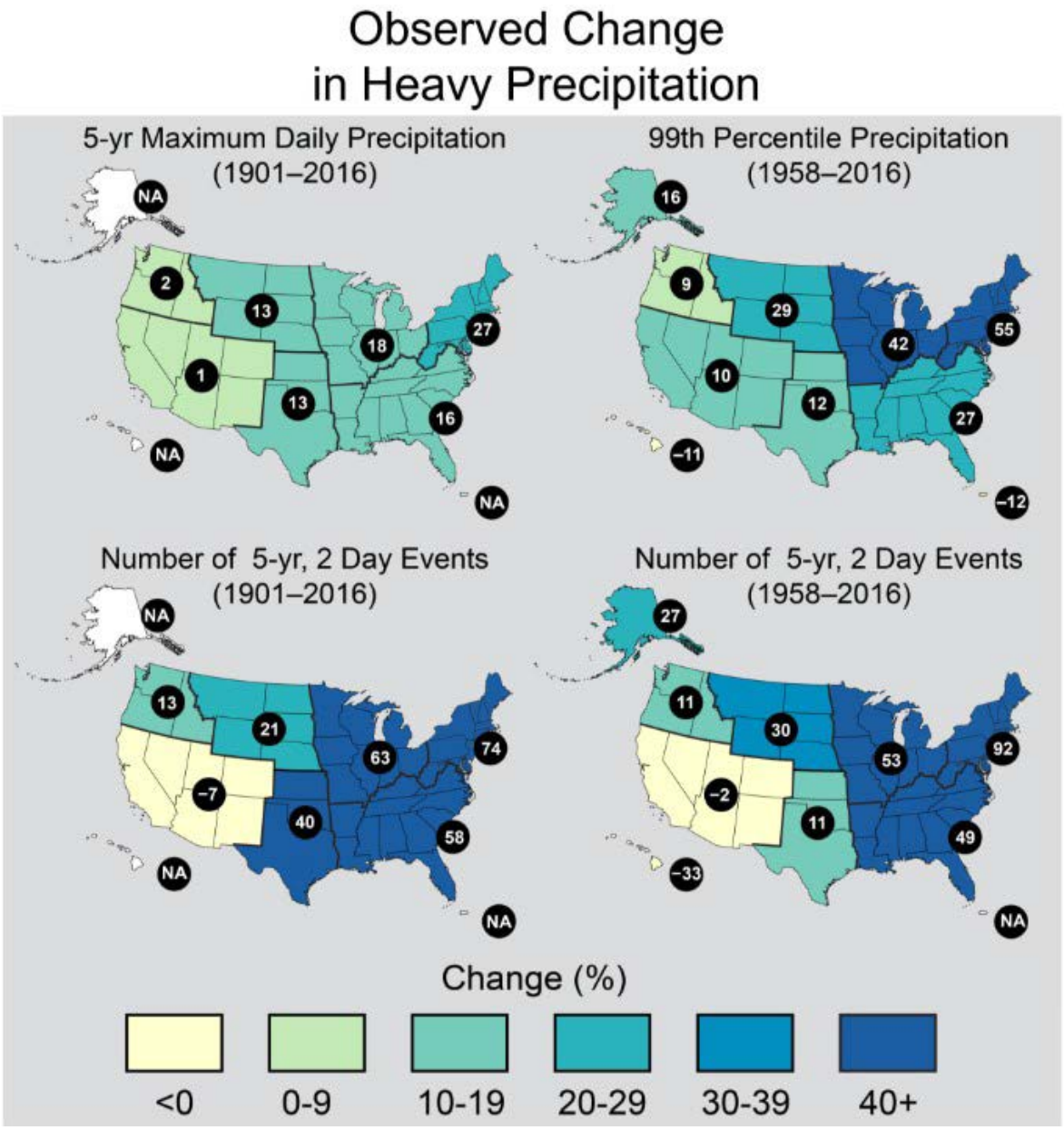

Figure 9-16. Changes in extreme precipitation. The percent change in maximum daily precipitation by 5-year periods (upper left), the percent change in the amount of precipitation falling in daily events that exceed the 99th percentile of precipitation days (upper right), the percent change in number of two day events with a precipitation total exceeding the largest two-day amount that would be expected to occur only once every five years based on data from 1901–2016 (lower left), and the percent change in number of two day events with a precipitation total exceeding the largest two-day amount that would be expected to occur only once every five years based on data from 1958–2016 (lower right) (Figure source: USGCRP 2017 p. 212).

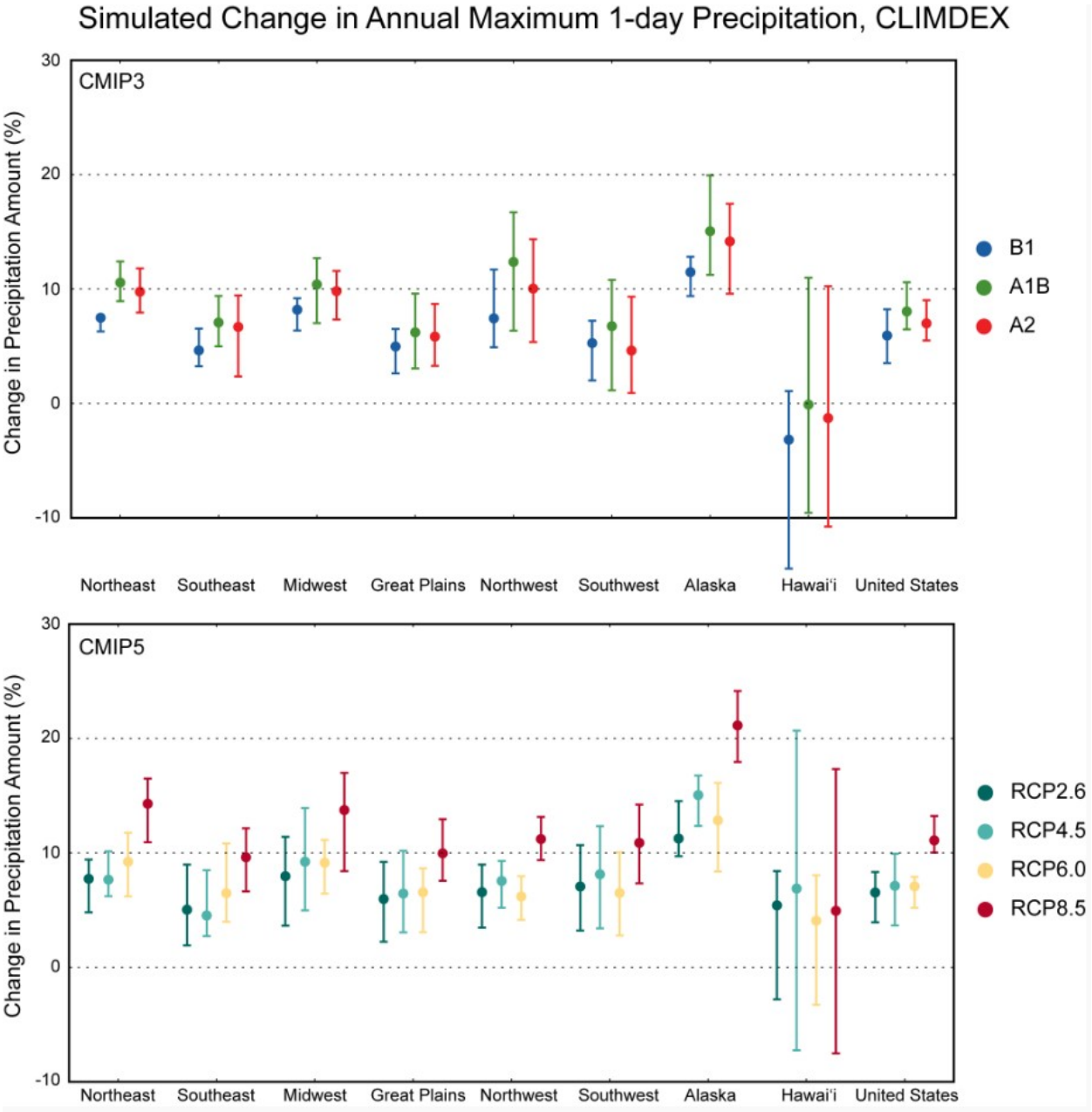

Figure 9-17. Simulated change in annual maximum 1-day precipitation (Rx1day) for each region and the contiguous United States, for 2046–2065 with respect to the reference period of 1981–2000. The upper panel shows values for the CLIMDEX SRES B1 (blue), A1B (green), and A2 (red) scenarios. The lower panel shows values for the CLIMDEX RCP2.6 (dark teal), 4.5 (light teal), 6.0 (yellow), and 8.5 (dark red) scenarios. Bars indicate the interquartile ranges of model values and circles depict the multi-model means (Figure source: Sun et al. 2015).

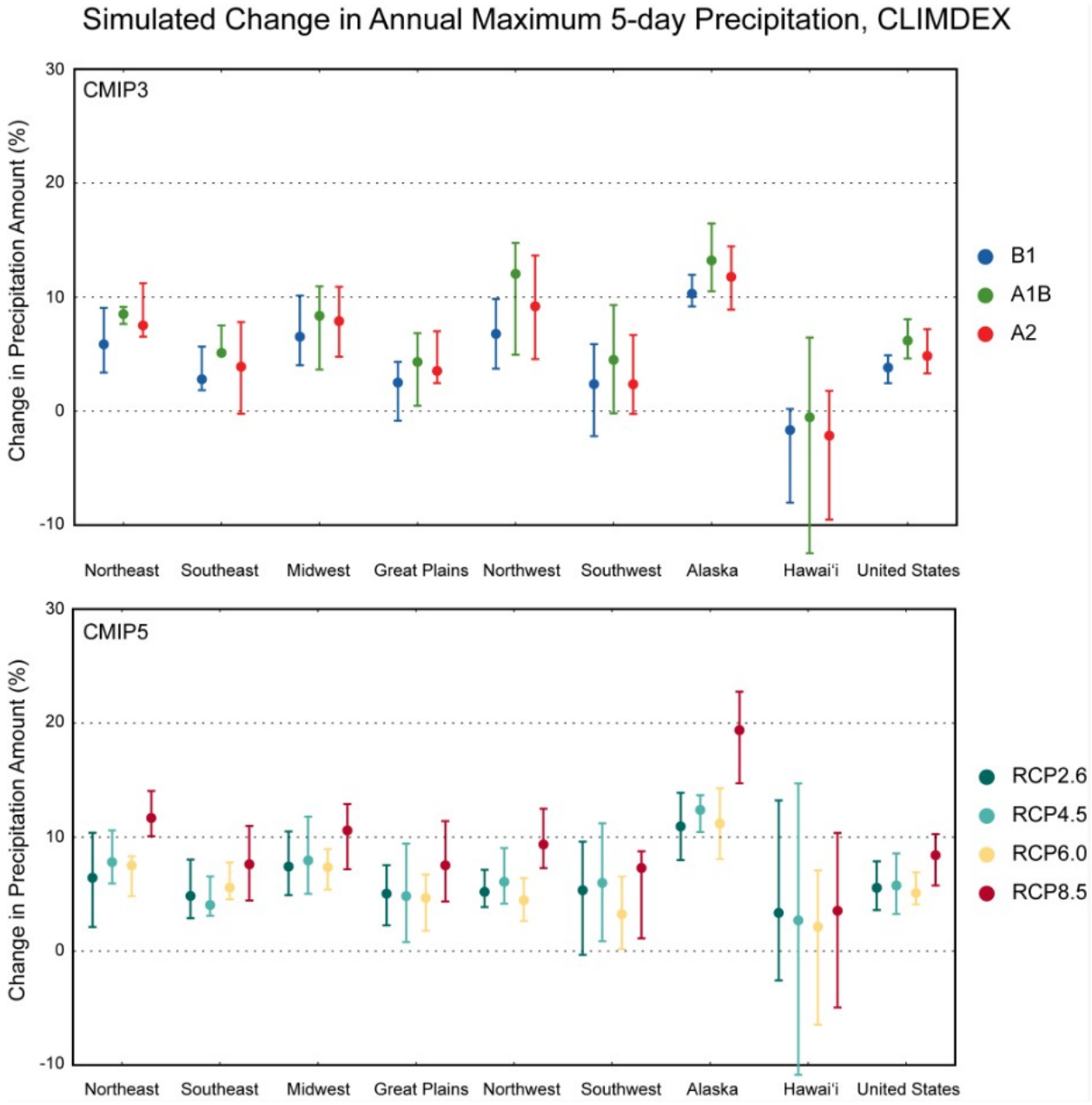

Figure 9-18. Simulated change in annual maximum 5-day precipitation (Rx5day) for each region and the contiguous United States, for 2046–2065 with respect to the reference period of 1981–2000. The upper panel shows values for the CLIMDEX SRES B1 (blue), A1B (green), and A2 (red) scenarios. The lower panel shows values for the CLIMDEX RCP2.6 (dark teal), 4.5 (light teal), 6.0 (yellow), and 8.5 (dark red) scenarios. Bars indicate the interquartile ranges of model values and circles depict the multi-model means (Figure source: Sun et al. 2015).

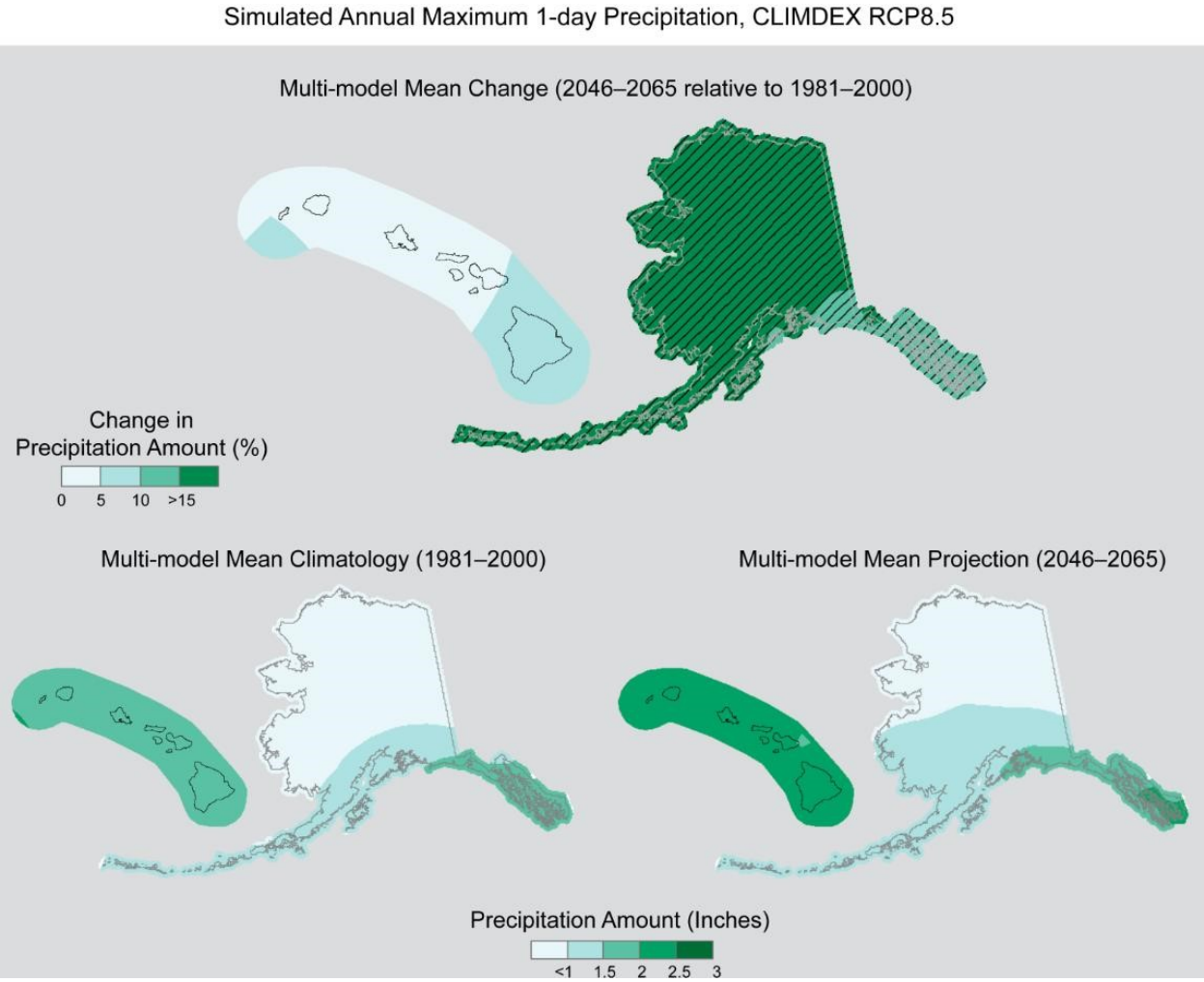

Figure 9-19. Simulated multi-model mean change in annual maximum 1-day precipitation (Rx1day) for Alaska and Hawai'i, for 2046–2065 with respect to the reference period of 1981–2000, using the CLIMDEX RCP8.5 scenario (top). Color only (category 1) indicates that less than 50% of the models show a statistically significant change. Color with hatching (category 3) indicates that more than 50% of the models show a statistically significant change, and more than 67% agree on the sign of the change. Multi-model mean climatology indicating the Rx1day for 1981–2000 is shown bottom left. Multi-model mean projection indicating the Rx1day for 2046–2065 is shown bottom right (Figure source: Sun et al. 2015).

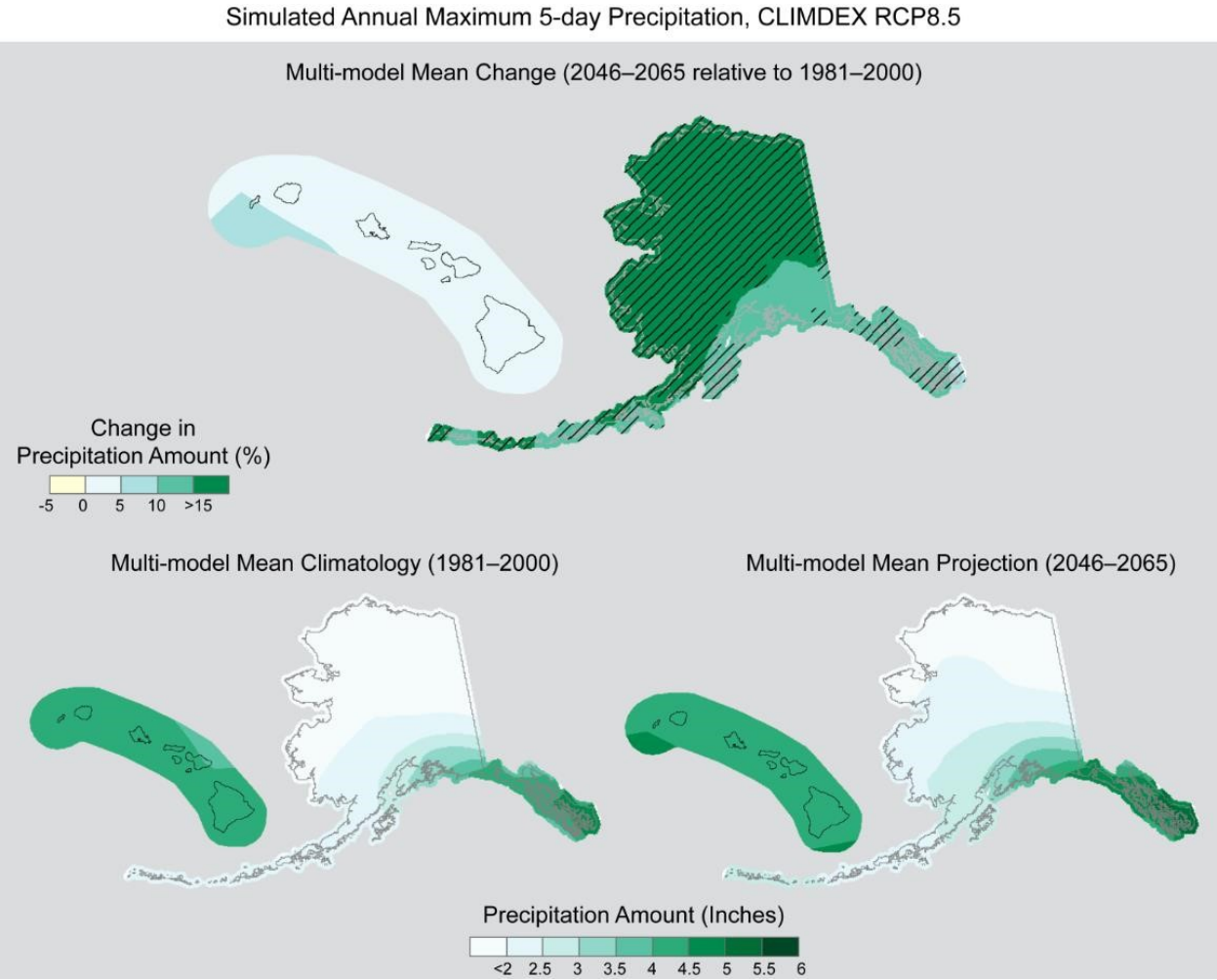

Figure 9-20. Simulated multi-model mean change in annual maximum 5-day precipitation (Rx5day) for Alaska and Hawai'i, for 2046–2065 with respect to the reference period of 1971–2000, using the CLIMDEX RCP8.5 scenario (top). Color only (category 1) indicates that less than 50% of the models show a statistically significant change. Color with hatching (category 3) indicates that more than 50% of the models show a statistically significant change, and more than 67% agree on the sign of the change. Multi-model mean climatology indicating the Rx5day for 1981–2000 is shown bottom left. Multi-model mean projection indicating the Rx5day for 2046–2065 is shown bottom right (Figure source: Sun et al. 2015).

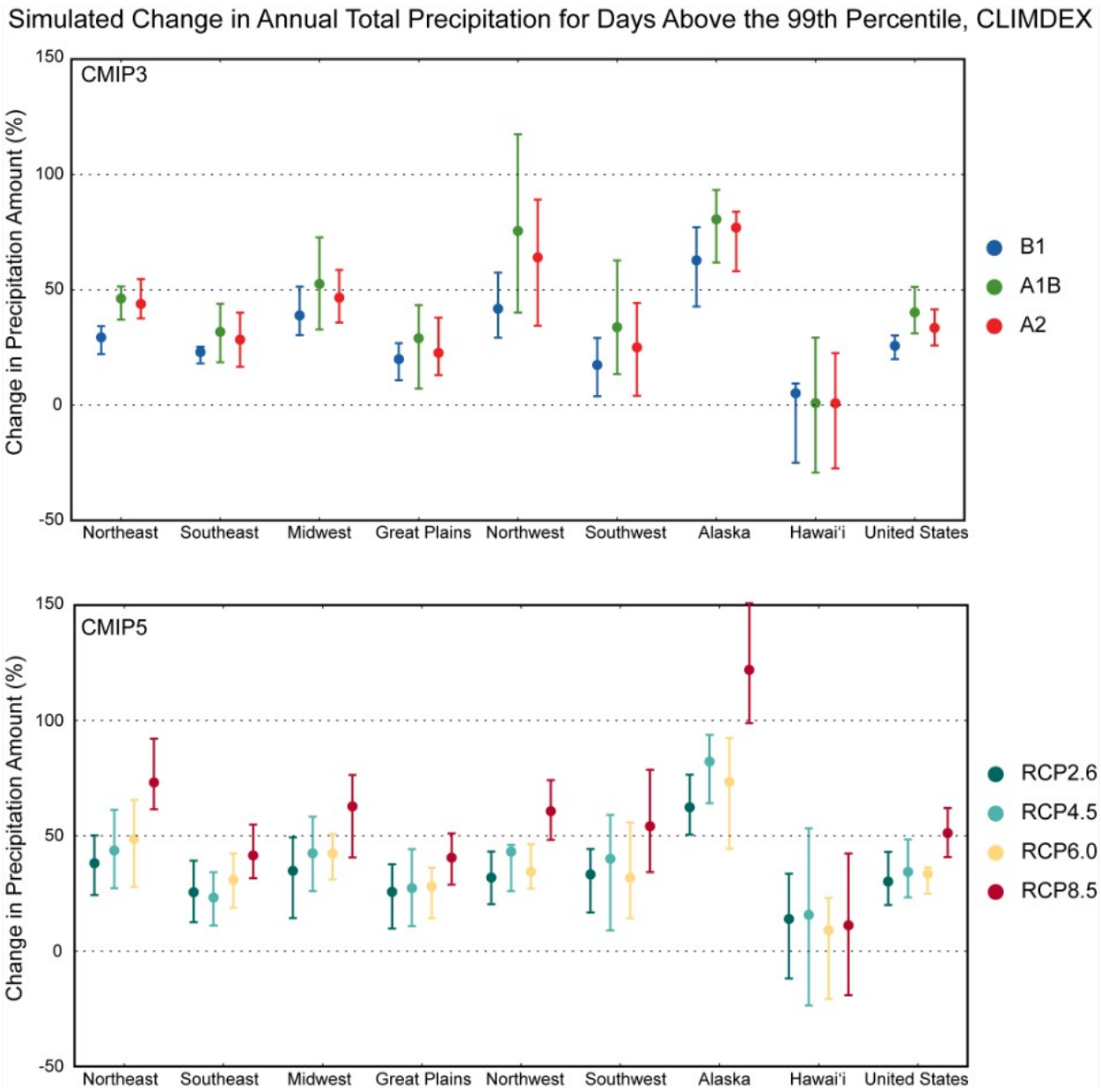

Figure 9-21. Simulated change in annual total precipitation for days above the 99th percentile (R99pTOT) for each region and the contiguous United State, for 2046–2065 with respect to the reference period of 1981–2000. The upper panel shows values for the CLIMDEX SRES B1 (blue), A1B (green), and A2 (red) scenarios. The lower panel shows values for the CLIMDEX RCP2.6 (dark teal), 4.5 (light teal), 6.0 (yellow), and 8.5 (dark red) scenarios. Bars indicate the interquartile ranges of model values and circles depict the multi-model means (Figure source: Sun et al. 2015).

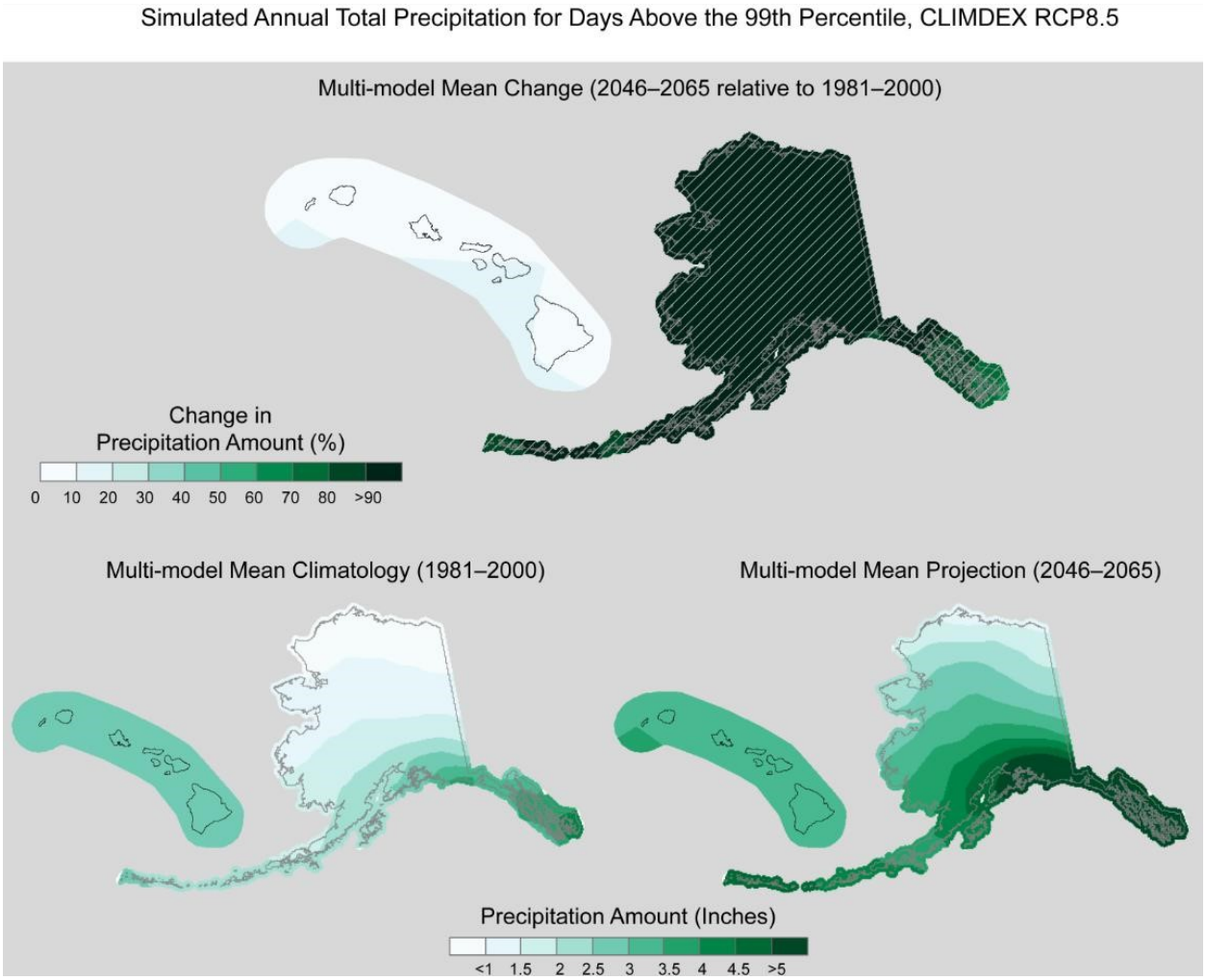

Figure 9-22. Simulated multi-model mean change in annual total precipitation for days above the 99th percentile (R99pTOT) for Alaska and Hawai‘i, for 2046–2065 with respect to the reference period of 1981–2000, using the CLIMDEX RCP8.5 scenario (top). Color only (category 1) indicates that less than 50% of the models show a statistically significant change. Color with hatching (category 3) indicates that more than 50% of the models show a statistically significant change, and more than 67% agree on the sign of the change. Multi-model mean climatology indicating the R99pTOT for 1981–2000 is shown bottom left. Multi-model mean projection indicating the R99pTOT for 2046–2065 is shown bottom right (Figure source: Sun et al. 2015).

Scenario	Period	Season	Lowest	25th Percentile	Median	75th Percentile	Highest
A2	2070-2099	DJF	10	21	30	38	48
		MAM	8	18	22	26	40
		JJA	5	14	21	25	30
		SON	11	17	24	30	35
B1	2070-2099	DJF	6	10	19	20	23
		MAM	-4	9	12	14	21
		JJA	7	10	12	14	19
		SON	6	10	11	17	23

Figure 9-23. Distribution of the simulated change in seasonal mean precipitation (%) from the 14 (B1) or 15 (A2) CMIP3 models for Alaska. The lowest, 25th percentile, median, 75th percentile and highest values are given for the high (A2) and low (B1) emissions scenarios, and for the 2070-2099 time period with respect to the reference period of 1971-1999 (Figure source: Stewart et al. 2013).

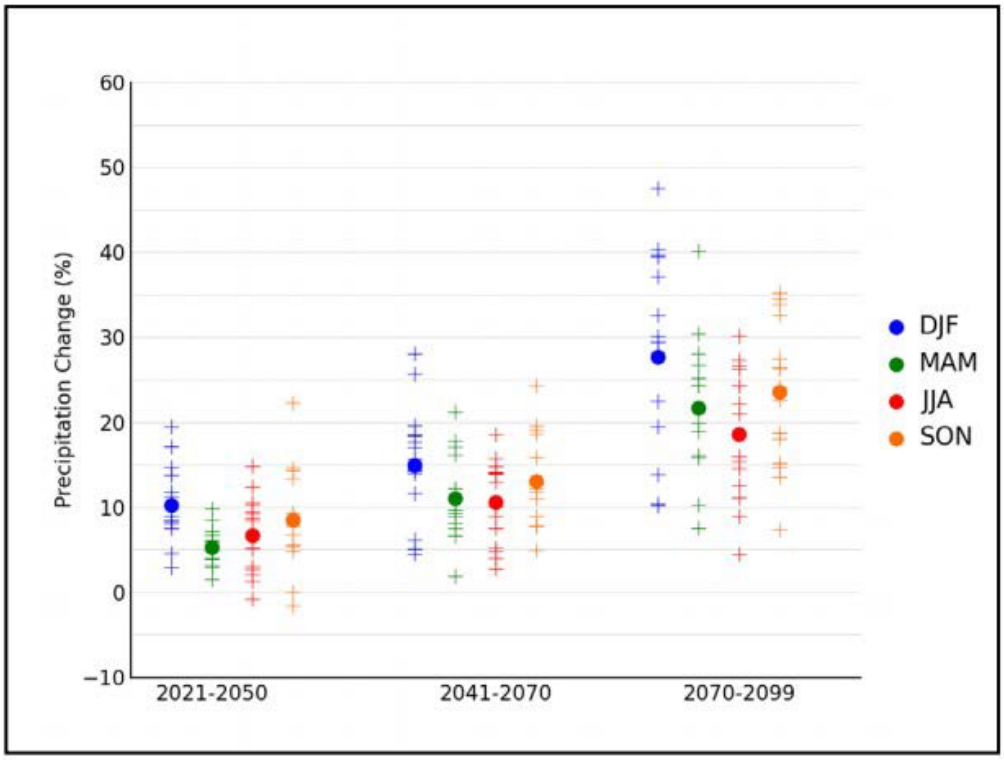

Figure 9-24. Simulated annual mean precipitation change (%) for Alaska for each future time period (2021-2050, 2041-2070, and 2070-2099) with respect to the reference period of 1971-1999. Values are given for all 15 CMIP3 models for the high (A2) emissions scenario. The small plus signs indicate each individual model and the circles depict the multi-model means. Seasons are indicated as follows winter (DFJ), spring (MAM), summer (JJA), and fall (SON). The ranges of the model-simulated changes are large compared to the mean changes and to difference between the seasons (Figure source: Stewart et al. 2013).

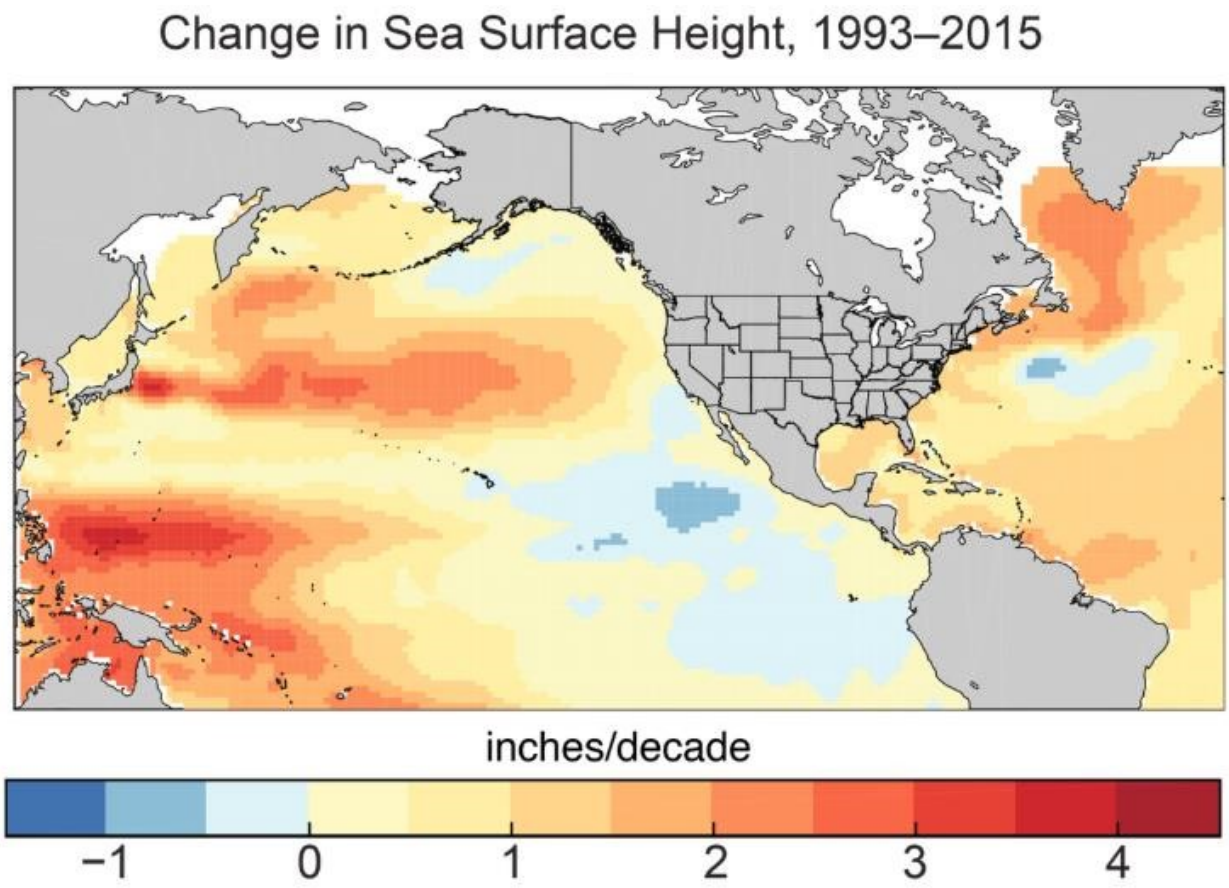

Figure 9-25. Rates of change from 1993 to 2015 in sea surface height from satellite altimetry data; updated from Kopp et al. using data updated from Church and White (Figure source: USGCRP 2017 p. 340).

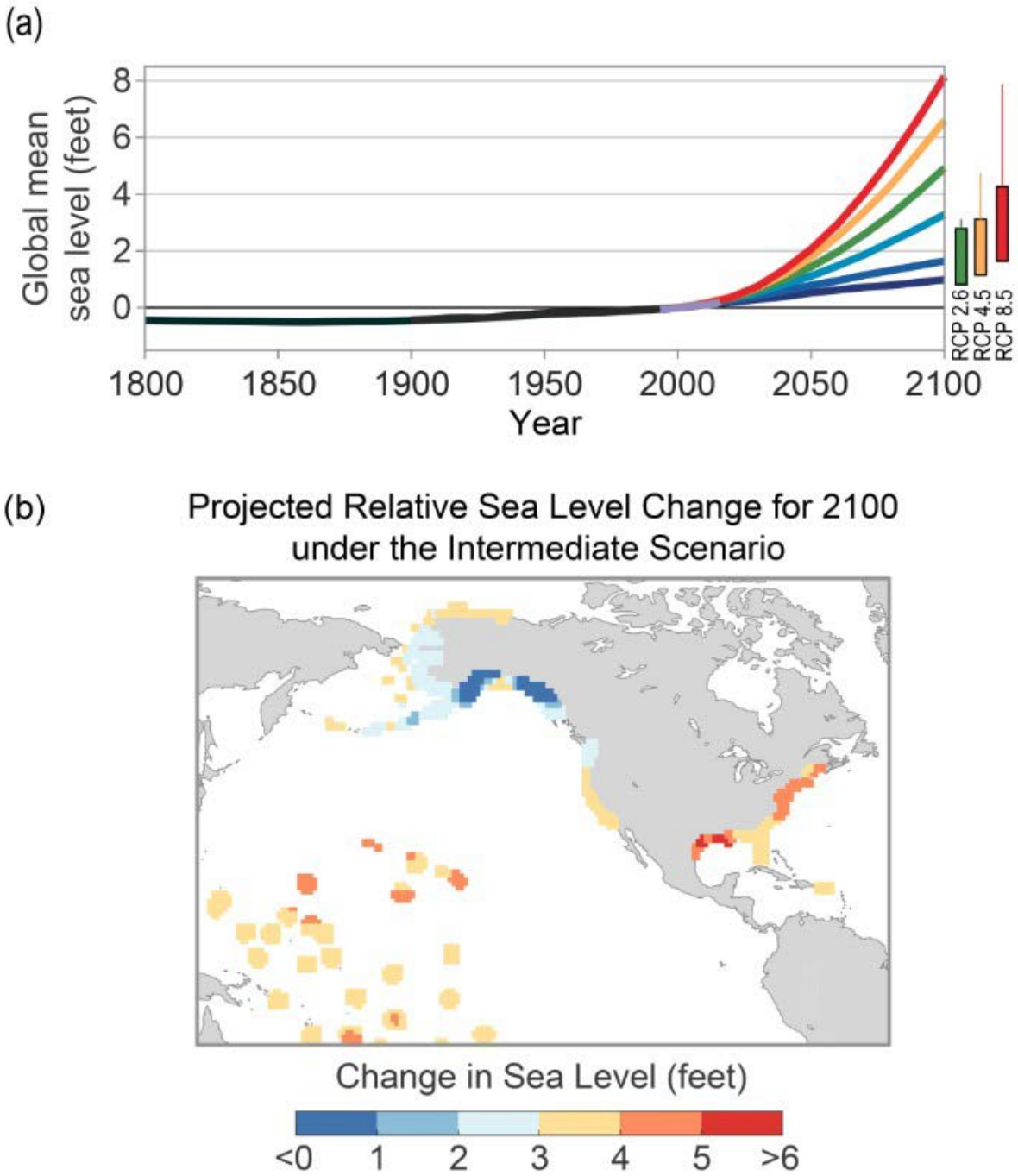

Figure 9-26. (a) Global mean sea level (GMSL) rise from 1800 to 2100, based on Figure 12.2b from 1800 to 2015, the six Interagency GMSL scenarios (navy blue, royal blue, cyan, green, orange, and red curves), the very likely ranges in 2100 for different RCPs (colored boxes), and lines augmenting the very likely ranges by the difference between the median Antarctic contribution of Kopp et al. and the various median Antarctic projections of DeConto and Pollard. (b) Relative sea level (RSL) rise (feet) in 2100 projected for the Interagency Intermediate Scenario (1-meter [3.3 feet] GMSL rise by 2100) (Figure source: USGCRP 2017 p. 342).

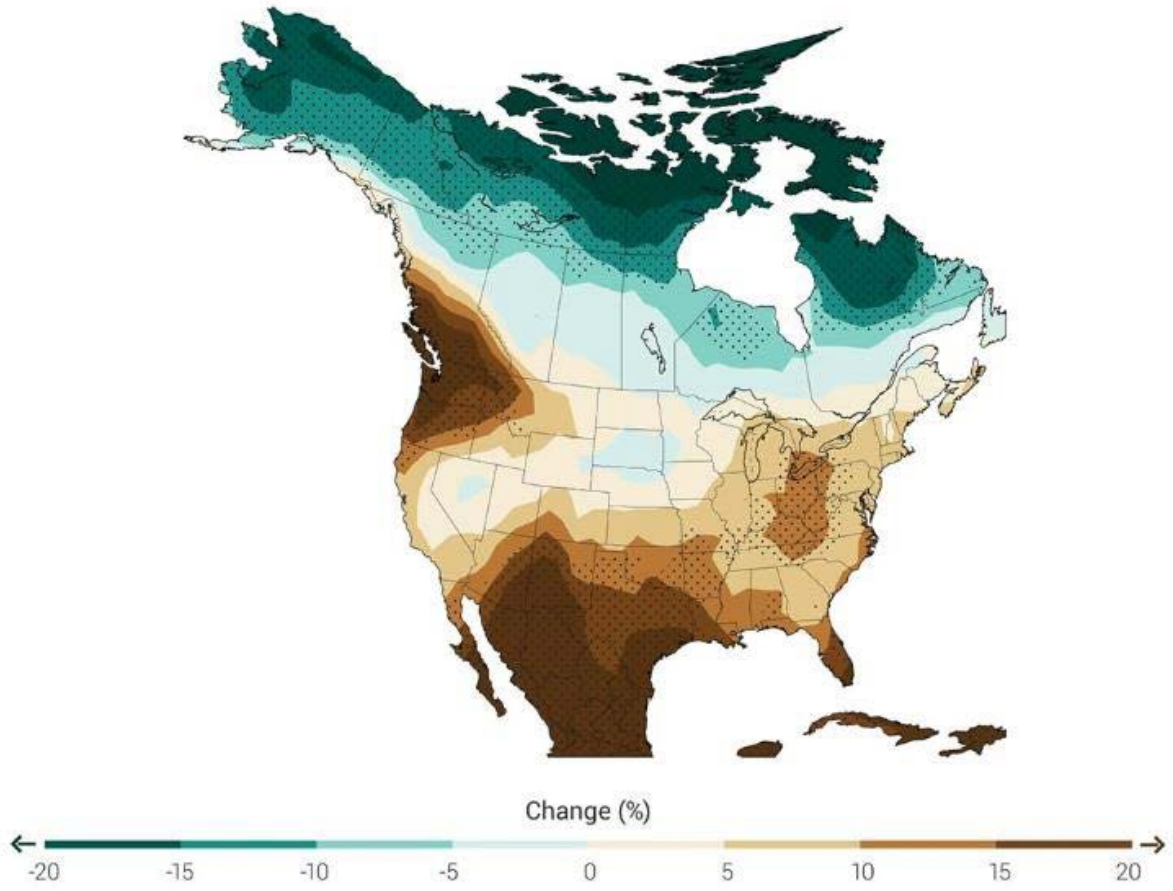

Figure 9-27. Change in the number of consecutive dry days (less than 0.04 inches (1mm) of precipitation) at the end of this century (2070-2099) relative to the end of the last century (1971-2000) under the higher scenario, RCP 8.5. Stippling indicates area where changes are consistent among at least 80% of the 25 models used in this analysis (Figure source: Melillo et al. 2014 p. 33).

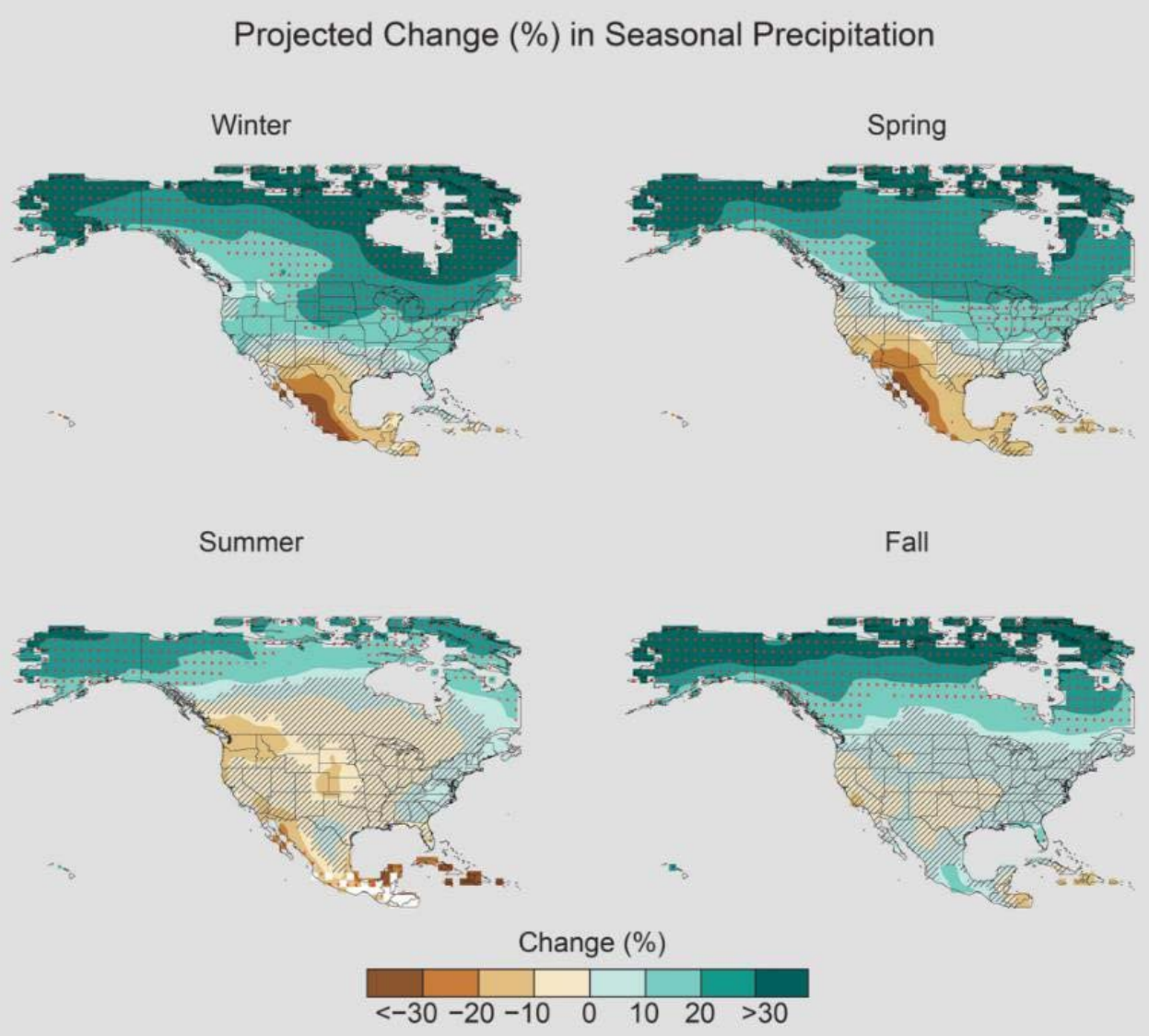

Figure 9-28. Projected change (%) in total seasonal precipitation from CMIP5 simulations for 2070–2099. The values are weighted multi-model means and expressed as the percent change relative to the 1976–2005 average. These are results for the higher scenario (RCP8.5). Stippling indicates that changes are assessed to be large compared to natural variations. Hatching indicates that changes are assessed to be small compared to natural variations. Blank regions (if any) are where projections are assessed to be inconclusive. Data source: World Climate Research Program's (WCRP's) Coupled Model Intercomparison Project (Figure source: USGCRP 2017 p. 217).

10 Hawai‘i

10.1 Summary of Climate Projections for Hawai‘i

10.1.1 Temperature

Hawai‘i has observed an increase in annual temperature of 1.26°F from the 1925-1960 average to the present-day average (1986-2016) (USGCRP 2017 p. 187). This warming is noted during all seasons (USGCRP 2017 p.193). Under both lower and higher emissions scenarios, Hawai‘i is expected to warm slightly by mid-century (Figure 10-1, Figure 10-2, and Figure 10-3). The models slightly diverge by late century (~4-6°F in high emissions, ~2-4°F in low emissions) but both suggest increased warming in Hawai‘i (USGCRP 2017 p.196). However, Hawai‘i's temperature changes will be largely dictated by the change in ocean temperatures. It is unlikely that annual temperatures decrease in Hawai‘i, unless ocean temperatures decrease, or other unforeseen changes occur.

Due to the limited ability of models to resolve surface temperature on small islands in the Pacific (model output only shows one grid box on Oahu, where Honolulu is), confidence is lower than other regions that temperature will increase on the islands. However, it remains more probable than not. This discussion does not apply for the peaks of Mauna Loa and other volcanos. Temperature trends are different at very high elevations and climate models do not have the spatial resolution to show trends in temperature for each volcano.

The climatological mean (1981-2000) hottest annual temperature for Hawai‘i is between 80-85 degrees. This is projected, according to Sun et al. (2015), to increase by 4-5°F by mid-century (2046-2065) relative to the climatological mean in high emissions scenarios (Figure 10-4). With Hawai‘i omitted from discussion on change in extreme annual temperatures in both NCA3 (Melillo et al. 2014) and the Climate Science Special Report (USGRP 2017), there may be some uncertainty to the magnitude of increase, especially in low emissions scenarios. Therefore, it seems probable that the hottest annual temperature will increase on Hawai‘i. Thus, there is low confidence that the magnitude of the hottest temperatures will decrease.

The climatological mean (1981-2000) lowest annual temperature for Hawai‘i is just over 60 degrees. This is projected, according to Sun et al. (2015), to increase by 2-4°F by mid-century (2046-2065) relative to the climatological mean in high emissions scenarios (Figure 10-5). With Hawai‘i omitted from discussion on change in extreme annual temperatures in both NCA3 (Melillo et al. 2014) and the Climate Science Special Report (USGRP 2017), there may be some uncertainty to the magnitude of increase, especially in low emissions scenarios. Therefore, it seems probable that the lowest annual temperature will increase on Hawai‘i. Thus, there is less confidence that the lowest annual temperatures will decrease.

According to the National Centers for Environmental Information, Hawai‘i saw a large number of days over 90°F from 1975 to 2000 when compared to the 1950-2014 average of about 6.5 days. This trend has not generally continued since 2000, with the five-year averages for 2005-2009 and 2010-2014 being about five and seven, respectively. A search of literature found no results on future projections of hot days in Hawai‘i. In addition, projections for days over 90°F in Hawai‘i are not discussed in any of the recent climate assessments (Karl et al. 2009, Melillo et al.

2014, and USGCRP 2017). Hawai‘i does not average very many days over 90°F due to its location in the central Pacific Ocean, which moderates air temperature. Therefore, it is entirely possible that 1950-2014 average of about 6.5 days over 90°F may only slightly increase, stay the same, or slightly decrease. The urban heat island effect may play a role in Honolulu and other developed areas. With increased development, these urban areas may experience increases in days over 90°F during the next century that adjacent rural areas may not.

Using the Warm Spell Duration Index (WSDI, defined as the annual count of days with at least 6 consecutive days when daily maximum temperatures are > 90th percentile), model projections from the CMIP3 and CMIP5 downscaled data sets indicate that the number of days with temperatures > 90th percentile will increase by over 200 days by mid-century (2046-2065; see Figure 10-6). The CMIP5 model ensemble with high (RCP8.5) emission scenario predicts that the WSDI will increase, with the increase considered statistically significant (see Figure 10-7).

With the exception of the peaks of Mauna Loa and other volcanos, Hawai‘i does not generally experience freezing temperatures. With warming annual temperatures, near sea-level Hawai‘i is extremely unlikely to see any freezing temperatures.

According to the National Centers for Environmental Information, Hawai‘i has seen an increase in minimum nighttime temperatures since 1950, and since 1980 these minimum temperatures have been above the 1950-2014 average. Hawai‘i is accustomed to warm nighttime temperatures, averaging well over 225 nights with temperatures over 68°F (Sun et al. 2015). According to Sun et al. (2015), there will be an increase of anywhere from 10-40 days with nighttime temperatures over 68°F across the island chain, under higher emissions scenarios by mid-century (2046-2065) compared to the 1981-2000 average. That increase would imply there would be an increase in minimum nighttime temperatures across the chain. Since Hawai‘i is expected to warm, it seems very unlikely the minimum nighttime temperatures will decrease. Uncertainty in these projections results from lack of detail in Sun et al. (2015) regarding other emissions scenarios and longer timescales.

Hawai‘i has seen a decrease in its diurnal temperature range over the past decade. The islands’ average annual maximum temperature has increased by 1.01°F while the average annual minimum temperature has increased by 1.49°F, when comparing the present-day average (1986-2016) to an average from (1925-1940). This differential warming leads to a decrease in the diurnal temperature range of 0.48°F. None of the previous three national climate assessments (Karl et al. 2009, Melillo et al. 2014, and USGCRP 2017) discuss the changes in diurnal temperature range for Hawai‘i during the next century. A search for literature on the subject also led to no result. A continuation of the current shrinking trend in the diurnal temperature range is possible, especially in the short-term, but with considerable uncertainty given the lack of information on the subject.

10.1.2 Precipitation

Unlike regions of the contiguous United States, Hawai‘i has experienced up to a five percent decrease in annual precipitation comparing the present-day average (1986-2015) to the average from 1925-1960 (USGCRP 2017 p. 209). According to Sun et al. (2015), only under the lowest emissions scenarios would a decrease in annual precipitation occur on Hawai‘i by mid-century

(2041-2070) compared to the 1971-2000 averages (Figure 10-8, Figure 10-9, Figure 10-10, and Figure 10-11). The decrease in precipitation was most notable and statistically significant by this time period in some of the lower emissions scenarios. Under no scenarios would an increase in annual precipitation be significant. Acknowledging that Hawai‘i is experiencing reduced precipitation with time and recognizing local effects, there still remains large uncertainty and a lack of conclusive statistical evidence for any increase.

In addition, terrain-enhanced precipitation as result of the trade winds may impact Hawai‘ian precipitation totals, especially on the Big Island. Sun et al. (2015) suggests that this island may see a slight increase (but not significant) in precipitation by mid-century, compared to the other islands. Windward sides of islands may see increased annual precipitation, while leeward sides of islands may see decreased amounts (NCEI).

Hawai‘i has experienced a decrease in heavy rainfall intensity, according to the Climate Science Special Report (USGCRP 2017 p. 211; Figure 10-12). This decrease is noted by 11% reduction in the amount of rainfall falling in the top 1% most significant events from 1956 to 2016 and a 33% reduction in the amount of rainfall falling in two-day events based on five-year averages. In terms of changes into the future, even the highest emissions scenarios show a limited, non-statistically significant increase in intensity by mid-century (Sun et al. 2015; Figure 10-13, Figure 10-14, Figure 10-15, and Figure 10-16). It seems likely that the precipitation intensity on rainy days will continue the downward trend or not change in the future, with considerable uncertainty in these projections.

Hawai‘i’s heavy rainfall events are generally found on the eastern side of each island, where terrain-induced precipitation dominates. On western slopes of the islands or islands with limited terrain very few, if any, heavy rainfall days occurred through 2005 compared to near 25 days on the eastern slopes (Chu et al. 2009). However, Chu et al. (2010) argues that there has been a negative trend over the past century in the number of heavy precipitation days. This trend is expected to continue in the future (Figure 10-17 and Figure 10-18) with relatively low confidence.

The Climate Science Special Report (USGCRP 2017 p. 209) shows that there has been a slight decrease (-5 to 0%) in precipitation for each season when comparing the present-day average (1986-2015) to the 1925-1960 averages. There does not seem to be any variability between islands. Climate model resolution for precipitation on Hawai‘i is poor (USGCRP 2017 p. 217). There is only one grid box overlaid on Oahu (Honolulu). Just drawing from that one grid box, precipitation is expected to slightly decline in the winter and spring, slightly increase in the summer, and significantly increase (>20%) in the fall by late century (2071-2100) in high emissions scenarios. Therefore, extrapolating that grid point out for the chain and accounting for uncertainty and the lack of spatial resolution available for the island chain, an increase in seasonality is probable by late century.

10.1.3 Other Stressors

Unlike inland regions, Hawai‘i is very vulnerable to sea level rise. While the peak elevation of some of the islands is over a thousand feet, a large portion of Hawai‘i’s population lives on the coast, including the city of Honolulu. According to the National Centers for Environmental Information, global sea levels are expected to continue to rise at an increasing rate. Sea levels could rise over two feet by 2050 compared to 2000 levels and could rise over six feet by 2100. There is very high confidence that sea level will continue to rise throughout the next century (Figure 10-19 and Figure 10-20). Unlike other regions, flooding due to rainfall probably will not be a main culprit. However, intense rainfall down steep slopes combined with increased impervious surfaces could cause flooding issues. Therefore, it is very unlikely that this region will experience a decreased chance of flooding or high water levels.

It is highly unlikely that Hawai‘i will experience low water levels. That being said, precipitation changes (seasonality and totals), may also cause drought unrelated to rising sea levels. In fact, the 3rd National Climate Assessment argues that increased temperatures and the chance of lower precipitation could lead to instances of drought that would stress fresh water supplies and food sources, despite rising sea levels (Melillo et al. 2014 p.542-545). Decreased chance of drought/low water level is difficult to assess, as Hawai‘i almost certainly will see a decreased chance of reduced water levels as a result of sea level rise, but also may become prone to drought.

Wildfires are most common during the dry summer season and their frequency has been documented to be affected by the El Niño-Southern Oscillation. Specifically, Chu et al. (2002) found that the spring and summer after an El Niño event had the most amount of acreage burned on Hawai‘i. Therefore, with summers projected to become slightly wetter into the future, it is probable that wildfires may become less frequent on the Hawai‘ian Islands. But this is countered by the possible drying out of the spring months (USGCRP 2017 p.217). However, neither the Climate Science Special Report (USGCRP 2017) nor the 3rd National Climate Assessment (Melillo et al. 2014) discusses the impact of wildfires on Hawai‘i. Therefore, changes in wildfire may occur but with low confidence.

While winter weather events (snow accumulation, freezing rain, etc.) were investigated, they occur so infrequently a discussion is not warranted.

10.2 Tables and Figures: Hawai‘i

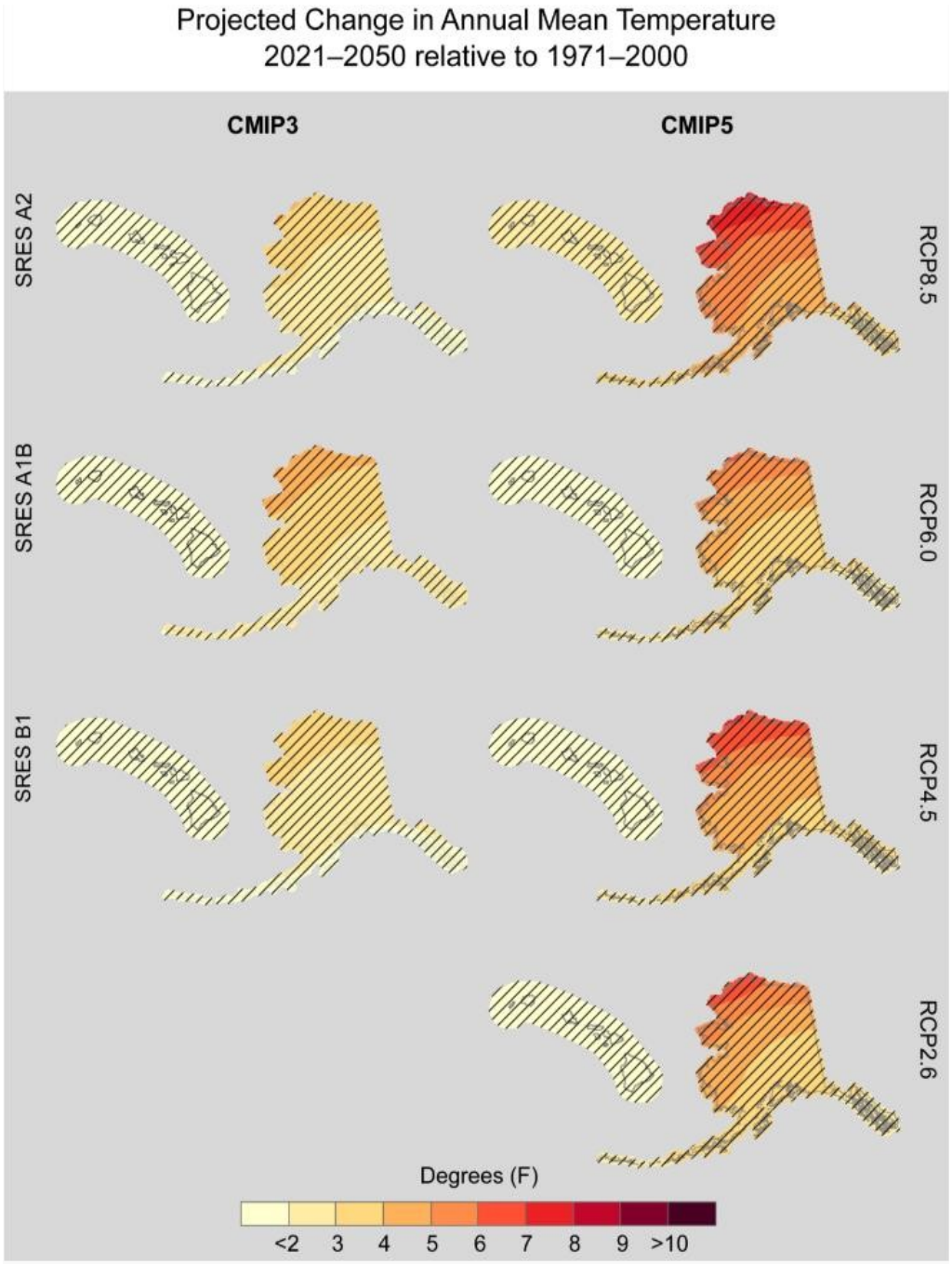

Figure 10-1. Projected change in annual mean temperature (°F) for Alaska and Hawai‘i, for 2021–2050 with respect to the reference period of 1971–2000. These are multi-model means using CMIP3 SRES A2, A1B, and B1 scenarios (left column), and CMIP5 RCP8.5, 6.0, 4.5, and 2.6 scenarios (right column). Color with hatching (category 3) indicates that more than 50% of the models show a statistically significant change, and more than 67% agree on the sign of the change (Figure source: Sun et al. 2015).

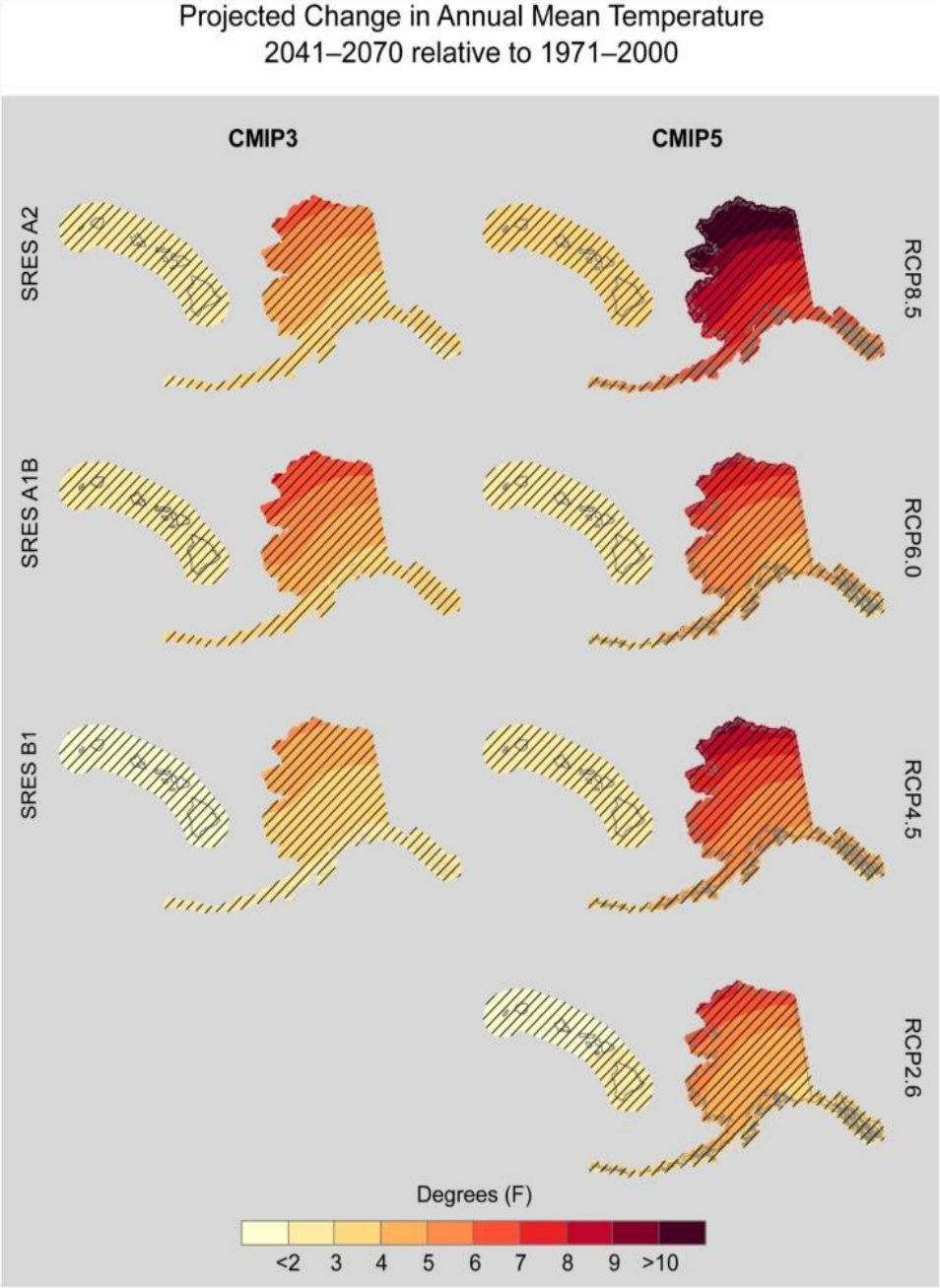

Figure 10-2. Projected change in seasonal mean temperature (°F) for Alaska and Hawai'i, for 2041–2070 with respect to the reference period of 1971–2000. These are multi-model means using CMIP3 SRES A2 (left column), and CMIP5 RCP8.5 (right column). Color with hatching (category 3) indicates that more than 50% of the models show a statistically significant change, and more than 67% agree on the sign of the change (Figure source: Sun et al. 2015).

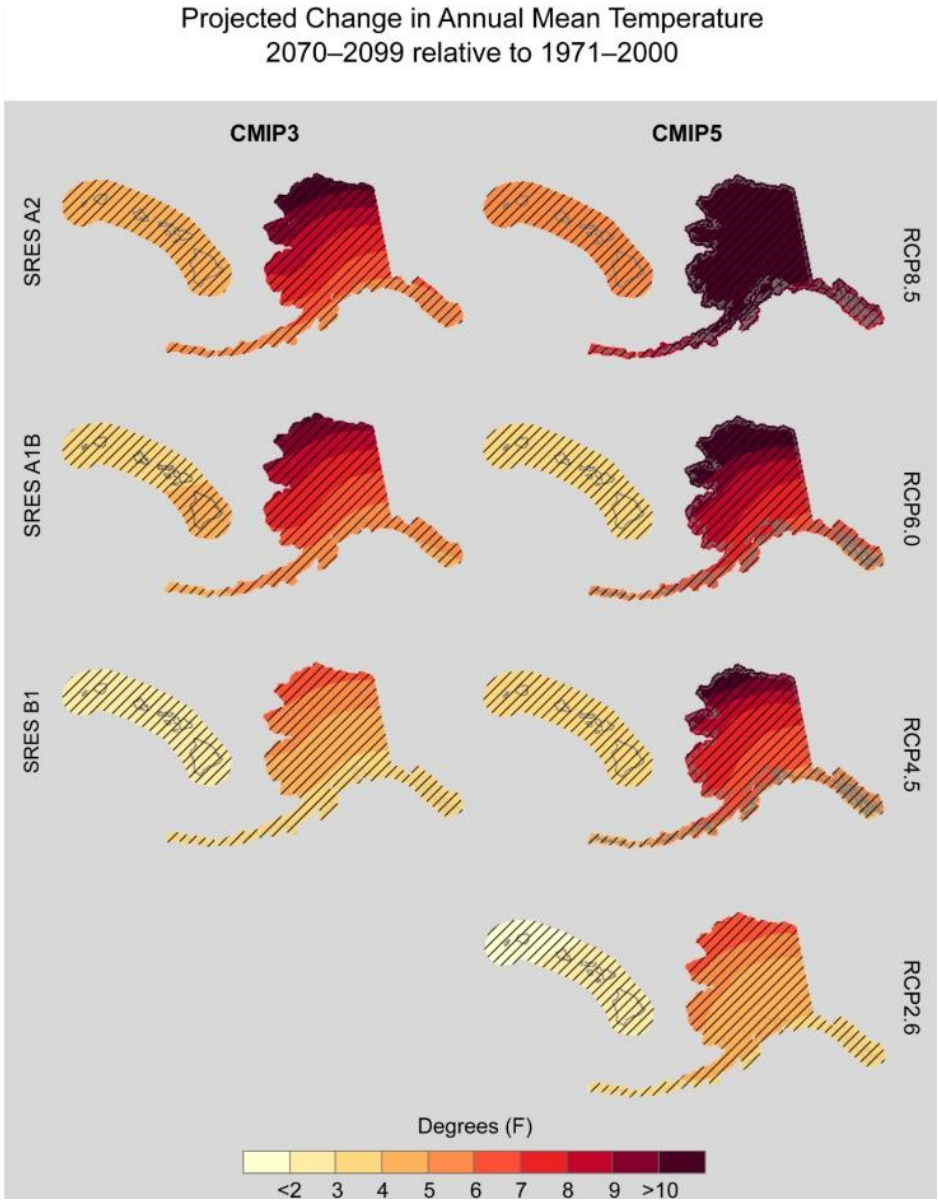

Figure 10-3. Projected change in annual mean temperature (°F) for Alaska and Hawai'i, for 2070–2099 with respect to the reference period of 1971–2000. These are multi-model means using CMIP3 SRES A2, A1B, and B1 scenarios (left column), and CMIP5 RCP8.5, 6.0, 4.5, and 2.6 scenarios (right column). Color with hatching (category 3) indicates that more than 50% of the models show a statistically significant change, and more than 67% agree on the sign of the change (Figure source: Sun et al. 2015).

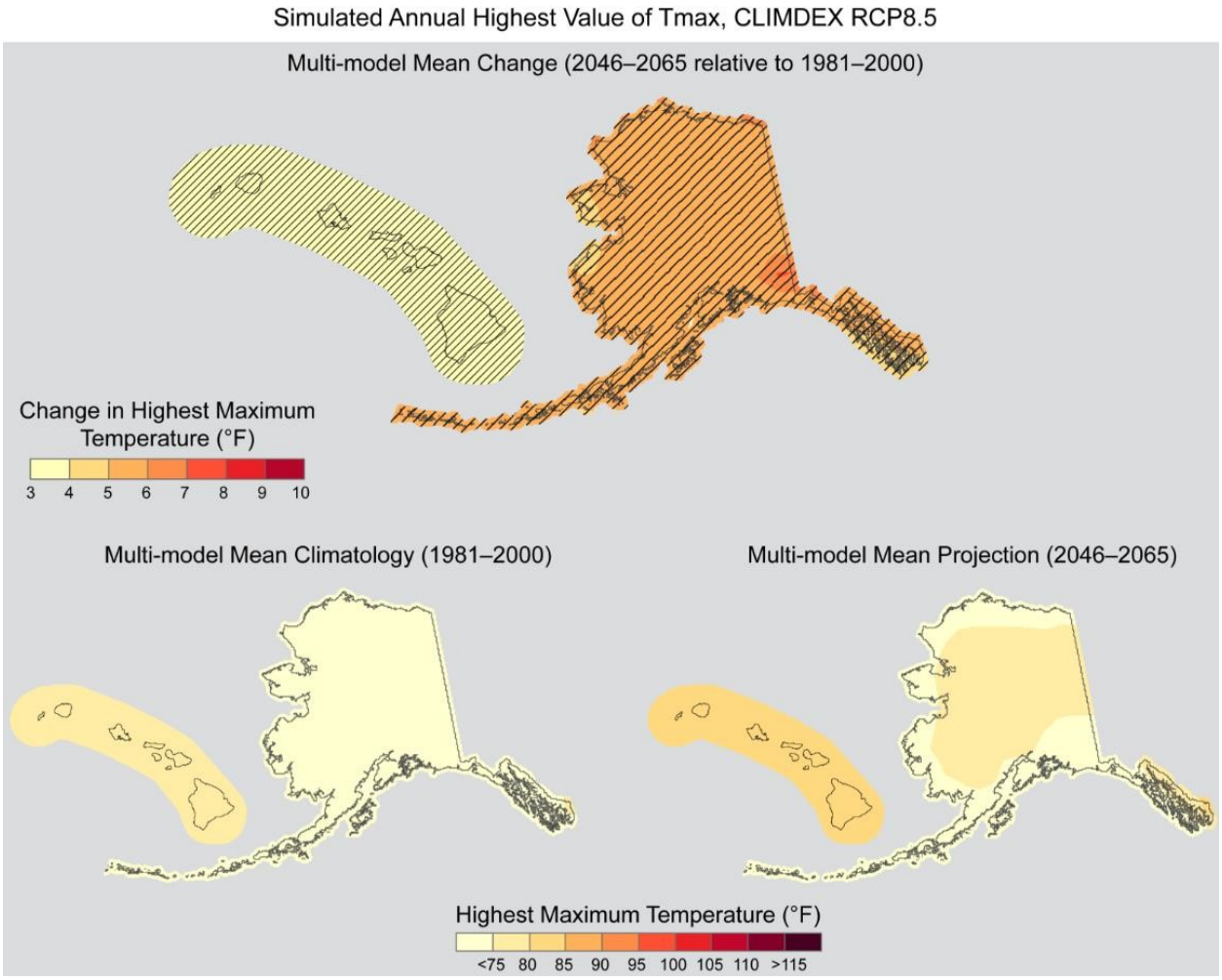

Figure 10-4. Simulated multi-model mean change in the annual highest value of daily maximum temperature (TXx) for Alaska and Hawai‘i, for 2046–2065 with respect to the reference period of 1981–2000, using the CLIMDEX RCP8.5 scenario (top). Color with hatching (category 3) indicates that more than 50% of the models show a statistically significant change, and more than 67% agree on the sign of the change. Multi-model mean climatology indicating the TXx for 1981–2000 is shown bottom left. Multi-model mean projection indicating the TXx for 2046–2065 is shown bottom right (Figure source: Sun et al. 2015).

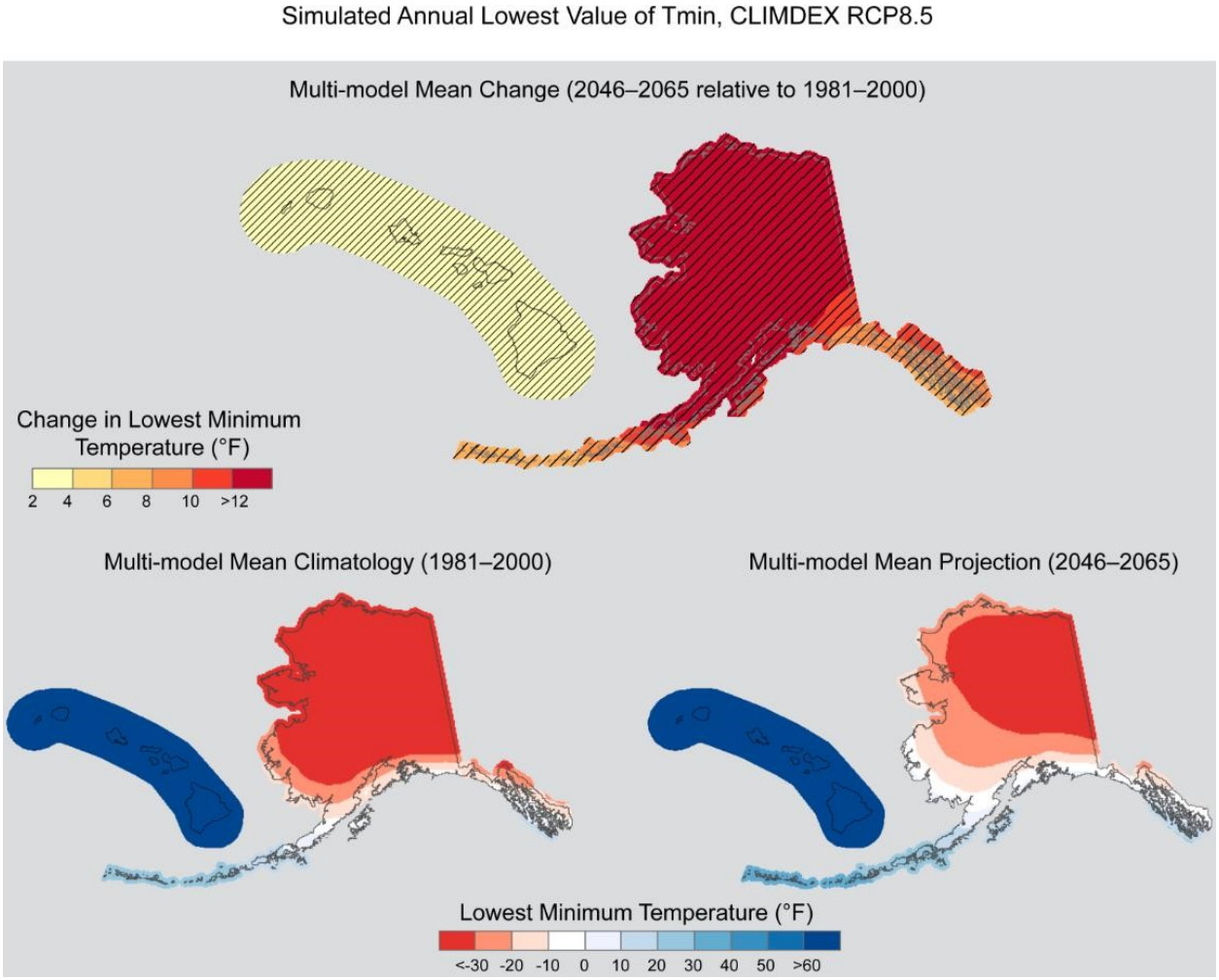

Figure 10-5. Simulated multi-model mean change in the annual lowest value of daily minimum temperature (TNn) for Alaska and Hawai'i, for 2046–2065 with respect to the reference period of 1981–2000, using the CLIMDEX RCP8.5 scenario (top). Color with hatching (category 3) indicates that more than 50% of the models show a statistically significant change, and more than 67% agree on the sign of the change. Multi-model mean climatology indicating the TNn for 1981–2000 is shown bottom left. Multi-model mean projection indicating the TNn for 2046–2065 is shown bottom right (Figure source: Sun et al. 2015).

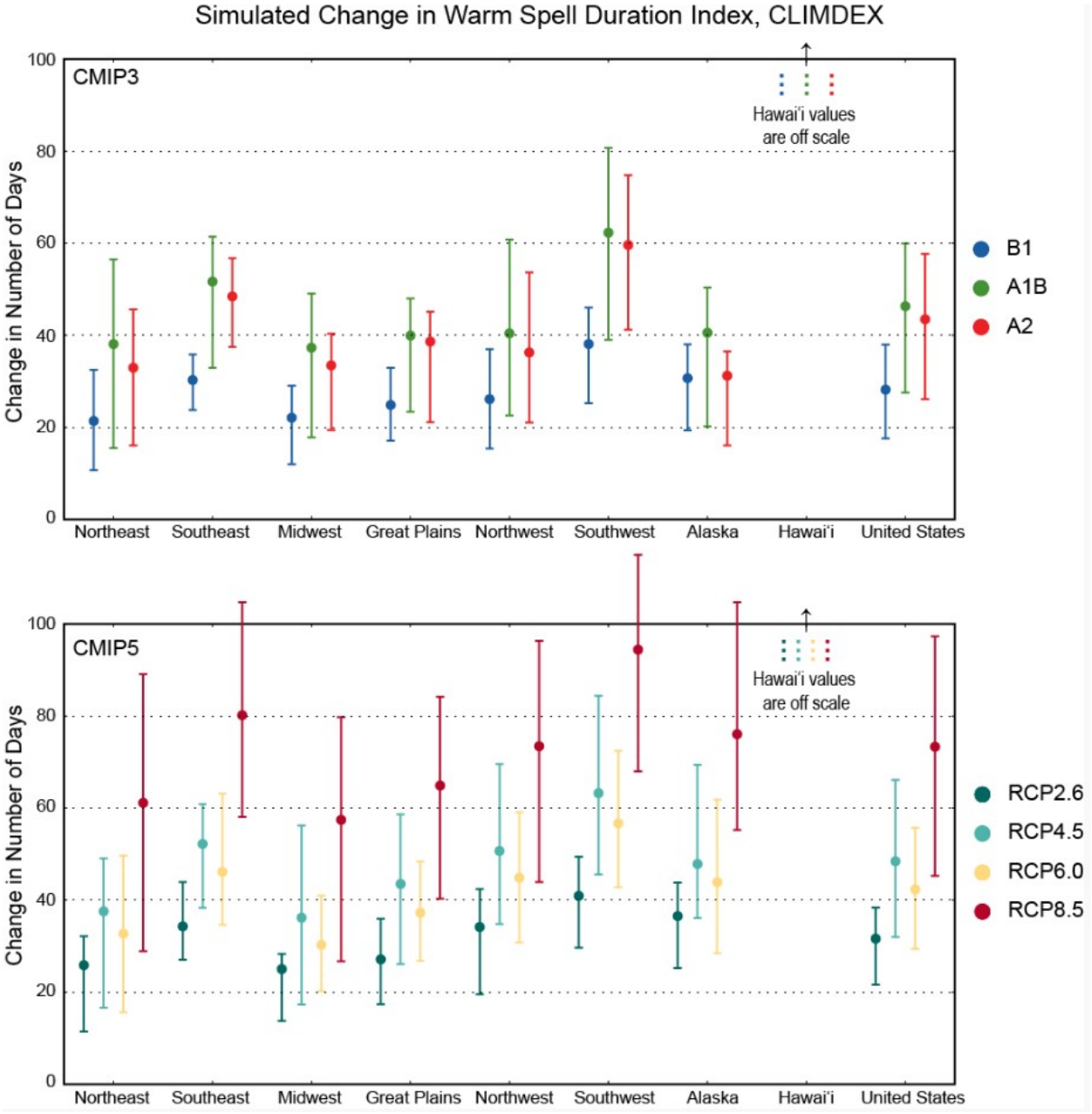

Figure 10-6. Simulated change in warm spell duration index (WSDI) for each region and the contiguous United States, for 2046–2065 with respect to the reference period of 1981–2000. The upper panel shows values for the CLIMDEX SRES B1 (blue), A1B (green), and A2 (red) scenarios. The lower panel shows values for the CLIMDEX RCP2.6 (dark teal), 4.5 (light teal), 6.0 (yellow), and 8.5 (dark red) scenarios. Bars indicate the interquartile ranges of model values and circles depict the multi-model means. Note: values for Hawai'i lie off the scale, with multi-model means ranging from 184.4 days for the RCP2.6 scenario, to 271.3 days for RCP8.5 (Figure source: Sun et al. 2015).

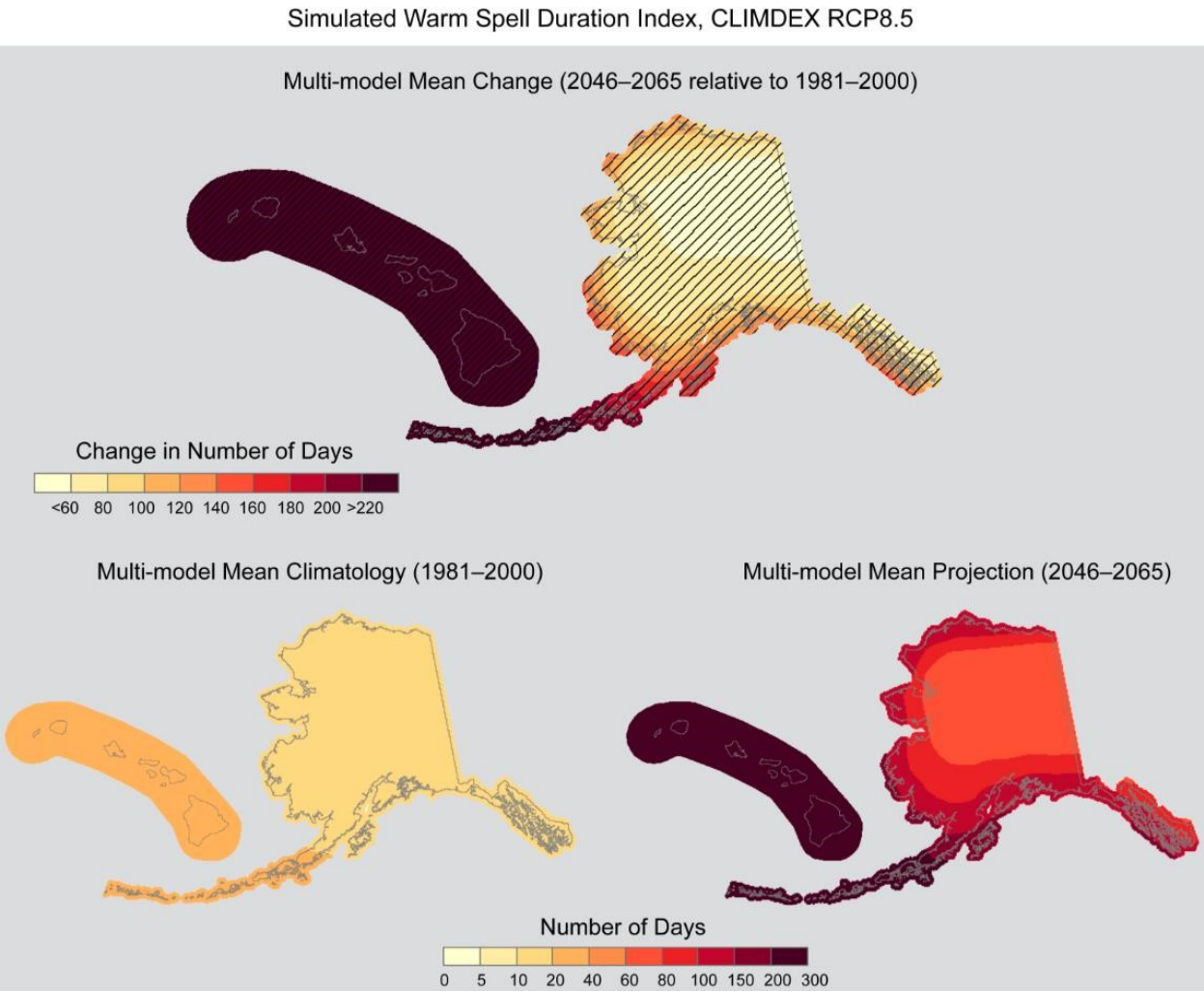

Figure 10-7. Simulated multi-model mean change in warm spell duration index (WSDI) for Alaska and Hawai'i, for 2046–2065 with respect to the reference period of 1981–2000, using the CLIMDEX RCP8.5 scenario (top). Color with hatching (category 3) indicates that more than 50% of the models show a statistically significant change, and more than 67% agree on the sign of the change. Multi-model mean climatology indicating the WSDI for 1981–2000 (bottom left). Multi-model mean projection indicating the WSDI for 2046–2065 (bottom right) (Figure source: Sun et al. 2015).

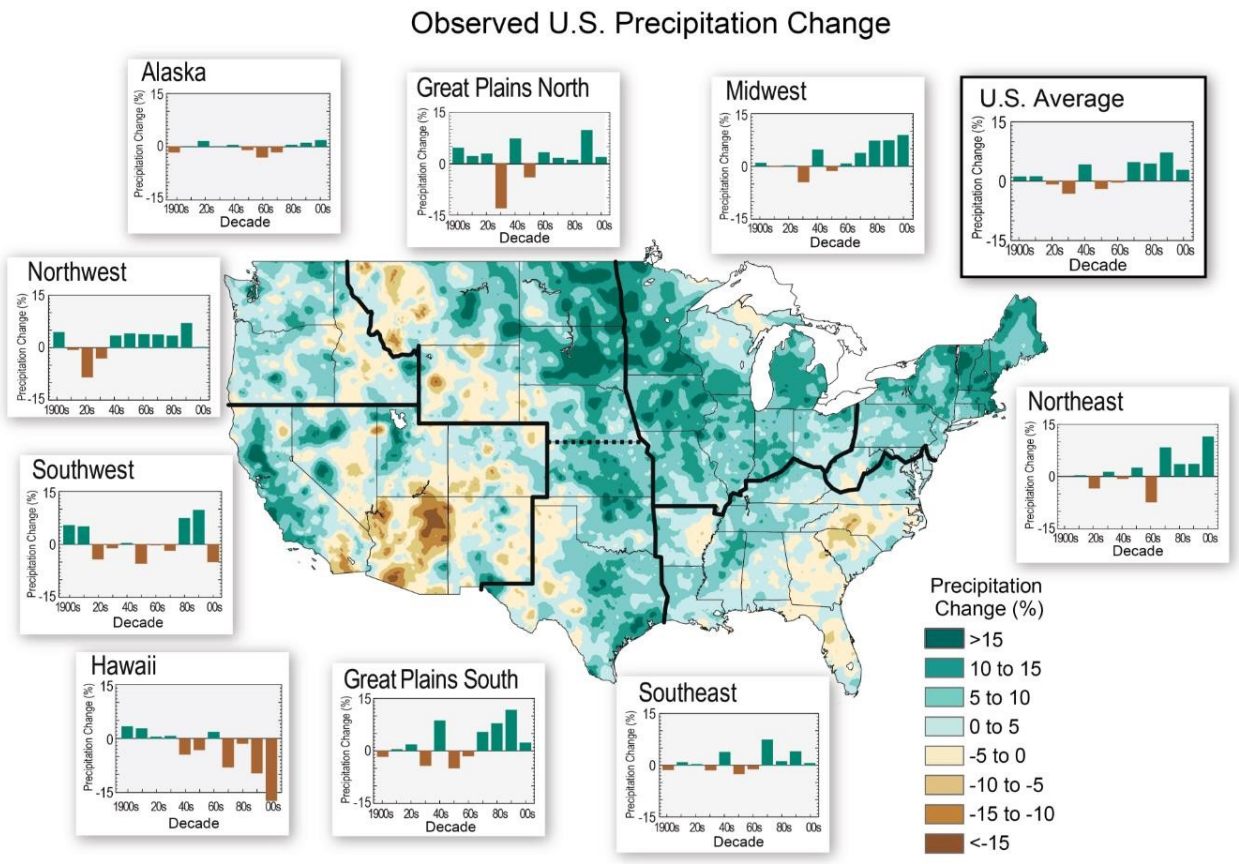

Figure 10-8. The colors on the map show annual total precipitation changes for 1991-2012 compared to the 1901-1960 average and show wetter conditions in most areas. The bars on the graphs show average precipitation differences by decade for 1901-2012 (relative to the 1901-1960 average) for each region. The far-right bar in each graph is for 2001-2012 (Figure source: Melillo et al. 2014 p. 32).

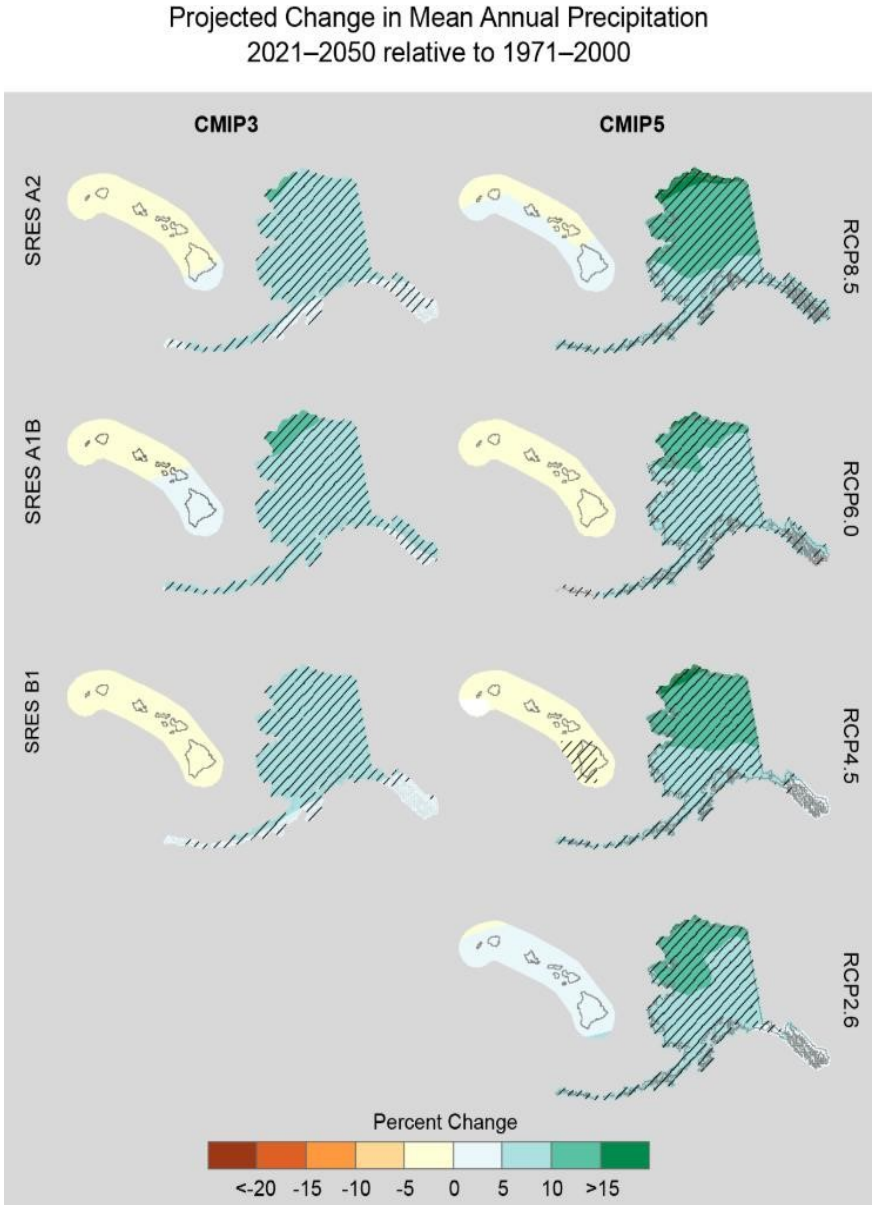

Figure 10-9. Projected change in mean annual precipitation (%) for Alaska and Hawai'i, for 2021–2050 with respect to the reference period of 1971–2000. These are multi-model means using CMIP3 SRES A2, A1B, and B1 scenarios (left column), and CMIP5 RCP8.5, 6.0, 4.5, and 2.6 scenarios (right column). Color only (category 1) indicates that less than 50% of the models show a statistically significant change. Whited out areas (category 2) indicate that more than 50% of the models show a statistically significant change, but less than 67% agree of the sign of the change. Color with hatching (category 3) indicates that more than 50% of the models show a statistically significant change, and more than 67% agree on the sign of the change (Figure source: Sun et al. 2015).

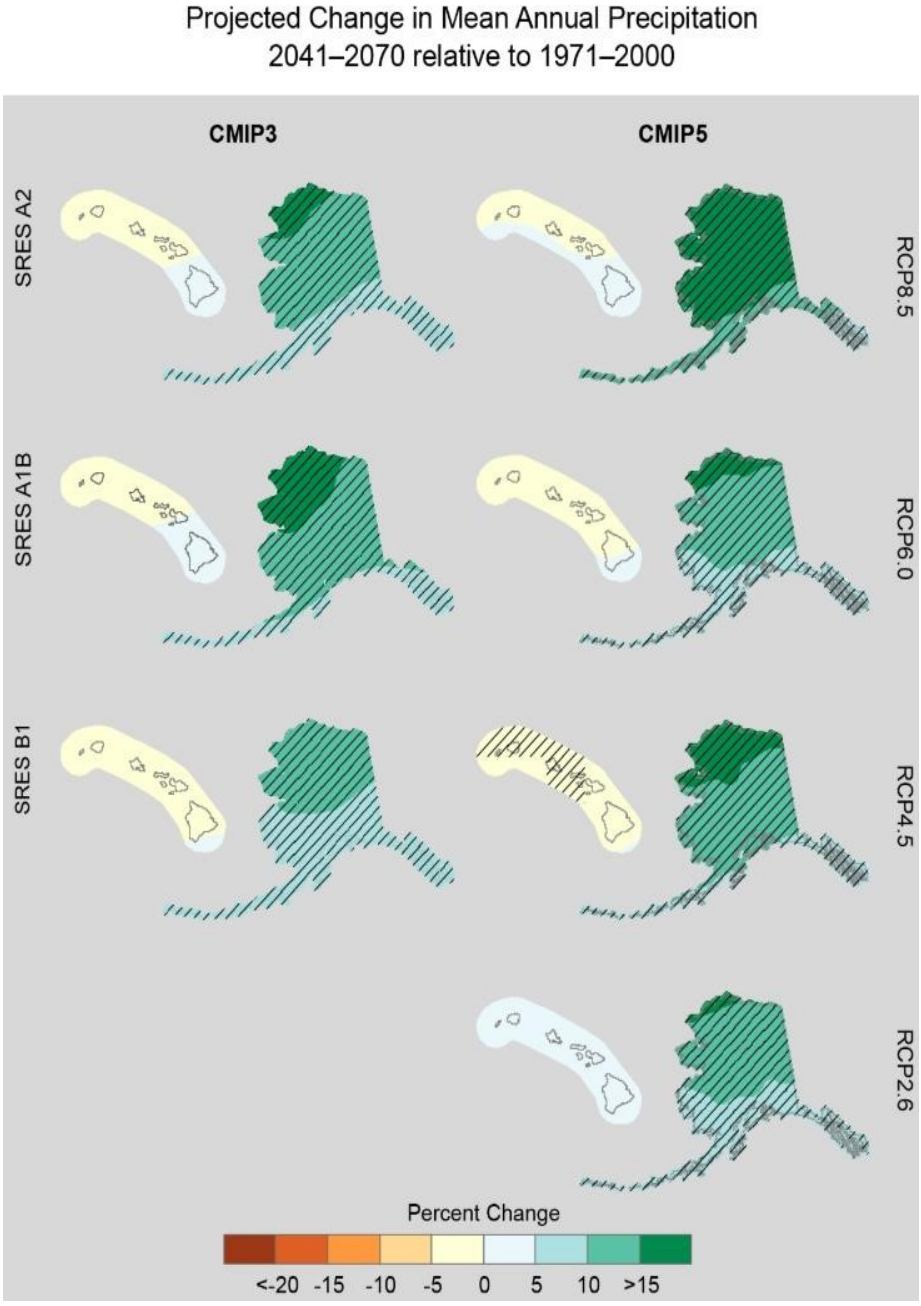

Figure 10-10. Projected change in mean annual precipitation (%) for Alaska and Hawai'i, for 2041–2070 with respect to the reference period of 1971–2000. These are multi-model means using CMIP3 SRES A2, A1B, and B1 scenarios (left column), and CMIP5 RCP8.5, 6.0, 4.5, and 2.6 scenarios (right column). Color only (category 1) indicates that less than 50% of the models show a statistically significant change. Color with hatching (category 3) indicates that more than 50% of the models show a statistically significant change, and more than 67% agree on the sign of the change (Figure source: Sun et al. 2015).

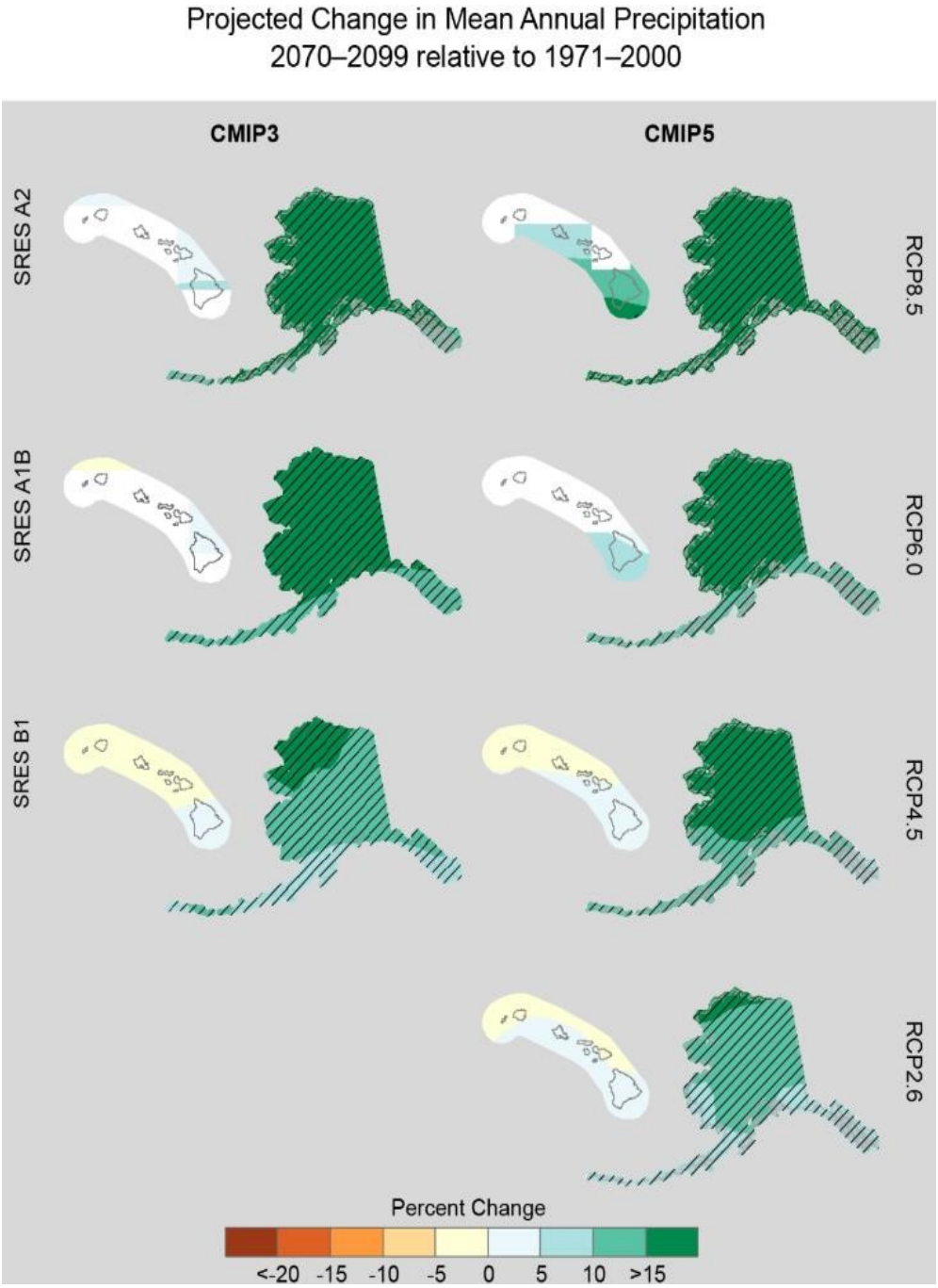

Figure 10-11. Projected change in mean annual precipitation (%) for Alaska and Hawai'i, for 2070–2099 with respect to the reference period of 1971–2000. These are multi-model means using CMIP3 SRES A2, A1B, and B1 scenarios (left column), and CMIP5 RCP8.5, 6.0, 4.5, and 2.6 scenarios (right column). Color only (category 1) indicates that less than 50% of the models show a statistically significant change. Whited out areas (category 2) indicate that more than 50% of the models show a statistically significant change, but less than 67% agree of the sign of the change. Color with hatching (category 3) indicates that more than 50% of the models show a statistically significant change, and more than 67% agree on the sign of the change (Figure source: Sun et al. 2015).

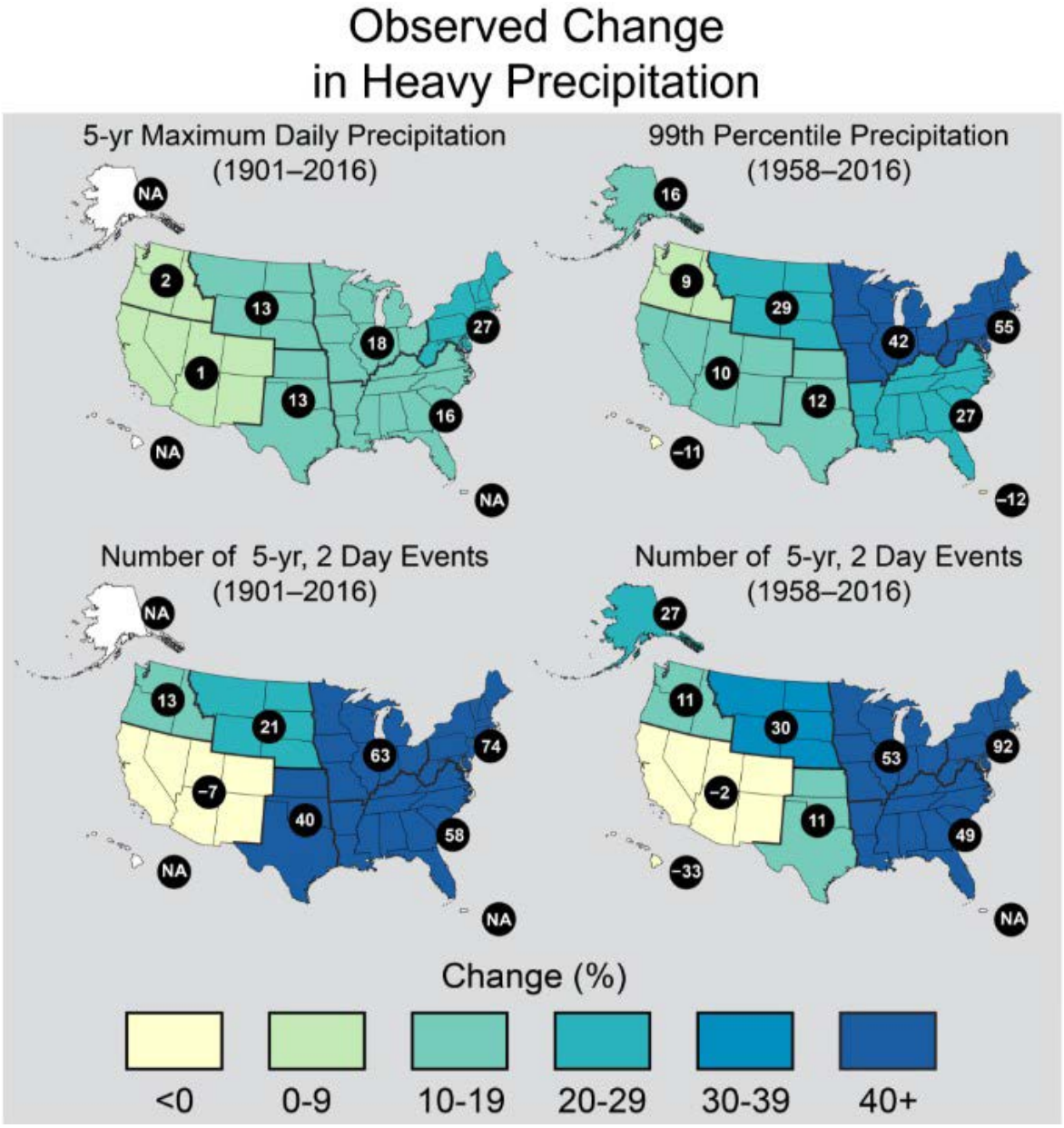

Figure 10-12. Changes in extreme precipitation. The percent change in maximum daily precipitation by 5-year periods (upper left), the percent change in the amount of precipitation falling in daily events that exceed the 99th percentile of precipitation days (upper right), the percent change in number of two-day events with a precipitation total exceeding the largest two-day amount that would be expected to occur only once every five years based on data from 1901–2016 (lower left), and the percent change in number of two-day events with a precipitation total exceeding the largest two-day amount that would be expected to occur only once every five years based on data from 1958–2016 (lower right) (Figure source: USGCRP 2017 p. 212).

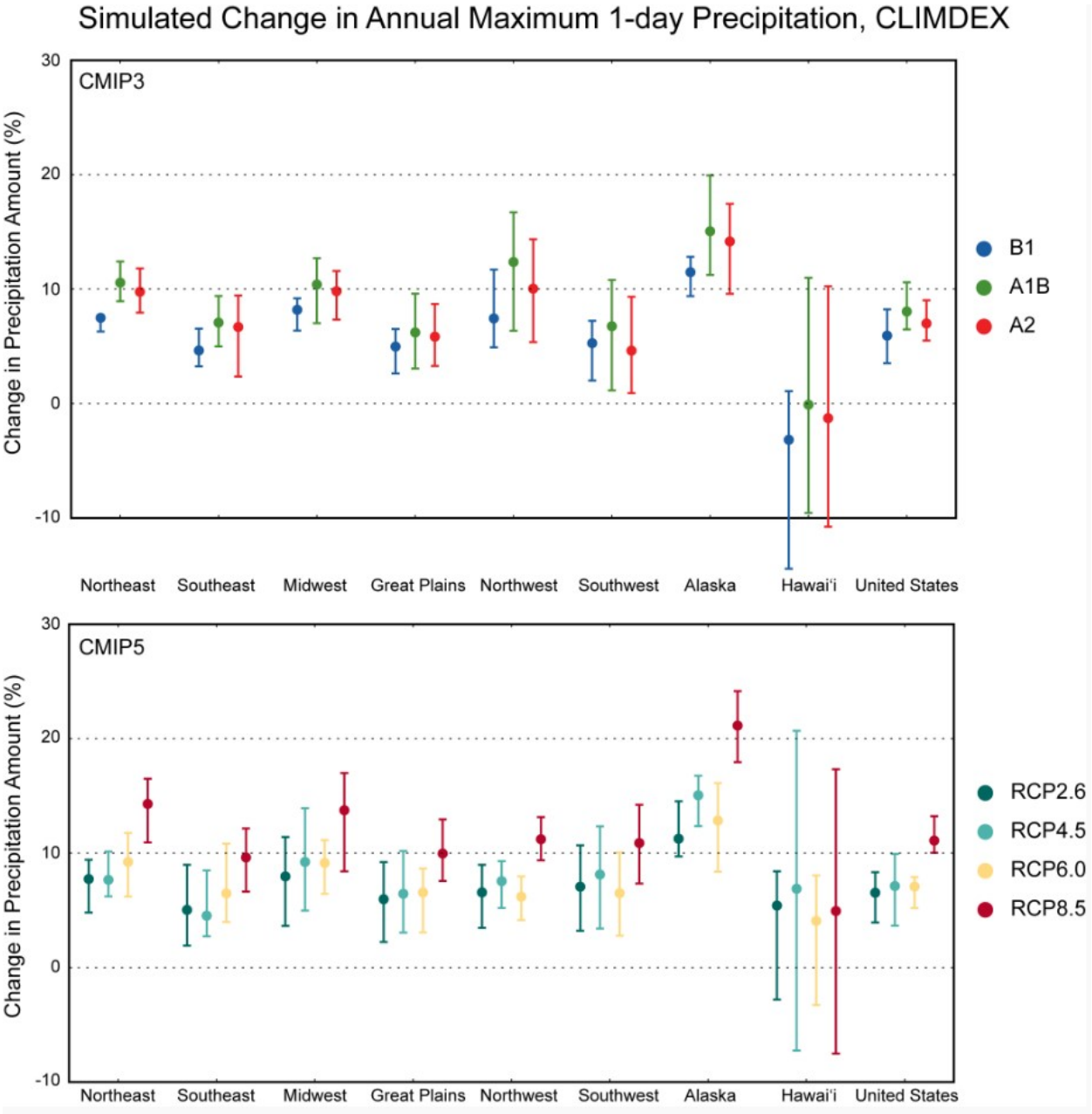

Figure 10-13. Simulated change in annual maximum 1-day precipitation (Rx1day) for each region and the contiguous United States, for 2046–2065 with respect to the reference period of 1981–2000. The upper panel shows values for the CLIMDEX SRES B1 (blue), A1B (green), and A2 (red) scenarios. The lower panel shows values for the CLIMDEX RCP2.6 (dark teal), 4.5 (light teal), 6.0 (yellow), and 8.5 (dark red) scenarios. Bars indicate the interquartile ranges of model values and circles depict the multi-model means (Figure source: Sun et al. 2015).

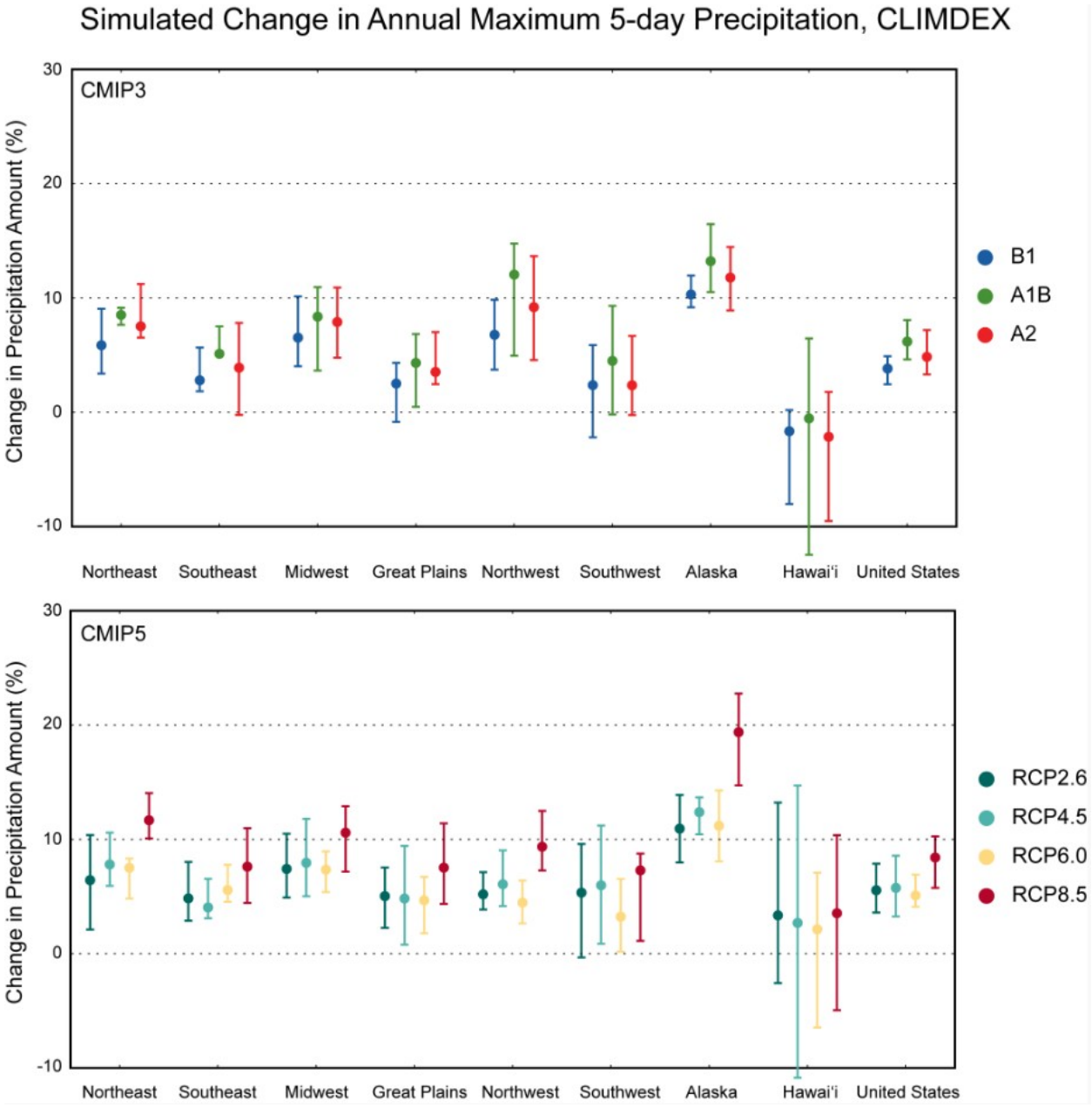

Figure 10-14. Simulated change in annual maximum 5-day precipitation (Rx5day) for each region and the contiguous United States, for 2046–2065 with respect to the reference period of 1981–2000. The upper panel shows values for the CLIMDEX SRES B1 (blue), A1B (green), and A2 (red) scenarios. The lower panel shows values for the CLIMDEX RCP2.6 (dark teal), 4.5 (light teal), 6.0 (yellow), and 8.5 (dark red) scenarios. Bars indicate the interquartile ranges of model values and circles depict the multi-model means (Figure source: Sun et al. 2015).

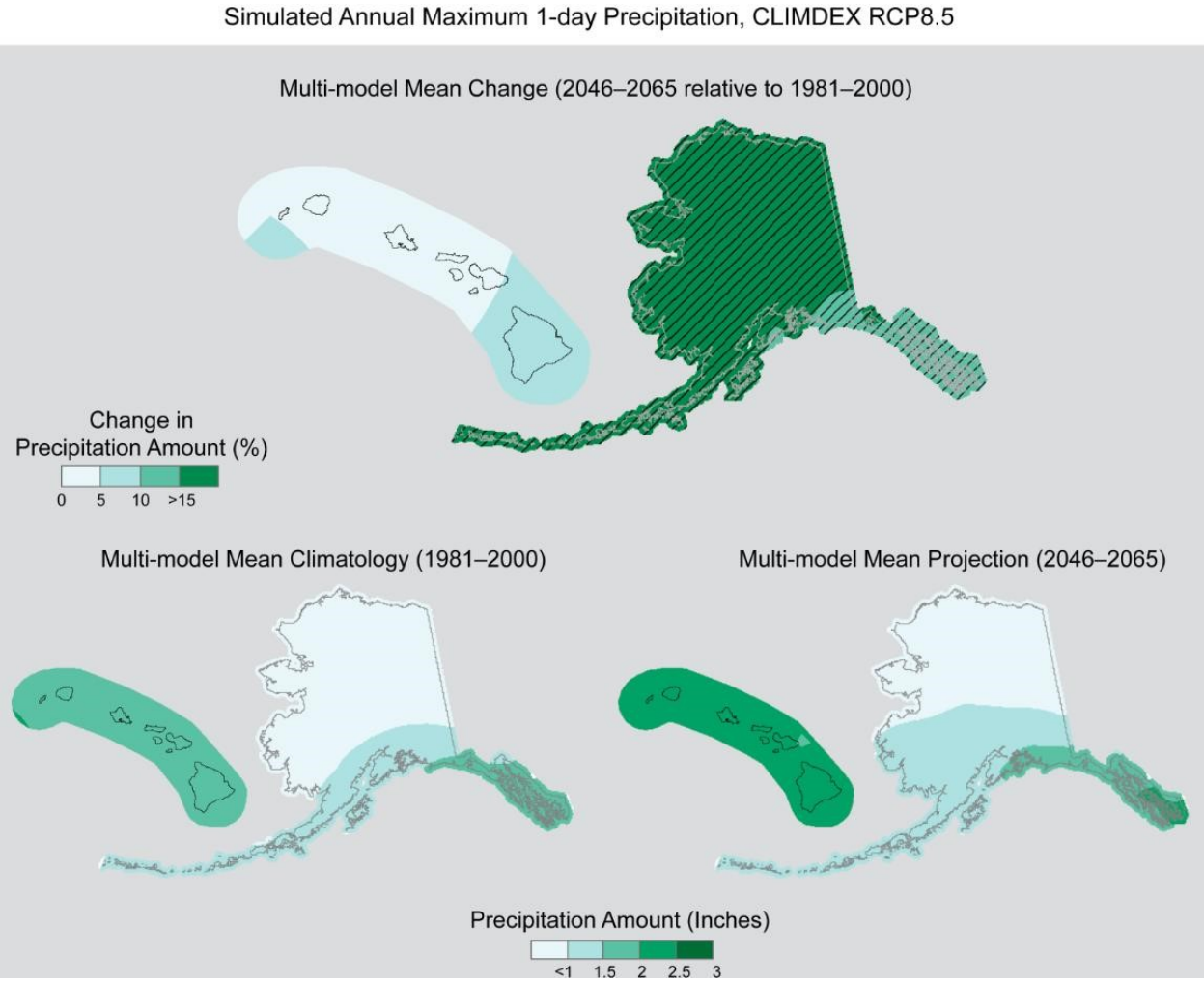

Figure 10-15. Simulated multi-model mean change in annual maximum 1-day precipitation (Rx1day) for Alaska and Hawai'i, for 2046–2065 with respect to the reference period of 1981–2000, using the CLIMDEX RCP8.5 scenario (top). Color only (category 1) indicates that less than 50% of the models show a statistically significant change. Color with hatching (category 3) indicates that more than 50% of the models show a statistically significant change, and more than 67% agree on the sign of the change. Multi-model mean climatology indicating the Rx1day for 1981–2000 is shown bottom left. Multi-model mean projection indicating the Rx1day for 2046–2065 is shown bottom right (Figure source: Sun et al. 2015).

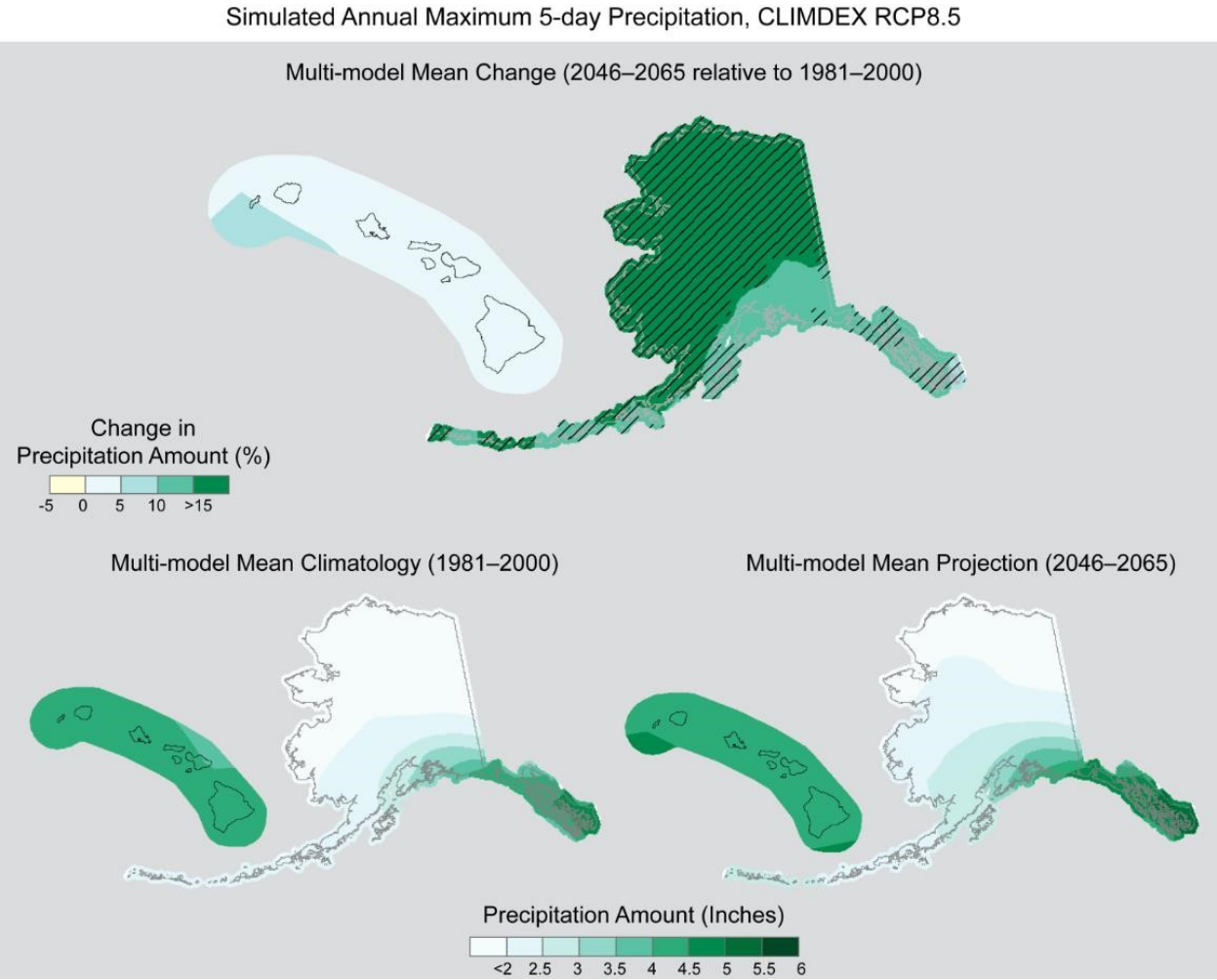

Figure 10-16. Simulated multi-model mean change in annual maximum 5-day precipitation (Rx5day) for Alaska and Hawai'i, for 2046–2065 with respect to the reference period of 1971–2000, using the CLIMDEX RCP8.5 scenario (top). Color only (category 1) indicates that less than 50% of the models show a statistically significant change. Color with hatching (category 3) indicates that more than 50% of the models show a statistically significant change, and more than 67% agree on the sign of the change. Multi-model mean climatology indicating the Rx5day for 1981–2000 is shown bottom left. Multi-model mean projection indicating the Rx5day for 2046–2065 is shown bottom right (Figure source: Sun et al. 2015).

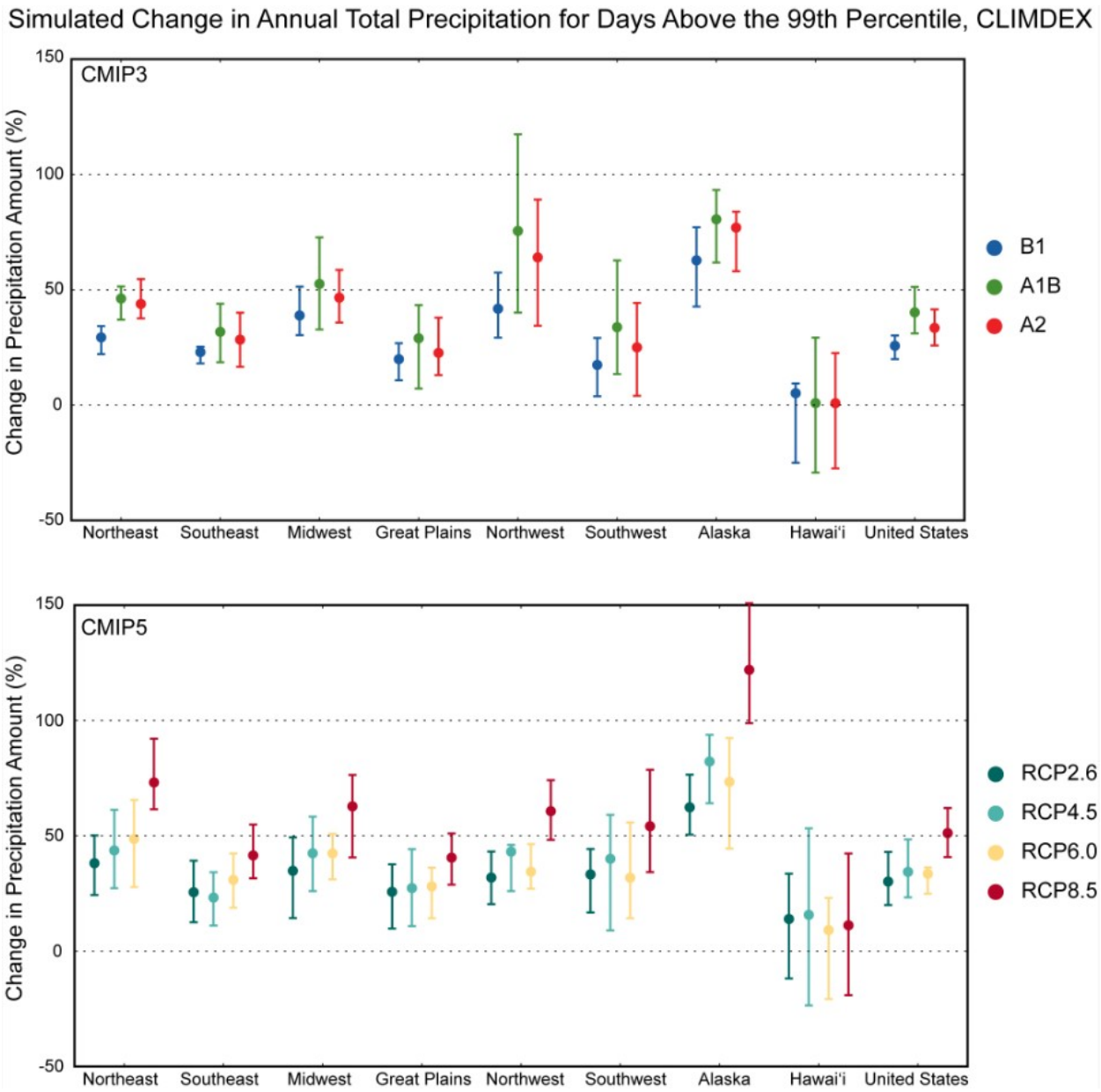

Figure 10-17. Simulated change in annual total precipitation for days above the 99th percentile (R99pTOT) for each region and the contiguous United State, for 2046–2065 with respect to the reference period of 1981–2000. The upper panel shows values for the CLIMDEX SRES B1 (blue), A1B (green), and A2 (red) scenarios. The lower panel shows values for the CLIMDEX RCP2.6 (dark teal), 4.5 (light teal), 6.0 (yellow), and 8.5 (dark red) scenarios. Bars indicate the interquartile ranges of model values and circles depict the multi-model means (Figure source: Sun et al. 2015).

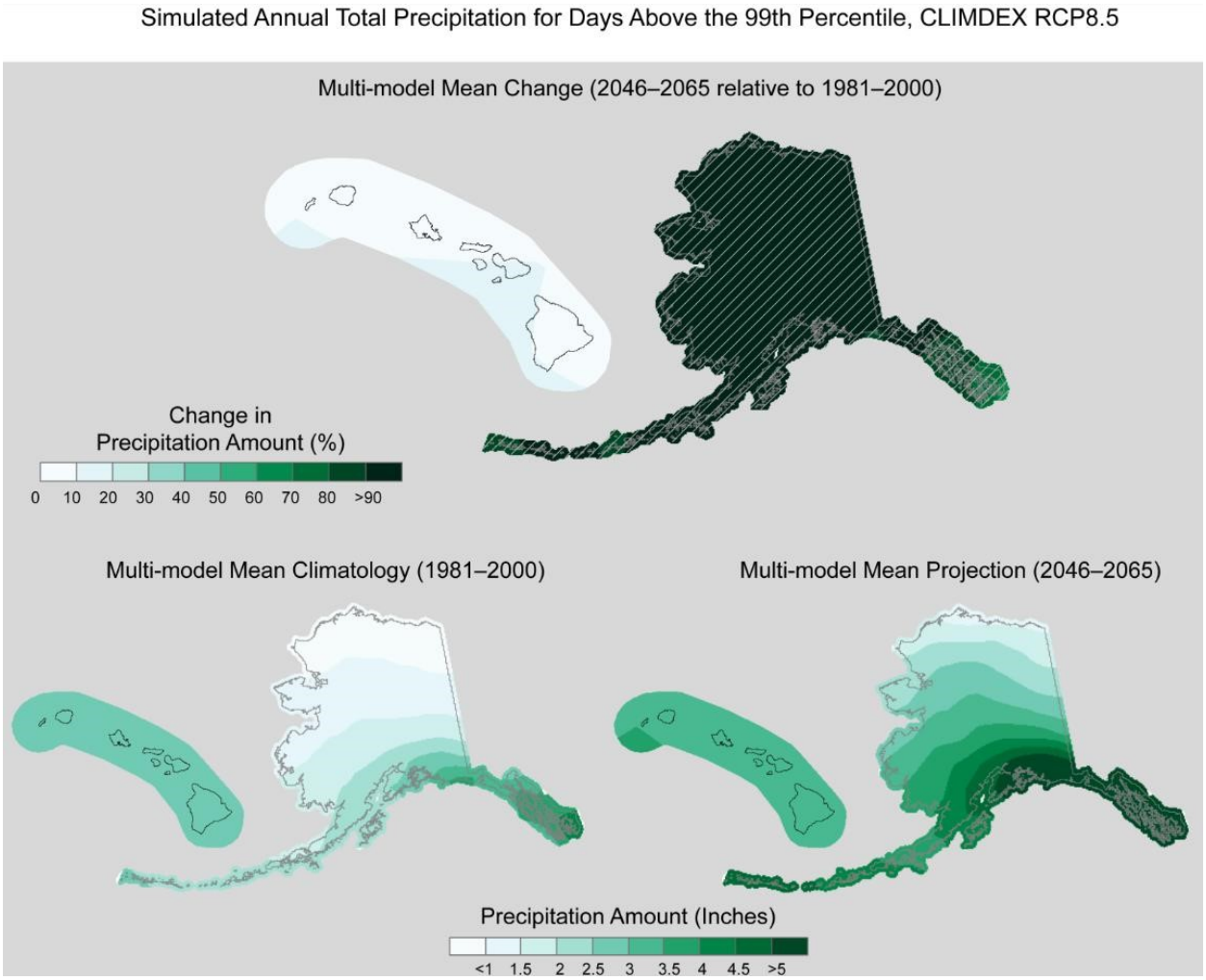

Figure 10-18. Simulated multi-model mean change in annual total precipitation for days above the 99th percentile (R99pTOT) for Alaska and Hawai‘i, for 2046–2065 with respect to the reference period of 1981–2000, using the CLIMDEX RCP8.5 scenario (top). Color only (category 1) indicates that less than 50% of the models show a statistically significant change. Color with hatching (category 3) indicates that more than 50% of the models show a statistically significant change, and more than 67% agree on the sign of the change. Multi-model mean climatology indicating the R99pTOT for 1981–2000 is shown bottom left. Multi-model mean projection indicating the R99pTOT for 2046–2065 is shown bottom right (Figure source: Sun et al. 2015).

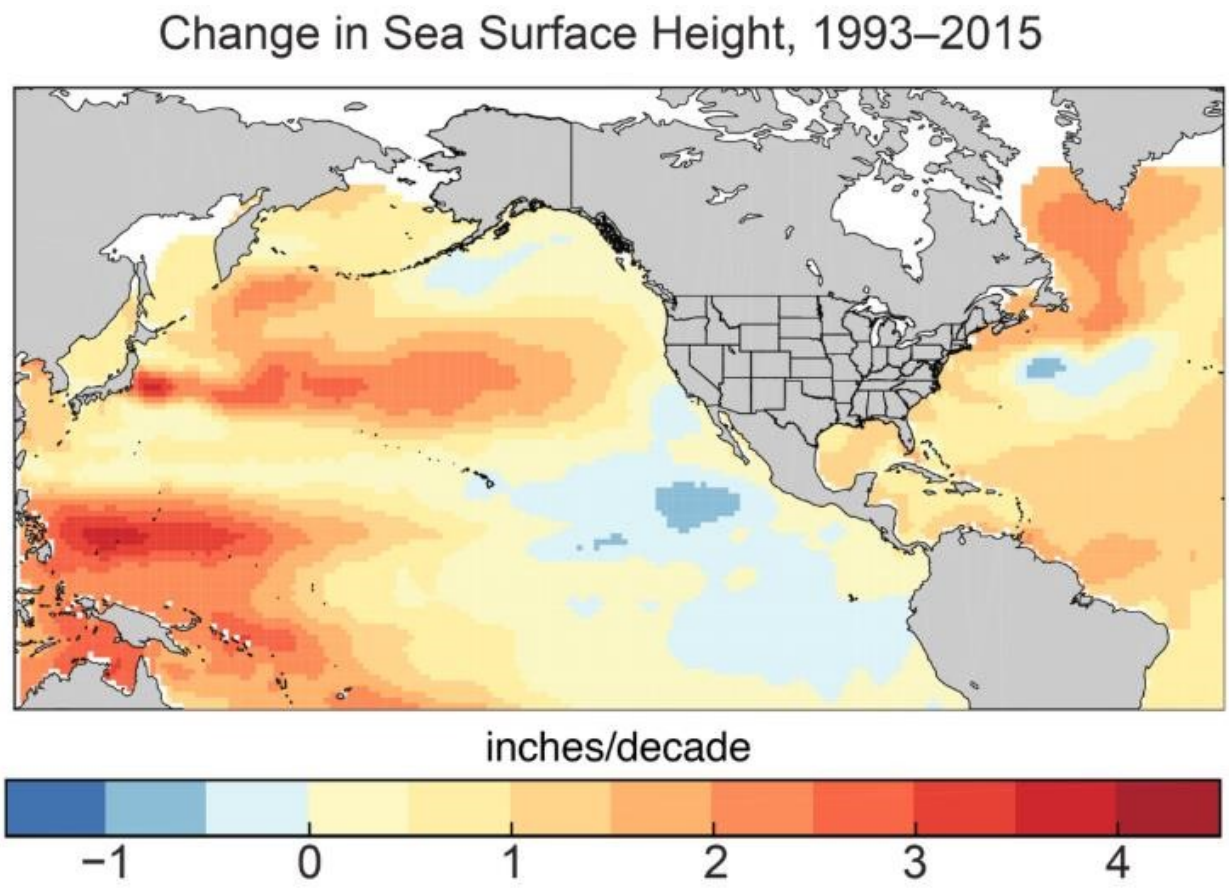

Figure 10-19. Rates of change from 1993 to 2015 in sea surface height from satellite altimetry data; updated from Kopp et al. using data updated from Church and White (Figure source: USGCRP 2017 p. 340).

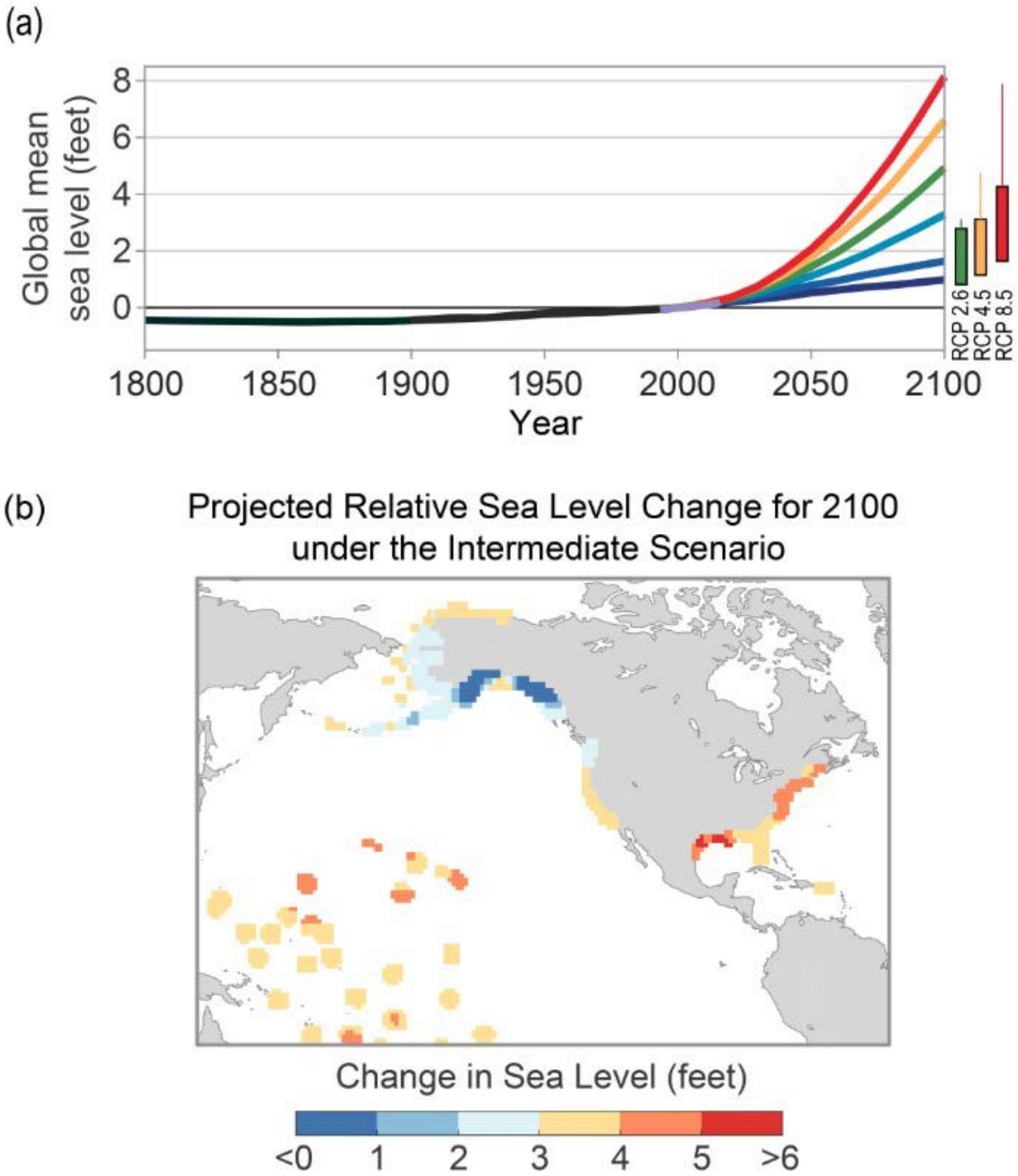

Figure 10-20. (a) Global mean sea level (GMSL) rise from 1800 to 2100, based on Figure 12.2b from 1800 to 2015, the six Interagency GMSL scenarios (navy blue, royal blue, cyan, green, orange, and red curves), the very likely ranges in 2100 for different RCPs (colored boxes), and lines augmenting the very likely ranges by the difference between the median Antarctic contribution of Kopp et al. and the various median Antarctic projections of DeConto and Pollard. (b) Relative sea level (RSL) rise (feet) in 2100 projected for the Interagency Intermediate Scenario (1-meter [3.3 feet] GMSL rise by 2100) (Figure source: USGCRP 2017 p. 342).

11 Other Stressors

11.1 Summary of Climate Projections for Other Stressors

11.1.1 Increase in Average Wind Speed

There is relatively good agreement across several General Circulation Models (GCMs) that average wind speed will increase across portions of the Southern Great Plains region. The majority of models in the CMIP5 ensemble suggest wind speed increases across parts of Kansas, the majority of Oklahoma, and across much of Texas (Figure 11-1). Model confidence is greatest along and south of the I-10 corridor from west of San Antonio to Houston. In this region, average annual wind speed is expected to increase as much as 0.25 meters/second (0.55 mi/hr, .49 knots). While these numbers are small, since they are an annual average this represents a relatively large shift in the wind regime. Coupled with the finding below that suggests a decrease in high wind days, this could indicate that wind speeds could be considerably higher than models indicate on days with high winds.

In all other regions, models generally suggest no increase in wind speed or are less consistent in their suggestions (i.e. fewer models within the ensemble suggest increases.).

11.1.2 Decrease in Average Wind Speed

As mentioned above, models suggest decreases in wind speed across much of the U.S. except the Southern Great Plains. Models are most consistent in suggesting these decreases across the Northern Great Plains, northern portions of the Southwest region (Utah, Colorado, Nevada), and across the Northwest region.

11.1.3 Increase in Number of Days with High Winds not Associated with Thunderstorms
Decrease in Number of Days with High Winds not Associated with Thunderstorms

Very little work has been done to explore the possible change in high wind days in the future. Global analysis of historical wind speeds in the 20th century (1901–2000) suggest a decrease in the number of high wind days (McVicar et al. 2012). A number of possible reasons for this have been suggested, including increasing land surface roughness due to increased vegetation cover globally; circulation changes related to the strength of El Niño/Southern Oscillation (ENSO); movement of large storms towards polar latitudes; expansion of the equatorial circulation regime (Hadley cell); and temperature increases in polar regions relative to tropical regions, resulting in a smaller temperature contrast between these regions and a reduction in winds. There is no obvious indication that the trend in high wind days would reverse in the future. In fact, this trend could accelerate in a warming world.

11.1.4 Increase in Humidity (Dewpoint)
Decrease in Humidity (Dewpoint)

Overall, it is very likely that average temperature will increase across the U.S. in the future. Warmer air has a greater capacity to "hold" water vapor than colder air (Figure 11-2). Given this, it is more likely than not that atmospheric moisture, as measured by the dewpoint temperature

will increase across most seasons and locations. There is little evidence to suggest that atmospheric moisture will decrease in the future.

11.1.5 Increase in Number of Days with Thunderstorms/Lightning
Decrease in Number of Days with Thunderstorms/Lightning
Increase in Occurrence of Severe Thunderstorms
Decrease in Occurrence of Severe Thunderstorms
Increase in Occurrence of Tornadoes
Decrease in Occurrence of Tornadoes

Changes in thunderstorms, severe thunderstorms (defined as those which produce hail greater than 1 inch or winds of 50 kts. or greater), and tornadoes are all related. Thunderstorms and tornadoes occur on relatively small scales (on the order of tens of miles) while GCMs operate at a relatively coarse resolution (hundreds of miles). Because of this, GCMs cannot directly simulate the occurrence of thunderstorms, severe thunderstorms or tornadoes in the future. However, we can examine the environmental conditions that lead to the formation of these storms in the past and see how these environments might change in the future.

The formation of a thunderstorm requires several ingredients. In general, air must be moved vertically (lift) with enough moisture for the formation of clouds and precipitation, and the air must be buoyant enough to continue rising after the initial lifting (instability). Each of these is expected to change under future climates. The ability of the atmosphere to hold moisture is dependent on temperature, and atmospheric moisture is expected to increase in the future as the climate warms. Because of the increase in temperatures and moisture, instability is also expected to increase (Brooks 2013; Trapp et al. 2007). These factors would suggest an increase in thunderstorm activity. The biggest question pertains to possible changes in lift, and no studies have systematically explored any possible changes in lift. Given this, it seems more likely than not that more thunderstorms will occur in the future, with considerable uncertainty given the possible change in lift.

The formation of severe thunderstorms and tornadoes require another ingredient beyond those mentioned above. Wind shear (a change in wind direction or speed vertically through the atmosphere) is required for severe thunderstorm formation. Studies indicate that wind shear will likely decrease in the future (Brooks 2013; Trapp et al. 2007). It is unknown if the increases in instability will offset the decreases in shear to produce more severe thunderstorms, or if the decrease in shear will lead to a decrease in severe thunderstorms. It is also possible that the decrease in wind shear will result in more thunderstorms with high winds and fewer thunderstorms that produce tornadoes. Overall, the frequency of environments favorable for thunderstorms and severe weather is projected to increase in all seasons, with the largest increases in the early spring (March and April).

11.1.6 Increase of Occurrence of Vector-Borne Disease

The 3rd National Climate Assessment states “Climate change is causing large-scale changes in the environment, increasing the likelihood of the emergence or reemergence of unfamiliar disease threats. Factors include shifting ranges of disease-carrying pests, lack of immunity and preparedness, inadequate disease monitoring, and increasing global travel” (Luber et al. 2014). However, the report notes that disease transmission is sensitive to small-scale changes in weather, human modifications of a particular area, animal hosts for disease in a region, and

human behavior. (Luber et al. 2014). As pathogens expand their geographic ranges in a warming world, it is fairly likely that increased numbers of non-immune people will be exposed.

11.1.7 Decrease in Water Quality

A number of decreases in water quality have already been noted across the U.S. (Georgakakos et al. 2014). Increased air temperatures have led to warming of waters, especially in lakes. This reduces mixing of waters, resulting in lower oxygen content in bottom waters along with the elimination of cold-water zones at the bottom of lakes. Models predict that continued warming will have negative effects on lake water quality and ecosystem health. In addition, major precipitation events increase runoff from land, increasing the amount of pollutants and sediment transported into larger bodies of water. Model projections suggest that the amount of sediment transported by rivers could increase anywhere from 25% to 55%. Major uncertainties exist in these projections and relate to the impact of future precipitation distributions, which may exhibit more extremes (increases in both dry spells and heavy rainfall events).

11.2 Tables and Figures: Other Stressors

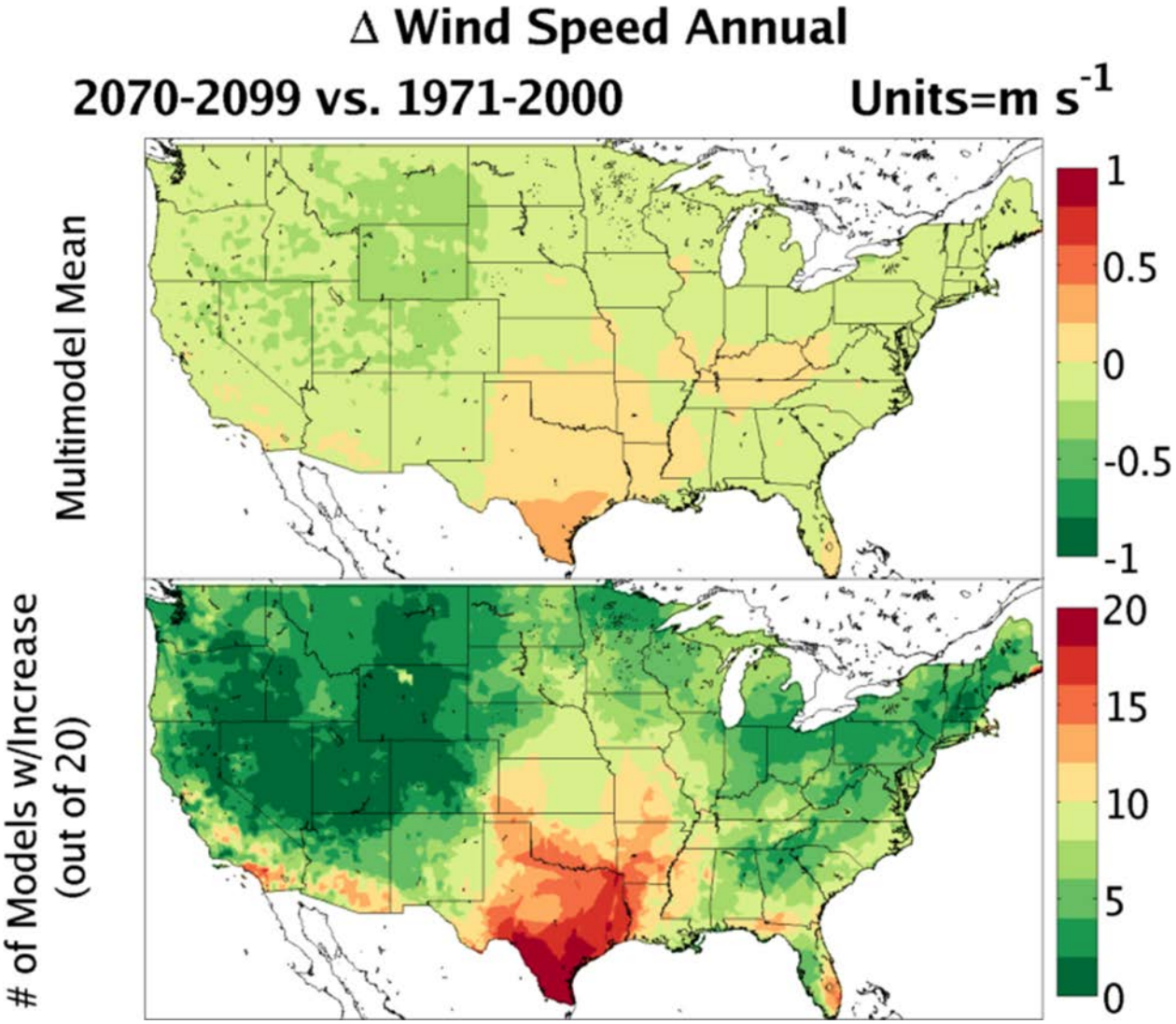

Figure 11-1. Top panel: Projected change in annual average wind speed in meters per second for the end of century period (2070–2099) as compared to the 1971–2000 reference period based on a 20 model ensemble. Increases are depicted in yellow/orange/red while decreases are depicted in green. Bottom panel: Model agreement on the prediction of wind speed increases depicted in the top panel. Warm colors (yellow/orange/red) indicate more of the models in the ensemble predicted an increase in wind speeds. Note the near unanimous model agreement in wind speed increase depicted across south Texas, while areas where wind speeds decreases are projected in the top panel (for example, Wyoming) have no models indicating an increase in the bottom panel (Figure source: Sweet et al. 2017).

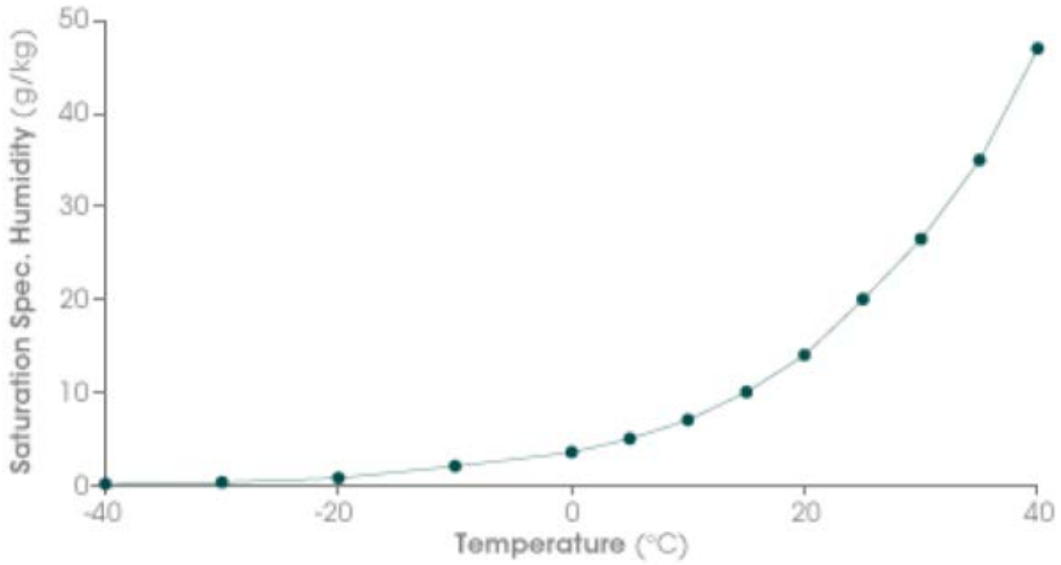

Figure 11-2. The relationship between temperature and atmospheric moisture. As temperature increases (x-axis), moisture capacity of the air increases as measured by the specific humidity (grams of water vapor per kilogram of air, y-axis) (Figure source: Sweet et al. 2017).

12 Coastal Regions

12.1 Summary of Climate Projections for Coastal Regions

12.1.1 Intensity of Hurricanes

Theoretical and numerical modeling indicate an increase in tropical cyclone intensity in a warmer global system. Globally averaged intensity is expected to increase 2–11% by 2100. Moreover, the number of intense or major tropical cyclones (Saffir-Simpson Category 4-5) is expected to modestly increase due to increases in available energy (Figure 12-1). Warmer ocean and air temperatures could create larger imbalances in mass which require a redistribution or balancing of energy. The IPCC AR5 for the late 21st century concluded a slight increase in average tropical cyclone intensity, precipitation rate (precipitation rates near storm center are expected to increase by 20%), and a decrease or little change in the global frequency. However, some models (post-IPCC AR5) indicate warming-induced intensification may not be as prevalent in the future, reducing confidence in the overall increase in intensity. Nonetheless, model projections for the North Atlantic are in agreement that intensities and precipitation rates will increase this century. There is an overall medium confidence that North Atlantic hurricanes will increase in intensity.

Global scale climate models have projected an increase in the potential intensity of tropical cyclones with anthropogenic global warming, forecasting that future storm intensity should increase (Emanuel 1987). Some studies suggest that warming sea surface temperatures (SSTs) have already caused an increase in the intensity of tropical cyclones (Elsner et al. 2008), while other studies focus on future projections. For example, as discussed above, Knutson et al. (2010) project a 2–11% increase in the average intensity of future tropical cyclones. Another example can be seen in Emanuel (2005) that found a relationship between the potential destructiveness of tropical cyclones and SSTs, proposing that future warming will result in stronger storms. Major tropical cyclones have also been investigated to determine if they may become stronger and more devastating. Kang and Elsner (2016) found that the strongest 10% of tropical cyclones are directly related to warming SSTs and suggest that stronger storm may get stronger and lead to a suppression in weaker tropical storms. This finding is in agreement with Bender et al. (2010) (and many others) in that stronger tropical cyclones will become more frequent at the expense of weaker storms. In fact, it has been suggested that a tradeoff exists between intensity and frequency of tropical cyclones. Kang and Elsner (2015) proposed that the global average intensity of tropical cyclones would increase while the frequency of weaker tropical cyclones would decrease. Additional consideration must also be given to upper-level wind shear, a factor that can determine if tropical cyclone formation will occur. It is projected that upper-level wind shear will increase in the future for the Northern Atlantic (Arpe and Leroy 2009), counteracting the influence of a warming ocean, and possibly limiting the strength of future tropical cyclones. A final consideration should be given to the effects of continental aerosols. These aerosols, which work to decrease the strength of tropical cyclones by causing premature convection that makes dissipation more likely prior to landfall (Khain et al. 2010), are projected to increase due to anthropogenic inputs. However, SSTs are projected to increase, and that single variable alone is believed to be the main ingredient in strengthening future tropical cyclones.

12.1.2 Frequency of Hurricanes

There is low confidence in long-term changes in tropical cyclone frequency. Historical data are highly heterogeneous and do not allow for unbiased analysis. This does not mean that increases or decreases have not occurred; rather, detectable trends cannot be given separated from natural variability. However, there is confidence that tropical cyclones are migrating poleward in the Northern Hemisphere. This is likely due to favorable conditions (warm sea surface temperatures, decreasing shear, increased spin (Coriolis)) moving poleward. Therefore, it is possible coastal locations in the Northeast could experience an increase in the frequency of tropical cyclones. However, some models suggest that track changes could dampen the effect in the U.S. Mid-Atlantic and Northeast, conflicting with theoretical evidence.

In the Atlantic, variability in tropical cyclones has been attributed to both natural (changes in overturning circulations, Atlantic Multi-Decadal Oscillation, ENSO, Saharan dust, etc.) and anthropogenic factors. However, there is confidence that the observed slight uptick in tropical cyclones since the 1970s is related to anthropogenic activities (mainly driven by increased sea surface temperatures).

Globally averaged, it is expected that tropical cyclones will decrease by 6-34% by 2100. However, there is low confidence in a change of storm track. Research has highlighted tracks of storms impacting Hawaii and suggest the state may be impacted by tropical cyclones more frequently in the future, but confidence is low.

Determining if frequency trends in tropical cyclone formation are natural variation or related to human activity is difficult. Ten of the twenty most active tropical cyclone seasons (seasons with the most named storms, 1851–2015) have occurred since 2000 (National Hurricane Center 2016). However, recent studies have shown a decrease in the number of intense tropical cyclones (at least 50 ms^{-1} sustained winds) in the last few decades in the North Atlantic (Landsea et al. 1996). Other studies have found increases in the frequency of tropical cyclones in other water bodies, such as the western North Pacific (Chan and Shi 1996). Countless other studies have continued to find conflicting results, leading some researchers to question tropical cyclone frequency trends due to their large annual variability paired with fluctuations in large-scale climate oscillations (Knutson et al. 2010; Emanuel 2005). It has been shown that large-scale climate oscillations influence the frequency of tropical cyclones annually (Gray 1984; Pielke and Landsea 1999; Trenberth 2007; Kim et al. 2011); however, any change (even small) in ocean temperature can influence long-term tropical cyclone frequency (Trenberth 2007). This theoretical framework (warming SSTs) has led researchers to seek answers in modeling. For example, some model projections forecast a reduction in the annual frequency of tropical cyclones by roughly 6–34% in a warming global climate (Knutson et al. 2010). Many other studies are in agreement, and conclude that the overall frequency of tropical cyclone will decrease under future climate warming (Knutson et al. 2008; Emanuel et al. 2008), while other studies conclude major tropical cyclones (Category 4 and 5's) may double in frequency by the end of the 21st century (Bender et al. 2010). However, disagreements do exist as some researchers conclude that the annual frequency of tropical cyclone may increase (Zhao et al. 2009), or conclude that the situation is not clear enough to draw conclusions on (Trenberth 2005).

12.1.3 Storm Surge

It is expected that storm surge will continue to increase for all locations that experience tropical cyclones. Sea level rise, subsidence, and increased impervious surfaces (surfaces that prevent water from reaching the underlying soil, such as asphalt or concrete) will combine to make the impact of storm surge worse when it occurs. Projections also indicate more intense storms will produce greater surges, whether it be localized higher heights or larger areas impacted.

If storm characteristics do not change, sea level rise alone will cause an increase in the frequency and extent of flooding of coastal storms (hurricanes and nor'easters). Relative sea level rise is projected to cause a nonlinear increase in storm surge heights in areas where there is a gentle slope of the solid surface of the Earth from land into sea (shallow bathymetry). One of the main variables that may offset projected increases in storm surge is a shift in storm tracks. Any decrease in tropical cyclone frequency or shift in storm track away from the coast will decrease the occurrence and severity of storm surge. If tracks and storm characteristics do not change noticeably, it is expected that storm surge from tropical cyclones will increase, putting more people and coastal locations at risk.

12.1.4 Sea Level

There is a strong correlation between global temperatures and sea level rise. There is high confidence that sea level rise will challenge coastal communities, ecosystems, and infrastructure in the future. Sea level rise will exacerbate coastal flooding, erosion of natural and manmade structures, and saltwater intrusion. Global mean sea level rise is driven by two factors; 1) thermal expansion of the ocean which increases the volume of water, and 2) larger inputs of water into oceans from melting glaciers and ice sheets (Antarctic and Greenland). Also of concern, but not nearly as influential, is the reduction of liquid water storage on land.

Global mean sea level has risen by about 8 inches since 1900 with roughly 40-50% of that occurring since 1993 (Figure 12-2), largely attributed to human activity. The rates of sea level rise observed in the past century are greater than what has been observed in the past 2,800 years. Relative to 2000, global sea level is likely to rise by 0.3–0.6 feet (9–18 cm) by 2030, 0.5–1.2 feet (15–38 cm) by 2050, and 1.0–4.3 feet (30–130 cm) by 2100 (Figure 12-3). It is also important to note that some scenarios conclude 8 feet of sea level rise is possible by 2100, but the likelihood of that specific outcome cannot be accurately assessed.

It is important to note that sea level rise changes will not be uniform globally. Some locations may see little to no change in relative sea level while others may even see a decrease. Reasons why a location may not experience sea level rise are 1) changes in ocean circulation and wind / pressure patterns may change sea surface heights 2) locations near melting ice sheets often see decreases in sea level because the reduced gravitonic pull or attraction of the ocean to the less heavy (melting) ice sheet 3) isostatic adjustment, where areas once covered by thick ice sheets rise causing relative sea levels to drop (Hudson Bay) while areas on the flanks of the ice sheet such as the East Coast of the U.S. subside, causing relative sea level to rise. Also of importance is the consideration of local factors such as ground water and fossil fuel extraction, which cause large amounts of subsidence.

Sea level rise is a natural process and geological records indicate that past sea levels were higher than sea levels observed today. Roughly 125,000 year ago global mean sea level was roughly 20-

30 feet higher than today. When the last Glacial Maximum (26,000 to 19,000 year ago) peaked and deglaciation occurred (17,000 to 8,000 years ago) global mean sea level rose at an average rate of roughly 0.5 inches per year, but faster rates did occur, up to 2 inches per year in some cases. However, prior to industrialization, global mean sea level exhibited small fluctuations in rate (roughly 3 inches). The rate of rise in the last century has been larger than what naturally has occurred, with a rise of about 5.5 inches per century.

12.1.5 Coastal Flooding

In the United States coastal flooding has become more frequent from a fixed elevation perspective and the frequencies of minor tidal flooding (or nuisance flooding of 1-2 feet) have increased 5 to 10-fold since 1960. These types of coastal flooding events can be triggered by tides, strong onshore winds, or frontal storm systems (non-tropical). Coastal flooding is becoming more frequent due to increased global mean sea level.

The extent and frequency of coastal flooding and high-water events is expected to increase in the future (medium confidence), attributed to high confidence in projected sea level rise. RCP based projections using tide gauge locations along the contiguous U.S. coastline estimate a median 8-fold increase in the annual number of floods exceeding the elevation of the current 100-year flood event (with respect to a 1991-2009 base sea level). The frequency of minor tidal flooding (with recurrence level generally <1) is estimated to increase even more and it is possible the start occurring on a daily basis. Local conditions will either exacerbate or mitigate the frequencies of these events (subsidence, uplift, reduction of natural coastline, barriers, etc.). Overall, as sea levels continue to rise, pending mitigation and local features, coastal flooding will continue to increase and become more severe in the future (Figure 12-4).

12.1.6 Coastal Erosion

When higher-than-normal sea levels occur, wave action increases, thus the likelihood for extensive coastal erosion and low-island over wash increases. During the coming century it is estimated that mean and maximum seasonal wave heights will increase in parts of the northeast Pacific, northwest Atlantic, and Gulf of Mexico which will increase coastal erosion. However, coastal erosion is highly dependent on local conditions such as shoreline geometry, structures in place (jetties, sand bars, barrier islands, etc.) and local wind patterns. Nonetheless, beach, coastal landforms, and barrier island are expected to experience continued erosion in the coming decades, primarily due to sea level rise and increased wave action.

12.2 Tables and Figures: Coastal Regions

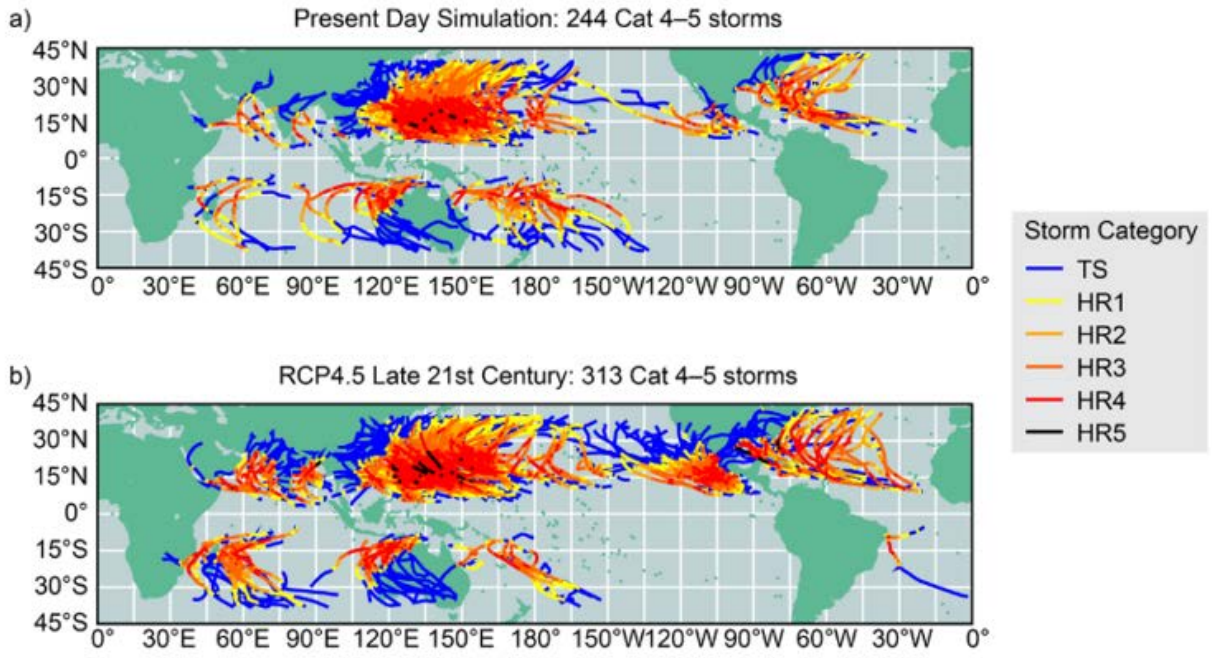

Figure 12-1. Tracks of simulated Saffir-Simpson (category 4-5 tropical cyclones) for (a) Present day or (b) late-21st-century conditions, based on the dynamical downscaling of climate conditions from the CMIP5 multi-model ensemble (lower scenario; RCP4.5). The tropical cyclones were initially simulated using a 50-km grid global atmospheric model, but each individual tropical cyclone was re-simulated at higher resolution using the GFDL hurricane model to provide more realistic storm intensities and structure. Storm categories or intensities are shown of the lifetime of each simulated storm. The categories are depicted by the track colors, varying from tropical storm (blue) to Category 5 (black; see legend) (Figure source: USGCRP 2017 p. 261).

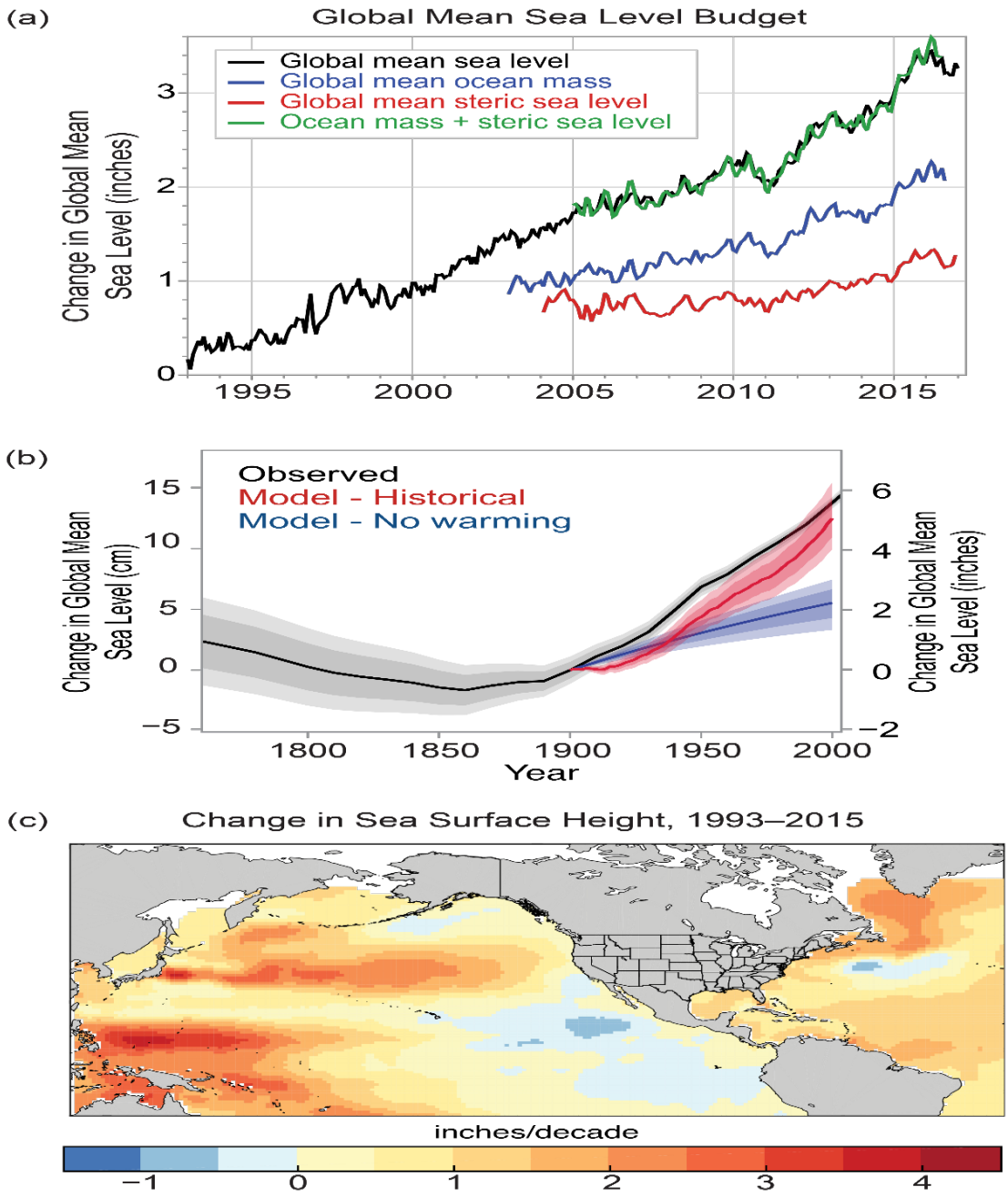

Figure 12-2. (a) Sea level rise contributions of ocean mass changes from land ice and land water storage (measured by satellite gravimetry) and ocean volume changes (or steric, primarily from thermal expansion measured by in situ ocean profilers) and their comparison to global mean sea level (GMSL) change (measured by satellite altimetry) since 1993. (b) An estimate of modeled GMSL rise in the absence of 20th century warming (blue), from the same model with observed warming (red) and compared to observed GMSL change (black). Heavy/light shading indicates the 17th–83rd and 5th–95th percentiles. (c) Rates of change from 1993 to 2015 in sea surface height from satellite altimetry data; updated from Kopp et al. using data updated from Church and White (Figure source: USGCRP 2017 p. 340).

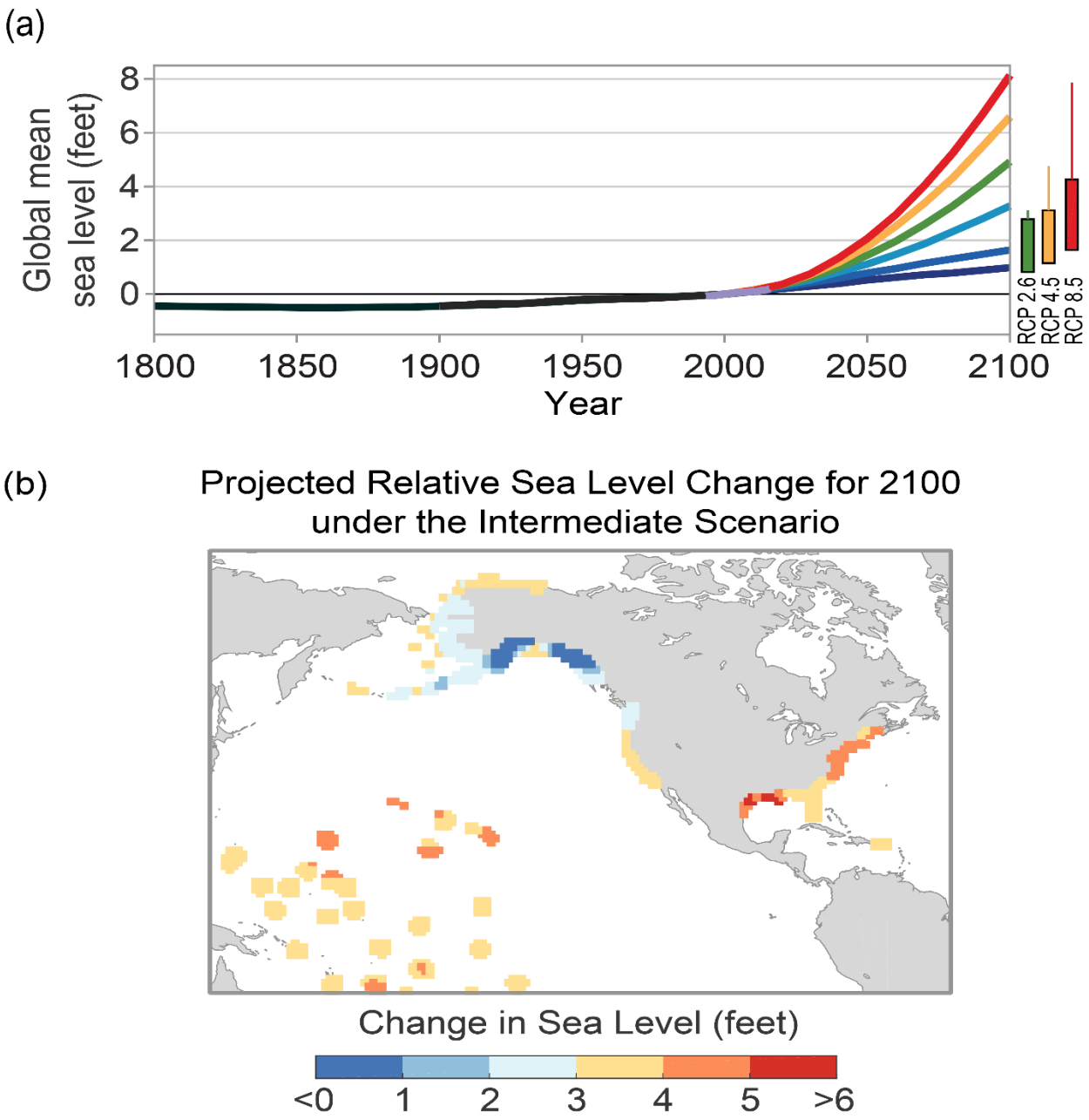

Figure 12-3. (a) Global mean sea level (GMSL) rise from 1800 to 2100, based on Figure 12.2b from 1800 to 2015, the six Interagency GMSL scenarios (navy blue, royal blue, cyan, green, orange, and red curves), the *very likely* ranges in 2100 for different RCPs (colored boxes), and lines augmenting the *very likely* ranges by the difference between the median Antarctic contribution of Kopp et al. and the various median Antarctic projections of DeConto and Pollard. (b) Relative sea level (RSL) rise (feet) in 2100 projected for the Interagency Intermediate Scenario (1-meter [3.3 feet] GMSL rise by 2100) (Figure source: USGCRP 2017 p. 342).

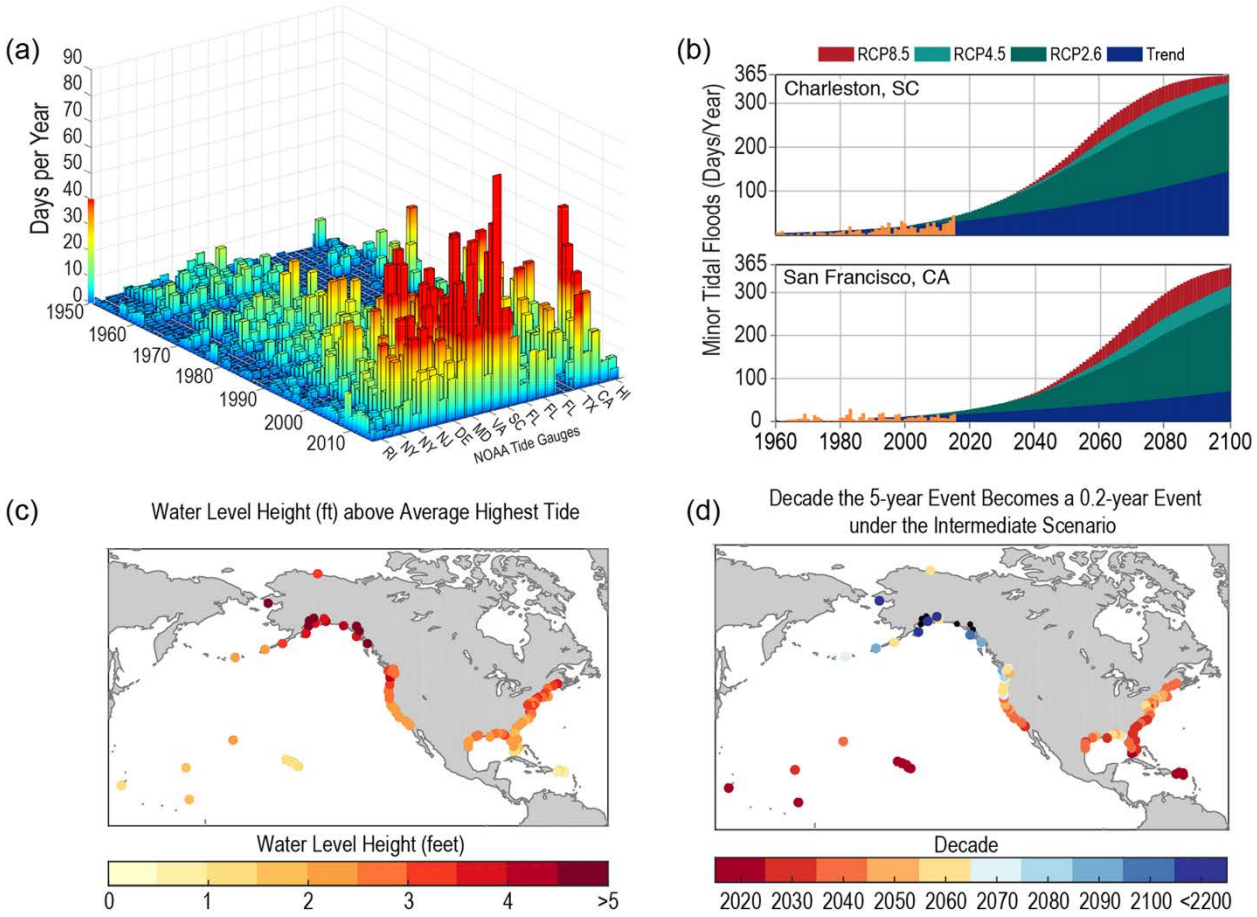

Figure 12-4. (a) Tidal floods (days per year) exceeding NOAA thresholds for minor impacts at 28 NOAA tide gauges through 2015. (b) Historical exceedances (orange), future projections through 2100 based upon the continuation of the historical trend (blue), and future projections under median RCP2.6, 4.5 and 8.5 conditions, for two of the locations—Charleston, SC and San Francisco, CA. (c) Water level heights above average highest tide associated with a local 5-year recurrence probability. (d) The future decade when the 5-year event becomes a 0.2-year (5 or more times per year) event under the Interagency Intermediate scenario; black dots imply that a 5-year to 0.2-year frequency change does not unfold by 2200 under the Intermediate scenario (Figure source: USGCRP 2017 p. 348).

13 References

Arpe, K., and S.A.G. Leroy. 2009. "Atlantic hurricanes—Testing impacts of local SSTs, ENSO, stratospheric QBO—Implications for global warming." *Quaternary International* 195, no. 1: 4-14.

Australian Research Council (ARC) Centre of Excellence for Climate System Science. "New Scenarios – SPM.1: Representative Concentration Pathways (RCPs)." Government of Australia. https://www.climatescience.org.au/content/379-new-scenarios-spm1-representative-concentration-pathways-rcps.

Bender, M.A., T.R. Knutson, R.E. Tuleya, J.J. Sirutis, G.A. Vecchi, S.T. Garner, and I.M. Held. 2010. "Modeled impact of anthropogenic warming on the frequency of intense Atlantic hurricanes." *Science* 327, no. 5964: 454-458.

Brooks, H. 2013. "Severe Thunderstorms and Climate Change." *Atmospheric Research* 123: 129–138.

Chan, J.C.L., and J. Shi. 1996. "Long-term trends and interannual variability in tropical cyclone activity over the western North Pacific." *Geophysical Research Letters* 23, no. 20: 2765-2767.

Chu, P. S., W. Yan, and F. Fujioka. 2002. "Fire-climate relationships and long-lead seasonal wildfire prediction for Hawaii." *International Journal of Wildland Fire*, 11, no. 1: 25-31.

Chu, P. S., X. Zhao, Y. Ruan, and M. Grubbs. 2009. "Extreme rainfall events in the Hawaiian Islands." *Journal of Applied Meteorology and Climatology*, 48, no. 3: 502-516.

Chu, P. S., Y.R. Chen, and T.A. Schroeder. 2010. "Changes in precipitation extremes in the Hawaiian Islands in a warming climate." *Journal of Climate*, 23, no. 18: 4881-4900.

Climate Central. 2012. "The Age of Western Wildfires." 23 pp. Available at http://www.climatecentral.org/wgts/wildfires/Wildfires2012.pdf.

Collins, M., R. Knutti, J. Arblaster, J.-L. Dufresne, T. Fichefet, P. Friedlingstein, X. Gao, W.J. Gutowski, T. Johns, G. Krinner, M. Shongwe, C. Tebaldi, A.J. Weaver, and M. Wehner. 2013. "Long-term Climate Change: Projections, Commitments and Irreversibility." in *Climate Change 2013: The Physical Science Basis. Contribution of Working Group I to the Fifth Assessment Report of the Intergovernmental Panel on Climate Change* [Stocker, T.F., D. Qin, G.-K. Plattner, M. Tignor, S.K. Allen, J. Boschung, A. Nauels, Y. Xia, V. Bex and P.M. Midgley (eds.)]. Cambridge University Press, Cambridge, United Kingdom and New York, NY, USA. http://www.climatechange2013.org/images/report/WG1AR5_Chapter12_FINAL.pdf.

Dai, A. 2011. "Drought under global warming: A review." Wiley Interdisciplinary Reviews: *Climate Change* 2, no. 1: 45-65. Available at https://onlinelibrary.wiley.com/doi/pdf/10.1002/wcc.81.

Easterling, D.R., K.E. Kunkel, J.R. Arnold, T. Knutson, A.N. LeGrande, L.R. Leung, R.S. Vose, D.E. Waliser, and M.F. Wehner. 2017. “Precipitation change in the United States.” in *Climate Science Special Report: Fourth National Climate Assessment, Volume I* [Wuebbles, D.J., D.W. Fahey, K.A. Hibbard, D.J. Dokken, B.C. Stewart, and T.K. Maycock (eds.)]. U.S. Global Change Research Program, Washington, DC, USA, pp. 207-230, DOI: 10.7930/J0H993CC.

Elsner, J.B., J.P. Kossin, and T.H. Jagger. 2008. "The increasing intensity of the strongest tropical cyclones." *Nature* 455, no. 7209: 92-95.

Emanuel, K.A. 1987. "The dependence of hurricane intensity on climate." *Nature* 326, no. 6112: 483-485.

Emanuel, K. 2005. "Increasing destructiveness of tropical cyclones over the past 30 years." *Nature* 436, no. 7051: 686-688.

Emanuel, K., R. Sundararajan, and J. Williams. 2008. "Hurricanes and global warming: Results from downscaling IPCC AR4 simulations." *Bulletin of the American Meteorological Society* 89, no. 3: 347.

Georgakakos, A., P. Fleming, M. Dettinger, C. Peters-Lidard, Terese (T.C.) Richmond, K. Reckhow, K. White, and D. Yates. 2014. “Ch. 3: Water Resources.” in *Climate Change Impacts in the United States: The Third National Climate Assessment*, J. M. Melillo, Terese (T.C.) Richmond, and G. W. Yohe, Eds., U.S. Global Change Research Program, 69-112. doi:10.7930/ J0G44N6T.

Gray, W.M. 1984. "Atlantic seasonal hurricane frequency. Part I: El Nino and 30 mb quasi-biennial oscillation influences." *Monthly Weather Review* 112, no. 9: 1649-1668.

Hayhoe, K., J. Edmonds, R.E. Kopp, A.N. LeGrande, B.M. Sanderson, M.F. Wehner, and D.J. Wuebbles. 2017. “Climate models, scenarios, and projections.” in *Climate Science Special Report: Fourth National Climate Assessment, Volume I* [Wuebbles, D.J., D.W. Fahey, K.A. Hibbard, D.J. Dokken, B.C. Stewart, and T.K. Maycock (eds.)]. U.S. Global Change Research Program, Washington, DC, USA, pp. 133-160, DOI: 10.7930/ J0WH2N54.

Hibbard, K.A., F.M. Hoffman, D. Huntzinger, and T.O. West. 2017. “Changes in land cover and terrestrial biogeochemistry.” in *Climate Science Special Report: Fourth National Climate Assessment, Volume I* [Wuebbles, D.J., D.W. Fahey, K.A. Hibbard, D.J. Dokken, B.C. Stewart, and T.K. Maycock (eds.)]. U.S. Global Change Research Program, Washington, DC, USA, pp. 277-302, DOI: 10.7930/J0416V6X.

IPCC. 2007. “Summary for Policymakers.” in *Climate Change 2007: The Physical Science Basis. Contribution of Working Group I to the Fourth Assessment Report of the Intergovernmental Panel on Climate Change* [Solomon, S., D. Qin, M. Manning, Z. Chen, M. Marquis, K.B. Averyt, M. Tignor and H.L. Miller (eds.)]. Cambridge University Press, Cambridge, United Kingdom and New York, NY, USA. https://www.ipcc.ch/site/assets/uploads/2018/02/ar4-wg1-spm-1.pdf.

Kang, N.Y., and J.B. Elsner. 2015. "Trade-off between intensity and frequency of global tropical cyclones." *Nature Climate Change* 5, no. 7: 661-664.

Kang, N.Y., and J.B. Elsner. 2016. "Climate Mechanism for Stronger Typhoons in a Warmer World." *Journal of Climate* 29, no. 3: 1051-1057.

Karl, T. R., J.M. Melillo, T.C. Peterson, and S.J. Hassol (Eds.). 2009. *Global climate change impacts in the United States*. Cambridge University Press.

Kasischke, E.S., D.L. Verbyla, T.S. Rupp, A.D. McGuire, K.A. Murphy, R. Jandt, J.L. Barnes, E.E. Hoy, P.A. Duffy, M. Calef, and M.R. Turetsky. 2010. "Alaska's changing fire regime—implications for the vulnerability of its boreal forests." *Canadian Journal of Forest Research*, 40, no. 7: 1313-1324.

Khain, A., B. Lynn, and J. Dudhia. 2010. "Aerosol effects on intensity of landfalling hurricanes as seen from simulations with the WRF model with spectral bin microphysics." *Journal of the Atmospheric Sciences* 67, no. 2: 365-384.

Kim, H.M., P.J. Webster, and J.A. Curry. 2011. "Modulation of North Pacific tropical cyclone activity by three phases of ENSO." *Journal of Climate* 24, no. 6: 1839-1849.

Knutson, T.R., J.J. Sirutis, S.T. Garner, G.A. Vecchi, and I.M. Held. 2008. "Simulated reduction in Atlantic hurricane frequency under twenty-first-century warming conditions." *Nature Geoscience* 1, no. 6: 359-364.

Knutson, T.R., J.L. McBride, J. Chan, K. Emanuel, G. Holland, C. Landsea, I. Held, J.P. Kossin, A. K. Srivastava, and M. Sugi. 2010. "Tropical cyclones and climate change." *Nature Geoscience* 3, no. 3: 157-163.

Kovacik, C., and K. Kloesel. 2014. "Changes in Ice Storm Frequency Across the United States." Southern Climate Impacts Planning Program, 21 pp. http://www.southernclimate.org/documents/Ice_Storm_Frequency.pdf.

Kunkel, K. E., M. Palecki, L. Ensor, K. G. Hubbard, D. Robinson, K. Redmond, and D. Easterling. 2009. "Trends in Twentieth-Century U.S. Snowfall Using a Quality-Controlled Dataset." *Journal of Atmospheric and Oceanic Technology* 26: 33-44. DOI: 10.1175/2008JTECHA1138.1.

Kunkel, K. E., L. E. Stevens, S. E. Stevens, L. Sun, E. Janssen, D. Wuebbles, K. T. Redmond, and J. G. Dobson. 2013. "Part 2. Climate of the Southeast U.S." in *Regional Climate Trends and Scenarios for the U.S. National Climate Assessment*. NOAA Technical Report NESDIS 142-6. 83 pp., National Oceanic and Atmospheric Administration, National Environmental Satellite, Data, and Information Service, Washington, D.C.

Kunkel, K. E., L. E. Stevens, S. E. Stevens, L. Sun, E. Janssen, D. Wuebbles, K. T. Redmond, and J. G. Dobson. 2013. "Part 5. Climate of the Southwest U.S." in *Regional Climate Trends and Scenarios for the U.S. National Climate Assessment*. NOAA Technical Report NESDIS 142-5. 87 pp., National Oceanic and Atmospheric Administration, National Environmental Satellite, Data, and Information Service, Washington, D.C.

Kunkel, K. E., L. E. Stevens, S. E. Stevens, L. Sun, E. Janssen, D. Wuebbles, K. T. Redmond, and J. G. Dobson. 2013. "Part 6. Climate of the Northwest U.S." in *Regional Climate Trends and Scenarios for the U.S. National Climate Assessment*. NOAA Technical Report NESDIS 142-6. 83 pp., National Oceanic and Atmospheric Administration, National Environmental Satellite, Data, and Information Service, Washington, D.C.

Kunkel, K. E., T.R. Karl, H. Brooks, J. Kossin, J.H. Lawrimore, D. Arndt, and K. Emanuel. 2013. "Monitoring and understanding trends in extreme storms: State of knowledge." *Bulletin of the American Meteorological Society*, 94, no. 4: 499-514.

Kunkel, K. E., T. R. Karl, D. R. Easterling, K. Redmond, J. Young, X. Yin, and P. Hennon. 2013. "Probable maximum precipitation and climate change." *Geophysical Research Letters*, 40: 1402–1408.

Landsea, C.W., N. Nicholls, W.M. Gray, and L.A. Avila. 1996. "Downward trends in the frequency of intense at Atlantic Hurricanes during the past five decades." *Geophysical Research Letters* 23, no. 13: 1697-1700.

Luber, G., K. Knowlton, J. Balbus, H. Frumkin, M. Hayden, J. Hess, M. McGeehin, N. Sheats, L. Backer, C. B. Beard, K. L. Ebi, E. Maibach, R. S. Ostfeld, C. Wiedinmyer, E. Zielinski-Gutiérrez, and L. Ziska. 2014. "Ch. 9: Human Health." in *Climate Change Impacts in the United States: The Third National Climate Assessment*, J. M. Melillo, Terese (T.C.) Richmond, and G. W. Yohe, Eds., U.S. Global Change Research Program, 220-256. DOI:10.7930/J0PN93H5.

McVicar, T.R., M.S. Roderick, R.J. Donohue, L.T. Li, T.G. Van Niel, A. Thomas, J. Grieser, D. Jhajharia, Y. Himri, N.M. Mahowald, A.V. Mescherskaya, A.C. Kruger, S. Rehman, and Y. Dinpashoh. 2012. "Global review and synthesis of trends in observed terrestrial near-surface wind speeds: implications for evaporation." *Journal of Hydrology* 416–417: 182–205.

Mearns, L.O., et al., 2007, updated 2014. *The North American Regional Climate Change Assessment Program dataset*, National Center for Atmospheric Research Climate Data Gateway data portal, Boulder, CO. Data downloaded 2019-10-08. https://doi.org/10.5065/D6RN35ST.

Melillo, J.M., T.C. Richmond, and G.W. Yohe, Eds., 2014: *Climate Change Impacts in the United States: The Third National Climate Assessment*. U.S. Global Change Research Program, 841 pp. doi:10.7930/J0Z31WJ2.

National Hurricane Center and Central Pacific Hurricane Center. 2016. "Tropical Cyclone Climatology." National Oceanic and Atmospheric Administration. https://www.nhc.noaa.gov/climo/.

Pielke Jr., R.A., and C.N. Landsea. 1999. "La nina, el nino and atlantic hurricane damages in the united states." *Bulletin of the American Meteorological Society* 80, no. 10: 2027.

Plucinski, M. 2011. "A review of wildfire occurrence research." *Bushfire Cooperative Research Centre, Australia*. http://www.bushfirecrc.com/sites/default/files/managed/resource/attachment_g_fire_occurrence_literature_review_0.pdf.

Pollina, J.B., B.A. Colle, and J.J. Charney. 2013. "Climatology and Meteorological Evolution of Major Wildfire Events over the Northeast United States." *Weather and Forecasting* 28: 175–193. DOI: 10.1175/WAF-D-12-00009.1.

Qu, M., J. Wan, and X. Hao. 2014. "Analysis of diurnal air temperature range change in the continental United States." *Weather and Climate Extremes* 4: 86-95.

Shafer, M., D. Ojima, J. M. Antle, D. Kluck, R. A. McPherson, S. Petersen, B. Scanlon, and K. Sherman. 2014. "Ch. 19: Great Plains." in *Climate Change Impacts in the United States: The Third National Climate Assessment*, J. M. Melillo, Terese (T.C.) Richmond, and G. W. Yohe, Eds., U.S. Global Change Research Program, 441-461. DOI:10.7930/J0D798BC. (3rd NCA).

Sillmann, J., V.V. Kharin, F. W. Zwiers, X. Zhang, and D. Bronaugh. 2013. "Climate extremes indices in the CMIP5 multimodel ensemble: Part 2. Future climate projections." *Journal of Geophysical Research: Atmospheres* 118: 2473-2493. DOI: 10.1002/jgrd.50188.

Stafford, J. M., G. Wendler, and J. Curtis. 2000. "Temperature and precipitation of Alaska: 50 year trend analysis." *Theoretical and Applied Climatology* 67: 33-44. Accessed at https://link.springer.com/content/pdf/10.1007%2Fs007040070014.pdf.

Stevens, L., R. Frankson, K. Kunkel, P-S. Shin, and W. Sweet. 2017. "Hawaii State Climate Summary." NOAA Technical Report NESDIS 149-HI, 4 pp.

Stewart, B. 2011. "Changes in Frequency of Extreme Temperature and Precipitation Events in Alaska." Master's Thesis, University of Illinois at Urbana-Champaign. Accessed at https://www.ideals.illinois.edu/bitstream/handle/2142/24093/Stewart_Brooke.pdf?sequence=1&isAllowed=y.

Stewart, B. C., K. E. Kunkel, L. E. Stevens, L. Sun, and J. E. Walsh. 2013. "Part 7. Climate of Alaska." in *Regional Climate Trends and Scenarios for the U.S. National Climate Assessment*. NOAA Technical Report NESDIS 142-7. 60 pp. National Oceanic and Atmospheric Administration, National Environmental Satellite, Data, and Information Service, Washington, D.C.

Sun, L., K.E. Kunkel, L.E. Stevens, A. Buddenberg, J.G. Dobson, and D.R. Easterling. 2015. "Regional Surface Climate Conditions in CMIP3 and CMIP5 for the United States: Differences, Similarities, and Implications for the U.S. National Climate Assessment." NOAA Technical Report NESDIS 144, 111 pp.

Sweet, W.V., R. Horton, R.E. Kopp, A.N. LeGrande, and A. Romanou. 2017: “Sea level rise.” in *Climate Science Special Report: Fourth National Climate Assessment, Volume I* [Wuebbles, D.J., D.W. Fahey, K.A. Hibbard, D.J. Dokken, B.C. Stewart, and T.K. Maycock (eds.)]. U.S. Global Change Research Program, Washington, DC, USA, pp. 333-363, doi: 10.7930/J0VM49F2.

Trapp, R.J., N.S. Diffenbaugh, H.E. Brooks, M.E. Baldwin, E.D. Robinson, and J.S. Pal. 2007. “Changes in severe thunderstorm environment frequency during the 21st century caused by anthropogenically enhanced global radiative forcing.” *Proceedings of the National Academy of Sciences* 104: 19719–19723.

Trenberth, K. 2005. "Uncertainty in hurricanes and global warming." *Science* 308, no. 5729: 1753-1754.

Trenberth, K.E. 2007. "Warmer oceans, stronger hurricanes." *Scientific American* 297, no. 1: 44-51.

United States Global Change Research Program (USGCRP). 2017: *Climate Science Special Report: Fourth National Climate Assessment, Volume I* [Wuebbles, D.J., D.W. Fahey, K.A. Hibbard, D.J. Dokken, B.C. Stewart, and T.K. Maycock (eds.)]. U.S. Global Change Research Program, Washington, DC, USA, 470 pp., DOI: 10.7930/J0J964J6.

Vose, R.S., D.R. Easterling, K.E. Kunkel, A.N. LeGrande, and M.F. Wehner, 2017. “Temperature changes in the United States.” in *Climate Science Special Report: Fourth National Climate Assessment, Volume I* [Wuebbles, D.J., D.W. Fahey, K.A. Hibbard, D.J. Dokken, B.C. Stewart, and T.K. Maycock (eds.)]. U.S. Global Change Research Program, Washington, DC, USA, pp. 185-206, DOI: 10.7930/J0N29V45.

Wehner, M.F., J.R. Arnold, T. Knutson, K.E. Kunkel, and A.N. LeGrande, 2017. “Droughts, floods, and wildfires.” in *Climate Science Special Report: Fourth National Climate Assessment, Volume I* [Wuebbles, D.J., D.W. Fahey, K.A. Hibbard, D.J. Dokken, B.C. Stewart, and T.K. Maycock (eds.)]. U.S. Global Change Research Program, Washington, DC, USA, pp. 231-256, doi: 10.7930/J0CJ8BNN.

Winski, D., E. Osterberg, D. Ferris, K. Kreutz, C. Wake, S. Campbell, and M. Handley. 2017. “Industrial-age doubling of snow accumulation in the Alaska Range linked to tropical ocean warming.” *Scientific reports*, *7*(1): 17869.

Zhao, M., I.M. Held, S-J. Lin, and G.A. Vecchi. 2009. "Simulations of global hurricane climatology, interannual variability, and response to global warming using a 50-km resolution GCM." *Journal of Climate* 22, no. 24: 6653-6678.